Potential New γ-globin Regulators: *in vivo* Analysis of Their Role in the Hematopoietic System.

Silvia Hoeboer

ISBN: 978-94-6375-518-4

Cover: Silvia Hoeboer, image from ©Adobe Stock, Alexandr Mitiuc
Layout: Silvia Hoeboer
Printing: Ridderprint BV Ridderkerk, The Netherlands

The research presented inn this thesis was performed at the department of Cell Biology at the Erasmus University Medical Centre, Rotterdam, the Netherlands, and was supported by The Netherlands Organization for Scientific Research (NWO/ZonMw 40/00812-98-12128 and DN82-301), Landsteiner Foundation for Blood Transfusion Research (LSBR 1040, The Netherlands Genomics Initiative (NGI Zenith 93511036), and EU fp7 Specific Cooperation Research Project THALAMOSS (306201).

Carpe diem

Potential New γ-globin Regulators: *in vivo* analysis of their role in the Hematopoietic System.

Potentiele Nieuwe γ-globine Regulatoren: *in vivo* analyse van hun rol in het Hematopoeitische Systeem.

Proefschrift

ter verkrijging van de graad van de doctor aan de
Erasmus Universiteit Rotterdam
op gezag van de
rector magnificus

Prof.dr. R.C.M.E. Engels

en volgens besluit van het College voor Promoties.
De openbare verdediging zal plaatsvinden op

Dinsdag 3 September 2019 om 15:30 uur.

Silvia Astrid Hoeboer
geboren te Rotterdam

Erasmus University Rotterdam

Promotiecommissie:

Promotor:	**Prof. Dr. J.N.J. Philipsen**
Overige leden:	**Prof. Dr. J.H. Gribnau** **Prof. Dr. F.G. Grosveld** **Prof. Dr. M. de Haas**
Copromotor:	**Dr. T.B. van Dijk** **Dr. M. von Lindern**

LIST OF COMMONLY USED ABBREVATIONS

ADMA	asymmetric Ψ-NG,NG-arginine demethylation
baso-EB	basophilic erythroblast
BCL11A	B cell CLL/lymphoma 11A
BFU-E	burst forming unit erythroid
BM	bone marrow
BSA	bovine serum albumin
bp	base pairs
CB	cord blood
cKO	conditional knock out
cDCs	conventinal dentritic cells
L-DCs	immature dendritic cells
CFU-E	colony forming unit erythroid
CHTOP	Chromatin target of protein arginine methyltransferase 1
CLP	common lymphoid progenitors
CML	chronic myeloid leukemia
CMP	common myeloid progenitors
CRISPR	Clustered Regularly Interspaced Short Palindromic Repeats
DCs	dentritic cells
DMSO	dimethyl sulfoxide
DN	double negative
DOX	doxycycline
DP	double positive
EPO	erythropoietin
EpoR	Epo Receptor locus
FL	fetal liver
gRNA	guideRNA
GMP	granulocyte-macrophage progenitor
GWAS	genome-wide association studies
Hb	hemoglobin
HBB	human-β-globin locus
HbA	Adult hemoglobin
HbF	Fetal hemoglobin
HbS	sickle cell hemoglobin
HCT	hematocrit
HEK	human embryonic kidney
HGB	hemoglobin
HEP	human erythroid progenitor
HPFH	hereditary persistence of fetal hemoglobin
HS	hypersensitivity
HSCs	hematopoietic stem cells
HUDEP	human umbilcal cord blood erythroid progenitor

IFN	interferon
ISP	immature single positive
JHDM1D	jumonji C domain containing histone demethylase 1 homolog D
KLF1	Krüppel-like factor 1, eKLF
KDM7A	Lysine demethylase 7A
LCR	locus control region
LRF	Leukemia/Lymphoma Related Factor
LT-HSCs	long-term repopulating hematopoietic stem cells
MCV	Mean Corpuscular Volume
MCH	Mean Corpuscular Hemoglobin
MCHC	Mean Corpuscular Hemoglobin Concentration
RDW	RBC distribution width
MPV	mean platelet volume
MEP	myeloid-erythroid progenitor
MMA	Ψ-NG-monomethyl arginine
MPP	Multipotent progenitor
MYB	Myeloblastosis oncogene
NK	Natural Killer
ortho-EB	orthochromatic erythroblast
pDCs	plasmacytoid dendritic cells
PHZ	phenylhydrazine
pIpC	poly-inosinic:poly-cytidylic acid
PLT	platelets
poly-EB	polychromatic-erythroblast
PRMT	protein arginine methyltransferase
Pro-EB	pro-erythroblast
RBC	red blood cells
SC	subcutaneously
SCD	sickle cell disease
sDMA	symmetric Ψ-NG,NG-arginine demethylation
SP	single positive
ST-HSCs	short-term repopulating hematopoietic stem cells
Vec-Cre	vascular endothelial cadherin-Cre recombinase
WBC	white blood cells
WT	wild type

Table of contents

Chapter 1

Introduction and scope of the thesis

Chapter 1. Introduction and scope of the thesis

Hematopoiesis

Blood is one of the most important tissues in our body. It consists of red and white blood cells, platelets, and blood plasma. Essential functions of blood are the transport of nutrients and hormones, but also oxygen delivery and removal of waste products throughout the body via a dense system of blood vessels and capillaries that enter deep into all tissues.

An adult human has between 4-6 litres of blood. Red blood cells (RBCs) or erythrocytes are the most common cells in the blood. Every microliter of blood contains 4-6 million erythrocytes. For comparison, in one microliter there are 150,000-400,000 platelets (thrombocytes) and 4,000-11,000 white blood cells (WBCs or leukocytes).[1,2]

Erythrocytes are produced within the bone marrow (BM). The average lifespan of a human RBC is about 110-120 days.[3] Under steady-state conditions, every second about 2 million RBCs are released into the blood stream to replace worn-out RBCs which are cleared by the reticulo-endothelial system mainly in the spleen and liver.[1]

Although the other cells within the blood are less abundant, their functions are very important. All blood cells are derived from hematopoietic stem cells (HSCs; see also Figure 1).[2,4] During differentiation, progenitor cells become more and more committed to the mature cell lineages. After leaving the HSC compartment, they become multipotent progenitor cells, common lymphoid progenitors (CLP) or common myeloid progenitors (CMP). Furthermore, there are committed progenitors for each mature differentiated cell type, such as the myeloid-erythroid progenitor (MEP). Although HSC provide for life-long replenishment of the hematopoietic cells, the HSC divide rarely. Instead the proliferation speed is highest at the multipotent and committed progenitor cell stages.[5]

Each component of the blood has its own role in the physiology of the organism. There are many cell surface markers available for identification of blood cell types by flow cytometry, some of which will be discussed later in this chapter.

Lymphocytes can be categorized in three major cell types: T cells, B cells and Natural Killer (NK) cells. These three groups are part of the immune system which protects the body against pathogens.

T cells, T lymphocytes or thymocytes develop within thymus, from which they derive their name, and tonsils.[6,7] Mature T cells can be distinguished from the other lymphocytes by the presence of the T cell receptor (TCR) on the cell surface. There are many types of T cells marked by different surface markers: effector, helper, cytotoxic, memory, regulatory and natural killer T cells.

Their functions vary from assisting maturation of B cells to the destruction of bacteria, virus-infected cells and tumour cells. T cells are only activated after they are presented with an antigen by antigen-presenting cells such as dendritic cells. T cells can only function for a short period of time when activated.[6]

B cells secrete antibodies, which are also known as immunoglobulins.[9,10] They were named after the bursa of Fabricius in birds, where they were first found. In mammals, B cells develop in the bone marrow.[10] There are different types of B cells: plasmablasts, effector (plasma cells)-, lympho-plasmacytoid-, memory-, follicular-, marginal zone-, B1/B2-, and regulatory B cells.[9,11-14] B cells in general are controlled by the activation of the B cell receptor (BCR).[15] The BCR can bind a specific antigen, against which a specific antibody response will be initiated. It is estimated that there

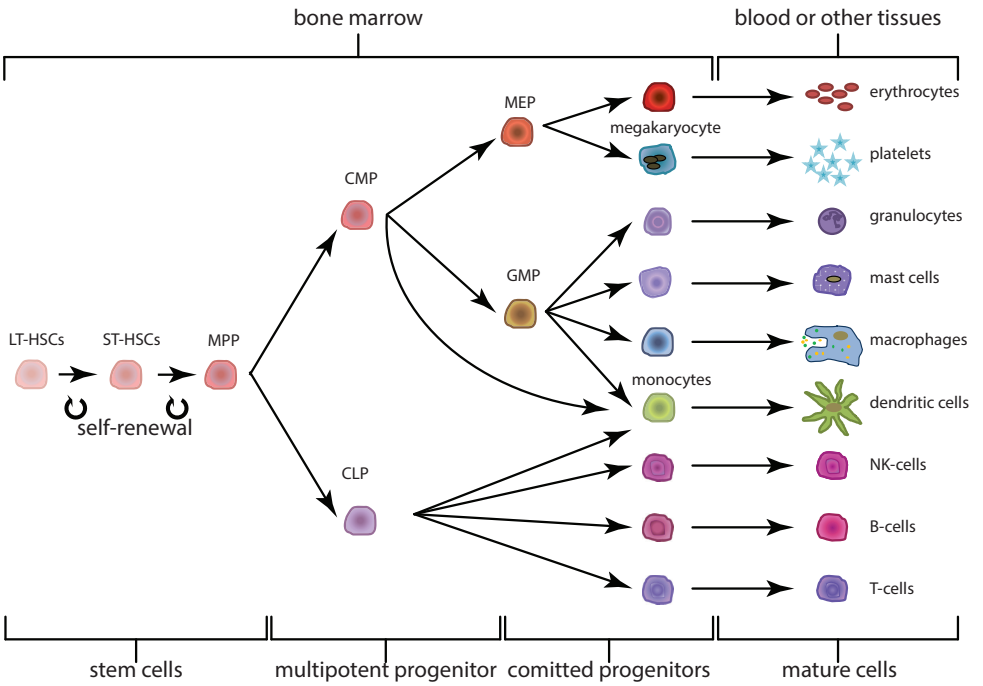

Figure 1. Hierarchy of the hematopoietic system in a schematic model to illustrate the different stages of differentiation that starts at the long-term repopulating hematopoietic stem cells (LT-HSCs). Differentiation proceeds through several steps: short term repopulating hematopoietic stem cell (ST-HSCs), multipotent progenitor (MPP), common lymphoid progenitor (CLP), common myeloid progenitor (CMP), megakaryocyte-erythroid progenitor (MEP), granulocyte-macrophage progenitor (GMP). The HSCs and MPP can still differentiate to all mature cells, but the progenitor cells become increasingly committed to a particular lineage. Most of the processes occur within the bone marrow, but other organs such as the lymph nodes, spleen, tonsils, and thymus are also involved. Figure adapted from ref [8].

are around 10^{11} different BCRs.[9,15]

NK cells respond rapidly to viral infections, protect against tumour formation, and can recognize stressed cells in the absence of antibodies.[16-18] They belong to the innate immune system. Before entering the bloodstream, the cells differentiate and mature in the BM, lymph nodes, spleen, tonsils and thymus.[19] Due to MHC-class I proteins, NK cells and cytotoxic T cells can distinguish virus infected cells from healthy cells.[6]

Dendritic cells (DCs) originate in general from the common myeloid progenitor (CMP) cells, but can also be generated by common lymphoid progenitor (CLP) cells.[20] DCs are also known as antigen-presenting cells or accessory cells. They sample the environment to present antigens to T cells. These cells are the communicators from the innate immune system, that signal to the adaptive system.[21] The innate immune system is the first line of defence against many common microorganisms and is essential in the control of bacterial infections.[22] Also changed body cells will be removed by the innate immune system. Some pathogens escape from this system, after 4-7 days the adaptive immune system will fight those escpated the foreign bodies and pathogens.[22]

Macrophages engulf anything that does not have the markers of a healthy cell, this can be a cancer cell, but also an unknown substance or pathogen. After engulfing

the substance, it will digest it.[6] Macrophages can be found in any tissue.[23] There are several types of macrophages. Their names depend on the tissue where they are located, e.g. Kupffer cells in the liver, alveolar macrophages in pulmonary alveoli and microglia in neural tissues.[24-26] Macrophages present antigens to T cells, and also produce anti-inflammatory cytokines, like IL-10.[27] In addition to their immunological role, macrophages are involved in wound healing, muscle regeneration, and play a major role in iron-homeostasis from iron that is released by ingested RBCs.[28-30]

Granulocytes are a group of leukocytes with granules in their cytoplasm. Most abundant are the neutrophilic granulocytes.[31] Eosinophilic and basophilic granulocytes are less common. They can be histologically distinguished using haematoxylin and eosin staining: neutrophilic granules are stained pink, basophilic granules are stained blue, and eosinophilic granules are stained red.[32] All types of granulocytes originate from the bone marrow, are associated with inflammation, and have their own signalling molecules.[9] Neutrophils are the most abundant type of white blood cells, are mainly found during the acute phase of an inflammation and are the major component of pus.[33] Basophils and eosinophils are associated with chronical inflammatory conditions such as asthma.[34,35]

Neutrophils phagocytose microorganisms and particles, and eosinophils degranulate in response to large (multicellular) parasites. In contrast, the basophils that are not associated with phagocytosis, but with histamine and serotonin release to initiate inflammatory responses.[33-35]

Mast cells also belong to the granulocytes. They contain many granules which are heparin and histamine rich. They play a role in allergic reactions like anaphylaxis and are involved in wound healing.[36] When activated, mast cells release granules into the environment, activating an inflammatory response.[36,37]

Thrombocytes, or platelets, have the capacity to clump to avoid excessive blood loss when injured.[38] These cell fragments are produced by megakaryocytes and don't have a nucleus.[39] They are about a 1/5 of the size of an RBC. In case of wound bleeding, they first attach to the endothelium, then they reshape and activate receptors to assemble other factors involved, and finally they aggregate to each other. These three steps describe the major functions of thrombocytes: adhesion, activation and aggregation.[40]

Erythropoiesis

The hematopoietic process of production and expansion of progenitor cells and the subsequent maturation towards red blood cells is called erythropoiesis. RBCs are the most abundant cell type in blood and are responsible for the O_2 transport from the lungs to the other parts of the body. After oxygen is released, the waste product CO_2 is transported by the RBCs from the tissues and released in the lungs.[6] The protein responsible for oxygen and CO_2 transport is hemoglobin (Hb). The average lifespan of an erythrocyte is 60 days in mice and 120 days in humans. As mentioned earlier, the first defined stage following the HSC phase is a multipotent progenitor (MPP) stem cell, followed by the common myeloid progenitor (CMP) stage. Additional stages in erythropoiesis are shown in Figure 2: the megakaryocytic-erythroid-progenitor (MEP) becomes more committed to the erythroid lineage.[41] The first erythroid-restricted progenitor is called the burst forming unit erythroid (BFU-E).[42] This cell will give rise to large colonies in specific cell culture conditions. The next more mature erythroid

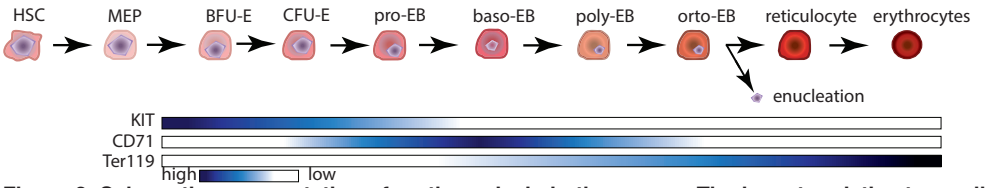

Figure 2. Schematic representation of erythropoiesis in the mouse. The hematopoietic stem cell (HSC) first gives rise to megakaryocytic-erythroid progenitor (MEP) cells. The MPP (multipotent progenitor) and CMP (common myeloid progenitor) stages are not shown. The MEP cells progressively develop through different stages: burst forming unit erythroid (BFU-E), colony forming unit erythroid (CFU-E), pro-erythroblast (pro-EB), basophilic erythroblast (baso-EB), polychromatic-erythroblast (poly-EB), and orthochromatic erythroblast (ortho-EB). Then, the nucleus is extruded from the cell, and a reticulocyte is formed. The cell subsequently reshapes to a biconcave disc and becomes a mature erythrocyte. During the entire process, the expression of surface markers KIT, CD71 and Ter119 changes dynamically. Figure adapted from ref.43.

progenitor is the colony forming unit erythroid (CFU-E), which gives rise to small colonies in the same culture conditions.[42] In the lower panel of Figure 2 the expression profiles of the cell surface markers KIT, CD71 and Ter119 are indicated. These markers are used in the following chapters to mark the different erythroid stages by flow cytometry analysis.

Erythropoiesis takes place in a structure called the erythroblastic island.[44] This structure is composed of a central macrophage and is covered by proliferating erythroid progenitor cells. The central macrophage is also called the 'nurse' cell, since it regulates differentiation and provides nutrients to the erythroid progenitors.[30] During the next maturation steps the cells become smaller, but still have a nucleus which decreases in size: pro-erythroblast (pro-EB), basophilic erythroblast (baso-EB) and the orthochromatic erythroblast (ortho-EB).[45] From the ortho-EB stage the hemoglobin levels increase rapidly. Then enucleation will be accomplished with the help of macrophages.[46] The enucleated cells are called reticulocytes, these are released in the bloodstream, where they mature into erythrocytes. Reticulocytes still produce hemoglobin and have to adopt the typical biconcave shape of mature erythrocytes. [43,45,47,48] The biconcave shape increases the surface area/volume ratio, which promotes the exchange of O_2 and CO_2, and it enhances the deformability that is required for the RBCs to pass the small capillaries. [49-51]

Hemoglobin and the switch

The most important protein complex in erythrocytes is hemoglobin, a tetrameric structure of 2 α-like and 2 β-like globins. Each globin contains a heme-group that can bind oxygen (Figure 3A). It is estimated that every erythrocyte contains ~270 million hemoglobin molecules.[52,53] The molecular structure shows that each globin contains 8 α-helices that form a three-dimensional structure termed the globin fold.[53] There are many different globins produced in humans: ζ, α, ε, γ, β and δ can be found. In mice, they are called: ζ, α, εy, βh1, βmajor and βminor. The tetramers that are formed in humans are: adult hemoglobin (HbA): $\alpha_2\beta_2$ and HbA_2 $\alpha_2\delta_2$, fetal hemoglobin (HbF): $\alpha_2\gamma_2$, and embryonic hemoglobin: Hb Gower1 $\zeta_2\varepsilon_2$, and Hb, Gower2 $\alpha_2\varepsilon_2$ Hb Portland 1 $\zeta_2\gamma_2$, Hb Portland 2 $\zeta_2\beta_2$. In both humans and mice, the different globin genes are distributed over two different loci (Figure 3B). The α-globin locus can be found in humans on chromosome 16 and in mouse on chromosome

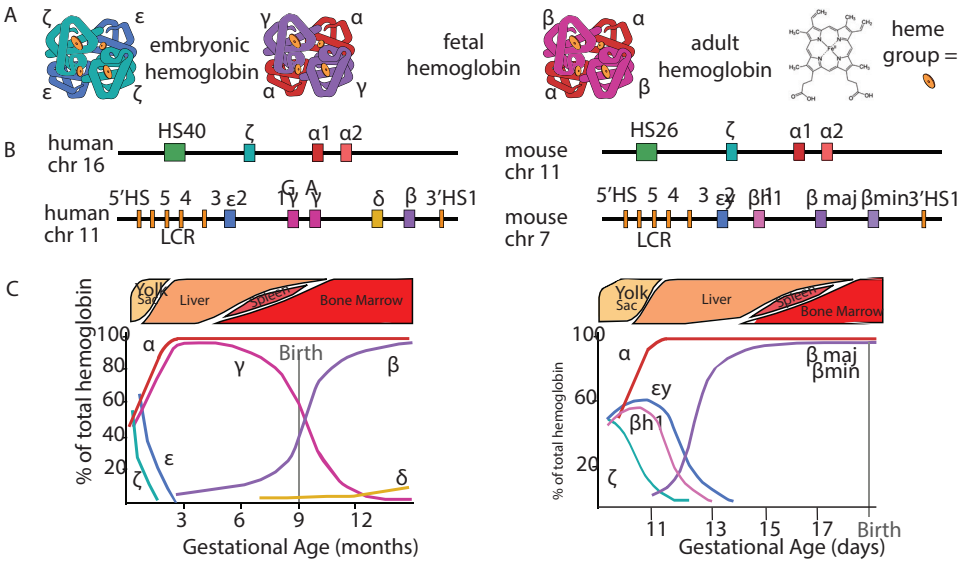

Figure 3. Schematic representation of (A) human embryonic, fetal and adult hemoglobin. On the right the molecular structure of a heme group, and its representation. (B) The human (left) and mouse (right) globin locus. On the a-globin locus 5' hypersensitivity site (HS)-40 is located. On the b-globin locus the genes are flanked by the locus control region (LCR) with multiple HS sites. (C) During embryonic and fetal stages of development the composition of hemoglobin changes, expression of human globins is represented on the left. On the right the expression pattern of mouse globins is shown on the right. During this process, the location of hematopoiesis changes from the yolk sac to the liver, spleen and finally bone marrow. Figure adapted from ref 56,57.

11. The embryonic ζ-globin gene is located upstream of the two α-globin genes α1 and α2. In humans, hypersensitivity site -40 (HS-40) is located further upstream. HS-40 is known as an erythroid specific enhancer that regulates the transcription of the α-like globin genes.[54,55] The β-globin locus is located at human chromosome 11 and on chromosome 7 in the mouse. Hypersensitivity sites are present in the locus control region (LCR). Located 5' of the human β-globin gene, there are the δ-globin -, γ-globin - and ε-globin genes. In mice, εy, βh1, βmajor and βminor-globin are found at the β globin locus.

Depending on the stage of life, the tetramers are composed of different globin combinations, due to globin gene and protein switches (Figures 3A and C). In humans, mice and other vertebrates, a tetramer is formed in a ratio of 2:2. In the early embryonic life phase of humans, the erythrocytes mainly contain ζ-globin and ε-globin polypeptides, forming Hb Gower1.[53]

Embryonic hemoglobins can only be found at the beginning of the first trimester. During fetal development, 2 α-globins form a tetramer with 2 γ-globins: the fetal hemoglobin or HbF.[53] This switch occurs halfway the first trimester of gestation. A second switch happens around birth, when adult hemoglobin, HbA, gradually replaces HbF. HbA is composed of 2 α-globin chains and 2 β-globin chains.[53]

In mice only one switch occurs within the β-globin locus. The early embryonic genes εγ and βh1 are expressed from E8.5 to E12.5. After the mouse globin switch, βmajor and βminor are the active β-like globin genes. Interestingly, transgenic mice carrying the human β-globin locus follow a switching pattern that is different from humans.[58]

Human γ-globin will be expressed from E8.5 and is silenced around E13.5. Human β-globin will be expressed from E11.5 onwards.

Hemoglobinopathies

The most common monogenetic disorders in the human population are hemoglobinopathies, which include sickle cell disease (SCD) and thalassemias. As a result of these diseases, oxygen transport is decreased and the erythrocytes have a shorter life span, leading to anemia.[59] As a consequence, hematopoiesis is disturbed and unbalanced.[60,61]

Despite the autosomal recessive inheritance around 300,000-400,000 patients are born every year worldwide.[62,63] Most patients live in the tropics and subtropics: Southeast Asia, Middle East, India, Africa and the Mediterranean countries, Figure 4.[63] Interestingly, the heterozygous condition is thought to provide some protection against the malaria parasite *Plasmodium falciparum* which causes cerebral malaria.[63,64] This provides a selective advantage for the disease carriers. When untreated, the homozygote condition is usually lethal. Due to migration, SCD and β-thalassemia are now common in many parts of the world.[63]

Thalassemia

About 4.83% of the worldwide population is carrier of a hemoglobinopathy mutation.[59] More than 200 different mutations are known that are linked to β-thalassemia.[63] These mutations affecting the *HBB* gene will lead to decreased (β^+-thalassemia) or absent (β^0-thalassemia) expression of β-globin, causing an imbalance with α-globin.[66]

Three different β-thalassemias can be distinguished. The first is called thalassemia trait, which is a heterozygous variant: β^+/β or β^0/β, with one normal and one affected allele of *HBB*.[67] Only mild anaemic symptoms are presented and in general there is no threat to life.[68] The second is β-thalassemia intermedia, which is caused by homozygous mutations in *HBB*, combining β^+/β^+ or β^0/β^+ alleles.[67] These patients usually suffer from moderate anaemia and may need blood transfusions to have a normal life. The transfusions cause an iron overload, which needs to be treated by iron chelation therapy.[68] The third type is β-thalassemia major, which is due to homozygosity of *HBB* for severe β^0/β^0 mutations[67] Patients showsymptoms soon after birth. They are transfusion-dependent, and consequently have to be treated

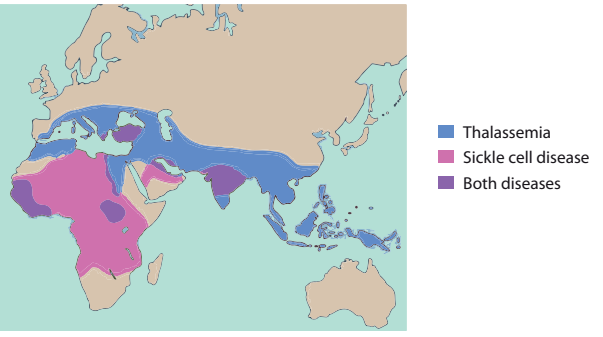

Figure 4. Representation of the distribution of thalassemia, sickle cell disease and both diseases in the tropic and subtropic regions: Southeast Asia, Middle East, India, Africa and the Mediterranean countries. Figure adapted from ref [63,65].

for iron overload.[68] Since the disease manifests itself already at a young age, organ damage will occur during life giving these patients a shorter life expectancy.[68,69]
In α-thalassemia the α-globin locus is affected. Deletions or mutations within the α-globin locus on chromosome 16 cause the anemia.[70] Severity of the disease is dependent on which mutation or deletion is present, and how many alleles are affected.[70] When all four alleles are affected, this is called α-thalassemia major. Since α-globin is also part of fetal HbF, foetuses die before delivery or shortly after birth.[70] When two (alpha thalassemia or thalassemia trait) or three alleles (hemoglobin H disease) are affected, the patients show several anemic symptoms and need to be treated.[70] When only one allele is affected, called silent α-thalassemia carrier, there are no signs of the disease, but the affected allele can be transmitted to the next generation.[70]

Sickle cell disease

In SCD, a point mutation *HBB*:c.20A>T causes an amino acid substitution in β-globin: a glutamic acid is replaced by a valine.[71,72] Due to this mutation, sickle cell hemoglobin (HbS) is formed by 2 α-globins and 2 β^s-globin peptides.[60] HbS is less soluble and leads to a disturbed environment within the erythrocyte.[60] Under low oxygen conditions, HbS polymerizes forcing the erythrocytes to adopt the characteristic sickled shape.[73] The lifespan of sickle cell erythrocytes is ~18 days, much shorter than the average lifespan of 120 days of normal erythrocytes. As the bone marrow cannot fully compensate the rate of destruction, this causes a shortage of RBCs (anemia). The sickled cells easily obstruct vessels and especially small capillaries, leading to a reduced oxygen delivery and causing painful crises and necrosis of the tissue.[74] Any organ can be affected; SCD patients suffer from a much higher risk of stroke, eye problems and, due to repeated splenic infarction, serious infections.[74,75]

Hereditary persistence of HbF

Hereditary persistence of fetal hemoglobin (HPFH) is a benign condition with persistent high levels of γ-globin in adult erythrocytes.[76] This can be caused by mutations in the *HBB* locus. In addition, mutations affecting the transcription factors KLF1, BCL11A, and MYB can also result in HPFH.[77-82] The percentage of γ-globin varies depending on the mutation. Patients with a β-hemoglobinopathy and HPFH combined, and having a HbF of 20% or higher, show a great reduction in clinical severity.[83]

Treatments

Since people with HPFH combined with SCD or β-thalassemia show less symptoms of the diseases, several therapies are aimed at raising levels of HbF in non-HPFH patients.[60] One of those treatments is the administration of hydroxyurea, which can increase HbF levels up to 10-15%.[84,85] Other studies revealed that >25% HbF is needed to ameliorate most of the symptoms of SCD patients.[60] Hydroxyurea is not a universal solution to SCD and β-thalassemia, because there is a high variability in the response rate of patients.[86] Due to the increased HbF levels, the transport ability of oxygen increases, the cellular hydration will increase and the cells are less likely to sickle.[87] The molecular mechanism behind hydroxyurea is not completely

understood. Long term side effects of hydroxyurea are not known yet, short term effects are: reduced neutrophil levels, bone marrow suppression, increase of liver enzymes, reduced appetite, weight loss and infertility.[87]
Other current treatments are blood transfusions, and bone marrow transplantations. Blood transfusions are always combined with iron chelation therapy to prevent iron overload due to the transfusion.[68] Iron overload will lead to damage of vital organs such as the heart and the liver. Bone morrow transplantation is dependent on availability of a suitable donor, is very invasive, risky and expensive, and not a realistic option in most of the countries with high disease incidence.[88]
Gene therapy for β-hemoglobinopathies has been applied successfully to small numbers of patients, but this state-of-the-art approach is unlikely to become available to the large majority of patients. Integration of the gene therapy vector in the host genome carries the risk of insertional mutagenesis.[89-91] Precisely targeting the affected globin locus, or regulatory genes, would circumvent that risk. With the development of highly efficient CRISPR (Clustered Regularly Interspaced Short Palindromic Repeats)-Cas9-based genome editing tools this approach has become a realistic option.[92-95] However, this is currently still in research phase. All these innovative treatments are not accessible for the thousands of people living in low income countries. Later in this chapter we will discuss some target genes. These include known erythropoiesis regulator genes, but also new potential regulator genes. All those genes might be interesting targets to develop new affordable and low risk therapeutic strategies.
Other potential therapies are, for example, histone deacetylase inhibitors such as butyrates, and the DNA methylation inhibitor 5-azacytidine.[96-99] Clinical trials using the butyrate HQK-1001 did not lead to a therapeutic agent: two out of three phase II clinical trials patients showed an increase HbF and hemoglobin levels, one trial stopped after the first evaluation since patients did not show an increased HbF but showed more pain crises.[100-102]
The DNA methyltransferase inhibitor 5-azacytidine increases γ-globin levels in β-hemoglobinopathies but does have potential mutagenic side effects.[98,99] Despite this, phase I clinical trials have recently been performed that combined the deoxy variant of 5-azacytidine (decitabine) with tetrahydrouridine. No short-term side effects were observed and an increase of 4%-9% HbF was achieved.[103]

Experimental research models

Cell culture systems

Much knowledge of erythropoiesis has been gained from a variety of cell culture models. One of the most widely used systems is the murine erythroleukemia (MEL) cell line.[97] By the addition of dimethyl sulfoxide (DMSO) MEL cells can differentiate, but will not enter the erythrocyte phase completely. Immortalized mouse fetal liver cells represent a more physiological system due to their growth factor dependence.[104,105] K562 cells are a widely-used cell line of human origin.[106] They are derived from a chronic myeloid leukemia (CML) patient. Addition of specific components such as hemin, butyric acid, 5-azacytidine, chromomycin or cisplatin analogs to the medium can induce erythroid differentiation of K562 cells.[107-112] A disadvantage of K562 cells is that they don't express HbA but only embryonic hemoglobin and HbF at low levels. The most recently created cell lines are the immortalized human umbilical cord blood

erythroid progenitor (HUDEP) cells.[113] There are 3 different HUDEP cell lines, they differ in maturation status and end stage after differentiation. HUDEP-2 cells are most commonly used as they faithfully model human adult erythropoiesis.
It is also possible to culture primary human erythroid progenitor (HEP) cells. This system is quite laborious and these cells have a limited life span.[114,115] When using peripheral blood or buffy coats, a homogenous cell culture system can be derived, although there will always be donor-to-donor variability. Of note, HEP cell cultures invariably display high HbF levels (5-7%), which is thought to be due to the stress invoked by the culture conditions. Despite these limitations, the HEP cell cultures are, together with the HUDEP-2 line, considered the best human erythroid model systems.

Animal models for the study of erythropoiesis

The nematode worm *Caenorhabditis elegans* and fruitfly *Drosophila melanogaster* do not rely on erythroid cells for gas transport; hence these widely used model animals are not suitable for the study of erythropoiesis. In contrast, the zebrafish *Danio rerio* has an erythroid system with many similarities to that of humans.[116] Zebrafish are easy to mutate, have a separate mesodermal site that functions like the mammalian yolk sac, and have thymus and aorta-gonad-mesonephros (AGM)-like structures.[117,118] Erythrocytes are responsible for oxygen transport, but remain nucleated and have an oval shape.[118,119] Research using zebrafish has contributed significantly to our understanding of hematopoiesis during embryonic development in particular, due to the easy access to large numbers of embryos at all stages of development. Given the large physiological differences between adult zebrafish and mammals, the contribution of the zebrafish model to understanding adult mammalian erythropoiesis has been far more limited.
Another animal model that has been used in research is the chicken (*Gallus gallus*). Their oval red blood cells are nucleated and develop in seven steps from a rubryblast (erythroblast) to a mature red blood cell.[120] In chicken, the proto-oncogene myb was correlated to hemoglobin regulation.[121] Furthermore, chicken hemoglobin has a lower oxygen affinity than human hemoglobin.[122] Chickens also have a hemoglobin switch during the development, where NF-E4 is a critical regulatory factor.[123-127]
The most commonly used animal model for human development and disease is the house mouse (*Mus musculus*). Mice are used for multiple reasons: they are easy to modify genetically, easy to handle, have a small size, reach adulthood quickly, have large litter sizes with a short gestation period of three weeks. The erythroid systems of mice and humans have many similarities but also a number of differences, such as the life span of erythrocytes (120 vs 42 days), mean corpuscular volume (MCV 90 vs 52 fl) and oxygen affinity (25 vs 40 mm Hg). Other differences can be found within the membrane protein structure which functions differently, leading to altered glucose, vitamin C, signalling pathways and different iron regulation.[128-131] LncRNAs are also differently regulated between mouse and human erythropoiesis.[132]
At the genetic level, many similarities are found between mouse and human. When aligning the mouse genome to the human genome, they will match for approximately 50%.[133,134] Furthermore, they share the same transcription factors, e.g. GATA1 and KLF1/EKLF are regulating expression of the erythroid globin genes.[132,134] The α-globin and β-globin loci have similar structures.[56] Another similarity are the erythroid

production sites. The first erythropoiesis happens in primitive streak mesoderm, this will be continued in the yolk sac, AGM and placenta.[135] Subsequently, it moves to the fetal liver and around birth it switches to the bone marrow. Also, erythropoiesis is EPO driven and the hematopoietic cells have several conserved cell surface markers.[136,137] Although there are many differences with humans, mice are considered to be a good animal model for hematological research. Results obtained in mice can be extrapolated, with caution, to human erythropoiesis. When possible, critical observations should be confirmed in humans.

Cre-recombinase

Cre-recombinase is a P1 bacteriophage-derived tyrosine site-specific recombinase.[138-141] The normally monomeric Cre dimerizes around loxP sites within the genome, due to its high affinity to loxP.[140,142,143] The loxP site is a 34 bp DNA sequence, when two loxP sites are linked within the genome, a so called synaptic complex is formed.[144,145] The synaptic complex is a mechanism used by all tyrosine recombinases.[140,141]

In recent years, many tissue-specific Cre-recombinase mouse lines were developed for instance by the International Mouse Phenotyping Consortium (IMPC) for different purposes. A search in the Mouse Genome Database shows almost 3000 matches for Cre.[146,147] For example, there are many tamoxifen-inducible ($CreER^{T2}$) Cre-recombinase lines.[148-150] Most common are constitutive tissue-specific Cre lines, for example Alb1-Cre is only expressed in the liver, Lck-Cre is expressed in thymocytes, and Tagln-Cre in smooth muscles.[146,147,151-153]

In this thesis, we used 4 different Cre-recombinase lines specific for the erythroid and hematopoietic cells. EpoR-Cre is controlled by the endogenous erythropoietin receptor promoter, which is active from the BFU-E stage with a maximal expression from the CFU-E stage, and its expression is restricted to erythroid cells.[154]

Vav1-Cre is an endothelial, germ cell and pan-hematopoietic Cre recombinase line. Expression of this Cre recombinase transgene is controlled by the promotor of the Vav1 gene.[155] Vav1 was first identified as an oncogene, but normally it is involved in B and T cell maturation and activation.[156,157] Vav1 functions as a guanidine nucleotide exchange factor.[158]

The vascular endothelial cadherin (Vec) Cre recombinase transgene is controlled by the promotor of the VE-cadherin gene.[159] VE-cadherin is a transmembrane protein that is involved in cell-to-cell adhesion.[160] Vec-Cre activity is first found at E7.5 within the yolk sac blood islands, at E9.5 it will become active within the whole vasculature, on E10.5 it is active in endothelial cells and several intra-arterial clusters, from E11.5 activity can be found within the fetal liver and within the blood cells and finally it can also be found within the adult bone marrow. [161]

Mx1-Cre is the only inducible Cre-recombinase we used. This Cre-recombinase transgene is controlled by the *Mx1* promotor, which is part of the defense against viruses. In healthy mice, this promotor is silent. It can be transiently induced using interferon (IFN) α or IFN-β. Also the IFN inducer poly-inosinic:poly-cytidylic acid (pIpC or pI:pC or poly IC) which is synthetic double-stranded RNA, can be used for Mx1-Cre induction.[162] Since it is an anti-viral mechanism, it is not tissue specific. In bone marrow, liver and spleen recombination efficiency of almost 100% can be reached, in other tissues such as brain and muscles there is a maximum of 40%.

Known and potential regulators of hemoglobin

There are several established and many more potential regulators of hemoglobin expression. Several genome-wide association studies (GWAS) have been performed in order to understand the mechanisms of hemoglobin regulation and the hemoglobin switch. Some of the genes that are known to be associated with γ-globin regulation are: *MYB, KLF1, SOX6, BCL11A,* and *ZBTB7A,* Figure 5.[77,78,163-167]

KLF1

Krüppel-like factor 1 (KLF1), also known as erythroid Krüppel-like factor (eKLF), is a transcription factor involved in hemoglobin regulation.[168] The zinc-finger motif will bind to a CACCC sequence in the *HBB* gene promotor.[168] Mutations within the CACCC box of the *HBB* promoter are connected to β-thalassemia.[169] KLF1 also regulates other erythroid associated genes.[170] KLF1 knockout mice die around E13.5 due to defects in fetal liver erythropoiesis.[170,171] In human HEP cells, γ-globin is increased in a KLF1 knockdown. The expression *in vivo* increases together with the development of the erythroid cell differentiation, but when the differentiation proceeds towards the megakaryocytes *KLF1* will be downregulated.[76,172,173] Interestingly, mutations in the *KLF1* gene were found in HPFH affected members of a Maltese family, but mutations in *KLF1* are also associated with inhibition of Lutheran blood group expression (In(Lu)), and different types of anemia like neonatal (Nan) anemia in the mouse.[76,174-177] Chromatin conformation capture (3C) experiments revealed that KLF1 is required for looping between the LCR and the mouse *Hbb-b1* gene.[178]

BCL11A

B cell CLL/lymphoma 11A (BCL11A) was identified as a γ-globin repressor during GWAS studies focussed on HbF levels.[77] High BCL11A is related with low levels of γ-globin and low levels of BCL11A are linked to high levels of γ-globin.[179] It has recently been shown that BCL11A binds directly to the γ-globin promoters in adult cells. Several HPFH-inducing mutations (-114 C>T/G/A, -117 G>A) disrupt the binding of BCL11A to these sites.[182] BCL11A was originally found to be a proto-oncogene in mice and humans.[179] In BCL11A-mediated silencing of γ-globin, the transcription factor SOX6 is co-expressed and interacts physically on the LCR.[180] Interestingly, *in vivo* studies in mice revealed that when BCL11A is depleted together with heterozygosity for KLF1 an even higher γ-globin level is reached.[181]

NuRD/FOG1/GATA1/LRF

NuRD is a nucleosome remodelling histone deacetylase, and is a critical cofactor in the complex with GATA1, FOG1 and BCL11A.[183,184] Although disruption of the FOG1/NuRD interaction in transgenic mice carrying the human β-globin locus does not affect γ-globin silencing, there is a significant reduction of HbA in bone marrow.[184] So, NuRD is required for FOG-1-dependent activation of adult-type globin gene expression *in vivo*.[184]

GATA1 is a zinc finger transcription factor, which was one of the first regulators identified controlling globin expression.[185] GATA1 is named after it zinc fingers recognition site the consensus motif (T/A)GATA(A/G).[186] GATA1 is expressed in many hematopoietic cell types, from erythrocytes and its progenitors to megakaryocytes and eosinophils.[187] GATA1 knockout cells are not able to differentiate to the erythrocyte stage due to apoptosis and *Gata1* knockout mice die around E10.5.[188,189] FOG1, Friend of GATA1, is a transcription factor essential for the erythroid and

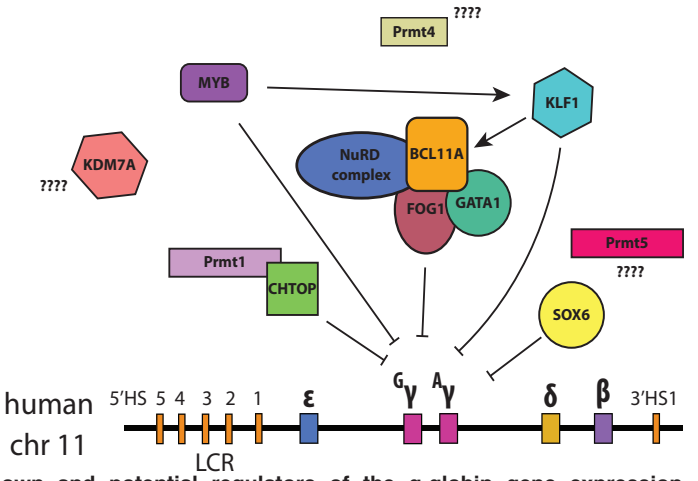

Figure 5. Known and potential regulators of the g-globin gene expression, silencing and erythropoiesis. Known regulators are MYB, KLF1, NuRD complex, SOX6, BCL11A, GATA1, FOG1, CHTOP. New candidate modifiers are PRMT1, PRMT4/CARM1, PRMT5 and KDM7A.

megakaryocyte development.[190] FOG1 dimerizes with GATA1, but is also able to dimerize with other GATA family members.[191] Depending on its partner, the transcription will be increased or decreased.
Another recently found transcription factor, that acts independently from BCL11A but works via the NuRD repressive complex, is the Leukemia/Lymphoma Related Factor (LRF). In LRF deficient erythroblasts, the fetal hemoglobin is induced.[192]

MYB

Myeloblastosis oncogene (MYB) gene is also originally found as a proto-oncogene, and act as a transcription factor in erythroid cells.[193,194] Experiments in K562 cells showed a reduction of γ-globin when MYB is overexpressed.[195] In addition, MYB shows a high expression profile in immature proliferating hematopoietic stem cells, and is down regulated during differentiation.[196,197] Different studies showed that the *MYB* gene is activating and bound by KLF1 and is involved in the FOG1/GATA1/LDB1 complex that shows interactions with the β-globin locus.[178,198,199]

CHTOP

Chromatin target of protein arginine methyltransferase 1 (CHTOP*)* was identified to play a role in HbF regulation.[167] In *in vitro* studies of cultured erythroid cells, a short hairpin mediated knockdown showed an increase of γ-globin up to 31%,.[167,200] In mice a full knockout of CHTOP is lethal due to many defects.[200] Later in this thesis the effect of different Cre-recombinases in a *Chtop* conditional knockout environment within the erythroid system are discussed.

PRMTs

Using mass spectroscopy, we identified PRMT1 and PRMT5 as CHTOP interaction partners.[167,200,201] Previous work linked PRMT1 and PRMT5 to γ-globin regulation.[65] Also PRMT1 was found to be essential for β-globin transcription activation by asymmetric dimethylation of histone 4 arginine 3 (H4R3) in mouse fetal liver cells.[202] PRMT4 (also known as CARM1), is linked to hematopoiesis via MYB-dependent transcription in hematopoietic cell lines and its depletion can result in deregulated cell

proliferation and differentiation.[203] *In vitro* experiments with PRMT5 drug inhibitors in K562 cells lead to increased γ-globin expression.[204]

The PRMT-family consists of 9 members, which are divided in 3 groups: Type I, II and III, Figure 6A.[207,208] PRMT stands for protein arginine methyltransferase. PRMTs catalyse the transfer of a methyl group from *S*-adenosyl-*L*-methionine (SAM) to the guanidino nitrogen atom of arginine molecule, Figure 6B. Type I enzymes are characterized by asymmetric ω-N^G,N^G-arginine dimethylation (ADMA), and include PRMT1, PRMT2, PRMT3, PRMT4/CARM1, PRMT6 and PRMT8.[208] Type II is characterized by symmetric ω-N^G,N^G-arginine dimethylation (sDMA), and includes *PRMT5* and *PRMT9*.[209,210] *PRMT7* is thus far the only Type III enzyme which is able to form ω-N^G-monomethyl arginine (MMA) on histones.[211] Most PRMTs methylate arginine- and glycine rich motifs, called RGG/RG motifs or GAR-domains, except for PRMT4/CARM1, which prefers proline, glycine and methionine (PGM)-rich motifs.[212]

In general, the effect of arginine methylation is the modification of interactions, due to steric effects of hydrogen bond interactions without changing the charge of the molecule.[213]

Many full knockouts of *Prmt*s in mice, for example, *Prmt1, Prmt4/Carm1* and *Prmt5* are lethal. [214-216] PRMTs are associated with many functions and roles *in vivo*: from the nerves, muscles and immune system to metabolic diseases, aging and cancer.[217,218]

In literature, we can find some *in vitro* studies linking PRMT1 and PRMT5 to globin expression. *PRMT1* induction in K562 cells promotes erythroid differentiation, and shRNA-mediated knockdown leads to suppressed erythroid differentiation.[219] PRMT1 expression enhances hemoglobin synthesis.[219] According to recent literature loss of PRMT4 does not affect erythropoiesis and hematopoiesis, but is essential for

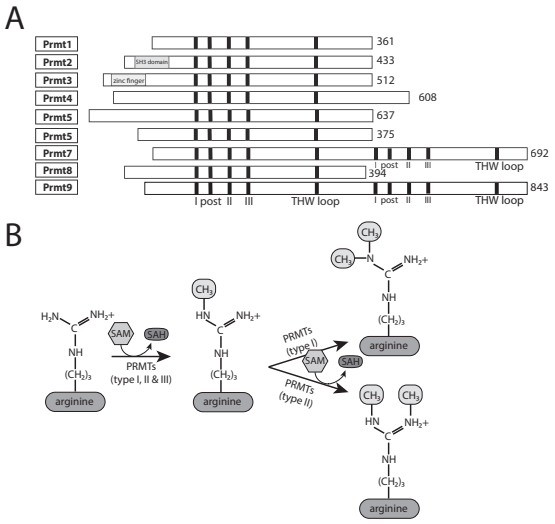

Figure 6.(A) The PRMT family consists of 9 members. They all carry one or two post I, II and II motifs and a THW loop. PRMT2 also contains a SH3 domain and PRMT3 a zinc finger. (B) Dimethyl arginine is generated by the PRMTs in two steps where a methyl group from S-adenosyl-L-methionine (SAM) is attached to the guanidino nitrogen atom of arginine molecule. Type I is arginine methylation symmetric, and Type II asymmetric. Type III only mono methylate. Figures adapted from ref 205,206.

myeloid leukomogenesis.[220]
Other K562 and human erythroid progenitor studies revealed that the PRMT5 protein binds to the γ-globin promotor, and is regulated via the nuclear zinc finger protein LYAR (Ly-1 antibody reactive clone) and DNA methyltransferase DNMT3A.[221,222] LYAR binds to the 5'untranslated region and silences γ-globin expression.[221] I*n vitro* studies using the methyl transferase inhibitor Adox led to inhibition of *PRMT5* and an increase of γ-globin expression in K562 cells.[223]
Given the multiplicity of the PRMT functions, we hope to be able to link them to γ-globin regulation and erythroid cell development *in vivo* using conditional gene inactivation approaches in mice.

KDM7A

In order to extend the list of new therapeutics, our laboratory compared gene expression profiles of high γ-globin expressing tissues (fetal liver), intermediate γ-globin expressing tissues (cord blood), and low γ-globin expressing tissues (adult peripheral blood). Genes expressed higher in peripheral blood, were assigned as potential γ-globin repressors. One of these candidate repressors is the histone lysine demethylase KDM7A. KDM7A is also known as KDM7 or JHDM1D (jumonji C domain containing histone demethylase 1 homolog D).[224]
KDM7A is a histone demethylase, and is known to demethylate H3K9me2, H3K27me2 and H4K20Me1.[225] More specifically, demethylase activity of KDM7A toward H3K9me2 is only active in absence of H3K4me3, the demethylation of H3K27me2 is not affected by H3K4me3 status. H4K20me1 demethylation is not active when restricted to the histone octamers, activity is specific for the complete nucleosomal context.[226] Dimethylation of H3K9 and H3K27 is associated with transcriptional repression.[227] It is known that is KDM7A is important during early neural differentiation via regulation of FGF4.[228] Full knockouts are viable, but show an abnormal skin morphology, especially around the hair follicles.[229]

FACS markers

In this thesis, we made use of a number of pan-hematopoietic Cre recombinase lines. To observe the effects of depletion of potential γ-globin modifier genes on the other hematopoietic lineages, we performed a "pan-hematopoietic" flow cytometry analysis.

B-cells

The development of B cells starts at the HSC, Figure 1, after going to the MPP stage it will become a CLP, Figure 7. With every step in this linage, the cells aremore committed to become a mature B cell. In this thesis, we distinguished two different types of mature B cells: the marginal zone and follicular B cell. In Figure 7 the expression of the cell surface markers used for flow cytometry, B220, CD19, CD2, IgM, IgD, CD21 and CD23, are depicted with gradients indicating expression levels.

T cells

In T cell development, hematopoietic precursor cells move first from the BM to the outer cortex of the thymus. Here the cell surface markers CD4 and CD8 distinguish mature from progenitor cells, Figure 8. T cells are first double negative (DN) for CD4 and CD8. Here we can distinguish four different progenitor stages by CD25 and CD44 expression. Subsequently the cells become double positive (DP) for CD4/

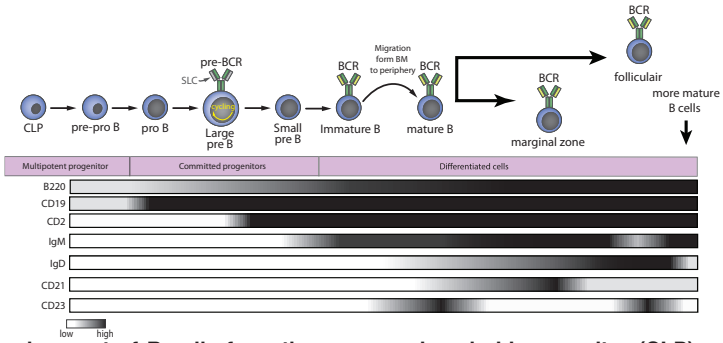

Figure 7. Development of B cells from the common lymphoid progenitor (CLP) cell via several intermediate steps to a mature B cell. We show two types of mature B cells: the marginal zone and follicular B cell. In the lower panel the expression profiles of the surface markers used for flow cytometry are presented as gradients. BCR is the B-cell receptor. Figure adapted from ref52,230-234.

CD8. Then they become single positive (SP) for either CD4 or CD8. From there they follow their own but similar final maturation, by CD3/CD44/CD62L expression different memory T cells can be distinguished: memory stem cell, central memory, follicular memory, effector memory and the resident memory. Between some stages cells can differentiate directly in both directions.

Myeloid cells

There are many different types of myeloid cells, all originated from the HSC. Via the CMP and GMP they differentiate to granulocytes, monocytes, erythrocytes and platelets. In the pan-hematopoietic flow cytometry analysis we performed a separate staining specific for the erythrocyte lineage using Ter119/KIT/CD71 (Figure 2). For the other myeloid cells, we focussed attention on mature cells: granulocytes, monocytes and macrophages, Figure 9. For the granulocytes, we distinguished eosinophils and neutrophils. The monocytes were divided into novel/resident monocytes and inflammatory monocytes. Dendritic cells were subdivided into 4 dendritic cell populations: pDCs, CD11c DCs, CD11b DCs and CD11b/CD11c DCs. For this we used the cell surface markers SiglecF/F4-80/CD11b/Ly6G/Ly6C/CD11c.

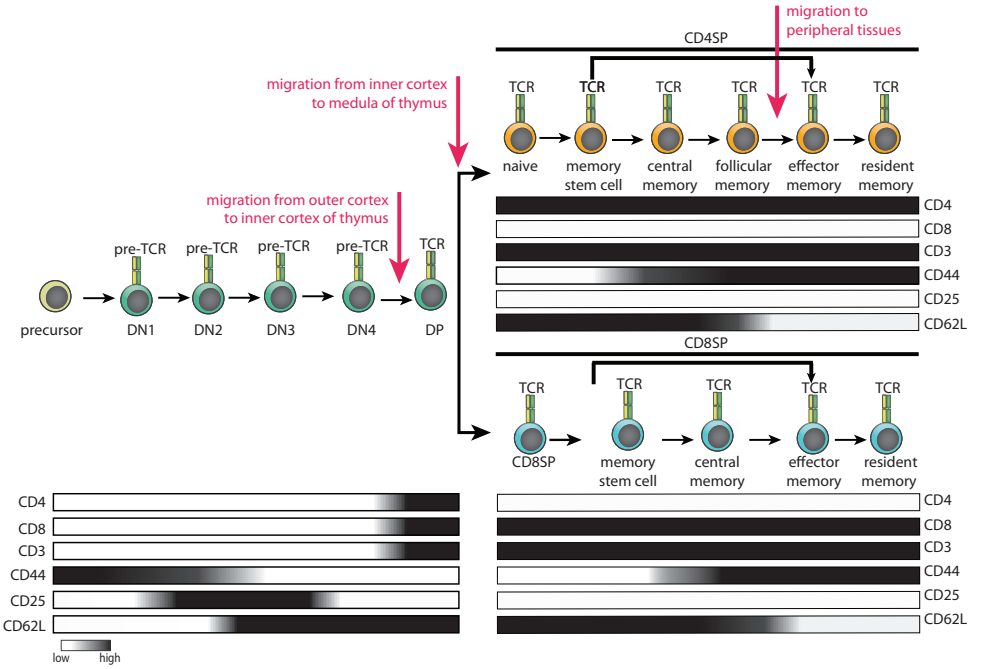

Figure 8. Simplified graphical representation of the differentiation from a committed precursor to different types of T cells. DN are double negatives for CD4/CD8. After becoming DP (double positive for CD4/CD8) the cells become SP (single positive for CD4 or CD8). CD4 SP and CD8 SP cells follow subsequently their own but similar final maturation steps. TCR is the T cell receptor. Expression of surface markers used for flow cytometry is shown in gradients. Figure is based on ref 52,234-238.

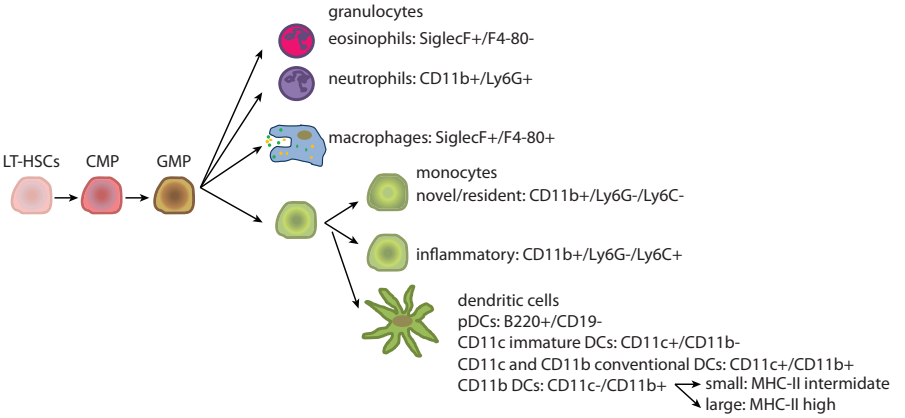

Figure 9. Schematic overview of the differentiation steps from hematopoietic stem cell (HSC) via common myeloid progenitor (CMP) and granulocyte-macrophage progenitor (GMP) to granulocytes (eosinophils and neutrophils), macrophages, novel/resident and inflammatory monocytes and four different types of dendritic cells: pDCs, CD11c+, CD11c+/CD11b+ and CD11b DCs. At every cell type the cell surface markers for flow cytometry are indicated (SiglecF/F4-80/ CD11b/Ly6G/CD11c/Ly6C/ MHC-II). Figure based on refs 239-24.

Scope of this thesis

For many years, the hematopoietic field has been a major topic of interest for many researchers. Despite this, SCD and β-thalassemia are still the most common monogenetic disorders with approximately 300,000 new patients born ever year, and no low-threshold solutions have been developed in order to ban the impact of these diseases from the world. Recent progress indicates that we are coming closer to a permanent and satisfactory solution. It is well known that increased γ-globin ameliorates the symptoms of β-hemoglobinopathy patients. Genome-wide association studies and linkage analysis have revealed transcription factors that were shown experimentally to be directly involved in hemoglobin switching. Since these transcription factors are poor targets for pharmacological intervention, the challenge is now to identify and functionally characterize the co-factors and epigenetic regulators interacting with these transcription factors.

In this thesis, I show the results of the analysis of new candidate γ-globin modifiers, and their role during hematopoiesis *in vivo*. **Chapter 1** provides a general introduction to the work described in my thesis. **Chapter 2 to 4** are experimental chapters, where we used transgenic mice carrying the human *HBB* locus, conditional knockout alleles for candidate γ-globin modifiers, and a Cre recombinase active within the hematopoietic system.

In **Chapter 2** the findings concerning the histone demethylase KDM7A are shown. We investigated the effects of KDM7A depletion within the hematopoietic system, including a pan-hematopoietic flow cytometry analysis. In **Chapter 3** I describe the effects of *Prmt1, Prmt4 and Prmt5* conditional knockouts mice within the hematopoietic system. In the case of *Prmt4* I observed, in agreement with the literature, a T cell phenotype, but there was very little effect on the other cell lineages including the erythroid lineage, and hemoglobin switching. For *Prmt1* and *Prmt5* I observed selection for non-recombined cells, indicating a crucial role for these PRMTs, but precluding further interpretation of their roles in hematopoiesis.

The topic of **Chapter 4** is CHTOP. Here I investigated its role during hematopoiesis, the importance of rigorously checking recombination efficiency, and the efficiency of several erythroid and pan-hematopoietic Cre-recombinase lines. A general discussion about all experimental chapters can be found in **Chapter 5.**

References

1 Higgins, J. M. Red blood cell population dynamics. *Clin Lab Med* **35**, 43-57, doi:10.1016/j.cll.2014.10.002 (2015).

2 Orkin, S. H. & Zon, L. I. Hematopoiesis: an evolving paradigm for stem cell biology. *Cell* **132**, 631-644, doi:10.1016/j.cell.2008.01.025 (2008).

3 Franco, R. S. Measurement of red cell lifespan and aging. *Transfus Med Hemother* **39**, 302-307, doi:10.1159/000342232 (2012).

4 Morrison, S. J. & Weissman, I. L. The long-term repopulating subset of hematopoietic stem cells is deterministic and isolatable by phenotype. *Immunity* **1**, 661-673 (1994).

5 Passegue, E., Wagers, A. J., Giuriato, S., Anderson, W. C. & Weissman, I. L. Global analysis of proliferation and cell cycle gene expression in the regulation of hematopoietic stem and progenitor cell fates. *J Exp Med* **202**, 1599-1611, doi:10.1084/jem.20050967 (2005).

6 Alberts, B. J., A.; Lewis, J.; Raff, M.;Roberts, K; Walter, P. (Garland Science, 2008).

7 Woosley, R. L. Pharmacokinetics and pharmacodynamics of antiarrhythmic agents in patients with congestive heart failure. *Am Heart J* **114**, 1280-1291 (1987).

8 Weissman, I. L. & Shizuru, J. A. The origins of the identification and isolation of hematopoietic stem cells, and their capability to induce donor-specific transplantation tolerance and treat autoimmune diseases. *Blood* **112**, 3543-3553, doi:10.1182/blood-2008-08-078220 (2008).

9 Kenneth, M., Paul, T., Mark, W. & Charles, J. Janeway's immunobiology. *New York, NY: Garland Science* (2012).

10 Cooper, M. D. The early history of B cells. *Nat Rev Immunol* **15**, 191-197, doi:10.1038/nri3801 (2015).

11 Nutt, S. L., Hodgkin, P. D., Tarlinton, D. M. & Corcoran, L. M. The generation of antibody-secreting plasma cells. *Nat Rev Immunol* **15**, 160-171, doi:10.1038/nri3795 (2015).

12 Ribourtout, B. & Zandecki, M. Plasma cell morphology in multiple myeloma and related disorders. *Morphologie* **99**, 38-62, doi:10.1016/j.morpho.2015.02.001 (2015).

13 Pillai, S., Cariappa, A. & Moran, S. T. Marginal zone B cells. *Annu Rev Immunol* **23**, 161-196, doi:10.1146/annurev.immunol.23.021704.115728 (2005).

14 Baumgarth, N. The double life of a B-1 cell: self-reactivity selects for protective effector functions. *Nat Rev Immunol* **11**, 34-46, doi:10.1038/nri2901 (2011).

15 Saito, T. & Batista, F. D. *Immunological synapse.* (Springer, 2010).

16 Lee, S. H., Miyagi, T. & Biron, C. A. Keeping NK cells in highly regulated antiviral warfare. *Trends Immunol* **28**, 252-259, doi:10.1016/j.it.2007.04.001 (2007).

17 Smyth, M. J., Hayakawa, Y., Takeda, K. & Yagita, H. New aspects of natural-killer-cell surveillance and therapy of cancer. *Nat Rev Cancer* **2**, 850-861, doi:10.1038/nrc928 (2002).

18 Bottino, C., Castriconi, R., Moretta, L. & Moretta, A. Cellular ligands of activating NK receptors. *Trends Immunol* **26**, 221-226, doi:10.1016/j.it.2005.02.007 (2005).

19 Yu, J., Freud, A. G. & Caligiuri, M. A. Location and cellular stages of natural killer cell development. *Trends Immunol* **34**, 573-582, doi:10.1016/j.it.2013.07.005 (2013).

20 Manz, M. G., Traver, D., Miyamoto, T., Weissman, I. L. & Akashi, K. Dendritic cell potentials of early lymphoid and myeloid progenitors. *Blood* **97**, 3333-3341 (2001).

21 Cooper, M. A., Fehniger, T. A., Fuchs, A., Colonna, M. & Caligiuri, M. A. NK cell and DC interactions. *Trends Immunol* **25**, 47-52 (2004).

22 Janeway, C. A., Travers, P., Walport, M. & Shlomchik, M. J. Immunobiology: the immune system in health and disease. (2005).

23 Ovchinnikov, D. A. Macrophages in the embryo and beyond: much more than just giant phagocytes. *Genesis* **46**, 447-462, doi:10.1002/dvg.20417 (2008).

24 Naito, M., Hasegawa, G. & Takahashi, K. Development, differentiation, and maturation of Kupffer cells. *Microsc Res Tech* **39**, 350-364, doi:10.1002/(SICI)1097-0029(19971115)39:4<350::AID-JEMT5>3.0.CO;2-L (1997).

25 Lambrecht, B. N. Alveolar macrophage in the driver's seat. *Immunity* **24**, 366-368 (2006).

26 Ginhoux, F., Lim, S., Hoeffel, G., Low, D. & Huber, T. Origin and differentiation of microglia. *Front Cell Neurosci* **7**, 45, doi:10.3389/fncel.2013.00045 (2013).

27 Hammer, M. *et al.* Control of dual-specificity phosphatase-1 expression in activated macrophages by IL-10. *Eur J Immunol* **35**, 2991-3001, doi:10.1002/eji.200526192 (2005).

28 De la Torre, J. & Sholar, A. Wound healing: Chronic wounds. *Emedicine. com* (2006).

29 St Pierre, B. A. & Tidball, J. G. Differential response of macrophage subpopulations to soleus muscle reloading after rat hindlimb suspension. *J Appl Physiol (1985)* **77**, 290-297, doi:10.1152/jappl.1994.77.1.290 (1994).

30 Soares, M. P. & Hamza, I. Macrophages and Iron Metabolism. *Immunity* **44**, 492-504, doi:10.1016/j.immuni.2016.02.016 (2016).

31 Breedveld, A., Groot Kormelink, T., van Egmond, M. & de Jong, E. C. Granulocytes as modulators of dendritic cell function. *J Leukoc Biol* **102**, 1003-1016, doi:10.1189/jlb.4MR0217-048RR (2017).

32 Brown, G. Basic staining: the hematoxylin and eosin technique. *An introduction to histotechnology-a manual for the student, practicing technologist, and resident-in-pathology*, 207-216 (1978).

33 Malech, H. L., Deleo, F. R. & Quinn, M. T. The role of neutrophils in the immune system: an overview. *Methods Mol Biol* **1124**, 3-10, doi:10.1007/978-1-62703-845-4_1 (2014).

34 Galli, K. M. S. in *eLS*.

35 Uhm, T. G., Kim, B. S. & Chung, I. Y. Eosinophil Development, Regulation of Eosinophil-Specific Genes, and Role of Eosinophils in the Pathogenesis of Asthma. *Allergy Asthma Immunol Res* **4**, 68-79 (2012).

36 da Silva, E. Z., Jamur, M. C. & Oliver, C. Mast cell function: a new vision of an old cell. *J Histochem Cytochem* **62**, 698-738, doi:10.1369/0022155414545334 (2014).

37 Nanninga, L. B. & Guest, M. M. Preparation and properties of anticoagulant split product of fibrinogen and its determination in plasma. *Thromb Diath Haemorrh* **17**, 440-451 (1967).

38 Laki, K. Our ancient heritage in blood clotting and some of its consequences. *Ann N Y Acad Sci* **202**, 297-307 (1972).

39 Machlus, K. R., Thon, J. N. & Italiano, J. E., Jr. Interpreting the developmental dance of the megakaryocyte: a review of the cellular and molecular processes mediating platelet formation. *Br J Haematol* **165**, 227-236, doi:10.1111/bjh.12758 (2014).

40 Yip, J., Shen, Y., Berndt, M. C. & Andrews, R. K. Primary platelet adhesion receptors. *IUBMB Life* **57**, 103-108, doi:10.1080/15216540500078962 (2005).

41 Pronk, C. J. *et al.* Elucidation of the phenotypic, functional, and molecular topography of a myeloerythroid progenitor cell hierarchy. *Cell Stem Cell* **1**, 428-442, doi:10.1016/j.stem.2007.07.005 (2007).

42 Wong, P. M., Chung, S. W., Chui, D. H. & Eaves, C. J. Properties of the earliest clonogenic hemopoietic precursors to appear in the developing murine yolk sac. *Proc Natl Acad Sci U S A* **83**, 3851-3854 (1986).

43 Dzierzak, E. & Philipsen, S. Erythropoiesis: development and differentiation. *Cold Spring Harb Perspect Med* **3**, a011601, doi:10.1101/cshperspect.a011601 (2013).

44 Chasis, J. A. & Mohandas, N. Erythroblastic islands: niches for erythropoiesis. *Blood* **112**, 470-478, doi:10.1182/blood-2008-03-077883 (2008).

45 Palis, J. Primitive and definitive erythropoiesis in mammals. *Front Physiol* **5**, 3, doi:10.3389/fphys.2014.00003 (2014).

46 Keerthivasan, G., Wickrema, A. & Crispino, J. D. Erythroblast enucleation. *Stem Cells Int* **2011**, 139851, doi:10.4061/2011/139851 (2011).

47 Hoffman, J. F. Biconcave shape of human red-blood-cell ghosts relies on density differences between the rim and dimple of the ghost's plasma membrane. *Proc Natl Acad Sci U S A* **113**, 14847-14851, doi:10.1073/pnas.1615452113 (2016).

48 Allen, T. D. & Dexter, T. M. Ultrastructural aspects of erythropoietic differentiation in long-term bone marrow culture. *Differentiation* **21**, 86-94 (1982).

49 Waugh, R. E., Mantalaris, A., Bauserman, R. G., Hwang, W. C. & Wu, J. H. Membrane instability in late-stage erythropoiesis. *Blood* **97**, 1869-1875 (2001).

50 Griffiths, R. E. *et al.* The ins and outs of human reticulocyte maturation: autophagy and the endosome/exosome pathway. *Autophagy* **8**, 1150-1151, doi:10.4161/auto.20648 (2012).

51 Diez-Silva, M., Dao, M., Han, J., Lim, C. T. & Suresh, S. Shape and Biomechanical Characteristics of Human Red Blood Cells in Health and Disease. *MRS Bull* **35**, 382-388 (2010).

52 Stadhouders, R. *Transcription Factors, Chromatin Loops & Blood Cells*, Erasmus University Rotterdam, (2014).

53 Schechter, A. N. Hemoglobin research and the origins of molecular medicine. *Blood* **112**, 3927-3938, doi:10.1182/blood-2008-04-078188 (2008).

54 Weatherall, D. & Clegg, J. (Blackwell Scientific, Oxford UK, 2001).

55 Higgs, D. *et al.* Understanding α-Globin Gene Regulation: Aiming to Improve the Management of Thalassemia. *Annals of the New York Academy of Sciences* **1054**, 92-102 (2005).

56 Kioussis, D., Vanin, E., deLange, T., Flavell, R. A. & Grosveld, F. G. Beta-globin gene inactivation by DNA translocation in gamma beta-thalassaemia. *Nature* **306**, 662-666 (1983).

57 Cantù, I. *KLF1 in Erythroid Differentiation*, Erasmus University Rotterdam, (2015).

58 Strouboulis, J., Dillon, N. & Grosveld, F. Developmental regulation of a complete 70-kb human beta-globin locus in transgenic mice. *Genes Dev* **6**, 1857-1864 (1992).

59 Urbinati, F., Madigan, C. & Malik, P. Pathophysiology and therapy for haemoglobinopathies. Part II: thalassaemias. *Expert Rev Mol Med* **8**, 1-26, doi:10.1017/S1462399406010805 (2006).

60 Noguchi, C. T., Rodgers, G. P. & Schechter, A. N. Intracellular polymerization of sickle hemoglobin: disease severity and therapeutic goals. *Prog Clin Biol Res* **240**, 381-391 (1987).

61 Cunningham, M. J. & Nathan, D. G. New developments in iron chelators. *Curr Opin Hematol* **12**, 129-134 (2005).

62 Weatherall, D. J. & Clegg, J. B. Inherited haemoglobin disorders: an increasing global health problem. *Bull World Health Organ* **79**, 704-712 (2001).

63 Williams, T. N. & Weatherall, D. J. World distribution, population genetics, and health burden of the hemoglobinopathies. *Cold Spring Harb Perspect Med* **2**, a011692, doi:10.1101/cshperspect.a011692 (2012).

64 Weatherall, D. & Clegg, J. Distribution and population genetics of the thalassaemias. *The Thalassaemia Syndromes, Fourth Edition*, 237-284 (2001).

65 Mikropoulou, M. *An shRNA Screen for the Discovery of Suppressors of Fetal Hemoglobin*, Erasmus University Rotterdam, (2016).

66 Cunningham, M. J. & Nathan, D. G. New developments in iron chelators. *Current opinion in hematology* **12**, 129-134 (2005).

67 Jha, R. & Jha, S. *Beta thalassemia - a review*. Vol. 4 (2014).

68 Aydinok, Y., Kattamis, A. & Viprakasit, V. Current approach to iron chelation in children. *Br J Haematol* **165**, 745-755, doi:10.1111/bjh.12825 (2014).

69 Martin, A. & Thompson, A. A. Thalassemias. *Pediatr Clin North Am* **60**, 1383-1391, doi:10.1016/j.pcl.2013.08.008 (2013).
70 Harteveld, C. L. & Higgs, D. R. Alpha-thalassaemia. *Orphanet J Rare Dis* **5**, 13, doi:10.1186/1750-1172-5-13 (2010).
71 Pauling, L., Itano, H. A. & et al. Sickle cell anemia, a molecular disease. *Science* **109**, 443 (1949).
72 Ingram, V. M. A specific chemical difference between the globins of normal human and sickle-cell anaemia haemoglobin. *Nature* **178**, 792-794 (1956).
73 Kumar, V., Abbas, A. K., Fausto, N. & Aster, J. C. *Robbins and Cotran pathologic basis of disease, professional edition e-book*. (elsevier health sciences, 2014).
74 Steinberg, M. H. Sickle cell anemia, the first molecular disease: overview of molecular etiology, pathophysiology, and therapeutic approaches. *ScientificWorldJournal* **8**, 1295-1324, doi:10.1100/tsw.2008.157 (2008).
75 Madigan, C. & Malik, P. Pathophysiology and therapy for haemoglobinopathies. Part I: sickle cell disease. *Expert Rev Mol Med* **8**, 1-23, doi:10.1017/S1462399406010659 (2006).
76 Borg, J. *et al.* Haploinsufficiency for the erythroid transcription factor KLF1 causes hereditary persistence of fetal hemoglobin. *Nat Genet* **42**, 801-805, doi:10.1038/ng.630 (2010).
77 Uda, M. *et al.* Genome-wide association study shows BCL11A associated with persistent fetal hemoglobin and amelioration of the phenotype of beta-thalassemia. *Proc Natl Acad Sci U S A* **105**, 1620-1625, doi:10.1073/pnas.0711566105 (2008).
78 Lettre, G. *et al.* DNA polymorphisms at the BCL11A, HBS1L-MYB, and beta-globin loci associate with fetal hemoglobin levels and pain crises in sickle cell disease. *Proc Natl Acad Sci U S A* **105**, 11869-11874, doi:10.1073/pnas.0804799105 (2008).
79 Chang, Y. C., Smith, K. D., Moore, R. D., Serjeant, G. R. & Dover, G. J. An analysis of fetal hemoglobin variation in sickle cell disease: the relative contributions of the X-linked factor, beta-globin haplotypes, alpha-globin gene number, gender, and age. *Blood* **85**, 1111-1117 (1995).
80 Chang, Y. P. *et al.* The relative importance of the X-linked FCP locus and beta-globin haplotypes in determining haemoglobin F levels: a study of SS patients homozygous for beta S haplotypes. *Br J Haematol* **96**, 806-814 (1997).
81 Garner, C. P., Tatu, T., Best, S., Creary, L. & Thein, S. L. Evidence of genetic interaction between the beta-globin complex and chromosome 8q in the expression of fetal hemoglobin. *Am J Hum Genet* **70**, 793-799, doi:10.1086/339248 (2002).
82 Labie, D. *et al.* Common haplotype dependency of high G gamma-globin gene expression and high Hb F levels in beta-thalassemia and sickle cell anemia patients. *Proc Natl Acad Sci U S A* **82**, 2111-2114 (1985).
83 Sankaran, V. G. Targeted Therapeutic Strategies for Fetal Hemoglobin Induction. *ASH Education Program Book* **2011**, 459-465, doi:10.1182/asheducation-2011.1.459 (2011).
84 Platt, O. S. Hydroxyurea for the treatment of sickle cell anemia. *N Engl J Med* **358**, 1362-1369, doi:10.1056/NEJMct0708272 (2008).
85 Lanzkron, S. *et al.* Systematic review: Hydroxyurea for the treatment of adults with sickle cell disease. *Ann Intern Med* **148**, 939-955 (2008).
86 Silva, D. G. *et al.* Genetic and biochemical markers of hydroxyurea therapeutic response in sickle cell anemia. *BMC Med Genet* **14**, 108, doi:10.1186/1471-2350-14-108 (2013).
87 Agrawal, R. K., Patel, R. K., Shah, V., Nainiwal, L. & Trivedi, B. Hydroxyurea in sickle cell disease: drug review. *Indian J Hematol Blood Transfus* **30**, 91-96, doi:10.1007/s12288-013-0261-4 (2014).
88 Lucarelli, G., Isgro, A., Sodani, P. & Gaziev, J. Hematopoietic stem cell transplantation in thalassemia and sickle cell anemia. *Cold Spring Harb Perspect Med* **2**, a011825, doi:10.1101/cshperspect.a011825 (2012).
89 Thompson, A. A. *et al.* Gene Therapy in Patients with Transfusion-Dependent beta-Thalassemia. *N Engl J Med* **378**, 1479-1493, doi:10.1056/NEJMoa1705342 (2018).
90 Arumugam, P. & Malik, P. Genetic therapy for beta-thalassemia: from the bench to the bedside. *Hematology Am Soc Hematol Educ Program* **2010**, 445-450, doi:10.1182/asheducation-2010.1.445 (2010).
91 Malik, P. & Arumugam, P. I. Gene Therapy for beta-thalassemia. *Hematology Am Soc Hematol Educ Program*, 45-50, doi:10.1182/asheducation-2005.1.45 (2005).
92 Dever, D. P. *et al.* CRISPR/Cas9 beta-globin gene targeting in human haematopoietic stem cells. *Nature* **539**, 384-389, doi:10.1038/nature20134 (2016).
93 Lee, C. *et al.* Gene Editing with Crispr-Cas9 for Treating Beta-Hemoglobinopathies. *Blood* **126**, 3376-3376 (2015).
94 Ran, F. A. *et al.* Genome engineering using the CRISPR-Cas9 system. *Nature protocols* **8**, 2281-2308, doi:10.1038/nprot.2013.143 (2013).
95 Sanjana, N. E., Shalem, O. & Zhang, F. Improved vectors and genome-wide libraries for CRISPR screening. *Nat Methods* **11**, 783-784, doi:10.1038/nmeth.3047 (2014).
96 Ikuta, T., Kan, Y. W., Swerdlow, P. S., Faller, D. V. & Perrine, S. P. Alterations in protein-DNA interactions in the gamma-globin gene promoter in response to butyrate therapy. *Blood* **92**, 2924-2933 (1998).
97 Glauber, J. G., Wandersee, N. J., Little, J. A. & Ginder, G. D. 5'-flanking sequences mediate butyrate stimulation of embryonic globin gene expression in adult erythroid cells. *Mol Cell Biol* **11**, 4690-4697 (1991).
98 Dover, G. J., Charache, S. H., Boyer, S. H., Talbot, C. C., Jr. & Smith, K. D. 5-Azacytidine increases fetal hemoglobin production in a patient with sickle cell disease. *Prog Clin Biol Res* **134**, 475-488 (1983).
99 Ley, T. J. *et al.* 5-azacytidine selectively increases gamma-globin synthesis in a patient with beta+ thalassemia. *N Engl J Med* **307**, 1469-1475, doi:10.1056/NEJM198212093072401 (1982).
100 Kutlar, A. *et al.* A dose-escalation phase IIa study of 2,2-dimethylbutyrate (HQK-1001), an oral fetal globin

inducer, in sickle cell disease. *Am J Hematol* **88**, E255-260, doi:10.1002/ajh.23533 (2013).
101 Patthamalai, P. *et al.* A phase 2 trial of HQK-1001 in HbE-beta thalassemia demonstrates HbF induction and reduced anemia. *Blood* **123**, 1956-1957, doi:10.1182/blood-2013-11-538470 (2014).
102 Reid, M. E. *et al.* A double-blind, placebo-controlled phase II study of the efficacy and safety of 2,2-dimethylbutyrate (HQK-1001), an oral fetal globin inducer, in sickle cell disease. *Am J Hematol* **89**, 709-713, doi:10.1002/ajh.23725 (2014).
103 Molokie, R. *et al.* Oral tetrahydrouridine and decitabine for non-cytotoxic epigenetic gene regulation in sickle cell disease: A randomized phase 1 study. *PLoS Med* **14**, e1002382, doi:10.1371/journal.pmed.1002382 (2017).
104 Dolznig, H. *et al.* Establishment of normal, terminally differentiating mouse erythroid progenitors: molecular characterization by cDNA arrays. *FASEB J* **15**, 1442-1444 (2001).
105 Kooren, J. *et al.* β-*Globin Active Chromatin Hub Formation in Differentiating Erythroid Cells and in p45 NF-E2 Knock-out Mice*. Vol. 282 (2007).
106 Grosveld, G. *et al.* The chronic myelocytic cell line K562 contains a breakpoint in bcr and produces a chimeric bcr/c-abl transcript. *Mol Cell Biol* **6**, 607-616 (1986).
107 Bianchi, N. *et al.* Induction of erythroid differentiation of human K562 cells by cisplatin analogs. *Biochem Pharmacol* **60**, 31-40 (2000).
108 Rutherford, T. R., Clegg, J. B. & Weatherall, D. J. K562 human leukaemic cells synthesise embryonic haemoglobin in response to haemin. *Nature* **280**, 164-165 (1979).
109 Bianchi Scarra, G. L. *et al.* Terminal erythroid differentiation in the K-562 cell line by 1-beta-D-arabinofuranosylcytosine: accompaniment by c-myc messenger RNA decrease. *Cancer Res* **46**, 6327-6332 (1986).
110 Gambari, R. *et al.* Human leukemia K-562 cells: induction of erythroid differentiation by 5-azacytidine. *Cell Differ* **14**, 87-97 (1984).
111 Gambari, R. *et al.* Human leukemic K562 cells: suppression of hemoglobin accumulation by a monoclonal antibody to human transferrin receptor. *Biochim Biophys Acta* **886**, 203-213 (1986).
112 Bianchi, N. *et al.* The DNA-binding drugs mithramycin and chromomycin are powerful inducers of erythroid differentiation of human K562 cells. *Br J Haematol* **104**, 258-265 (1999).
113 Kurita, R. *et al.* Establishment of immortalized human erythroid progenitor cell lines able to produce enucleated red blood cells. *PLoS One* **8**, e59890, doi:10.1371/journal.pone.0059890 (2013).
114 Panzenbock, B., Bartunek, P., Mapara, M. Y. & Zenke, M. Growth and differentiation of human stem cell factor/erythropoietin-dependent erythroid progenitor cells in vitro. *Blood* **92**, 3658-3668 (1998).
115 van den Akker, E., Satchwell, T. J., Pellegrin, S., Daniels, G. & Toye, A. M. The majority of the in vitro erythroid expansion potential resides in CD34(-) cells, outweighing the contribution of CD34(+) cells and significantly increasing the erythroblast yield from peripheral blood samples. *Haematologica* **95**, 1594-1598, doi:10.3324/haematol.2009.019828 (2010).
116 Carradice, D. & Lieschke, G. J. Zebrafish in hematology: sushi or science? *Blood* **111**, 3331-3342, doi:10.1182/blood-2007-10-052761 (2008).
117 Kimmel, C. B., Warga, R. M. & Schilling, T. F. Origin and organization of the zebrafish fate map. *Development* **108**, 581-594 (1990).
118 Kulkeaw, K. & Sugiyama, D. Zebrafish erythropoiesis and the utility of fish as models of anemia. *Stem Cell Res Ther* **3**, 55, doi:10.1186/scrt146 (2012).
119 Paffett-Lugassy, N. *et al.* Functional conservation of erythropoietin signaling in zebrafish. *Blood* **110**, 2718-2726, doi:10.1182/blood-2006-04-016535 (2007).
120 Martinho, F. Blood transfusion in birds. *Revista Lusófona de Ciência e Medicina Veterinária* **5** (2012).
121 Beug, H., von Kirchbach, A., Doderlein, G., Conscience, J. F. & Graf, T. Chicken hematopoietic cells transformed by seven strains of defective avian leukemia viruses display three distinct phenotypes of differentiation. *Cell* **18**, 375-390 (1979).
122 Chicken, D. M. C. D. M. 286 Properties of Blood of Domestic Fowl. *The Journal of Biological Chemistry* **110**, 285.
123 Jane, S. M., Nienhuis, A. W. & Cunningham, J. M. Hemoglobin switching in man and chicken is mediated by a heteromeric complex between the ubiquitous transcription factor CP2 and a developmentally specific protein. *The EMBO journal* **14**, 97-105 (1995).
124 Groudine, M., Peretz, M. & Weintraub, H. Transcriptional regulation of hemoglobin switching in chicken embryos. *Molecular and Cellular Biology* **1**, 281-288 (1981).
125 Choi, O. R. & Engel, J. D. Developmental regulation of beta-globin gene switching. *Cell* **55**, 17-26 (1988).
126 Hashimoto, K. & Wilt, F. H. The heterogeneity of chicken hemoglobin. *Proceedings of the National Academy of Sciences* **56**, 1477-1483, doi:10.1073/pnas.56.5.1477 (1966).
127 Jane, S. M., Nienhuis, A. W. & Cunningham, J. M. Hemoglobin switching in man and chicken is mediated by a heteromeric complex between the ubiquitous transcription factor CP2 and a developmentally specific protein. *EMBO J* **14**, 97-105 (1995).
128 Chen, D. & Kaul, D. K. Rheologic and hemodynamic characteristics of red cells of mouse, rat and human. *Biorheology* **31**, 103-113 (1994).
129 Subramanian, S., Tsai, R. & Discher, D. E. The 'metabolon,' CD47, and the 'phagocytic synapse': molecular co-localization and species divergence. *Transfus Clin Biol* **13**, 31-38, doi:10.1016/j.tracli.2006.02.009 (2006).
130 Delpire, E. & Mount, D. B. Human and murine phenotypes associated with defects in cation-chloride cotransport. *Annu Rev Physiol* **64**, 803-843, doi:10.1146/annurev.physiol.64.081501.155847 (2002).
131 Makley, A. T. *et al.* Murine blood banking: characterization and comparisons to human blood. *Shock* **34**, 40-

45, doi:10.1097/SHK.0b013e3181d494fd (2010).
132 Pishesha, N. *et al.* Transcriptional divergence and conservation of human and mouse erythropoiesis. *Proc Natl Acad Sci U S A* **111**, 4103-4108, doi:10.1073/pnas.1401598111 (2014).
133 An, X., Schulz, V. P., Mohandas, N. & Gallagher, P. G. Human and murine erythropoiesis. *Curr Opin Hematol* **22**, 206-211, doi:10.1097/MOH.0000000000000134 (2015).
134 Hardison, R. C. Evolution of hemoglobin and its genes. *Cold Spring Harb Perspect Med* **2**, a011627, doi:10.1101/cshperspect.a011627 (2012).
135 Teitell, M. A. & Mikkola, H. K. Transcriptional activators, repressors, and epigenetic modifiers controlling hematopoietic stem cell development. *Pediatr Res* **59**, 33R-39R, doi:10.1203/01.pdr.0000205155.26315.c7 (2006).
136 Sykes, S. M. & Scadden, D. T. Modeling human hematopoietic stem cell biology in the mouse. *Semin Hematol* **50**, 92-100, doi:10.1053/j.seminhematol.2013.03.029 (2013).
137 Semenza, G. L. & Wang, G. L. A nuclear factor induced by hypoxia via de novo protein synthesis binds to the human erythropoietin gene enhancer at a site required for transcriptional activation. *Mol Cell Biol* **12**, 5447-5454 (1992).
138 Abremski, K. & Hoess, R. Bacteriophage P1 site-specific recombination. Purification and properties of the Cre recombinase protein. *J Biol Chem* **259**, 1509-1514 (1984).
139 Ikeda, H. & Tomizawa, J. Prophage P1, and extrachromosomal replication unit. *Cold Spring Harb Symp Quant Biol* **33**, 791-798 (1968).
140 Grindley, N. D., Whiteson, K. L. & Rice, P. A. Mechanisms of site-specific recombination. *Annu Rev Biochem* **75**, 567-605, doi:10.1146/annurev.biochem.73.011303.073908 (2006).
141 Van Duyne, G. D. Cre Recombinase. *Microbiology Spectrum* **3**, doi:doi:10.1128/microbiolspec.MDNA3-0014-2014 (2015).
142 Mack, A., Sauer, B., Abremski, K. & Hoess, R. Stoichiometry of the Cre recombinase bound to the lox recombining site. *Nucleic Acids Res* **20**, 4451-4455 (1992).
143 Ringrose, L. *et al.* Comparative kinetic analysis of FLP and cre recombinases: mathematical models for DNA binding and recombination. *J Mol Biol* **284**, 363-384, doi:10.1006/jmbi.1998.2149 (1998).
144 Ghosh, K., Guo, F. & Van Duyne, G. D. Synapsis of loxP sites by Cre recombinase. *J Biol Chem* **282**, 24004-24016, doi:10.1074/jbc.M703283200 (2007).
145 Hamilton, D. L. & Abremski, K. Site-specific recombination by the bacteriophage P1 lox-Cre system. Cre-mediated synapsis of two lox sites. *J Mol Biol* **178**, 481-486 (1984).
146 Blake, J. A. *et al.* The Mouse Genome Database (MGD): premier model organism resource for mammalian genomics and genetics. *Nucleic Acids Res* **39**, D842-848, doi:10.1093/nar/gkq1008 (2011).
147 Eppig, J. T. *et al.* The Mouse Genome Database (MGD): comprehensive resource for genetics and genomics of the laboratory mouse. *Nucleic Acids Res* **40**, D881-886, doi:10.1093/nar/gkr974 (2012).
148 Smedley, D., Salimova, E. & Rosenthal, N. Cre recombinase resources for conditional mouse mutagenesis. *Methods* **53**, 411-416, doi:10.1016/j.ymeth.2010.12.027 (2011).
149 Murray, S. A., Eppig, J. T., Smedley, D., Simpson, E. M. & Rosenthal, N. Beyond knockouts: cre resources for conditional mutagenesis. *Mamm Genome* **23**, 587-599, doi:10.1007/s00335-012-9430-2 (2012).
150 Indra, A. K. *et al.* Temporally-controlled site-specific mutagenesis in the basal layer of the epidermis: comparison of the recombinase activity of the tamoxifen-inducible Cre-ER(T) and Cre-ER(T2) recombinases. *Nucleic Acids Res* **27**, 4324-4327 (1999).
151 Yakar, S. *et al.* Normal growth and development in the absence of hepatic insulin-like growth factor I. *Proc Natl Acad Sci U S A* **96**, 7324-7329 (1999).
152 Wang, Q., Strong, J. & Killeen, N. Homeostatic competition among T cells revealed by conditional inactivation of the mouse Cd4 gene. *J Exp Med* **194**, 1721-1730 (2001).
153 Holtwick, R. *et al.* Smooth muscle-selective deletion of guanylyl cyclase-A prevents the acute but not chronic effects of ANP on blood pressure. *Proc Natl Acad Sci U S A* **99**, 7142-7147, doi:10.1073/pnas.102650499 (2002).
154 Heinrich, A. C., Pelanda, R. & Klingmuller, U. A mouse model for visualization and conditional mutations in the erythroid lineage. *Blood* **104**, 659-666, doi:10.1182/blood-2003-05-1442 (2004).
155 Stadtfeld, M. & Graf, T. Assessing the role of hematopoietic plasticity for endothelial and hepatocyte development by non-invasive lineage tracing. *Development* **132**, 203-213, doi:10.1242/dev.01558 (2005).
156 Katzav, S. Vav1: an oncogene that regulates specific transcriptional activation of T cells. *Blood* **103**, 2443-2451, doi:10.1182/blood-2003-08-2834 (2004).
157 Hebeis, B., Vigorito, E., Kovesdi, D. & Turner, M. Vav proteins are required for B-lymphocyte responses to LPS. *Blood* **106**, 635-640, doi:10.1182/blood-2004-10-3919 (2005).
158 Turner, M. & Billadeau, D. D. VAV proteins as signal integrators for multi-subunit immune-recognition receptors. *Nat Rev Immunol* **2**, 476-486, doi:10.1038/nri840 (2002).
159 Chen, M. J., Yokomizo, T., Zeigler, B. M., Dzierzak, E. & Speck, N. A. Runx1 is required for the endothelial to haematopoietic cell transition but not thereafter. *Nature* **457**, 887-891, doi:10.1038/nature07619 (2009).
160 Lampugnani, M. G. *et al.* The molecular organization of endothelial cell to cell junctions: differential association of plakoglobin, beta-catenin, and alpha-catenin with vascular endothelial cadherin (VE-cadherin). *J Cell Biol* **129**, 203-217 (1995).
161 Chen, W. The late stage of T cell development within mouse thymus. *Cell Mol Immunol* **1**, 3-11 (2004).
162 Kuhn, R., Schwenk, F., Aguet, M. & Rajewsky, K. Inducible gene targeting in mice. *Science* **269**, 1427-1429, doi:10.1126/science.7660125 (1995).

163 Thein, S. L., Menzel, S., Lathrop, M. & Garner, C. Control of fetal hemoglobin: new insights emerging from genomics and clinical implications. *Hum Mol Genet* **18**, R216-223, doi:10.1093/hmg/ddp401 (2009).

164 Wahlberg, K. *et al.* The HBS1L-MYB intergenic interval associated with elevated HbF levels shows characteristics of a distal regulatory region in erythroid cells. *Blood* **114**, 1254-1262, doi:10.1182/blood-2009-03-210146 (2009).

165 Wienert, B. *et al.* KLF1 drives the expression of fetal hemoglobin in British HPFH. *Blood* **130**, 803-807, doi:10.1182/blood-2017-02-767400 (2017).

166 Karkashon, S. *et al.* Intermediaries of branched chain amino acid metabolism induce fetal hemoglobin, and repress SOX6 and BCL11A, in definitive erythroid cells. *Blood Cells Mol Dis* **55**, 161-167, doi:10.1016/j.bcmd.2015.05.006 (2015).

167 van Dijk, T. B. *et al.* Fetal globin expression is regulated by Friend of Prmt1. *Blood* **116**, 4349-4352, doi:10.1182/blood-2010-03-274399 (2010).

168 Perkins, A. C., Sharpe, A. H. & Orkin, S. H. Lethal beta-thalassaemia in mice lacking the erythroid CAC-CC-transcription factor EKLF. *Nature* **375**, 318-322, doi:10.1038/375318a0 (1995).

169 Feng, W. C., Southwood, C. M. & Bieker, J. J. Analyses of beta-thalassemia mutant DNA interactions with erythroid Kruppel-like factor (EKLF), an erythroid cell-specific transcription factor. *J Biol Chem* **269**, 1493-1500 (1994).

170 Perkins, A. C., Peterson, K. R., Stamatoyannopoulos, G., Witkowska, H. E. & Orkin, S. H. Fetal expression of a human Agamma globin transgene rescues globin chain imbalance but not hemolysis in EKLF null mouse embryos. *Blood* **95**, 1827-1833 (2000).

171 Nuez, B., Michalovich, D., Bygrave, A., Ploemacher, R. & Grosveld, F. Defective haematopoiesis in fetal liver resulting from inactivation of the EKLF gene. *Nature* **375**, 316-318, doi:10.1038/375316a0 (1995).

172 Miller, I. J. & Bieker, J. J. A novel, erythroid cell-specific murine transcription factor that binds to the CACCC element and is related to the Kruppel family of nuclear proteins. *Mol Cell Biol* **13**, 2776-2786 (1993).

173 Frontelo, P. *et al.* Novel role for EKLF in megakaryocyte lineage commitment. *Blood* **110**, 3871-3880, doi:10.1182/blood-2007-03-082065 (2007).

174 White, R. A. *et al.* Hematologic characterization and chromosomal localization of the novel dominantly inherited mouse hemolytic anemia, neonatal anemia (Nan). *Blood Cells Mol Dis* **43**, 141-148, doi:10.1016/j.bcmd.2009.03.009 (2009).

175 Siatecka, M. *et al.* Severe anemia in the Nan mutant mouse caused by sequence-selective disruption of erythroid Kruppel-like factor. *Proc Natl Acad Sci U S A* **107**, 15151-15156, doi:10.1073/pnas.1004996107 (2010).

176 Arnaud, L. *et al.* A dominant mutation in the gene encoding the erythroid transcription factor KLF1 causes a congenital dyserythropoietic anemia. *Am J Hum Genet* **87**, 721-727, doi:10.1016/j.ajhg.2010.10.010 (2010).

177 Singleton, B. K., Burton, N. M., Green, C., Brady, R. L. & Anstee, D. J. Mutations in EKLF/KLF1 form the molecular basis of the rare blood group In(Lu) phenotype. *Blood* **112**, 2081-2088, doi:10.1182/blood-2008-03-145672 (2008).

178 Drissen, R. *et al.* The active spatial organization of the beta-globin locus requires the transcription factor EKLF. *Genes Dev* **18**, 2485-2490, doi:10.1101/gad.317004 (2004).

179 Sankaran, V. G. *et al.* Human fetal hemoglobin expression is regulated by the developmental stage-specific repressor BCL11A. *Science* **322**, 1839-1842, doi:10.1126/science.1165409 (2008).

180 Xu, J. *et al.* Transcriptional silencing of {gamma}-globin by BCL11A involves long-range interactions and cooperation with SOX6. *Genes Dev* **24**, 783-798, doi:10.1101/gad.1897310 (2010).

181 Esteghamat, F. *et al.* Erythropoiesis and globin switching in compound Klf1::Bcl11a mutant mice. *Blood* **121**, 2553-2562, doi:10.1182/blood-2012-06-434530 (2013).

182 Psatha, N. *et al.* Disruption of the BCL11A Erythroid Enhancer Reactivates Fetal Hemoglobin in Erythroid Cells of Patients with beta-Thalassemia Major. *Mol Ther Methods Clin Dev* **10**, 313-326, doi:10.1016/j.omtm.2018.08.003 (2018).

183 Miccio, A. *et al.* NuRD mediates activating and repressive functions of GATA-1 and FOG-1 during blood development. *EMBO J* **29**, 442-456, doi:10.1038/emboj.2009.336 (2010).

184 Miccio, A. & Blobel, G. A. Role of the GATA-1/FOG-1/NuRD pathway in the expression of human beta-like globin genes. *Mol Cell Biol* **30**, 3460-3470, doi:10.1128/MCB.00001-10 (2010).

185 Evans, T. & Felsenfeld, G. The erythroid-specific transcription factor Eryf1: a new finger protein. *Cell* **58**, 877-885 (1989).

186 Ko, L. J. & Engel, J. D. DNA-binding specificities of the GATA transcription factor family. *Mol Cell Biol* **13**, 4011-4022 (1993).

187 Gutiérrez Gutiérrez, L. *Studies on Gata1: Cell Cycle, Survival and Differentiation*, (2005).

188 Fujiwara, Y., Browne, C. P., Cunniff, K., Goff, S. C. & Orkin, S. H. Arrested development of embryonic red cell precursors in mouse embryos lacking transcription factor GATA-1. *Proc Natl Acad Sci U S A* **93**, 12355-12358 (1996).

189 Pevny, L. *et al.* Development of hematopoietic cells lacking transcription factor GATA-1. *Development* **121**, 163-172 (1995).

190 Vannucchi, A. M. *et al.* Abnormalities of GATA-1 in megakaryocytes from patients with idiopathic myelofibrosis. *Am J Pathol* **167**, 849-858, doi:10.1016/S0002-9440(10)62056-1 (2005).

191 Cantor, A. B. *et al.* Antagonism of FOG-1 and GATA factors in fate choice for the mast cell lineage. *J Exp Med* **205**, 611-624, doi:10.1084/jem.20070544 (2008).

192 Masuda, T. *et al.* The LRF/ZBTB7A Transcription Factor Is a BCL11A-Independent Repressor of Fetal Hemo-

globin. *Blood* **126**, 2-2 (2015).
193 Mucenski, M. L. *et al.* A functional c-myb gene is required for normal murine fetal hepatic hematopoiesis. *Cell* **65**, 677-689 (1991).
194 Lipsick, J. S. & Baluda, M. A. The myb oncogene. *Gene Amplif Anal* **4**, 73-98 (1986).
195 Jiang, J. *et al.* cMYB is involved in the regulation of fetal hemoglobin production in adults. *Blood* **108**, 1077-1083, doi:10.1182/blood-2006-01-008912 (2006).
196 Gonda, T. J. & Metcalf, D. Expression of myb, myc and fos proto-oncogenes during the differentiation of a murine myeloid leukaemia. *Nature* **310**, 249-251 (1984).
197 Emambokus, N. *et al.* Progression through key stages of haemopoiesis is dependent on distinct threshold levels of c-Myb. *EMBO J* **22**, 4478-4488, doi:10.1093/emboj/cdg434 (2003).
198 Stadhouders, R. *et al.* Dynamic long-range chromatin interactions control Myb proto-oncogene transcription during erythroid development. *EMBO J* **31**, 986-999, doi:10.1038/emboj.2011.450 (2012).
199 Cantor, A. B. & Orkin, S. H. Hematopoietic development: a balancing act. *Curr Opin Genet Dev* **11**, 513-519 (2001).
200 van Dijk, T. B. *et al.* Friend of Prmt1, a novel chromatin target of protein arginine methyltransferases. *Mol Cell Biol* **30**, 260-272, doi:10.1128/MCB.00645-09 (2010).
201 Fanis, P. *et al.* Five friends of methylated chromatin target of protein-arginine-methyltransferase[prmt]-1 (chtop), a complex linking arginine methylation to desumoylation. *Mol Cell Proteomics* **11**, 1263-1273, doi:10.1074/mcp.M112.017194 (2012).
202 Li, X. *et al.* H4R3 methylation facilitates β-globin transcription by regulating histone acetyltransferase binding and H3 acetylation. *Blood* **115**, 2028-2037, doi:10.1182/blood-2009-07-236059 (2010).
203 Streubel, G. *et al.* PRMT4 is a novel coactivator of c-Myb-dependent transcription in haematopoietic cell lines. *PLoS Genet* **9**, e1003343, doi:10.1371/journal.pgen.1003343 (2013).
204 Cannon, M. *et al.* Targeting The PRMT5 Enzyme To Induce γ-Globin Gene Derepression In Sickle Cell Anemia. *Blood* **122**, 1007-1007 (2013).
205 Molina-Serrano, D., Schiza, V. & Kirmizis, A. Cross-talk among epigenetic modifications: lessons from histone arginine methylation. *Biochemical Society Transactions* **41**, 751-759, doi:10.1042/bst20130003 (2013).
206 Bedford, M. T. & Richard, S. Arginine Methylation: An Emerging Regulatorof Protein Function. *Molecular Cell* **18**, 263-272, doi:https://doi.org/10.1016/j.molcel.2005.04.003 (2005).
207 Gray, K. A., Yates, B., Seal, R. L., Wright, M. W. & Bruford, E. A. Genenames.org: the HGNC resources in 2015. *Nucleic Acids Res* **43**, D1079-1085, doi:10.1093/nar/gku1071 (2015).
208 Gary, J. D. & Clarke, S. RNA and protein interactions modulated by protein arginine methylation. *Prog Nucleic Acid Res Mol Biol* **61**, 65-131 (1998).
209 Yang, Y. *et al.* PRMT9 is a type II methyltransferase that methylates the splicing factor SAP145. *Nat Commun* **6**, 6428, doi:10.1038/ncomms7428 (2015).
210 Huang, J., Vogel, G., Yu, Z., Almazan, G. & Richard, S. Type II arginine methyltransferase PRMT5 regulates gene expression of inhibitors of differentiation/DNA binding Id2 and Id4 during glial cell differentiation. *J Biol Chem* **286**, 44424-44432, doi:10.1074/jbc.M111.277046 (2011).
211 Zurita-Lopez, C. I., Sandberg, T., Kelly, R. & Clarke, S. G. Human protein arginine methyltransferase 7 (PRMT7) is a type III enzyme forming omega-NG-monomethylated arginine residues. *J Biol Chem* **287**, 7859-7870, doi:10.1074/jbc.M111.336271 (2012).
212 Cheng, D., Côté, J., Shaaban, S. & Bedford, M. T. The Arginine Methyltransferase CARM1 Regulates the Coupling of Transcription and mRNA Processing. *Molecular Cell* **25**, 71-83, doi:10.1016/j.molcel.2006.11.019.
213 Fuhrmann, J., Clancy, K. W. & Thompson, P. R. Chemical biology of protein arginine modifications in epigenetic regulation. *Chem Rev* **115**, 5413-5461, doi:10.1021/acs.chemrev.5b00003 (2015).
214 Yadav, N. *et al.* Specific protein methylation defects and gene expression perturbations in coactivator-associated arginine methyltransferase 1-deficient mice. *Proceedings of the National Academy of Sciences* **100**, 6464-6468 (2003).
215 Pawlak, M. R., Scherer, C. A., Chen, J., Roshon, M. J. & Ruley, H. E. Arginine N-methyltransferase 1 is required for early postimplantation mouse development, but cells deficient in the enzyme are viable. *Molecular and cellular biology* **20**, 4859-4869 (2000).
216 Tee, W.-W. *et al.* Prmt5 is essential for early mouse development and acts in the cytoplasm to maintain ES cell pluripotency. *Genes & development* **24**, 2772-2777 (2010).
217 Bedford, M. T. & Clarke, S. G. Protein Arginine Methylation in Mammals: Who, What, and Why. *Molecular Cell* **33**, 1-13, doi:10.1016/j.molcel.2008.12.013 (2009).
218 Blanc, R. S. & Richard, S. Arginine Methylation: The Coming of Age. *Mol Cell* **65**, 8-24, doi:10.1016/j.molcel.2016.11.003 (2017).
219 Hua, W. K. *et al.* Protein arginine methyltransferase 1 interacts with and activates p38alpha to facilitate erythroid differentiation. *PLoS One* **8**, e56715, doi:10.1371/journal.pone.0056715 (2013).
220 Greenblatt, S. M. *et al.* CARM1 Is Essential for Myeloid Leukemogenesis but Dispensable for Normal Hematopoiesis. *Cancer Cell* **33**, 1111-1127 e1115, doi:10.1016/j.ccell.2018.05.007 (2018).
221 Ju, J. *et al.* Human fetal globin gene expression is regulated by LYAR. *Nucleic Acids Res* **42**, 9740-9752, doi:10.1093/nar/gku718 (2014).
222 Rank, G. *et al.* Identification of a PRMT5-dependent repressor complex linked to silencing of human fetal globin gene expression. *Blood* **116**, 1585-1592, doi:10.1182/blood-2009-10-251116 (2010).
223 He, Y. *et al.* Induction of human fetal hemoglobin expression by adenosine-2',3'-dialdehyde. *J Transl Med* **11**, 14, doi:10.1186/1479-5876-11-14 (2013).

224 Nawrocki, M. J. *et al.* JHDM1D and HDAC1-3 mRNA expression levels in peripheral blood mononuclear cells of patients with systemic lupus erythematosus. *Z Rheumatol* **74**, 902-910, doi:10.1007/s00393-015-1619-9 (2015).

225 Tsukada, Y.-i., Ishitani, T. & Nakayama, K. I. KDM7 is a dual demethylase for histone H3 Lys 9 and Lys 27 and functions in brain development. *Genes & Development* **24**, 432-437, doi:10.1101/gad.1864410 (2010).

226 Qi, H. H. *et al.* Histone H4K20/H3K9 demethylase PHF8 regulates zebrafish brain and craniofacial development. *Nature* **466**, 503-507, doi:http://www.nature.com/nature/journal/v466/n7305/abs/nature09261.html#supplementary-information (2010).

227 Horton, J. R. *et al.* Enzymatic and structural insights for substrate specificity of a family of jumonji histone lysine demethylases. *Nat Struct Mol Biol* **17**, 38-43, doi:http://www.nature.com/nsmb/journal/v17/n1/suppinfo/nsmb.1753_S1.html (2010).

228 Huang, C. *et al.* Dual-specificity histone demethylase KIAA1718 (KDM7A) regulates neural differentiation through FGF4. *Cell research* **20**, 154-165, doi:10.1038/cr.2010.5 (2010).

229 Liakath-Ali, K. *et al.* Novel skin phenotypes revealed by a genome-wide mouse reverse genetic screen. *Nat Commun* **5**, 3540, doi:10.1038/ncomms4540 (2014).

230 Baker, D., Marta, M., Pryce, G., Giovannoni, G. & Schmierer, K. Memory B Cells are Major Targets for Effective Immunotherapy in Relapsing Multiple Sclerosis. *EBioMedicine* **16**, 41-50, doi:10.1016/j.ebiom.2017.01.042 (2017).

231 Allman, D. & Pillai, S. Peripheral B cell subsets. *Curr Opin Immunol* **20**, 149-157, doi:10.1016/j.coi.2008.03.014 (2008).

232 Shapiro-Shelef, M. & Calame, K. Regulation of plasma-cell development. *Nat Rev Immunol* **5**, 230-242, doi:10.1038/nri1572 (2005).

233 Lund, F. E. Cytokine-producing B lymphocytes-key regulators of immunity. *Curr Opin Immunol* **20**, 332-338, doi:10.1016/j.coi.2008.03.003 (2008).

234 Mauri, C. & Bosma, A. Immune regulatory function of B cells. *Annu Rev Immunol* **30**, 221-241, doi:10.1146/annurev-immunol-020711-074934 (2012).

235 Yu, X.-Z. & Anasetti, C. Memory stem cells sustain disease. *Nature Medicine* **11**, 1282, doi:10.1038/nm1205-1282 (2005).

236 Zhang, Q. & Lakkis, F. G. Memory T Cell Migration. *Frontiers in Immunology* **6**, doi:10.3389/fimmu.2015.00504 (2015).

237 Caramalho, Í., Nunes-Cabaço, H., Foxall, R. B. & Sousa, A. E. Regulatory T-Cell Development in the Human Thymus. *Frontiers in Immunology* **6**, doi:10.3389/fimmu.2015.00395 (2015).

238 Zuniga-Pflucker, J. C. T-cell development made simple. *Nat Rev Immunol* **4**, 67-72, doi:10.1038/nri1257 (2004).

239 Hey, Y.-Y., Tan, J. K. H. & O'Neill, H. C. Redefining Myeloid Cell Subsets in Murine Spleen. *Frontiers in Immunology* **6**, doi:10.3389/fimmu.2015.00652 (2016).

240 Salomon, B. t., Cohen, J. L., Masurier, C. & Klatzmann, D. Three Populations of Mouse Lymph Node Dendritic Cells with Different Origins and Dynamics. *The Journal of Immunology* **160**, 708-717 (1998).

241 Murdoch, C., Muthana, M., Coffelt, S. B. & Lewis, C. E. The role of myeloid cells in the promotion of tumour angiogenesis. *Nature Reviews Cancer* **8**, 618, doi:10.1038/nrc2444 (2008).

Chapter 2

Hematopoietic conditional knockout of mouse Kdm7a.

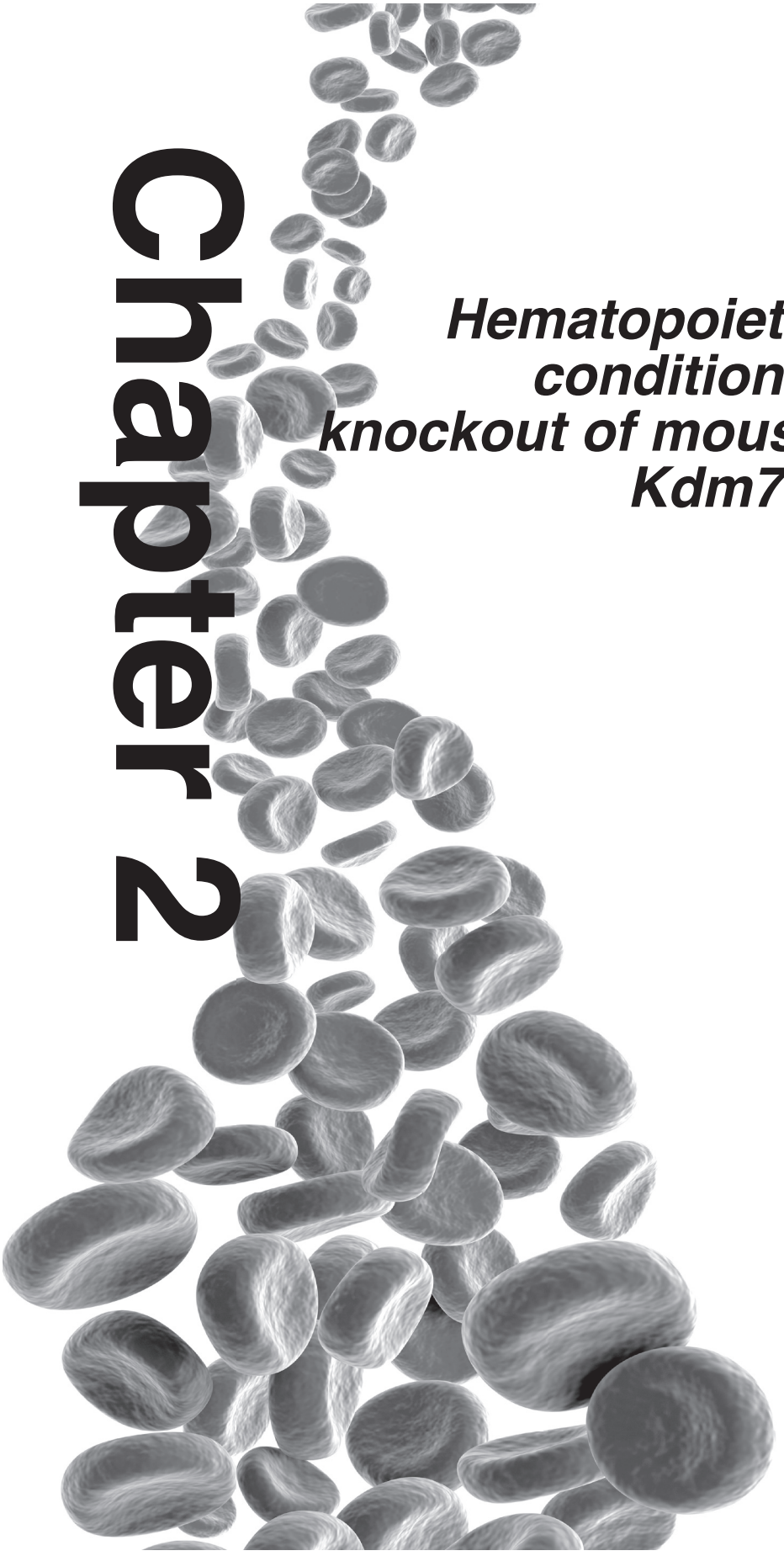

Chapter 2 Hematopoietic conditional knockout of the mouse *Kdm7a* gene.

Silvia Astrid Hoeboer[1], Nynke Gillemans[1], Ryo Kurita[2], Yukio Nakamura[2], Marjolein de Bruijn[3], Rudi Hendriks[3], Anne Korporaal[1], Thamar Bryn van Dijk[1] and Sjaak Philipsen[1]

[1] Department of Cell Biology, Erasmus MC, Rotterdam, The Netherlands
[2] Cell Engineering Division, RIKEN, BioResource Center, Tsukuba, Ibaraki, Japan
[3] Department of Pulmonary Medicine, Erasmus MC, Rotterdam, The Netherlands.

Manuscript in preparation

Abstract

Sickle cell disease and β-thalassemia are very common disorders caused by mutations affecting the HBB gene, encoding β-globin. Reactivation of the *HBG1/2* genes, encoding the fetal β-like Aγ and Gγ globins, would ameliorate the symptoms of these patients. Since the current treatment options for the large majority of patients are very limited, we would like to extend the list of therapeutic targets aimed at reactivation of the *HBG1/2* genes. We previously identified the histone demethylase KDM7A as a potential repressor of fetal hemoglobin expression. Here we show results of different conditional knockouts of the Kdm7a gene in a mouse model which also carries the human HBB locus. Erythroid-specific recombination by *EpoR*-Cre was efficient but did not affect erythropoiesis. Since recombination by *EpoR*-Cre occurs late during erythroid differentiation, we extended the observations to pan-hematopoietic deletion by *Mx1*-Cre. Induction of Cre expression by pIpC injection resulted in highly efficient recombination at the *Kdm7a* locus. Although we observed minor changes in some hematopoietic cell populations, these changes did not influence the balance in the complete hematopoietic system. We conclude that KDM7A is dispensable for hematopoiesis and does not have a role in repressing the HBG1/2 genes in adult erythropoiesis.

Introduction

The most common monogenetic disorders in the human population are sickle cell disease (SCD) and β-thalassemia. It is estimated that every year ~300,000 children are born with these diseases.[1] There is a high frequency of β-hemoglobinopathies in the Mediterranean, South-East Asia and sub-Saharan Africa. Because of migration, the diseases are widely spread around the world. Originally, the high frequency of SCD correlated with the prevalence of the malaria parasite *Plasmodium falciparum*. SCD is caused by a missense mutation, *HBB*:c.20A>T, in codon 6 of the *HBB* gene. This changes glutamic acid to valine, i.e. from a charged to a hydrophobic residue. As a consequence, hemoglobin under low oxygen conditions the globins aggregate and the circular biconcave shape of the erythrocytes changes to the sickle shape characteristic for the disease. β-thalassemia is caused by insufficient levels of β-globin, due to mutations in the β-globin gene or its regulatory elements. The symptoms of SCD and β-thalassemia can be ameliorated by high levels of γ-globin, a β-like globin protein that is normally expressed during fetal stages of development. After birth, when erythropoiesis shifts to the bone marrow (BM), γ-globin is silenced and β-globin is activated.[2] For this reason SCD and β-thalassemia patients start displaying disease symptoms during the first year of life. Fetal haemoglobin (HbF; α2γ2) can substitute for adult hemoglobin (HbA; α2β2). Currently, HbF is elevated in a subset of SCD patients using hydroxyurea.[3,4] The mechanism behind the increase of γ-globin due to hydroxyurea is incompletely understood. Novel therapeutic strategies are necessary for better curative and specific results not limited to a subset of patients.

The benign condition hereditary persistence of fetal hemoglobin (HPFH) leads to high levels of HbF in adulthood.[5] Deletions in the *HBB* locus or mutations in the *HBG1/2* promoters can cause HPFH.[6,7] For example, a mutation from G to A at -117 of the *HBG1* promoter leads to an HPFH phenotype. HPFH in combination with a β-hemoglobinopathy ameliorates disease severity, due to the increased HbF levels. Population studies have led to the identification of three loci, *HBB*, *HSB1L-MYB* and *BCL11A*, important for repression of the *HBG1/2* genes in adults. [8-11] Other transcription factors known to play a role in developmental regulation of erythropoiesis include CHD4, CHTOP, GATA1, LRF, LSD1, KLF1, SOX6 and TR2/TR4.[12,13]

In order to extend this list with new druggable therapeutic targets, we compared high γ-globin expressing cells (fetal liver), intermediate γ-globin expressing cells (cord blood), and low γ-globin expressing cells (adult peripheral blood). Genes expressed higher in peripheral blood were assigned as potential γ-globin repressors. One of these candidate repressors is Lysine demethylase 7A (KDM7A), also known as KDM7 or JHDM1D.14 KDM7A is a histone demethylase, and is known to demethylate H3K9me2, H3K27me2 and H4K20me1.[15] More specifically, demethylase activity of KDM7A towards H3K9me2 is only active in absence of H3K4me3, while demethylation of H3K27me2 is not affected by H3K4me3. H4K20me1 demethylation by KDM7A only occurs in the context of the complete nucleosome.[16] Dimethylation of H3K9 and H3K27 is associated with transcriptional repression.[17] It is known that KDM7A is important during early neural differentiation via regulation of FGF4 expression.[18]

The aim of this study was to characterise the potential role of KDM7A in erythropoiesis and developmental regulation of globin expression *in vivo* and *in vitro*. To achieve this aim, we used mice carrying conditional knockout alleles of *Kdm7a* and a single-copy

transgene of the complete human *HBB* locus (PAC8.1). These mice were crossed with *Cre* lines to inactivate the *Kdm7a* gene in a tissue-specific manner.

Material and Methods

Mice

All animal studies were approved by the Erasmus MC Animal Ethics Committee. In this study, transgenic mouse strains were used: human *HBB* locus PAC8.1[19]; *Kdm7a* floxed alleles (Eucomm)[20,21] (Supplementary Figure 1). We used two lines with Cre recombinase active in the hematopoietic system: the Epo Receptor locus (*EpoR*-Cre)[22] and the interferon inducible *Mx1-Cre* transgene[23]. Genotyping was performed by PCR using genomic DNA isolated from toe biopsies. Primers are listed in Supplementary Table 1. Embryos were collected between embryonic day (E) 11.5 and E16.5; genotyping was performed by PCR on head DNA. Adults were analysed with a maximum age of 21 weeks. To detect Cre-mediated recombination of the *Kdm7a* locus, Southern blot analysis was done on erythroid tissues using probes listed in Supplementary Table 1. To induce *Mx1-Cre* mediated recombination, mice were injected subcutaneously (SC) 20mg/g bodyweight polyinosinic-polycytidylic ribonucleic acid (pIpC; P0913, Sigma Aldrich). Mice were collected after 1-2 weeks or they were subsequently treated with phenylhydrazine (PHZ P6926; Sigma Aldrich) to induce stress erythropoiesis. The mice were injected SC with 0.4% (w/v) PHZ in phosphate buffered saline (PBS) (12µl/g body weight) for 2 consecutive days (Day 1 and 2). Mice were collected at Day 5 for analysis.

Blood analysis

Peripheral blood was collected from the mandibular vein of adult mice >10 weeks. Standard blood parameters were measured using an automated hematologic analyser (Scil Vet ABC). We also performed flow cytometry on the blood. Leftovers were stored in TRI-reagent (93289, Sigma Aldrich) at 20°C for RNA isolation.

Flow cytometry analysis

Single cell suspensions from blood, bone marrow, spleen and thymus were made by flushing and crushing the material and passing through cell strainers (40 µm, 352340, BD Bioscience). The cells were diluted and washed in PBS containing 1mM EDTA. Before staining, the cells were washed in FACS buffer (PBS, 1% (w/v) bovine serum albumin (BSA) and 1 mM EDTA). ~10^6 cells were incubated for 30 minutes with the primary antibodies. Antibodies used are listed in Supplementary Table 2. Depending on the antibody combination, cells were washed in FACS buffer or PBS. Live cells were distinguished negatively by 7-aminoactinomycin D (7-AAD; A1310; Invitrogen) staining and were directly analysed. Alternatively, the cells were stained for 30 minutes using the Fixable Viability Dye eFluor 506 (eBioscience) and washed in PBS. Cells were measured on a Fortessa flow cytometer (BD Bioscience).

MACS selection of CD71+ BM cells

To check recombination in erythroid cells, we selected for CD71 using the FITC labelled antibody annotated in Supplementary Table 2. We used MACS separation columns (Miltenyi Biotec), or FACS tubes and the EasySep kit (#18555; Stem Cell Technologies), and a magnet (18000; Stem Cell Technologies), according to the manufacturer's instructions.

Southern blot analysis

Genomic DNA (20 μg) was digested with 20 units EcoRI at 37°C overnight. The fragments were separated on a 0.7% agarose gel, and subsequently transferred to a nylon membrane. Primers to generate the probe are listed in Supplementary Table 1. The probe of 416 bp was labelled with α^{32}P-dATP (PerkinElmer) using a nick translation kit (GE Healthcare) according to the manufacturer's recommendations. After hybridisation and washing the blot was exposed to a phosphor screen which was scanned using a Typhoon FLA9500 instrument (GE Healthcare). The floxed allele will be visualised at 3.8 kb and the recombined allele at 3.0 kb.

Cell culture

Human Umbilical cord blood-Derived Erythroid Progenitor (HUDEP-2) cells were cultured in StemSpan medium (Stem Cell Technologies), supplemented with doxycycline (DOX, 1 μg/ml), stem cell factor (SCF, 100 ng/ml, R&D Systems), erythropoietin (EPO, 2 units/ml, Janssen-Cilag), and dexamethasone (1 μM, Sigma) as described previously.[24] To induce differentiation we used StemSpan medium supplemented with 500 μg/mL iron-saturated transferrin (Scipac) and EPO (10 units/ml). For cell counting we used a CASY TTC instrument (Omni Life Science).

Lentiviral production, transduction and testing

For knockout experiments of KDM7A in HUDEP-2 cells we transduced the cells first with lentiCas9-Blast (Addgene plasmid # 52962).[25] The lentiviral particles were produced in Human Embryonic Kidney (HEK) 293T cells as described previously.[26] Supernatant from the HEK-293T cells was collected on Day 1, 2 and 3 after transfection. On the third day, the combined supernatant was filtered using a 0.45μm filter. The virus particles were collected using centrifugation of 20,000 rpm for 2:15 hours at 4°C. The HUDEP-2 cells were exposed to the lentivirus for 78-92 hours. Blasticidine 10 μg/mL (Life Technologies) was added for the selection of transduced cells. After selection, we performed a second transduction with a vector containing the guide RNA (gRNA). This vector was made from the pSpCas9(BB)-2A-Puro (PX459) V2.0 plasmid (Addgene plasmid # 62988).[27] The gRNAs were designed with the online CRISPR design tool of the Zhang lab at MIT (http://crispr.mit.edu/). As a threshold, we only used guides with a score higher than 85. Furthermore, we blasted the guide targets for predicted off target effects. The gRNA oligonucleotides (Integrated DNA Technologies) are listed in Supplementary Table 1. We transferred the U6 promoter-gRNA part to a lentivirus producing vector; pLKO.1 puro (Addgene plasmid # 8453).[28] After transduction, we added puromycin (1 μg/mL; Sigma) for 24 hours.

To check the effect of CRISPR we designed a PCR around the gRNA target region. Using Platinum Taq polymerase (Invitrogen) according to the manufacturer's instructions, we amplified a product of ~828 base pairs (bp). Subsequently, we used the Surveyor Mutation Detection kit (Integrated DNA Technologies) to detect heteroduplexes indicative of CRISPR-induced mutations.

Protein extraction and western blotting

Whole cell lysates of blood, BM, spleen and HUDEP-2 cells were prepared using RIPA buffer (20 mM Tris pH7.5, 150 mM NaCl, 1% NP40, 0.1% SDS, 0.5 mM EDTA, and 0.5% sodium deoxycholate) supplemented with complete protease inhibitor mix (Roche) and Pefablock (Roche).[53] The samples were lysed on ice for 15 minutes

before centrifugation for 15 minutes at 10,000 rpm at 4°C. Supernatant was collected and mixed with 4x Sample Buffer (0.05M Tris pH6.8, 8% SDS, 40% glycerol, few grains Bromophenol Blue, 5% β-mercapto-ethanol). To visualize γ-globin expression at the protein level, whole cell lysates were loaded on 10% or 12.5% SDS-PAGE, the gels were transferred to nitrocellulose membranes and probed with antibodies listed in Supplementary Table 2.

mRNA extraction and qRT-PCR

mRNA extraction was performed using TRI Reagent (Sigma-Aldrich) according to the manufactur's recommendation. RNA was precipitated using addition of 0.1 volume of 3M NaAc pH 4.8 and addition of 3 volumes of 100% ethanol, treated with DNase I (Invitrogen), and subsequently transcribed to cDNA using Super Script Reverse Transcriptase IV (Invitrogen) in the presence of the RNAseOut RNAse inhibitor (Invitrogen) and Oligo(dT)$_{12\text{-}18}$ (for qRT-PCRs on globins), or a random primer mix (for Kdm7a qRT-PCRs). The qRT-PCRs were performed on cDNA using primers described in Supplementary Table 1 and Platinum Taq Polymerase (Invitrogen). The amplification was monitored using SYBR Green (Sigma Aldrich).

Results

In previous studies from our laboratory we identified a number of potential γ-globin repressors including *Kdm7a* that encodes a histone demethylase.[29] This gene is also known as *Jhdm1d*, *KIAA1718* and *Kdm7*. To study its role in the erythroid system and during hemoglobin switching, we crossed mice with the Eucomm conditional knockout allele of the *Kdm7a* gene (Supplementary Figure 1) with mice carrying a single-copy *HBB* locus transgene, PAC8.1, and Cre recombinase located in the Epo Receptor locus (*EpoR*-Cre) (Supplementary Figure 2). We started with the analysis of blood taken from the mandibular vein on the Vet ABC Counter (Figure 1 A). There were no significant changes observed between *PAC8*.1/wt; *Kdm7a* fl/fl and *PAC8*.1/wt; *Kdm7a* fl/fl; *EpoR*-Cre/wt animals. Although the white blood cells (WBC) appeared to be decreased, this was not a significant difference (p=0.38) due to high variability between the animals. We decided to analyse these animals in more detail. We weighed the animals and their spleens, but there was no significant difference between the two groups (Figure 1 B). We prepared single cell suspensions of spleen and bone marrow and performed flow cytometry analysis. To check recombination of the floxed alleles, we performed Southern blotting. In Supplementary Figure 1 the location of the probe is described and the primers used to generate the probe are listed in Supplementary Table 1.

The recombination efficiency in CD71+ MACS selected BM cells is almost 100% (Figure 1C). Indeed, RT-qPCR analysis showed an almost complete loss of *Kdm7a* mRNA (Figure 1D).

Subsequently, we tested γ-globin expression levels in BM samples using qRT-PCR; we did not observe any changes after *EpoR*-Cre mediated knock-out (Figure 1E). Although the Kdm7a mRNA levels are reduced, it is possible that there is still protein present. Unfortunately, good antibodies to check KDM7a protein levels by western blotting are currently not available.

We also performed flow cytometry on bone marrow and spleen cells. Differentiation of erythroid progenitors proceeds from CD71-/Ter119-; CD71+/Ter119+; CD71 intermediate (im.)/Ter119+ and finally CD71-/Ter119+. Although the flow cytometry

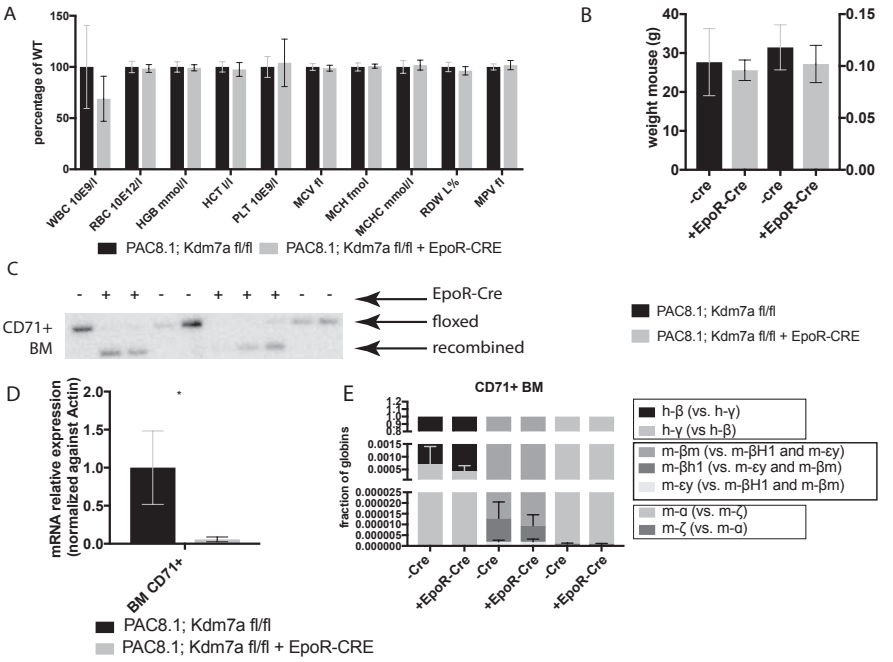

Figure 1. In the PA*C*8.1/wt; *Kdm7a* fl/fl; *EpoR*-Cre/wt mice there are no significant differences between the mice with and without Cre. (N=5 for each condition.) (A) Measured blood parameters: WBC (white blood cells); RBC (red blood cells); HGB (hemoglobin); HCT (hematocrit); PLT (platelets); MCV (Mean Corpuscular Volume); MCH (Mean Corpusc ular Hemoglobin); MCHC (Mean Corpuscular Hemoglobin Concentration); RDW (RBC distribution width); MPV (mean platelet volume). B) The mice were weighed (left panel), after sacrifice also the spleen weight was determined (right panel). (C) Southern blot of CD71+ MACS-selected bone marrow (BM) cells. (D) qRT-PCR for *Kdm7a* normalized using *Actin*; WT levels are set to 1. (E) Expression of human g-globin in BM, ratio of g/(g+b), x/(bH1+bm+ey) and z/(z+a) control vs. with *EpoR*-Cre determined by qRT-PCR in *PAC8*.1; *Kdm7a* fl/fl mice with and without EpoR-Cre.

plots suggest there might be some differences in the CD71+/Ter119+ populations in BM and spleen of the EpoR-Cre/Kdm7a knockout animals (Figure 2A), quantification shows that these differences do not reach statistical significance, due to variation between individual animals (Figure 2B).

As a last test to observe differences between the *EpoR*-Cre mediated knockout adult mice and their control littermates, we induced acute anemia by administering phenylhydrazine (PHZ) to the animals.

We measured the blood parameters before and after PHZ treatment. Before treatment, we observed similar values as in the experiments of Figure 1 and 2. After PHZ treatment, we observed a slight reduction in white blood cell counts in the animals with *EpoR*-Cre, but this did not reach statistical significance (Figure 3A and B). The red blood cell (RBC) counts and hemoglobin (HGB) levels were lower (P-value 0.03), so were significantly different in the *EpoR*-Cre/Kdm7a knockout mice after PHZ treatment. The hematocrit and platelet levels displayed a higher variability and were not significantly different between the two groups. It is possible that the animals with *EpoR*-Cre recover slower from PHZ treatment than the animals

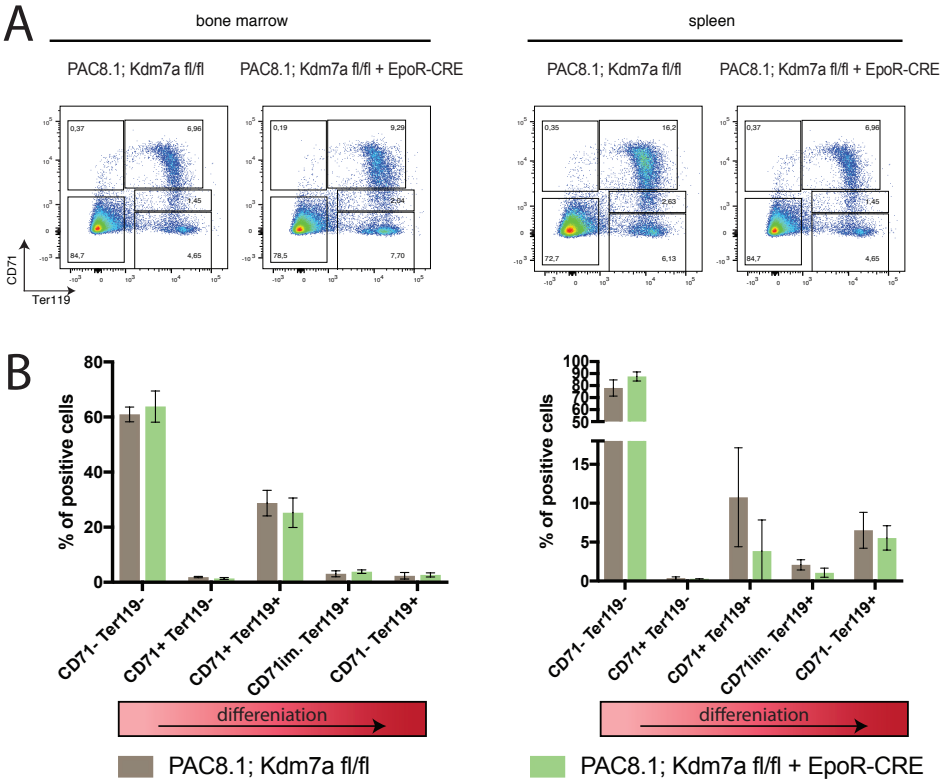

Figure 2. Flow cytometry of *PAC8*.1; *Kdm7a* fl/fl; *EpoR*-Cre. (N=5 for each condition). (A) Examples of flow cytometry profiles of CD71/Ter119 staining of bone marrow and spleen. (B) Quantification of different CD71+ and – Ter119 + and - populations progenitor cells (left panel) and on the right more differentiated erythrocytes (right panel).

without *EpoR*-Cre. Of note, the raw values (not shown) illustrate the effect of PHZ on many blood parameters. For instance, significant changes (p-value > 0.05) were detected for the WBC, MCH and MCHC parameters which were increased in contrast to the RBC, HCT and MCV parameters which were decreased due to PHZ treatment. Furthermore, we measured the weight of the animals before and after PHZ treatment, as well as spleen weight (Figure 3C). This revealed that induction of stress erythropoiesis does not affect the weight of the animals. Moreover, spleen weights were similar between the two groups indicating that the *EpoR*-Cre mice could mount a normal stress response. Figure 3D shows the plots of the erythrocytes from the Vet ABC counter these show that there is a new population of larger RBCs present in the blood after PHZ treatment. These are reticulocytes which are maturing into erythrocytes. The increased number of reticulocytes indicates that the animals have activated stress erythropoiesis in response to the PHZ treatment. However, there was no significant difference between the *EpoR*-Cre mice and control animals. Using qRT-PCR we observed a decrease in expression of the *Kdm7a* gene (Figure 3E), but this was not significant. Expression of the globin genes was not affected (Figure 3F and G).

Using flow cytometry with the erythroid markers CD71/Ter119, we did not observe any significant differences between the cell populations in blood, bone marrow and

spleen (Figure 4). Thus, while we observed slightly decreased numbers of RBCs in *EpoR-Cre* animals after PHZ treatment, the balance within erythropoiesis was not disturbed due to the absence of
Kdm7a gene in erythroid cells. To study the role of erythropoiesis during embryonic development, we tested cord blood (CB) and fetal liver (FL) cells at E11.5 until E16.5 of gestation. Using flow cytometry, we tested the different erythroid cell populations (Figure 5). In CB, we measured that most of the cells are as expected mature erythrocytes, but the balance between progenitor stages changed over time. There were no significant differences between the *PAC8*.1; *Kdm7a* fl/fl mice and *PAC8*.1; *Kdm7a* fl/fl; *EpoR*-Cre mice.
In the FL we observed as expected more progenitor cells and fewer mature erythrocytes. Over time, this balance is changed in favour of more mature progenitor cells.

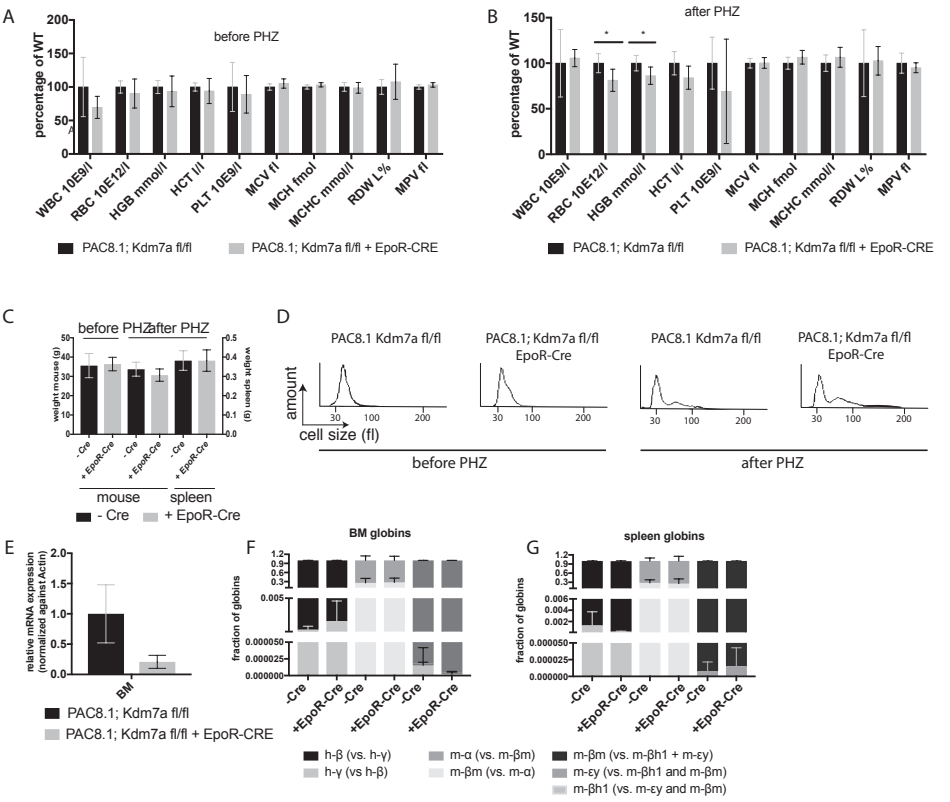

Figure 3. *PAC8*.1/wt; *Kdm7a* fl/fl; *EpoR*-Cre/wt mice were treated with PHZ (Supplementary Figure 3C) to activate the stress erythropoiesis. (N=5 for each condition) * indicates a p-value <0.05. (A) Measured blood parameters before PHZ treatment WBC (white blood cells); RBC (red blood cells); HGB (hemoglobin); HCT (hematocrit); PLT (platelets); MCV (Mean Corpuscular Volume); MCH (Mean Corpuscular Hemoglobin); MCHC (Mean Corpuscular Hemoglobin Concentration); RDW (RBC distribution width); MPV (mean platelet volume). (B) Measured blood parameters after PHZ. (C) The mice were weighed before and after the treatment, after sacrificing also the spleen weight was determined. (D) Size distribution of RBCs before and after PHZ treatment. (E) qRT-PCR for *Kdm7a* normalized using *Actin* relative to WT. (F) and (G) Expression of different globins measured by qRT-PCR, shown are the fractions of the related globins. Measurements are relative to control littermates.

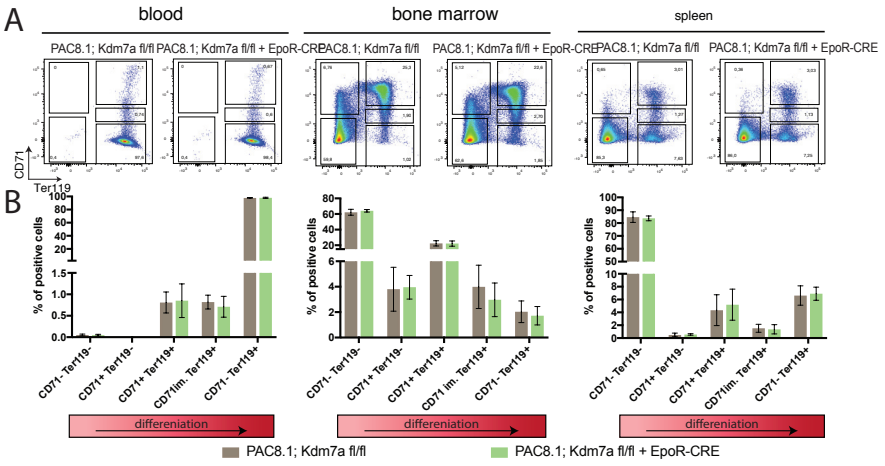

Figure 4. Flow cytometry of PAC8.1; Kdm7a fl/fl; EpoR-Cre mice after PHZ treatment. (N=5 for each condition) (A) Examples of flow cytometry profiles of CD71/Ter119 staining of blood, bone marrow and spleen cells. (B) Quantification of different CD71+ and – Ter119 + and - populations.

Although most stages do not show a difference, the appearance of progenitors within the FL of *PAC8*.1; *Kdm7a* fl/fl mice and *PAC8*.1; *Kdm7a* fl/fl; *EpoR*-Cre mice seems delayed.

In Figure 6 (A-D) we tested by qRT-PCR the relative expression of the different mouse and human globins at E12.5 until E16.5 of gestation. Looking at for example γ-globin levels in E12.5, there is an increase in expression, but due to the limited number of samples this is not significant. Between the different stages of development, the globin levels vary a lot and no significant differences in the relative expression of the globins were detected. Subsequently, in Figure 6D we tested the levels of *Kdm7a* relative to *Actin* and normalized to WT using qRT-PCR in FL cells. The expression of *Kdm7a* is reduced at E12.5, we were not able to measure this at other time points due to technical problems.

Because of the lack of phenotypical changes in the *PAC8*.1; *Kdm7a* fl/fl; *EpoR*-Cre mice, we decided to follow a broader approach by using the pIpC inducible *Mx1*-Cre line. This Cre recombinase is expressed in the hematopoietic stem cell compartment after pIpC induction. We injected mice of 4 months for 4 times with pIpC/PBS (Supplementary Figure 3A). 2 weeks after the last injection, the animals were sacrificed, and the erythroid organs (blood, spleen and BM) analyzed.In the size distribution of RBCs there is no difference (Figure 7A). Also in other blood parameters measured, there are no significant changes after pIpC induction of *Mx1*-Cre (Figures 7B_C). Both mouse and spleen weights are slightly reduced, but these changes do not reach significance (Figure 7D). Southern blot analysis of the genomic DNA shows that activation of Mx1-Cre results in a high recombination efficiency in CD71+ and CD71– BM cells of these mice (Figure 7E). In the spleen, there is less recombination as compared to the bone marrow. This can be explained since the recombination percentage in spleen is lower compared to BM. In addition, spleen size is also lower in *Mx1*-Cre mice. Anemia is compensated specifically by expansion of the erythroblast compartment in the spleen. Given that *Kdm7a*-deficient erythroblasts

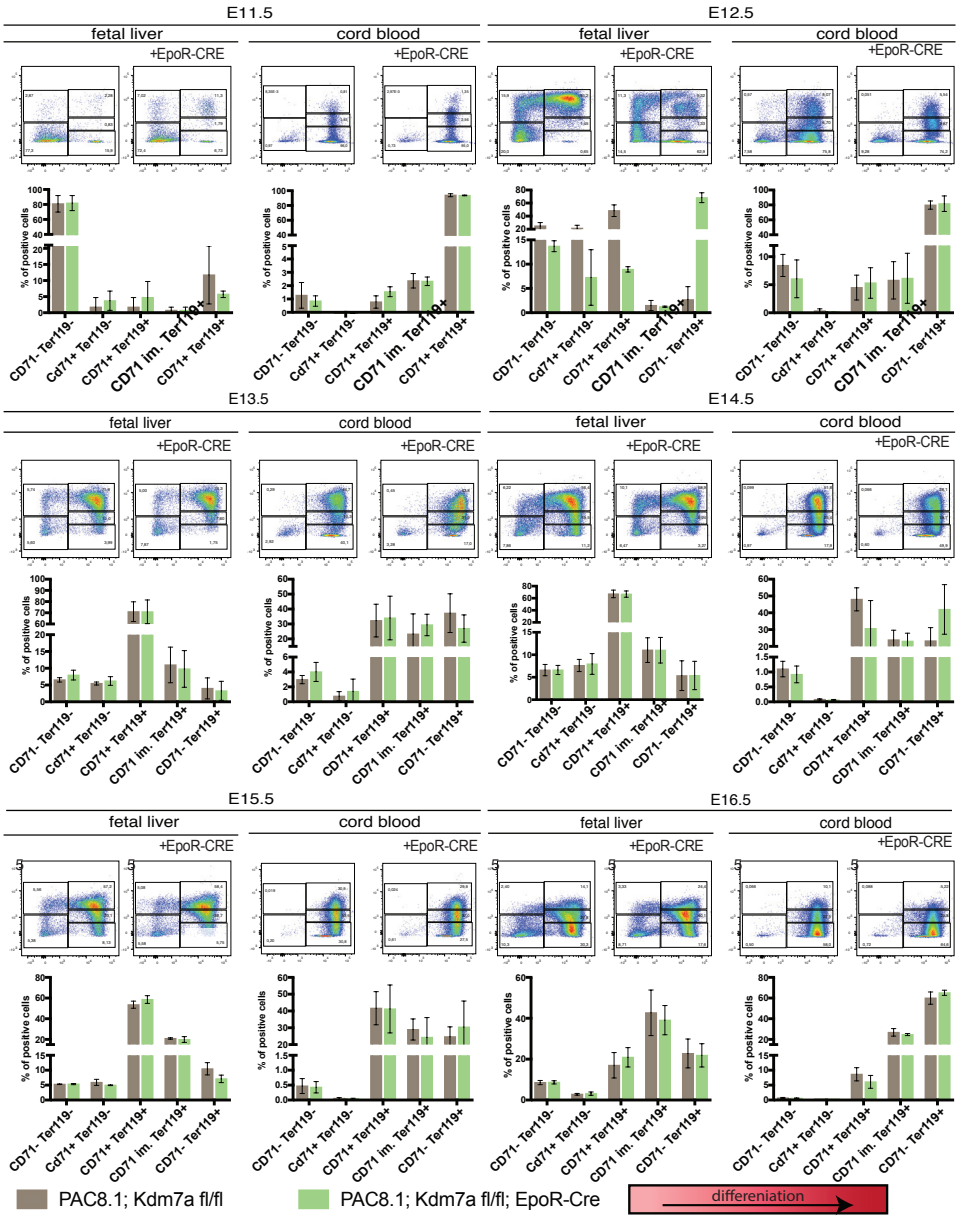

Figure 5. Flow cytometry plots of CD71/Ter119 antibody staining of fetal liver and cord blood at E11.5 until E16.5 of gestation and their quantification (E11.5/E12.5/E14.5/E15.5 WT n=5 and cKO n=3; E13.5 WT n=4 cKO n=5; E16.5 WT n=3 cKO n=3).

demonstrated reduced initiation of the progenitor compartment in fetal liver, reduced correction of RBC and HCT following PHZ treatment, it can be expected that non-recombined erythroblasts expand in the spleen whereas recombined erythroblasts contribute much less to spleen erythropoiesis. This skews the recombination percentage in the regenerating spleen compared to the BM where steady state

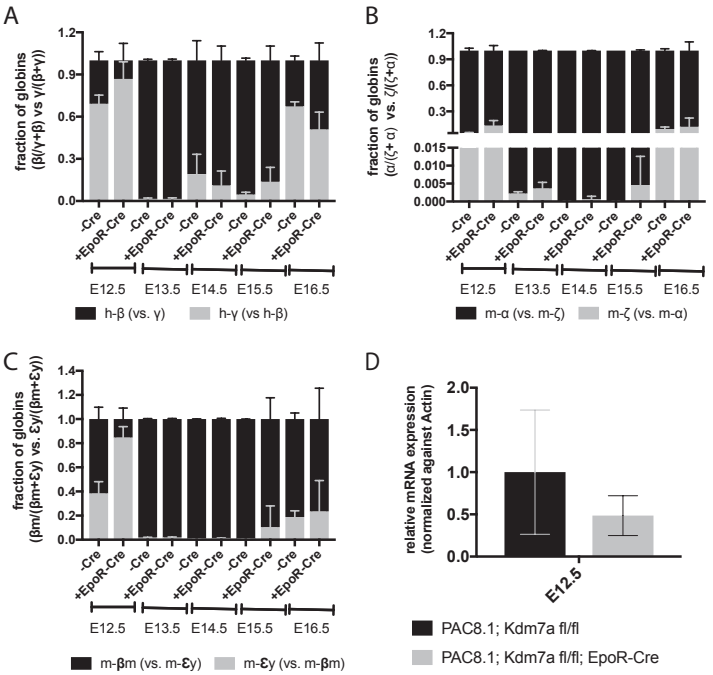

Figure 6. Relative expression of different hemoglobins and the *Kdm7a* gene in fetal livers at E12.5 until E16.5 of gestation. (E12.5 WT n=2 cKO n=2; E13.5/ E14.5/E15.5/E16.5 WT n=3 cKO n=3) (A) fraction of human g-globin relative to human b-globin. (B) fraction of mouse z-globin relative to mouse a-globin. (C) mouse e-globin relative to mouse bm-globin. (D) levels of the *Kdm7a* gene relative to *Actin*.

erythropoiesis occurs. Testing the mRNA levels of the globins in spleen and CD71+ BM cells, we didn't observe any changes (Figure 7G and H). Unfortunately, we cannot measure the protein levels of Kdm7a. As we induced *Mx1*-Cre in adult mice, it is possible that there is still protein left within the cells that masks the knockout phenotype.

To test this hypothesis, we induced *Mx1*-Cre a few days after the mice were born. Since the animals are small at the start of the experiment, we could not test the blood parameters before injection. Figure 8A and D represent the measurements of the Vet ABC counter after 4 months just before sacrificing the animals. No significant changes were observed for any of the blood parameters measured. After sacrificing the animals their body and spleen weights were measured. The total body weight was not affected by the conditional knockout, but the spleen weights were significantly smaller in the *Kdm7a* cKO mice after pIpC induction (Figure 8B; p-value 0.0079). Figure 8C shows that the recombination was very efficient in the different hematopoietic organs analyzed (spleen, BM and thymus). Of note, the BM cells were analyzed without prior selection for CD71+ cells, indicating pan-hematopoietic inactivation of *Kdm7a* upon pIpC treatment.

Testing the human and mouse globins using qRT-PCR, we observed an apparent decrease of ζ-globin versus α-globin and εy-globin versus βh1-globin, but this was not statistically significant (Figures 8E-F).

Of note, we observed an almost complete reduction of the *Kdm7a* mRNA in bone marrow and spleen of *Kdm7a* cKO mice after pIpC induction (Figure 8G). Because we induced the *Mx1*-Cre recombinase soon after birth, any protein left should be

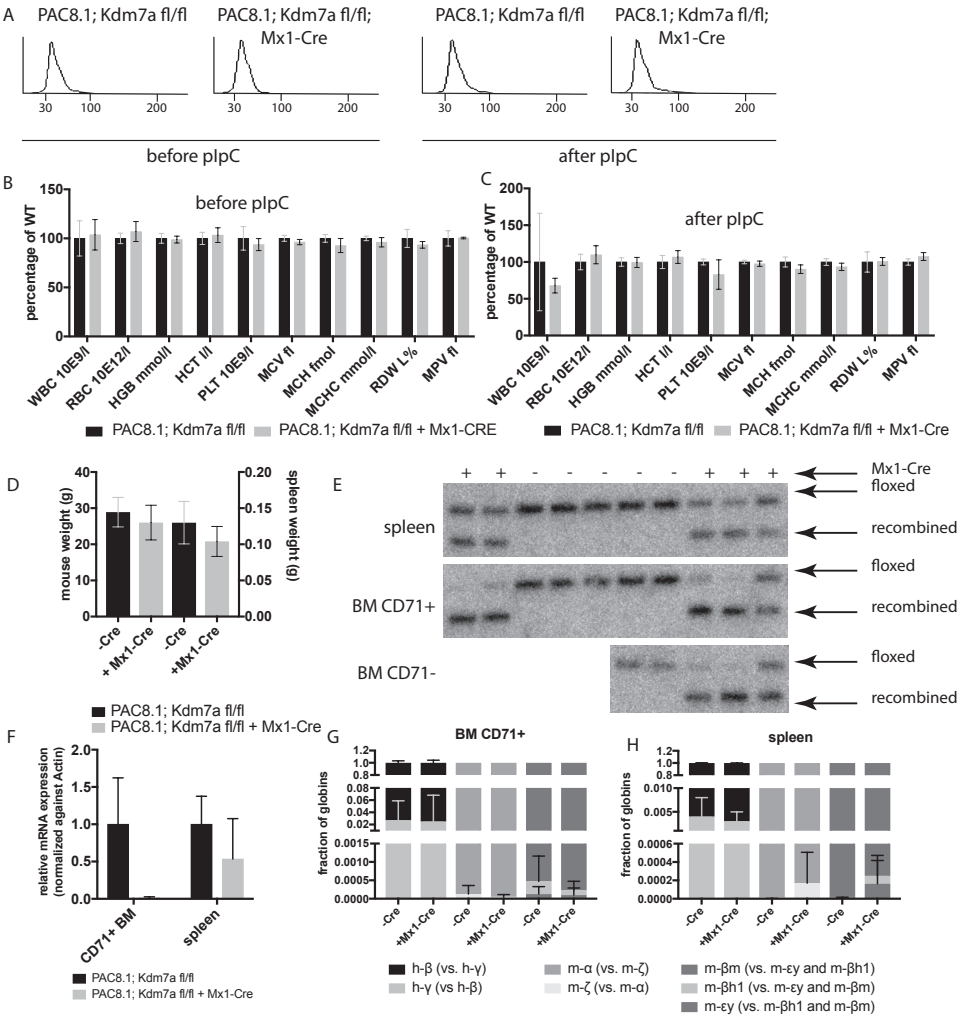

Figure 7. *PAC8*.1; *Kdm7a* fl/fl; *Mx1*-Cre pIpC injected mice. (n=5 for each condition). (A) Size distribution of RBCs before and after pIpC treatment. (B) and (C) Measured blood parameters WBC (white blood cells); RBC (red blood cells); HGB (hemoglobin); HCT (hematocrit); PLT (platelets); MCV (Mean Corpuscular Volume); MCH (Mean Corpuscular Hemoglobin); MCHC (Mean Corpuscular Hemoglobin Concentration); RDW (RBC distribution width); MPV (mean platelet volume) before and after pIpC induction. (D) Graphical representation of the mice and spleen weights after pIpC treatment. (E) Southern blot of spleen cells and CD71+ and - selected bone marrow cells. (F) Relative expression of *Kdm7a* normalized to *Actin* and relative to WT expression. (G) Expression of different globins RT-qPCR represented as a fraction. For example fractions were calculated as b/(b+g) and g/(b+g). Samples with and without *Mx1*-Cre in CD71+ selected bone marrow cells, and (H) spleen are shown.

diluted after multiple cell divisions. From this, we can conclude that *Kdm7a* does not affect the globin expression levels.

Because *Mx1*-Cre is active from the early hematopoietic stem cell stage, this may affect also other hematopoietic cell populations. We therefore set up a pan-

hematopoietic flow cytometry analysis.
For the erythroid cells, we performed CD71/KIT staining to mark the progenitor cells in blood, BM and spleen, and CD71/Ter119 staining to mark the more mature cells. The gating strategies are displayed in Supplementary Figure 5. In blood, we observed as expected mostly mature cells and almost no progenitor cells (Figure 9). The *PAC8*.1; *Kdm7a* fl/fl and *PAC8*.1; *Kdm7a* fl/fl; *Mx1-Cre* mice did not display significant differences between the populations of these cells. In BM, as expected there are more progenitor cells found than in blood. After pIpC treatment, there were two populations affected differently between the *PAC8*.1; *Kdm7a* fl/fl and *PAC8*.1; *Kdm7a* fl/fl; *Mx1*-Cre mice, it is the erythroid specific compartment that is reduced upon loss of *Kdm7a*: the early progenitors BFU/CFU erythroblasts (CD71-; c-KIT+) were slightly increased from 9,7% in the control to 12,3 % in the cKO animals and the poly/orthochromatic erythroblast cell populations (CD71 intermediate; Ter119+) were decreased from 20,6% in the control to 13,3% in the cKO animals. A reduced regenerative capacity is shown, what is compensated by increase of the input cells c-KIT+ BFU-E cells. In the other cell populations, including the earliest stem cells and progenitors, no differences were found. In spleen, there was a small but significant decrease from 13,9% in the control to 8,8% in the control animals in the population of mature erythroid cells.
In the flow cytometry plots of the spleen cells, the double negative population is not specifically the erythroid cell population, but may also be other spleen cells. In conclusion, there were some subtle differences between progenitor cell populations in the conditional knockouts and their floxed littermates, but this did not change the overall balance of erythroid cells in BM and spleen.
Next, we performed stainings to mark different T cell populations in the spleen and thymus. The gating strategy between these organs differs slightly (Supplementary Figure 5). In spleen, the NK1.1-/CD3+ general T cell population was reduced from 34% in the controls to 21,6% in the cKO animals. (Figure 10). In Figure 8B we showed that the spleen sizes are also decreased in the *PAC8*.1; *Kdm7a* fl/fl; *Mx1-Cre* mice compared to the PAC8.1; *Kdm7a* fl/fl mice. Within the T cell population, the balance between the CD8/CD4 populations did not change drastically (Figure 10). Only the double positives decreased from 0.72% to 0.45% with a p-value of 0.03. Subsequently, the CD4+/CD8- (T-helper cells) and CD4-/CD8+ (cytotoxic T cells) populations were further gated using CD44/CD62L. Within the CD4 positive T-helper cells, the CD62L negative cells are the memory cells, and the CD62L positive cells are naïve T-helper cells.
Within the CD8 positive cytotoxic T cell group we can distinguish activated, effector and naïve cytotoxic T cells, using CD62L/CD44. In none of the CD62L/CD44 cell populations significant differences were found (Figure 10). In conclusion, the total number of T cells in the spleen was slightly reduced; this reflects the smaller spleen sizes of the knockout animals. What is caused by the reduced regenerative capacity of the erythroblast in the spleen. The balance between the differentiated T cell populations was not changed.
The thymus is the organ where the T cells develop. We performed a similar staining on these cells, although the gating strategy is more laborious (Supplementary Figure 5). We started with NK1.1/FSC-A where we took the NK1.1 negative cells (Figure 11). Then we continued to distinguish the different CD4/CD8 populations.

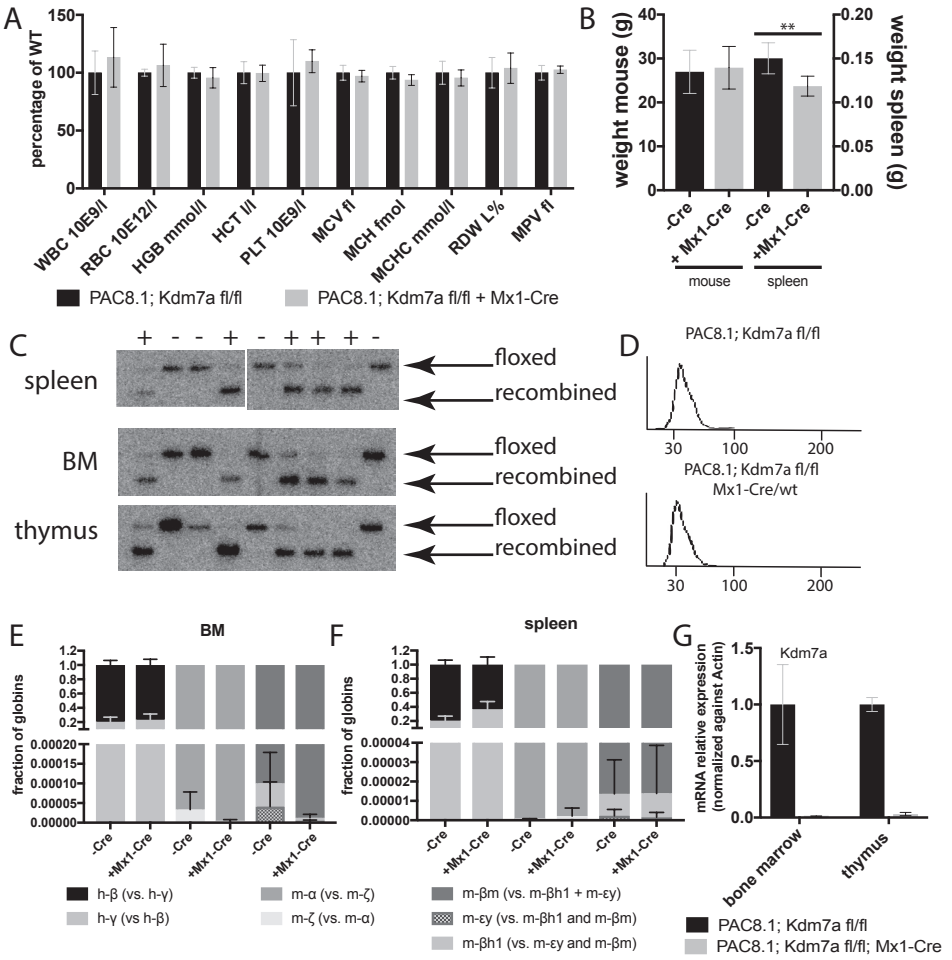

Figure 8. PAC8.1; *Kdm7a* fl/fl; Mx1-Cre pIpC injected mice. (WT n=4 vs cKO n=5) (A) Measured blood parameters WBC (white blood cells); RBC (red blood cells); HGB (hemoglobin); HCT (hematocrit); PLT (platelets); MCV (Mean Corpuscular Volume); MCH (Mean Corpuscular Hemoglobin); MCHC (Mean Corpuscular Hemoglobin Concentration); RDW (RBC distribution width); MPV (mean platelet volume) after pIpC induction. (B) Graphical representation of the mice and spleen weights after pIpC treatment. ** p-value > 0,01. (C) Southern blot of spleen cells, bone marrow and thymus cells. (D) Size distribution of RBCs. (E) Expression of the fraction of different globins in bone marrow, and (F) spleen. (G) Relative expression of *Kdm7a* normalized to actin and WT.

In the capsule of the thymus the T cells start as CD4-/CD8- cells and are called precursor thymocytes.[30] After moving to the cortex they become double positive (DP) for CD4/CD8. Subsequently, the cells move to the medulla of the thymus, where they become single positive (SP) for CD4 or CD8. Compared to the controls, the different populations did not change in the conditional knockout mice (Figure 11). We then looked into more detail to specify the subpopulations of these different T cell stages. Within the immature double-negative (DN) CD4-/CD8- cells we gated for CD3-/FSC-A medium/high cells to select the most immature T cells. From this group, we

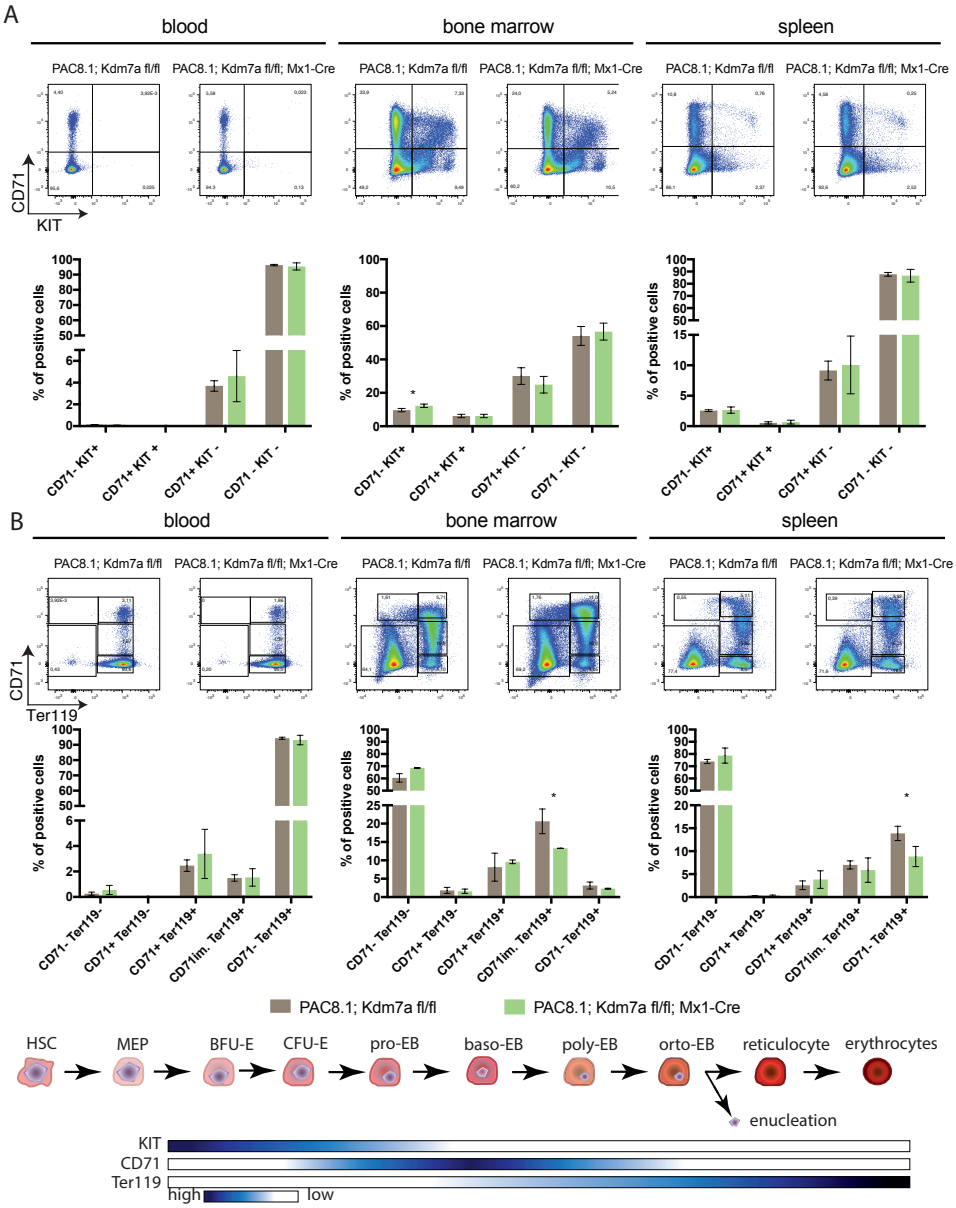

Figure 9. Erythroid flow cytometry in young injected PAC8.1; *Kdm7a* fl/fl mice vs. PAC8.1; *Kdm7a* fl/fl; Mx1-cre mice. After life/dead gating (see Supplementary Figure 5) (A) CD71/KIT is used to mark different progenitor cell stages, while (B) CD71/Ter119 is used to distinguish more differentiated cells. CD71/KIT maturation goes counter clock wise, while CD71/Ter119 goes clock wise. * indicates a p-value of < 0,05. (WT n=4 vs cKO n=5)

can further specify four different immature DN stages of those cells using CD44/CD25. During maturation, immature T cells start as DN1 cells with CD25-/CD44^{high}, then in DN2 they become CD25+/CD44+ DP. Subsequently, the cells lose CD44 and are CD25 SP in DN3, and finally in DN4 the cells lose CD25 expression and

become DN for those markers. In our PAC8.1; *Kdm7a* fl/fl; *Mx1-Cre* mice we found an increase from 21,7% in the controls to 31,1% of the DN3 cells. Looking at the other DN stages, we observed some minor increases or decreases, but these differences did not reach statistical significance.

For the more mature cells we went back to the CD4/CD8 gating, where we also looked at the SP cells.[31] For the CD4+ and CD8+ SP cells we gated for CD3/FSC-A, but here we took the CD3+ cells to select for the mature cells. Then we continued with CD62L/CD44. We can distinguish effector T cells CD62L-/CD44+, central memory T cells CD62L+/CD44+, and naïve T cells which are CD62L+/CD44-. The CD3 positive cell population of the CD8 SP cells, we also can mark the immature single positives (ISP) cells as a CD3-negative population. These gating strategies were applied on thymus cells from PAC8.1; *Kdm7a* fl/fl; *Mx1*-Cre mice and their *PAC8.*1; *Kdm7a* fl/fl littermates. We didn't observe any significant differences in those T cell populations between the conditional knockout animals and the controls. Thus, the change we observed at the DN3 stage does not appear to affect the mature cell populations.

To mark different B cell populations in spleen and BM we used a cocktail of B220/CD19/CD23/CD21/CD2/IgM and IgD, see Figure 12. After gating for single living cells and using the FSC-A and SSC-A parameters (Supplementary Figure 5) we continued with a B220/CD19 gating. Here we mark the plasmacytoid Dendritic Cells (pDC)s and B cells. Subsequently, we used CD23/CD21 to distinguish follicular (CD23+/CD21 medium), marginal zone (CD23-/CD21+) and newly formed B cells (CD23-/CD21-). In BM, we further analysed the newly formed cell population CD23-/CD21- using CD2/FSC-A to mark the pro/pre-B cells and small pre-B cells. The only significant differences we observed were in the spleen, were the pDCs are decreased from 2,1% in the controls to 1,5% in the cKO animals and the B-cell

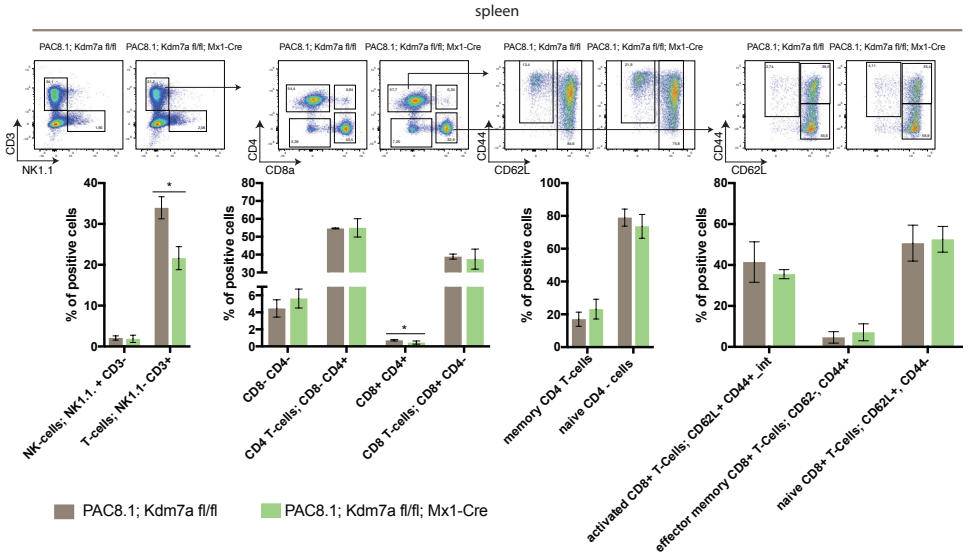

Figure 10. T cell staining of spleen cells. After live/dead marking (not shown) CD3/NK1.1 was used to distinguish between NK-cells and T cells. This is followed by CD4/CD8 staining, which mark different populations of T cells. Within the CD4+ population is CD62L/CD44 gated to distinguish CD4 memory and naïve CD4 T cells. Within the CD8+ population CD62L/CD44 mark activated, effector memory and naïve CD8+ T cells. (WT n=4 vs cKO n=5) * indicates a p-value of < 0.05.

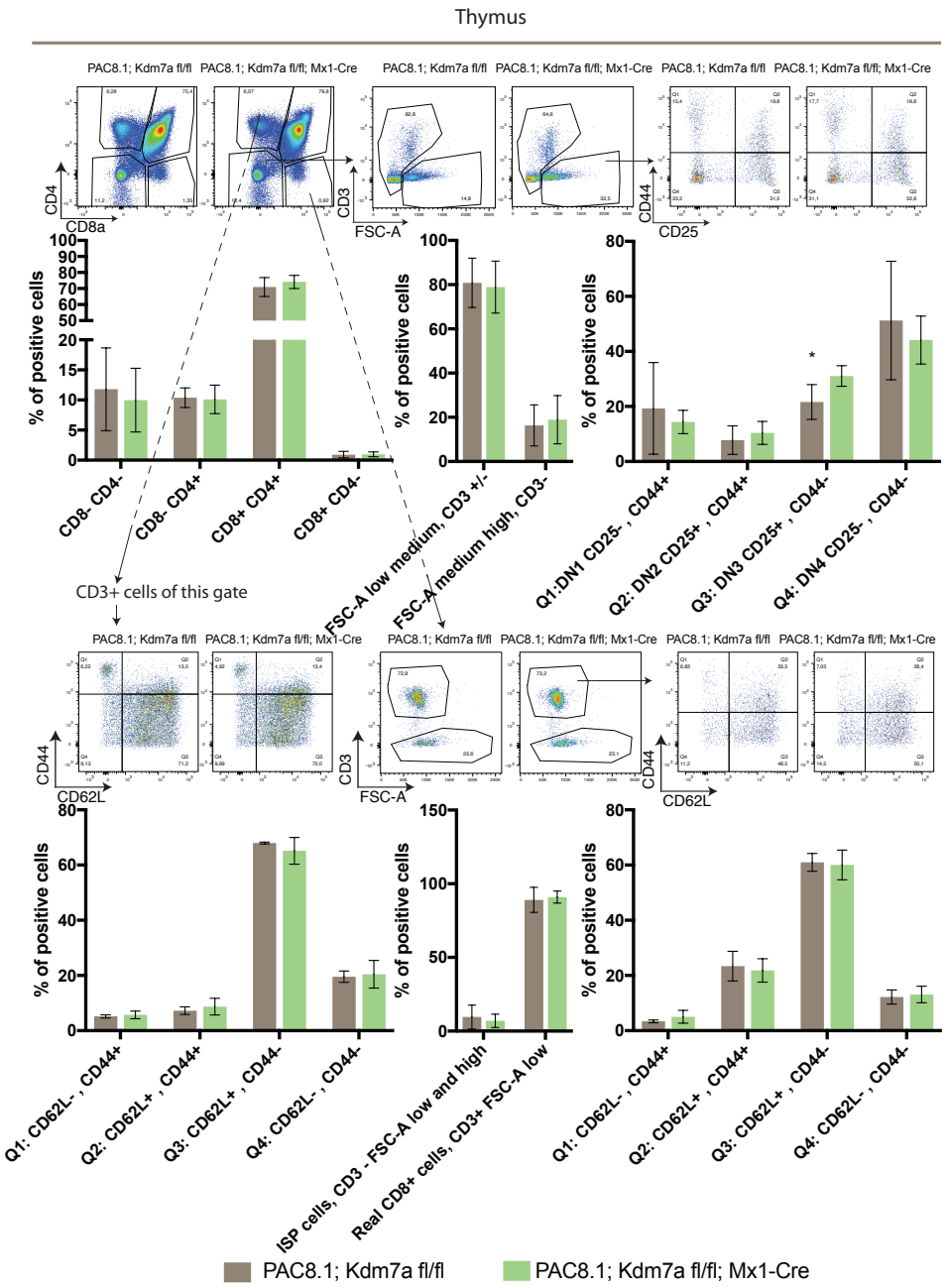

Figure 11. T cell staining of thymus cells. After gating for life/dead cells and using the FSC-A/ SSC-A, we used NK1.1 negative cells to continue (Supplementary Figure 5). Then the T cells are subdivided in double negative immature (DN:CD4-/CD8-), double positive precursors (DP:CD4+/ CD8+), and mature single positives (SP:CD4+ or CD8+). Subsequently, the DN and SPs are further analyzed using CD3/FSC-A which mark the immature (CD3-) or mature (CD3+) cells. The immature cells are further marked using CD25/CD44 which mark the maturation stadia. The mature SPs are further analyzed using CD62L/CD44. CD44+/CD62L- are effector T cells, CD44+/CD62L+ are central memory T cells; and CD44-/CD62L+ cells are naïve T cells. For CD8+SPs also the immature cells are marked as ISP using the CD3/FSC-A. (WT n=4 vs cKO n=5). * indicates a p-value of < 0.05.

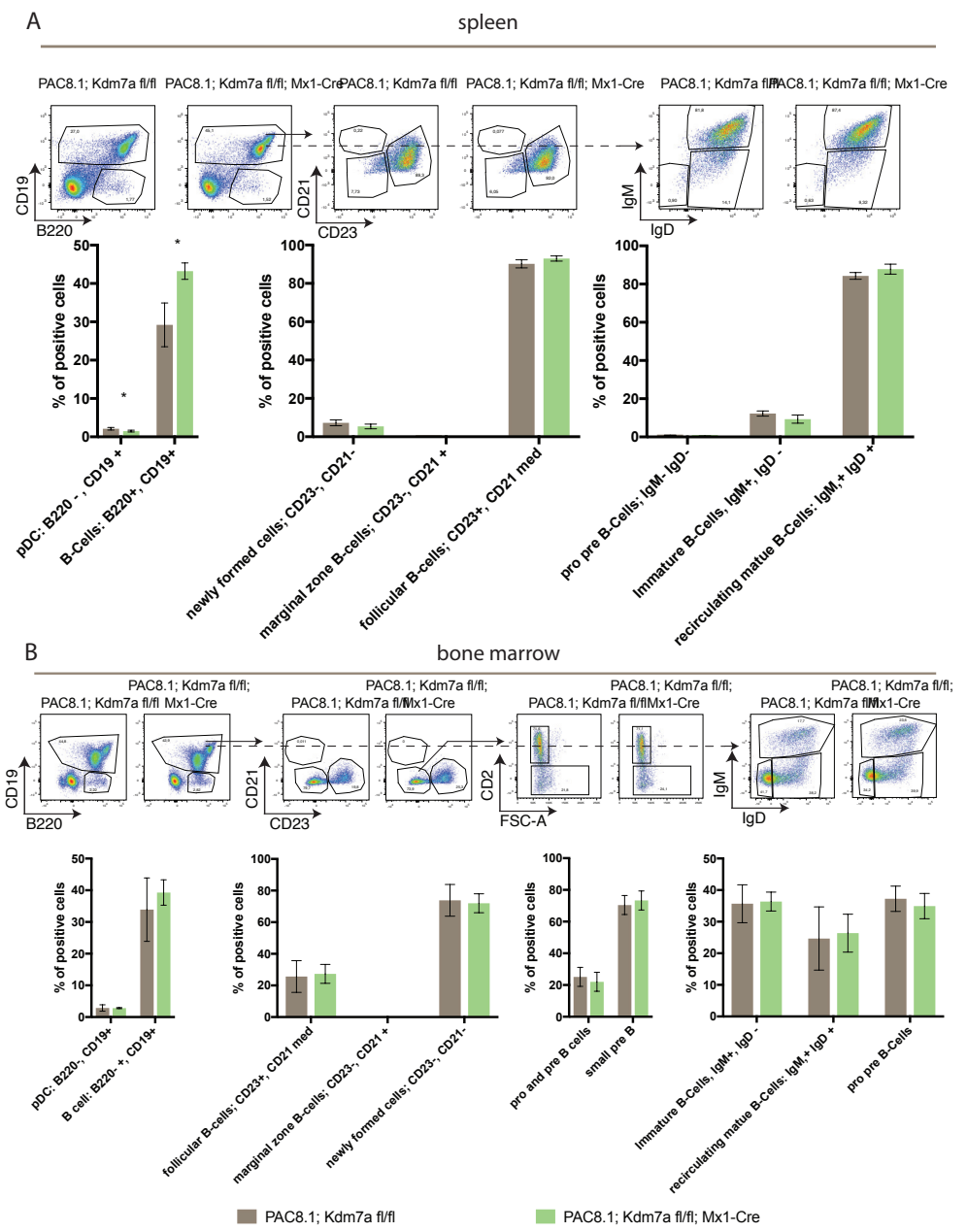

Figure 12. B cell staining of (A) spleen and (B) BM cells; after gating for live cells, single cells and lymphocytes. We used the B220/CD19 staining to distinguish plasmacytoid dendritic cells (pDC) and B cells. We continued with the B cell population for a CD23/CD21 gating. Here we gate for CD21/CD23 where we gate for follicular, marginal zone and newly formed B cells. In BM, the subpopulation of newly formed cells are subsequently gated by CD2/FSC-A to distinguish pro/ pre-B cells and small pre-B cells. From the B cell population we also checked the Immature, recirculating mature and pro/pre-B cells using IgM/IgD. (WT n=4 vs cKO n=5) * marks a p-value < 0.05

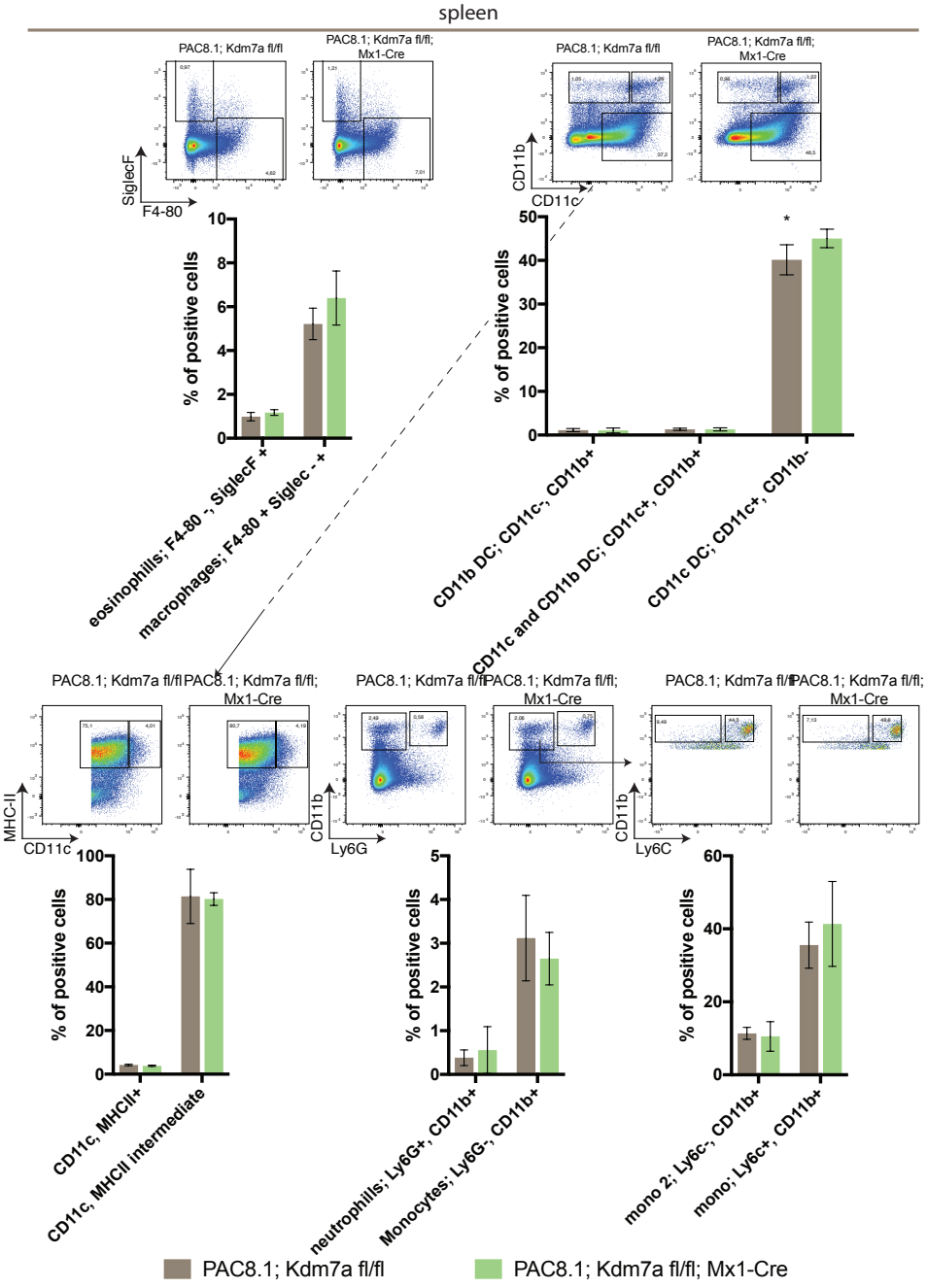

Figure 13. Myeloid flow cytometry analysis on spleen cells. After gating for granulocytes and living cells, we gated for eosinophils and macrophages using SiglegF/F4-80. To distinguish myeloid cells from dendritic cells (DCs) we used CD11b/CD11c. Subsequently, CD11c+ DCs were further gated using CD11c/MHCII to mark small and large DCs. CD11b/Ly6G was used to distinguish neutrophils and monocytes within the living cell population. Within the monocytes, we used CD11b/Ly6C to mark novel/resident and inflammatory monocytes. (WT n=4 vs cKO n=5) * marks a p-value < 0.05

population is increased from 22,2% to 43,2% in *PAC8*.1; *Kdm7a* fl/fl; *Mx1*-Cre mice. Since the balance between the more specified cell types has not changed, this might be an effect of the smaller spleen sizes of the conditional knockout animals (Figure 8B).

Finally, we checked the myeloid cells for changes due to the conditional knockout in *PAC8*.1; *Kdm7a* fl/fl and *PAC8*.1; Kdm7a fl/fl; *Mx1*-Cre mice (Figure 13). For this we used SiglegF/F4-80 to distinguish eosinophils (F4-80-/SiglegF+) and macrophages (F4-80+/SiglegF-).[32] To mark the different dendritic cell populations, we used CD11b/CD11c and MHCII/CD11c.[33] Myeloid cells are characterized by CD11b+/CD11c-, conventional dendritic cells (cDCs) are double positive for CD11b+/CD11c+, and the immature dendritic cells (L-DCs) are CD11b-/CD11+. This group is further analysed using MHCII and CD11c.[34] Here we can distinguish small and large DCs. The monocytes and neutrophils are analysed using CD11b/Ly6G. Neutrophils are DP for CD11b/Ly6G, while monocytes are SP for CD11b. To invest the monocyte population more specifically, we used CD11b/Ly6C. Novel/resident monocytes are CD11b+/Ly6C- and inflammatory monocytes are CD11b+/Ly6C+. In our mice, we only observed an increase of the CD11c SP DCs in conditional knockout animals (p=0.0238). There were minor changes in the monocyte populations, but these did not reach statistical significance.

CRISPR-mediated knock out of the KDM7A *gene in HUDEP-2 cells*

Recently HUDEP-2, a human umbilical cord-derived cell line, was developed.[24] Using CRISPR-Cas9 technology we aimed to knock out the *KDM7A* gene in HUDEP-2 cells.[25-28] We first transduced HUDEP-2 cells with lentiCRISPR-blast to obtain cells stably expressing Cas9 protein. After blasticidin selection and confirming expression of Cas9 protein, the cells were transduced with a pLKO vector carrying the guide RNA targeting *KDM7A*. After puromycin selection, we isolated protein and genomic DNA of the pool of cells. On the genomic DNA we performed a surveyor assay to detect heteroduplexes and with the protein lysates we did a western blot (Figure 14). The surveyor assay detected two extra fragments after digestion specific for gRNA treated cells, showing successful modification of *KDM7A*. To test the effect of the generated mutations on KDM7Aa expression at the protein level, we used a human-specific antibody against KDM7A. Unfortunately, this revealed that the protein level was not affected. Because of limited availability of material we could not test further characteristics of the cells.

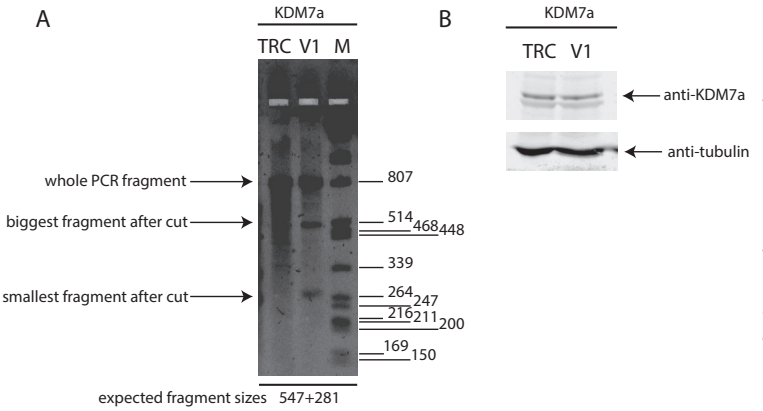

Figure 14. (A) Surveyor assay of PCR products of genomic DNA from the pool HUDEP-2 cells after blasticidin and puromycin selection. (B) Western blot of RIPA lysates SDS-PAGE stained for KDM7A and tubulin.

Discussion

Hematopoiesis is a complex process in which many factors play an important role. In order to understand this mechanism better and find new molecular targets for pharmacological treatment of SCD and β-thalassemia, we investigated the function of *Kdm7a* in conditional knockout-mice that carry the human *HBB* locus PAC8.1, and Cre recombinase specific for erythropoiesis or hematopoiesis.

First, we started with the *EpoR*-Cre line, which targets Cre to the erythroid lineage. This approach turned out to be ineffective. Due to the lack of a good antibody for mouse KDM7A, we were unable to check KDM7A protein levels. We observed efficient recombination at the genome level, but *Kdm7a* mRNA was not efficiently reduced in the erythroid lineage.

In the normal situation at the moment there should be feedback control, there is no difference, but after PHZ treatment and in the beginning of the fetal erythropoiesis the production of RBC should be optimal, then the production *Kdm7a* recombined cells stays behind.

Subsequently, we chose a Cre recombinase already active in the hematopoietic stem- and progenitor cell compartment: *Mx1*-Cre. Upon pI:pC induction of Cre recombinase in adult animals, we observed efficient recombination at the *Kdm7a* locus, accompanied by reduction of *Kdm7a* mRNA levels. However, compared to the controls the hemaglobin type remained unaffected in the conditional knockout animals. Nevertheless we see a decreased regenerative capicity in those ainimase. We observe a smaller spleen and there alre less RBC and a lower hematocrite level. Also the smaller spleen size show less recombination, what is caused by this reduced regererative capicity.

We then induced Cre recombinase in P7-P10 pups and analysed the animals at 4 months. We observed smaller spleens in the conditional knockout mice. As a consequence, several cell populations residing in the spleen, e.g. T- and B cells, are affected. The percentages of the total T cell population are decreased in the spleen, while the percentages of the total B cell population are increased.

This relative change does not affect the distribution between specified T- and B cell populations, e.g. CD4+ or CD8+ memory or naive T cells or the different types of B cells.

Because of the efficient recombination, as shown by the Southern blots, together with the RT-qPCR data that shows a reduced mRNA level, we can conclude that depletion of *Kdm7a* does not impair hematopoiesis such that the cell populations in peripheral blood are affected.

In HUDEP-2 cells we tested one guide RNA to modify the *KDM7A* gene. Although the surveyor assay shows some alterations due to this gRNA, no changes were detectable at the protein level. Effects could also be measured using single cell analysis methods to avoid background of the unaffected cells within the cell pool.

In addition to this, lack of higher γ-globin levels does not make KDM7A a new potential target for treatment of SCD and β-thalassemia patients.

References

1 Angastiniotis, M. & Modell, B. Global epidemiology of hemoglobin disorders. *Ann N Y Acad Sci* **850**, 251-269 (1998).

2 Stamatoyannopoulos, G. *The Molecular Basis of Blood Diseases.* (W.B. Saunders, 2001).

3 Gambari, R. Foetal haemoglobin inducers and thalassaemia: novel achievements. *Blood Transfus* **8**, 5-7, doi:10.2450/2009.0137-09 (2010).

4 Steinberg, M. H. Therapies to increase fetal hemoglobin in sickle cell disease. *Curr Hematol Rep* **2**, 95-101 (2003).

5 Borg, J. *et al.* Haploinsufficiency for the erythroid transcription factor KLF1 causes hereditary persistence of fetal hemoglobin. *Nat Genet* **42**, 801-805, doi:10.1038/ng.630 (2010).

6 Collins, F. S., Cole, J. L., Lockwood, W. K. & Iannuzzi, M. C. The deletion in both common types of hereditary persistence of fetal hemoglobin is approximately 105 kilobases. *Blood* **70**, 1797-1803 (1987).

7 Edward, H. L. *et al.* Analysis of (δβ)⁰ Thalassemia and HPFH Deletions Suggest a Hierarchy of Cis-Acting Elements Regulating Fetal Hemoglobin Gene Expression. *Blood* **124**, 54-54 (2014).

8 Lettre, G. *et al.* DNA polymorphisms at the BCL11A, HBS1L-MYB, and beta-globin loci associate with fetal hemoglobin levels and pain crises in sickle cell disease. *Proc Natl Acad Sci U S A* **105**, 11869-11874, doi:10.1073/pnas.0804799105 (2008).

9 Uda, M. *et al.* Genome-wide association study shows BCL11A associated with persistent fetal hemoglobin and amelioration of the phenotype of beta-thalassemia. *Proc Natl Acad Sci U S A* **105**, 1620-1625, doi:10.1073/pnas.0711566105 (2008).

10 Menzel, S. *et al.* The HBS1L-MYB intergenic region on chromosome 6q23.3 influences erythrocyte, platelet, and monocyte counts in humans. *Blood* **110**, 3624-3626, doi:10.1182/blood-2007-05-093419 (2007).

11 Thein, S. L. *et al.* Intergenic variants of HBS1L-MYB are responsible for a major quantitative trait locus on chromosome 6q23 influencing fetal hemoglobin levels in adults. *Proc Natl Acad Sci U S A* **104**, 11346-11351, doi:10.1073/pnas.0611393104 (2007).

12 Thein, S. L., Menzel, S., Lathrop, M. & Garner, C. Control of fetal hemoglobin: new insights emerging from genomics and clinical implications. *Hum Mol Genet* **18**, R216-223, doi:10.1093/hmg/ddp401 (2009).

13 van Dijk, T. B. *et al.* Fetal globin expression is regulated by Friend of Prmt1. *Blood* **116**, 4349-4352, doi:10.1182/blood-2010-03-274399 (2010).

14 Nawrocki, M. J. *et al.* JHDM1D and HDAC1-3 mRNA expression levels in peripheral blood mononuclear cells of patients with systemic lupus erythematosus. *Z Rheumatol* **74**, 902-910, doi:10.1007/s00393-015-1619-9 (2015).

15 Tsukada, Y.-i., Ishitani, T. & Nakayama, K. I. KDM7 is a dual demethylase for histone H3 Lys 9 and Lys 27 and functions in brain development. *Genes & Development* **24**, 432-437, doi:10.1101/gad.1864410 (2010).

16 Qi, H. H. *et al.* Histone H4K20/H3K9 demethylase PHF8 regulates zebrafish brain and craniofacial development. *Nature* **466**, 503-507, doi:http://www.nature.com/nature/journal/v466/n7305/abs/nature09261.html#supplementary-information (2010).

17 Horton, J. R. *et al.* Enzymatic and structural insights for substrate specificity of a family of jumonji histone lysine demethylases. *Nat Struct Mol Biol* **17**, 38-43, doi:http://www.nature.com/nsmb/journal/v17/n1/suppinfo/nsmb.1753_S1.html (2010).

18 Huang, C. *et al.* Dual-specificity histone demethylase KIAA1718 (KDM7A) regulates neural differentiation through FGF4. *Cell research* **20**, 154-165, doi:10.1038/cr.2010.5 (2010).

19 de Krom, M., van de Corput, M., von Lindern, M., Grosveld, F. & Strouboulis, J. Stochastic patterns in globin gene expression are established prior to transcriptional activation and are clonally inherited. *Mol Cell* **9**, 1319-1326 (2002).

20 Strausberg, R. L. *et al.* Generation and initial analysis of more than 15,000 full-length human and mouse cDNA sequences. *Proc Natl Acad Sci U S A* **99**, 16899-16903, doi:10.1073/pnas.242603899 (2002).

21 Koscielny, G. *et al.* The International Mouse Phenotyping Consortium Web Portal, a unified point of access for knockout mice and related phenotyping data. *Nucleic Acids Res* **42**, D802-809, doi:10.1093/nar/gkt977 (2014).

22 Heinrich, A. C., Pelanda, R. & Klingmuller, U. A mouse model for visualization and conditional mutations in the erythroid lineage. *Blood* **104**, 659-666, doi:10.1182/blood-2003-05-1442 (2004).

23 Kuhn, R., Schwenk, F., Aguet, M. & Rajewsky, K. Inducible gene targeting in mice. *Science* **269**, 1427-1429, doi:10.1126/science.7660125 (1995).

24 Kurita, R. *et al.* Establishment of immortalized human erythroid progenitor cell lines able to produce enucleated red blood cells. *PLoS One* **8**, e59890, doi:10.1371/journal.pone.0059890 (2013).

25 Sanjana, N. E., Shalem, O. & Zhang, F. Improved vectors and genome-wide libraries for CRISPR screening. *Nat Methods* **11**, 783-784, doi:10.1038/nmeth.3047 (2014).

26 Zufferey, R., Nagy, D., Mandel, R. J., Naldini, L. & Trono, D. Multiply attenuated lentiviral vector achieves efficient gene delivery in vivo. *Nature biotechnology* **15**, 871-875, doi:10.1038/nbt0997-871 (1997).

27 Ran, F. A. *et al.* Genome engineering using the CRISPR-Cas9 system. *Nature protocols* **8**, 2281-2308, doi:10.1038/nprot.2013.143 (2013).

28 Stewart, S. A. *et al.* Lentivirus-delivered stable gene silencing by RNAi in primary cells. *RNA (New York, N.Y.)* **9**, 493-501 (2003).

29 Mikropoulou, M. *An shRNA Screen for the Discovery of Suppressors of Fetal Hemoglobin*, Erasmus University Rotterdam, (2016).

30 Zuniga-Pflucker, J. C. T-cell development made simple. *Nat Rev Immunol* **4**, 67-72, doi:10.1038/nri1257 (2004).

31 Benichou, G., Gonzalez, B., Marino, J., Ayasoufi, K. & Valujskikh, A. Role of Memory T Cells in Allograft Rejection and Tolerance. *Front Immunol* **8**, 170, doi:10.3389/fimmu.2017.00170 (2017).

32 Hey, Y.-Y., Tan, J. K. H. & O'Neill, H. C. Redefining Myeloid Cell Subsets in Murine Spleen. *Frontiers in Immunology* **6**, doi:10.3389/fimmu.2015.00652 (2016).

33 Murdoch, C., Muthana, M., Coffelt, S. B. & Lewis, C. E. The role of myeloid cells in the promotion of tumour angiogenesis. *Nat Rev Cancer* **8**, 618-631, doi:10.1038/nrc2444 (2008).

34 Salomon, B. t., Cohen, J. L., Masurier, C. & Klatzmann, D. Three Populations of Mouse Lymph Node Dendritic Cells with Different Origins and Dynamics. *The Journal of Immunology* **160**, 708-717 (1998).

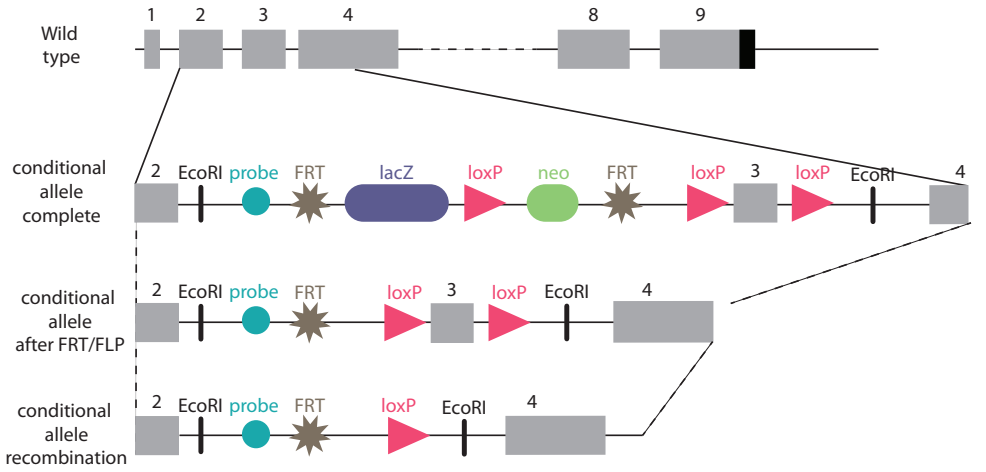

Supplementary Figure 1. Conditional knockout allele of *Kdm7a* gene. We used the conditional allele after FRT/FLP. EcoRI sites were used to check recombination efficiency by Cre recombinase using a probe at the location indicated. See Supplementary Table 1 for the primers to generate the probe.

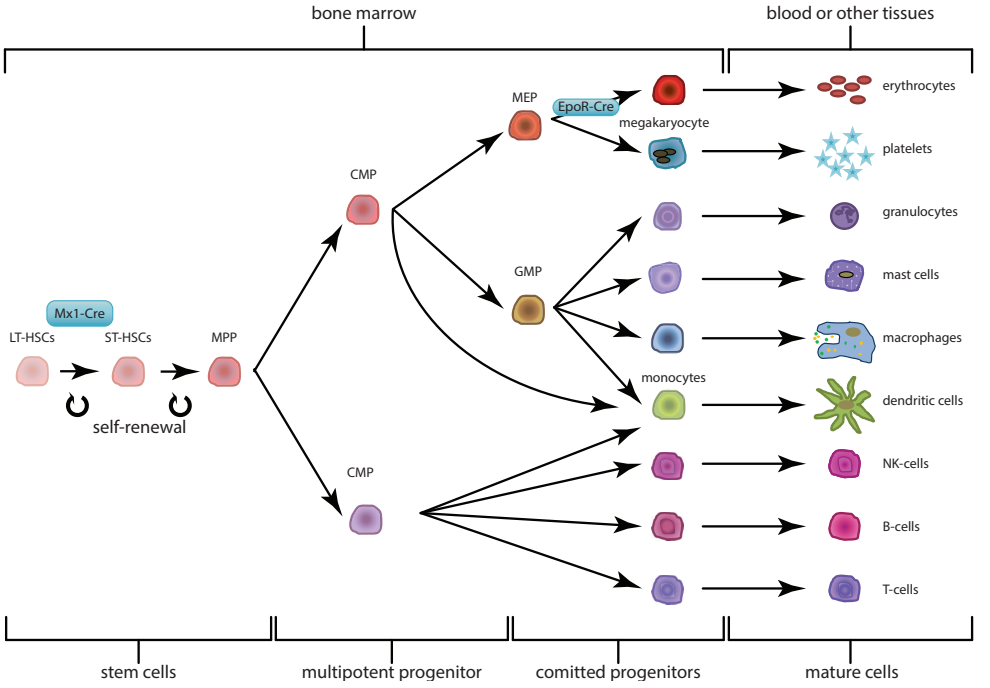

Supplementary Figure 2. Hematopoietic system and Cre recombinases used.

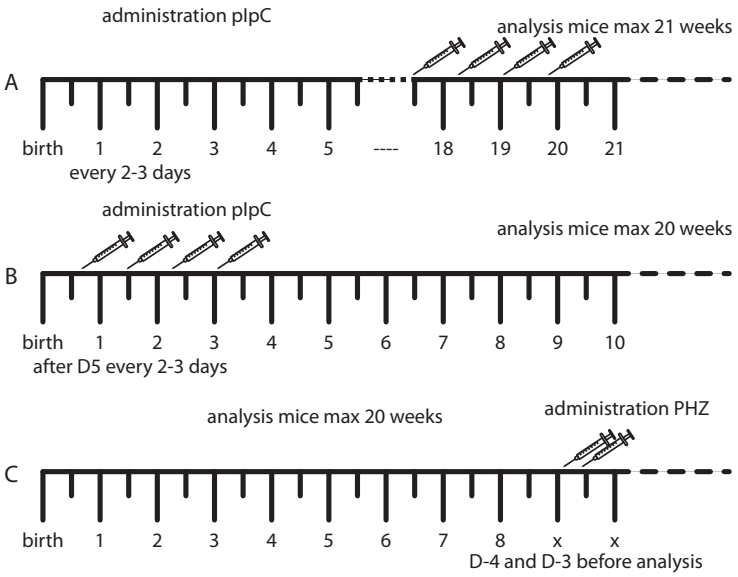

Supplementary Figure 3 Strategy to activate *Mx1-Cre* using pIpC administration, and to activate the erythroid stress response by PHZ administration.

Gating strategy erythroid stainings cord blood / fetal liver

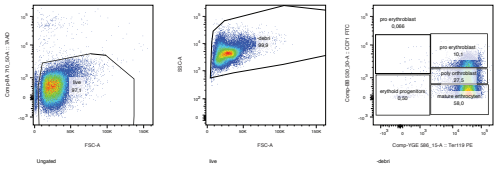

Gating strategy erythroid stainings blood / bone marrow / spleen --> compact

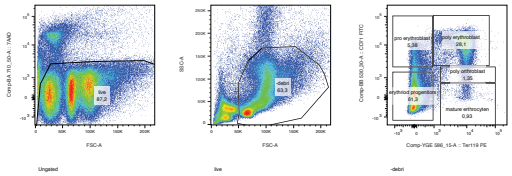

Gating strategy erythroid stainings blood / bone marrow / spleen --> extended

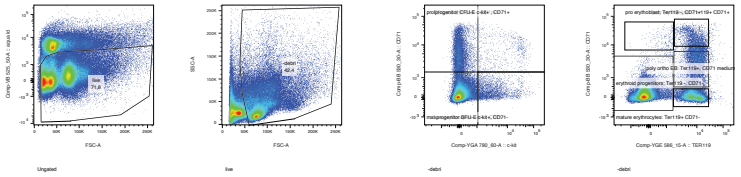

Supplementary Figure 4 Different gating strategies of erythroid stainings of cord blood, fetal liver, adult blood, bone marrow and spleen cells.

Gating strategy T-cells spleen

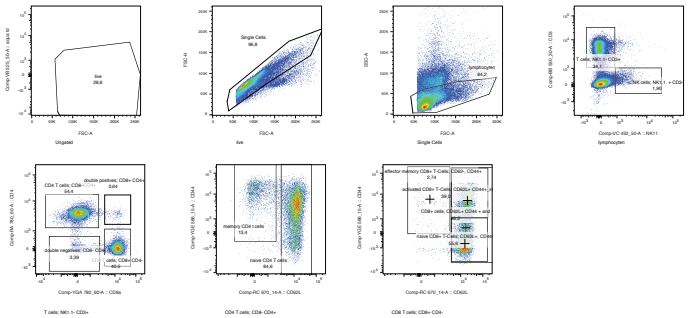

Gating strategy T-Cells Thymus

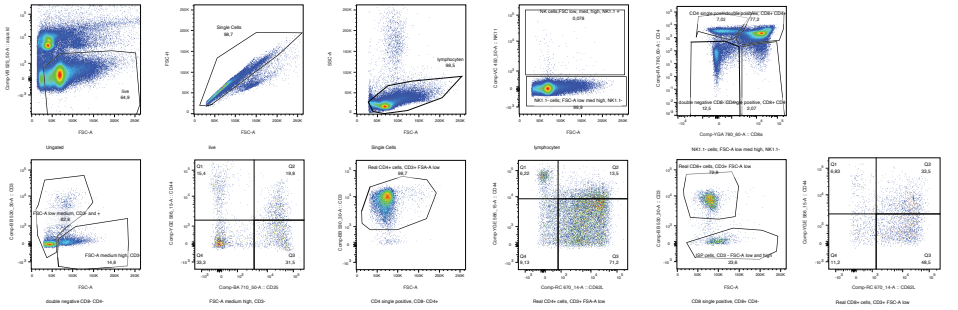

Gating strategy B-Cells bone marrow and spleen

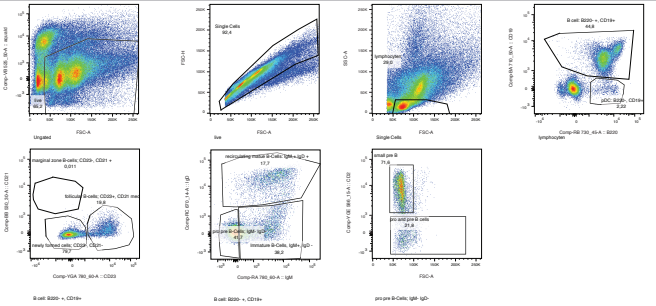

Gating strategy myeloid staining spleen

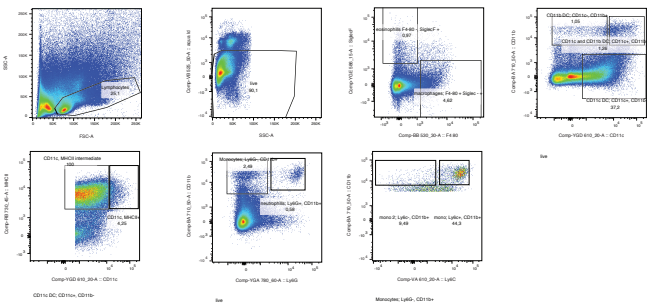

Supplementary Figure 5 Gating strategies of B-, T cell and myeloid flow cytometry staining.

Supplementary Table 1

Name / gene[1]	Sequence (5' to 3')	Purpose
KDM7A_cond_Fw	GAGTAGATGGTTTGGAAGATGTGG	Genotyping
KDM7A_cond_Rv	AGGCACAATGGAAACACTCAAGTG	Genotyping
KDM7A_probe_Fw	GGGTGGAGTAGGACTTAGATTT	Probe southern blotting
KDM7A_probe_Rv	CCACATCTTCCAAACCATCTAC	Probe southern blotting
PAC8.1_Fw	GCTGCTGTTATGACCACTAGAGGG	Genotyping
PAC8.1_Rv	AGACAGGGAAGGAGGTGTGG	Genotyping
EpoR-Cre_Fw	GTGTGGCTGCCCCTTCTGCCA	Genotyping
EpoR-Cre_Rv	CAGGAATTCAAGCTCAACCTCA	Genotyping
general-Cre_Fw	ACCCTGTTACGTATAGCCGA	Genotyping
general-Cre_Rv	CTCCGGTATTGAAACTCCAG	Genotyping
CAG_Flp_Fw	CCCATTCCATGCGGGGTATCG	Genotyping
CAG_Flp_Rv	GCATCTGGGAGATCACTGAG	Genotyping
KDM7A_m_qPCR_Fw	CCTTGACATTCTTGAGCTCC	qPCR
KDM7A_m_qPCR_Rv	TCTTTCGCTCTCCACTCAG	qPCR
Gapdh_m_qPCR_Fw	CTACTGGTGTCTTCACCACC	qPCR
Gapdh_m_qPCR_Rv	TCGTGGTTCACACCCATCAC	qPCR
α_m_qPCR_Fw	TTGGCTAGCCACCACCCT	qPCR
α_m_qPCR_Rv	CCAAGAGGTACAGGTGCA	qPCR
βmajor_m_qPCR_Fw	ATGGCCTGAATCACTTGGAC	qPCR
βmajor_m_qPCR_Rv	ACGATCATATTGCCCAGGAG	qPCR
βH1_m_qPCR_Fw	TGG ACA ACC TCA AGG AGA CC	qPCR
βH1_m_qPCR_Rv	ACC TCT GGG GTG AAT TCC TT	qPCR
εy_m_qPCR_Fw	TGGCCTGTGGAGTAAGGTCAA	qPCR
εy_m_qPCR_Rv	GAAGCAGAGCACAAGTTCCCA	qPCR
β_h_qPCR-Fw	TACAATTTGCTTCTGACACAAC	qPCR
β_h_qPCR-Rv	ACAGATCCCCAAAGGAC	qPCR
γ_h_qPCR-Fw	AGGTGCTGACTTCCTTGGG	qPCR
γ_h_qPCR-Rv	GGGTGAATTCTTTGCCGAA	qPCR
h_KDM7A_exF1	CACCGGGTTCCAAACCAGTGCAAGC	CRISPR guide
h_KDM7A_exR1	AAACGCTTGCACTGGTTTGGAACCC	CRISPR guide
h_KDM7Adeltest_F1	ACTGTGCTTATTTAGGGAGTAAGTC	CRISPR surveyor
h_KDM7Adeltest_R1	CCCAGTGTGCACATAGATGTAA	CRISPR surveyor

[1] _m_ = mouse; _h_=human; Fw = sense; Rv = antisense

Supplementary Table 2

Antibody	Manufacturer	Order #	Dilution
For flow cytometry			
CD71-FITC	BD Pharmingen	553266	1:400
Ter119-PE	BD Pharmingen	553673	1:400
cKit-PE-Cy7	BD Pharmingen	558163	1:200
CD44-APC	BD Pharmingen	559250	1:400
Ly6C-Brilliant Violet 605	BD Horizon	563011	1:500
2,4G2 block	Homemade	-	1:300
Fixable Viability Dye eFluor® 506	eBioscience	65-0866-14	1:400
CD3-FITC	BD Pharmingen	553062	1:320
CD25-PERCP-Cy5.5	BD Pharmingen	551071	1:160 for spleen or 1:640 for thymus
CD4-APC-Cy7	BD Pharmingen	560181	1:200
NK1.1-Pacific Blue	BD Horizon	560524	1:50
CD8a-PE-Cy7	eBioscience	25-0081-82	1:1600
CD44-PE	BD Pharmingen	553134	1:1000
CD62L-APC	eBioscience	17-0621-82	1:5000
CD21-FITC	eBioscience	11-0212-85	1:500
CD19-PERCP-Cy5.5	eBioscience	45-0193-82	1:320
B220-Alexa Fluor 700	eBioscience	56-0452-82	1:160
IgM-Bio	BD Pharmingen	553436	1:80
Streptavidin-APC-eFluor 780	eBioscience	47-4317-82	1:400
CD2-PE	eBioscience	12-0021-83	1:2500
CD23-PE-Cy7	eBioscience	25-0232-81	1:500
IgD-APC	eBioscience	17-5993-82	1:2500
F4/80-FITC	eBioscience	11-4801-85	1:100
CD11b-PERCP-Cy5.5	BD Pharmingen	550993	1:100
MHCII-Alexa Fluor 700	eBioscience	56-5321-82	1:400
Ly6C-Brilliant Violet 605	BD Horizon	563011	1:500
SiglecF-PE	PD Pharmingen	552126	1:320
Ly6G-PE-Cy7	BD Pharmingen	560601	1:500
CD11c-PertexRed	Invitrogen	MDC11c17	1:100
7-aminoactinomycin D	Invitrogen	A1310	1:400
For western blotting:			
Tubulin	Thermo Fisher	A11126	1:1000
KDM7A	Abiocode	R0234-2b	1:1000

Chapter 3

Conditional knockout of protein arginine methyl transferase 1, 4 and 5 in the hematopoietic system.

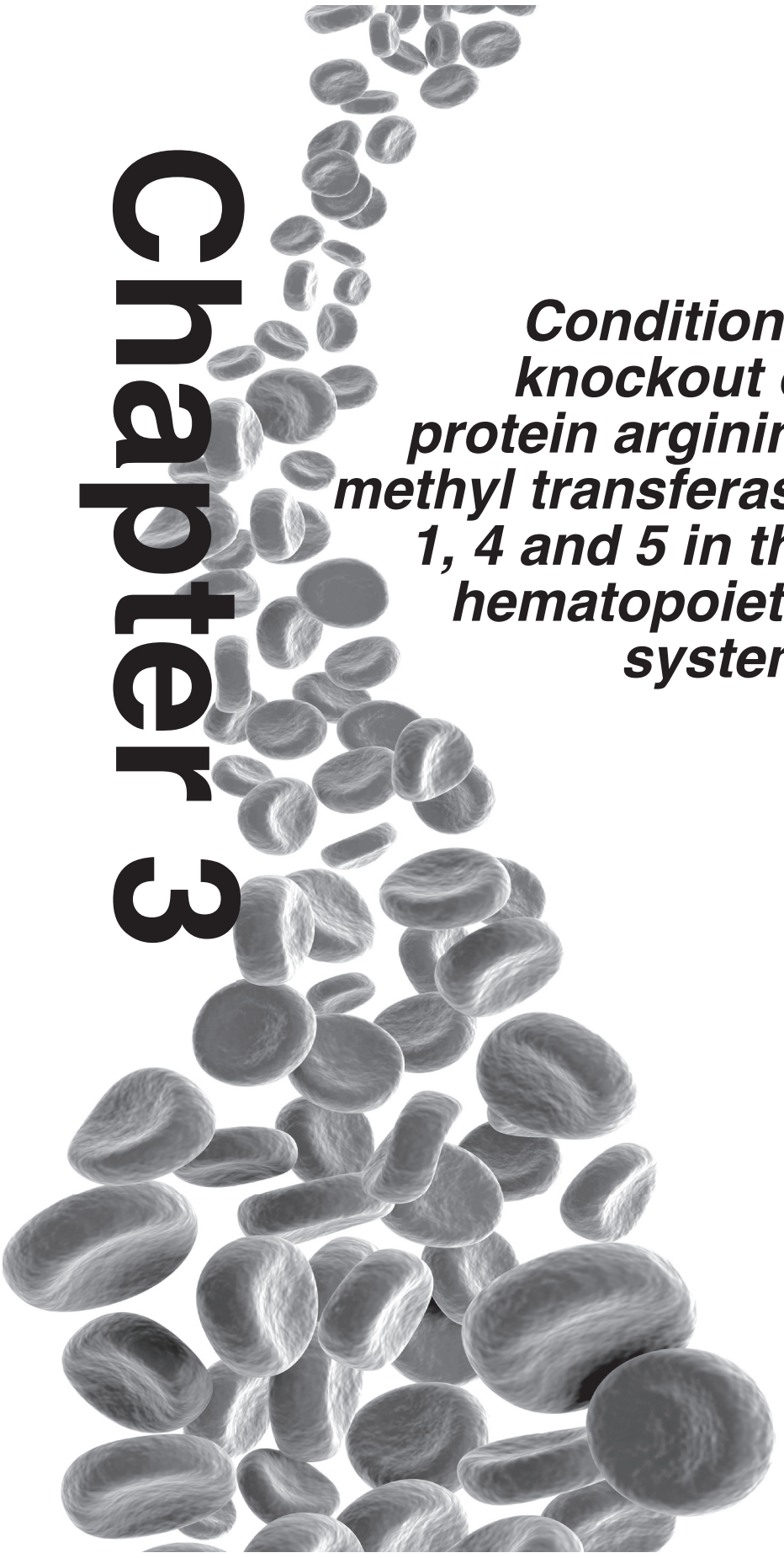

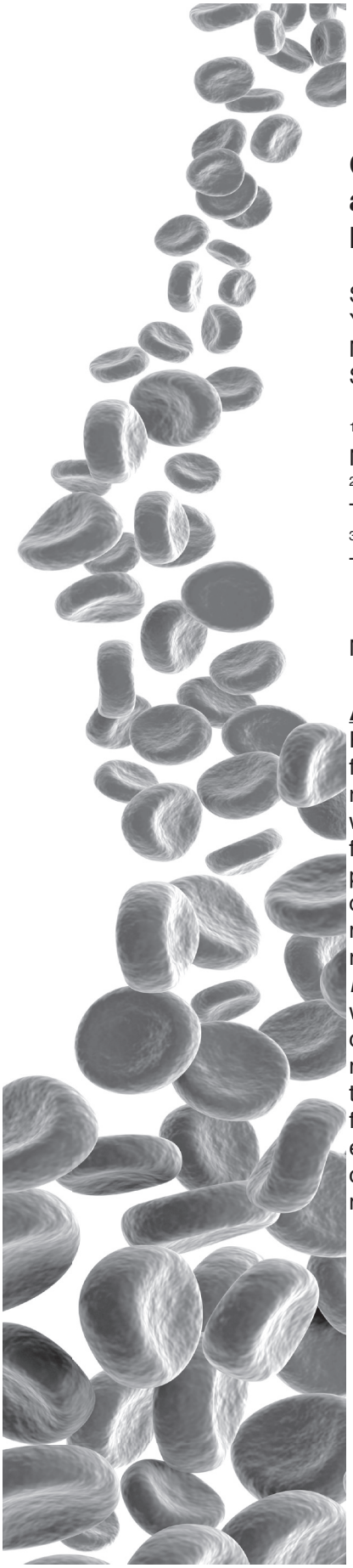

Chapter 3. Conditional knockout of protein arginine methyl transferase 1, 4 and 5 in the hematopoietic system.

Silvia Hoeboer[1], Nynke Gillemans[1], Alex Maas[1], Ryo Kurita[2], Yukio Nakamura[2], Anne Korporaal[1], Marco van Wingerden[1], Marjolein de Bruijn[3], Rudi Hendriks[3], Thamar Bryn van Dijk[1] and Sjaak Philipsen[1]

[1] Department of Cell Biology, Erasmus MC, Rotterdam, The Netherlands
[2] Cell Engineering Division, RIKEN, BioResource Center, Tsukuba Ibaraki, Japan
[3] Department of Pulmonary Medicine, Erasmus MC, Rotterdam, The Netherlands.

Manuscript in preparation

Abstract

Protein Arginine Methyl Transferases (PRMTs) are enzymes that function in a wide variety of cellular processes. To study their role in hematopoiesis *in vivo*, and in erythropoiesis specifically, we analzed the hematopoietic compartment in mice harbouring floxed alleles of *Prmt1*, *Prmt4* and *Prmt5* and the pIpC-inducible pan-hematopoietic *Mx1-Cre recombinase* gene. Recombination of the floxed *Prmt4* allele was very efficient. Deletion of *Prmt4* mainly affected T cell development, in agreement with previous reports. We observed a low recombination efficiency of the floxed *Prmt1* and *Prmt5* alleles, indicating selective survival of cells in which recombination had not occurred. Using tissue-specific constitutively active Cre lines, *Vav1-Cre* and *Vec-Cre*, we found more efficient recombination in *Prmt5* fl/wt mice compared to *Prmt5* fl/fl littermates. This supports the notion of selection for homozygous floxed cells that escaped recombination. The essential role of PRMT1 and PRMT5 in hematopoiesis was confirmed by CRISPR targeting in HUDEP-2 cells, a cell line modelling adult human erythropoiesis.

Introduction

Blood is composed of many different cell types, from immune cells to platelets, but the most common cells are the erythrocytes. When reticulocytes are released to the blood from the bone marrow (BM), they rapidly mature to erythrocytes that have an average lifespan of 120 days.[1] Erythrocytes are packed with hemoglobin (Hb), which facilitates oxygen uptake in the lungs and transport throughout the body to the organs. The composition of Hb changes during development. Before birth fetal hemoglobin (HbF) contains 2 α-globin and 2 γ-globin peptides to from a tetramer. After hemoglobin switching is completed during the first year of life, γ-globin is silenced to <1% and expression of adult β-globin is fully activated to form adult Hb (HbA), composed of 2 α-globin and 2 β-globin peptides.[2]

In sickle cell disease (SCD) and β-thalassemia the *HBB* gene, encoding β-globin, is affected. In SCD a point mutation *HBB*:c.20A>T leads to an amino acid substitution (p.Glu6Val) and creates sickle cell hemoglobin (HbS).[3,4] HbS is less soluble and leads to a disturbed environment within the erythrocyte.[4] As a response to low oxygen, HbS polymerizes and forces the erythrocytes to adopt a sickle shape. Sickled erythrocytes can block the microvasculature leading to local depletion of oxygen supply and promoting formation of more sickled erythrocytes. This leads to very painful sickle cell crises which may cause permanent damage to any organ.[5] In β-thalassemia mutations in the *HBB* gene cause reduced expression of the β-globin peptide, resulting in an imbalance with α-globin and insufficient levels of HbA.[6] In both diseases, most of the symptoms are ameliorated when combined with the benign condition of hereditary persistence of HbF (HPFH), which is characterized by high levels of HbF in adults.[7] Since β-hemoglobinopathy patients with HPFH display a more benign course of disease, therapies are aimed to raise levels of HbF in non-HPFH patients.[4] The only FDA-approved drug for SCD is hydroxyurea, which may increase the HbF levels up to 30% in some patients.[8,9] Other studies revealed that >25% HbF gives the best effects in SCD patients.[4] Hydroxyurea is not the definitive solution to SCD and β-thalassemia: there is a high variability in response between the patients, and the mechanisms behind hydroxyurea are poorly understood. Therefore, new therapeutic targets need to be revealed.

Several laboratory and genome-wide association studies (GWAS) have been performed in order to understand the mechanisms of high HbF and the hemoglobin switch. Some of the genes that are associated with γ-globin regulation are: *MYB*, *KLF*1, *SOX6*, *BCL11A* and *CHTOP*.[10-16]

We previously identified *CHTOP* to play a role in HbF repression.[14] *CHTOP* stands for Chromatin Target of *PRMT1*, and has been shown in *in vitro* studies to suppress HbF.[14] Upon lentiviral mediated CHTOP knockdown of human erythroid progenitor (HEP) cells and cultured mouse fetal liver (FL) cells carrying the human *HBB* locus PAC8, γ-globin levels increased up to 31% of total hemoglobin.[14] To identify CHTOP interacting partners, PRMT1 and PRMT5 were found using mass spectrometry.[14,17,18] We showed that both PRMT1 and PRMT5 can methylate CHTOP.

Previous work linked PRMT1 to *HBB* locus regulation[19] and PRMT5 to repression of the *HBG1/2* genes.[20,21] In addition, PRMT4 (also known as CARM1) is considered as a general cofactor for transcriptional activation.[22] The aim of this study was therefore to characterise the role of PRMT1, PRMT4/CARM1 and PRMT5 in erythropoiesis

and developmental regulation of globin expression. To achieve this aim, we used mice carrying conditional knockout alleles of *Prmt1*, *4* and *5*, and a single-copy transgene of the complete human *HBB* locus (PAC8.1). These mice were crossed with Cre lines to inactivate the floxed *Prmt* genes gene in a tissue-specific manner.

The mammalian protein arginine methyltransferase (PRMT) family consists of 9 members, and is divided in 3 groups: Type I, II and III.[23,24]. PRMTs catalyse the transfer of a methyl group from *S*-adenosyl-*L*-methionine (SAM) to the guanidino nitrogen atom of arginines. Type I is characterized by asymmetric ω-N^G,N^G-dimethylated arginines (ADMA), and includes PRMT1, PRMT2, PRMT3, PRMT4/CARM1, PRMT6 and PRMT8.[23] Type II is characterized by symmetric ω-N^G,N^G-dimethylation (sDMA), and includes PRMT5 and PRMT9.[25,26] PRMT7 is thus far the only Type III enzyme which is able to form ω-N^G-monomethylarginine (MMA) on histones.[27] Most PRMTs methylate arginine- and glycine rich motifs, called RGG/RG motifs or GAR-domains, except for PRMT4/CARM1, which prefers proline, glycine and methionine (PGM)-rich motifs.[28] In general the effect of arginine methylation is changing interacting partners, due to steric effects of hydrogen bond interactions without changing the charge of the molecule.[29]

In our study, we focussed on PRMT1, PRMT4/CARM1 and PRMT5. PRMT1 is a ~42 kDa protein that forms a homodimer.[30] In RAT1 fibroblast cells and mouse liver cells, PRMT1 is responsible for about 85% of the protein arginine methylation activity.[31] PRMT1 is associated with a number of proteins, including BTG1 and BTG2.[32] PRMT4/CARM1, a ~60 kDa protein, catalyses the methylation of other substrates than PRMT1, for example PABP1.[32] Loss of PRMT1 or PRMT4/CARM1 leads to perinatal death. The type II PRMT included in our study is PRMT5. This ~72 kDa protein is the major Type II enzyme and is able to from complexes in the cytoplasm as well as in the nucleus.[33-36] Cells lacking PRMT5 show problems with the splicing machinery.[37]

PRMTs can function both as activators and as repressors of transcription. PRMT1 and PRMT4/CARM1 are associated with active transcription by methylation of specific histones (H4R3me2a), and recruiting other transcriptional activators such as p300/CBP.[22,38] PRMT5 is associated with repressive functions through methylation of H3R3me2s, this will recruit DNA methyltransferase 3a (DNMT3a) leading to further gene repression by DNA methylation.[39] In contrast, PRMT5 is also able to fortify WDR5 mediated activation.[40] PRMTs are associated with many functions *in vivo*: from nerves, muscles and the immune system to metabolic diseases, aging and cancer.[22,41] PRMT1 induction in K562 cells promotes erythroid differentiation, and shRNA-mediated PRMT1 knockdown leads to suppressed erythroid differentiation.[42] PRMT1 expression enhances hemoglobin synthesis. According to recent literature loss of PRMT4 does not affect erythropoiesis and hematopoiesis, but is essential for myeloid leukomogenesis.[43] Other K562 and human erythroid progenitor *in vitro* studies revealed that the PRMT5 protein binds to the γ-globin promotor, via the nuclear zinc finger protein LYAR (Ly-1 antibody reactive clone) and DNA methyltransferase DNMT3A.[44,45] LYAR binds to the 5'untranslated region and silences γ-globin expression.[44] I*n vitro* studies using the methyl transferase inhibitor Adox led to a inhibition of PRMT5 and an increase of γ-globin expression in K562 cells.[46] Due to this multiplicity of the PRMT functions, we hope to be able to link them to γ-globin regulation and erythroid cell development. Since *Prmt1, Prmt4/Carm1* and *Prmt5* full knockouts die before birth, we used mice with floxed alleles of these genes in

combination with tissue-specific Cre recombinase knockin and transgenic lines.[47-49]

Material and Methods

Mice

All animal studies were approved by the Erasmus MC Animal Ethics Committee. In this study, transgenic mouse strains were used: human β-globin (*HBB*) locus PAC8.1; *Prmt1, Prmt4 and Prmt5* floxed alleles (Eucomm).[50,51] We used several Cre recombinase lines active in the hematopoietic system: endothelial, germ cell and pan hematopoietic *Vav1*-Cre[52]; vascular endothelial cadherin (*Vec*-Cre)[53], and the interferon inducible *Mx1*-Cre[54]. Genotyping was performed by PCR using genomic DNA isolated from toe biopsies. Primers are listed in Supplementary Table 1. Embryos were collected between embryonic day (E) 10.5 and E16.5; genotyping was performed by PCR on head DNA. Adults were analysed with a minimum age of 10 weeks and maximum age of 21 weeks. To detect Cre-mediated recombination of the *Prmt1, Prmt4 or Prmt5* locus, Southern blot analysis was done on BM, spleen and thymus using probes listed in Supplementary Table 1. To induce *Mx1*-Cre-mediated recombination, mice were injected subcutaneously (SC) with 20µg/g body weight polyinosinic-polycytidylic ribonucleic acid (pIpC; P0913, Sigma Aldrich) for 3 times every other day starting at the end of the first week after birth. Because the animals were still small, we could not take pre-treatment samples to measure blood parameters. Instead, we used blood samples from littermates without *Mx1*-Cre that were also treated with pIpC. After about 2 months, 1-2 weeks prior to analysis, the mice received a final pIpC injection. In some experiments, mice were subsequently treated with phenylhydrazine (PHZ P6926; Sigma Aldrich) to induce stress erythropoiesis. The mice were injected SC with 0.4% (w/v) PHZ in phosphate buffered saline (PBS) (12µl/g body weight) for 2 consecutive days (Day 1 and 2). Mice were collected at Day 5 for analysis.

Blood analysis

Peripheral blood was collected from the mandibular vein of adult mice >10 weeks. Standard blood parameters were measured using an automated hematologic analyser (Scil Vet ABC). All values were set at 100% for the control mice without Cre. We also performed flow cytometry on the blood. Leftovers were stored in TRI-reagent (93289, Sigma Aldrich) at -20°C for RNA isolation.

Flow cytometry analysis

Single cell suspensions from blood, bone marrow, spleen and thymus were made by flushing and crushing the material and passing through cell strainers (40 µm, 352340, BD Bioscience). The cells were diluted and washed in PBS containing 1mM EDTA. Before staining, the cells were washed in FACS buffer (PBS, 1% (w/v) bovine serum albumin (BSA) and 1 mM EDTA). ~10^6 cells were incubated for 30 minutes with the primary antibodies. Antibodies used are listed in Supplementary Table 2. Depending on the antibody combination, cells were washed in FACS buffer or PBS. Live cells were distinguished negatively by 7-aminoactinomycin D (7-AAD; A1310; Invitrogen) staining and were directly analysed. Alternatively, the cells were stained for 30 minutes using the Fixable Viability Dye eFluor 506 (eBioscience) and washed in PBS. Cells were measured on a Fortessa flow cytometer (BD Bioscience).

Southern blot analysis

Genomic DNA was isolated from bone marrow, spleen and thymus. No selection was

performed, unless depicted otherwise. Genomic DNA (20 μg) of *Prmt1* conditional knockout (cKO) mice was digested with 20 units of DraI enzyme overnight at 37°C, for *Prmt4* and *Prmt5* we used 20 units of EcoRI at 37°C overnight. The fragments were separated on a 0.7% agarose gel, and subsequently transferred to a nylon membrane. Primers to generate the probes are listed in Supplementary Table 1. The probes were labelled with α^{32}P-dATP (PerkinElmer) using a nick translation kit (GE Healthcare). For *Prmt1* the probe size was 492 base pairs (bp), *Prmt4* 522 bp and *Prmt5* 428 bp. After hybridisation and washing the blot was exposed to a phosphor screen which was scanned using a Typhoon FLA9500 instrument (GE Healthcare). The floxed *Prmt1* allele will be visualised at 4.87 kb and the recombined allele at 3.82 kb. The floxed *Prmt4* allele will be visualised at 6.8 kb and the recombined allele at 5.1 kb. The floxed *Prmt5* allele will be visualised at 2.65 kb and the recombined allele at 1.8 kb.

Cell culture

Human Umbilical cord blood-Derived Erythroid Progenitor (HUDEP-2) cells were cultured in StemSpan medium (Stem Cell Technologies), supplemented with doxycycline (DOX, 1 mg/ml), stem cell factor (SCF, 100 ng/ml, R&D Systems), erythropoietin (EPO, 2 units/ml, Janssen-Cilag), and dexamethasone ($1x10^{-6}$M, Sigma) as described previously.[55] To induce differentiation we used StemSpan medium supplemented with 500 μg/mL iron-saturated transferrin (Scipac), human AB plasma (3%, Sigma), and EPO (10 units/ml). For cell counting we used a CASY TTC instrument (Roche).

Lentiviral production and transduction

For knockout experiments of *PRMT1*, *PRMT4* and *PRMT5* in HUDEP-2 cells we transduced the cells first with lentiCas9-Blast (Addgene plasmid # 52962).[56] The lentiviral particles were produced in Human Embryonic Kidney (HEK) 293T cells as described previously.[57] Supernatant from the HEK-293T cells was collected on Day 1, 2 and 3 after transfection. On the third day, the supernatant was filtered using a 0.45μm filter. The virus particles were collected using centrifugation of 20,000 rpm for 2:15 hours at 4°C. The HUDEP-2 cells were exposed to the lentivirus for 78-92 hours. Blasticidin S (10 μg/ml; Santa Cruz) was added for the selection of transduced cells. After selection, we performed a second transduction with a vector containing the guide RNA (gRNA). This vector was made from the pSpCas9(BB)-2A-Puro (PX459) V2.0 plasmid, which was a gift from Dr. Feng Zhang (Addgene plasmid # 62988).[58] The gRNAs were designed with the online CRISPR design tool of the Zhang laboratory at MIT (http://crispr.mit.edu/). As a threshold, we only used guides with a score higher than 85. Furthermore, we blasted the guide targets for predicted off-target effects. The gRNA oligonucleotides (Integrated DNA Technologies) are listed in Supplementary Table 1. We transferred the gRNA part to a lentiviral vector; pLKO.1 puro which was a gift from Bob Weinberg (Addgene plasmid # 8453).[59] After transduction, we added puromycin (1 μg/mL; Sigma) for 24 hours to the cells.

To check the effect of the CRISPR we designed PCRs around the gRNA target regions. Using Platinum Taq polymerase (Invitrogen) according to the manufacturer's instructions, we amplified a product of ~523-553 bp. Subsequently, we used the Surveyor Mutation Detection kit (Integrated DNA Technologies) according to the manufacturer's instructions, to detect heteroduplexes indicative of CRISPR-induced

mutations.

PRMT5 inhibiting compound GSK591

The PRMT5 inhibiting compound GSK591 (Sigma ML1751) was dissolved in DMSO and used at different concentrations in HUDEP-2 cells.

Protein extraction and western blotting

Whole cell lysates of unselected cells of blood, BM, spleen and HUDEP-2 cells were prepared using RIPA buffer (20mM Tris pH7.4, 150 mM NaCl, 1% NP40, 0.1% SDS, 0.5 mM EDTA, and 0.5% sodium deoxycholate) supplemented with complete protease inhibitor mix (Roche) and Pefablock (Roche).[60] The samples were lysed on ice for 15 minutes before centrifugation 15 minutes at 10,000 rpm at 4°C. Supernatant was collected and mixed with 4x Sample Buffer (0.05M Tris pH6.8, 0.3 mg/mL, 8% SDS, 40% glycerol). Whole cell lysates were separated by 10% or 12.5% SDS-PAGE, the gels were transferred to nitrocellulose membranes (0.45 μm, GE Healthcare), and probed with antibodies listed in Supplementary Table 2.

TIDE

On the PCR fragments of genomic DNA we performed TIDE (Tracking of Indels by DEcomposition) analysis (https://tide.nki.nl/) to check the efficiency of the CRISPR guides.[61]

3

Results

PRMT4: analysis of normal hematopoiesis

In previous studies from our laboratory we identified a number of potential γ-globin repressors. Here we present our findings concerning the protein arginine methyltransferases PRMT1, PRMT4 and PRMT5.

According to literature, PRMT4/CARM1 is not essential for normal hematopoiesis but necessary for leukemogenesis.[43] To test whether PRMT4 modifies functional parameters of hematopoietic cells, we crossed with PAC8.1/wt; *Prmt4* fl/fl mice with *Mx1-Cre/wt* mice. Mx1-Cre is a pIpC-inducible Cre recombinase, which is active from the hematopoietic stem cell, we started the pIpC injection course within one week after birth. Blood parameters were analysed when mice were 10 weeks old. Blood samples from littermates without *Mx1*-Cre that were also treated with pIpC were used as controls.

We didn't observe significant differences in the blood parameters between PAC8.1/wt; *Prmt4* fl/fl mice with and without *Mx1-Cre* (Figure 1A). Cellularity of femur BM, spleen and thymus was calculated from cell suspensions using a CASY instrument, Figure 1B. Although the number of BM and spleen cells were lower in KO mice, this difference was not significant. The only significant difference observed with the total cell numbers was in the thymus. RBC size distribution (Figure 1C), and expression of globin genes measured by RT-qPCR using RNA isolated from bone marrow (figure 1D) and spleen (figure 1E) were also similar between animals with and without Mx1-Cre. We also found that the *Prmt4* cKO animals weighed slightly, but not significantly, less than the controls mice (Figure 1F). This could explain most of the observed reductions in cell counts, which were generally also not significant except for the thymus. We checked the recombination efficiency on genomic level (Figure 1G). Recombination efficiency was very high reaching 100% in some of the *Prmt4* cKO animals. Since *Mx1*-Cre is active from an early hematopoietic stem cell,

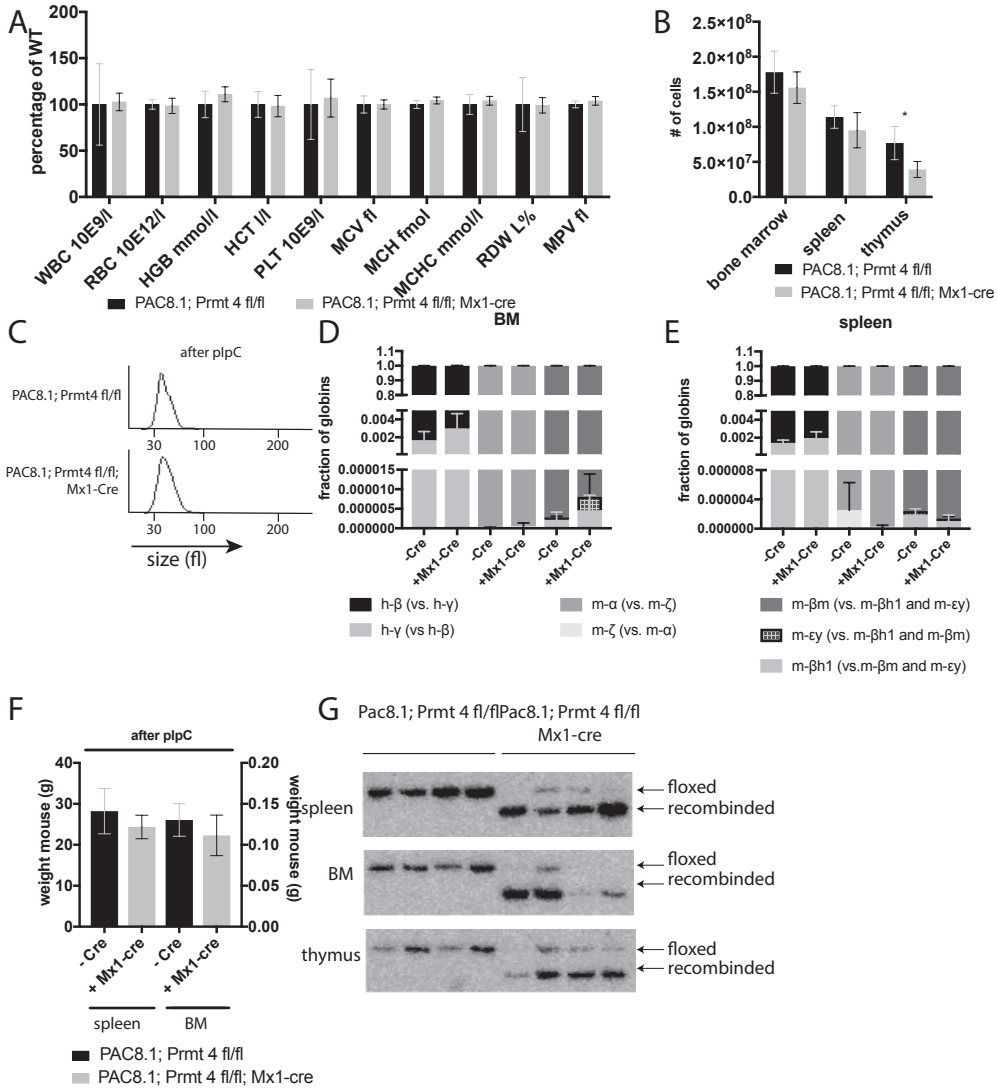

Figure 1. Control and Prmt4 cKO mice. (age 10 weeks WT n=4 and cKO n=4. * indicates a p-value <0,05.) (A) Measured blood parameters: WBC (white blood cells); RBC (red blood cells); HGB (hemoglobin); HCT (haematocrit); PLT (platelets); MCV (Mean Corpuscular Volume); MCH (Mean Corpuscular Hemoglobin); MCHC (Mean Corpuscular Hemoglobin Concentration); RDW (RBC distribution width); MPV (mean platelet volume) measured one day before sacrificing. (B) Number of cells per tissue counted using CASY TTC instrument. (C) Size distribution of RBCs. (D) and (E) Expression fraction of g-globin and mouse globins were determined using qRT-PCR. Fractions were calculated using g/g+b, z/(z+a) and bm/(bm+ey+bH1). (F) Mouse (left panel) and spleen weights (right panel). (G) Southern blot analysis of spleen, bone marrow and thymus DNA after pIpC treatment.

it might affect not only the erythroid cells, but also other cell types. So we extended these observations with a pan-hematopoietic flow cytometry analysis. From the literature it is known that *Prmt4* null embryos display aberrant T cell development and maturation in E18.5 embryos.[20,62] Here we report the effects of PRMT4 ablation

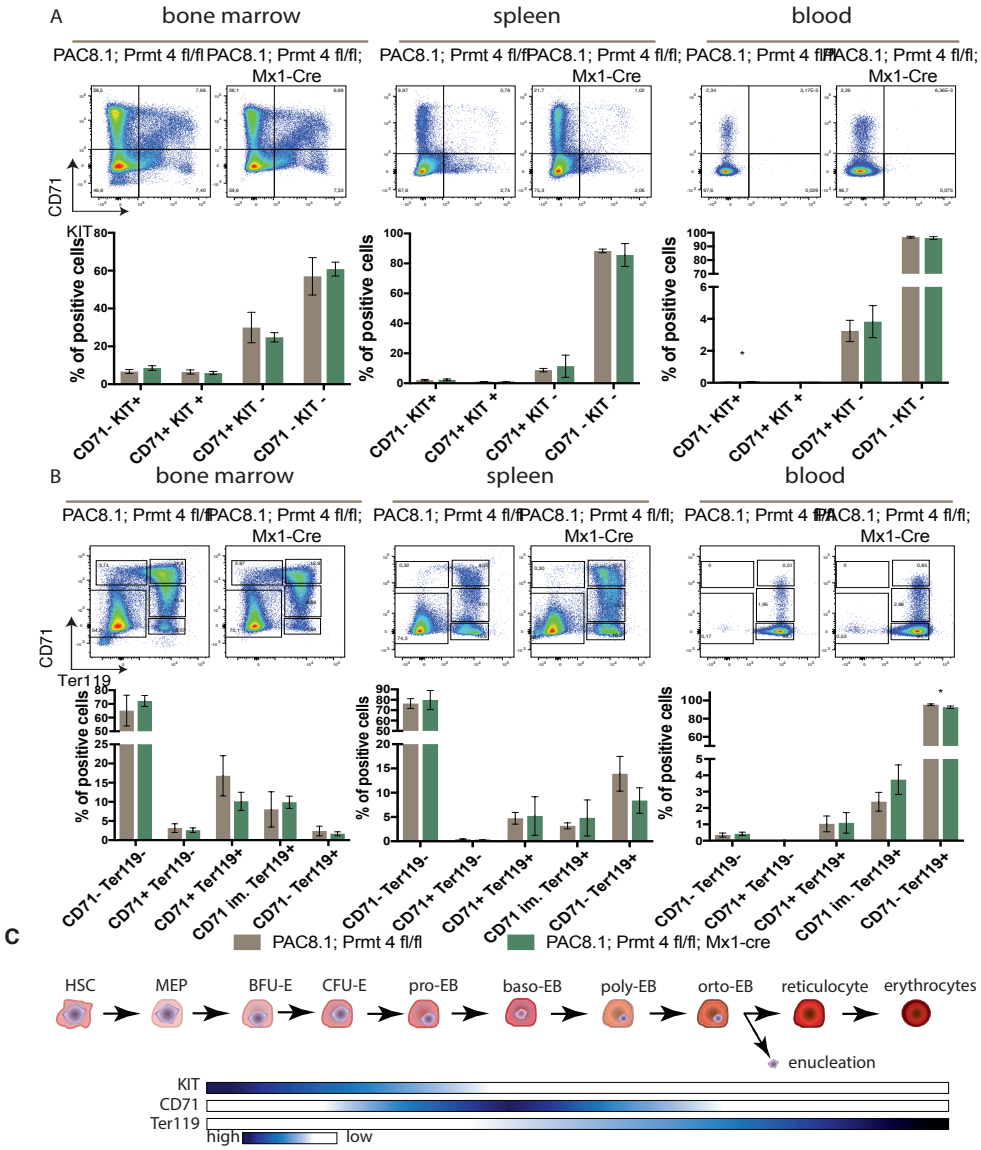

Figure 2. Flow cytometry analysis of erythroid cells in control and Prmt4 cKO mice. After live/dead gating, different erythroid progenitor cell populations were measured using CD71/Ter119 and CD71/KIT. (A) Maturation starts with CD71-/KIT+ and moves counter clock wise. (B) Using the Ter119 marker: maturation starts with CD71-/Ter119- and moves clock wise to the mature erythrocytes. (C) graphical repesentation of the distribution of the erythroid facs markers CD71, KIT and Ter119.(WT=4 vs cKO n=4. * indicates a p-value of <0.05).

on adult hematopoiesis.

To analyse the erythroid compartment in more detail, we stained BM, spleen and blood with CD71, Ter119 and KIT, Figure 2. Maturation from erythroid cells goes from KIT single positive, panel A, then they become KIT/CD71 double positive. After they lose the KIT marker, cells will become CD71/Ter119 positive, Figure 2 panel B. Subsequently they will lose the CD71 marker as a mature erythroid cell. In *Prmt4* cKO mice we observed

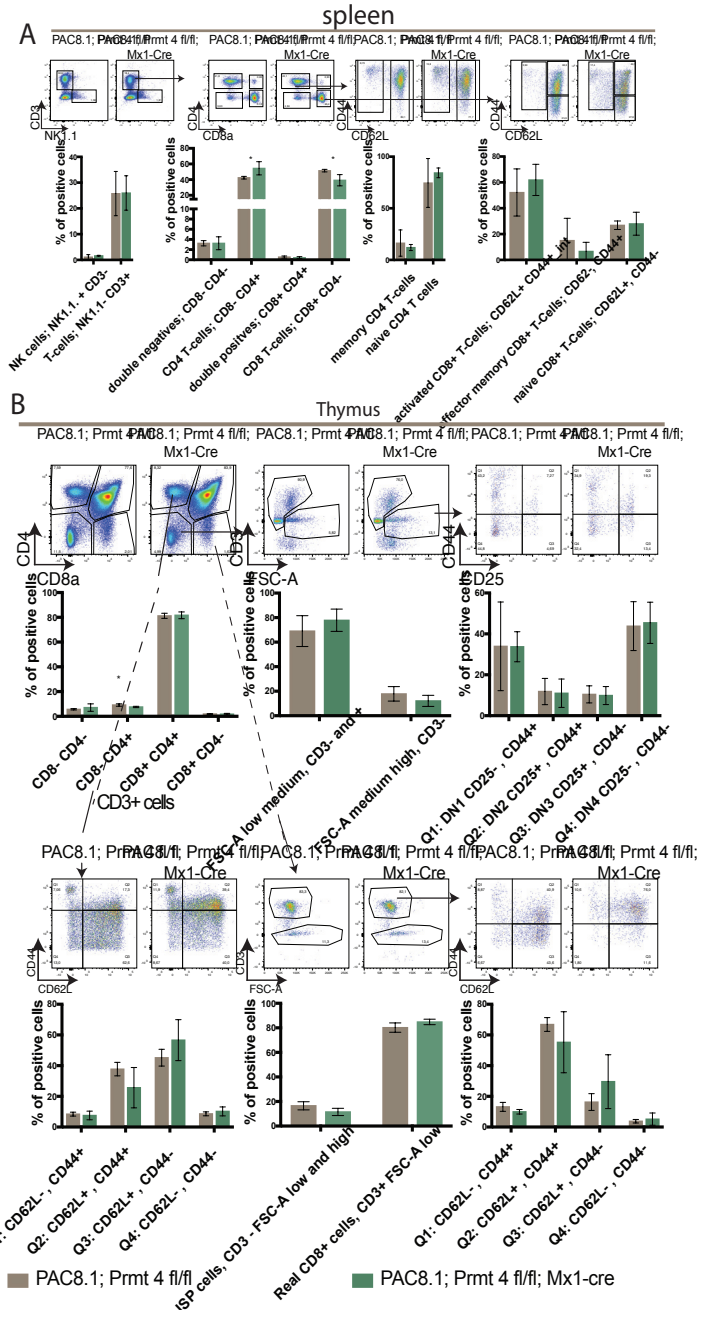

Figure 3. T cell flow cytometry analysis of control and Prmt4 cKO (A) spleen and (B) thymus. After live/dead marking (not shown) CD3/NK1.1 or NK1.1/FSC-A was used to distinguish between NK-cells (NK1.1+) and T cells (NK1.1- /(CD3+)). Different populations of T cells are further specified using CD4/CD8. CD4-/CD8- double negative (DN) cells are immature T cells, in thymus they are located in the capsule. In the thymus (panel A), they move to the cortex and become CD8+/CD4+ double positive (DP) which are precursor cells. Mature T cells are characterized which are located in the medulla of the thymus are marked as single positive (SP) for CD4 or CD8. From here the gating strategy differs between spleen and thymus. In spleen (panel B) the CD4+ population is CD62L/CD44 used to distinguish CD4 memory (CD62L-/CD44+) and naïve CD4 T cells (CD62L+/CD44-and+). Within the CD8+ population we can specify activated (CD62L+/CD44+), effector (CD62L-/CD44+) and naïve (CD62L+/CD44-) T cells. In thymus DN and SPs are further categorized using CD3/FSC-A, to distinguish immature negative and mature positive cells. Subsequently, different maturation stadia of the DN immature cells are marked using CD25/CD44. DN1 is CD25-/CD44+, DN2 CD25+/CD44+, DN3 CD25+/CD44- and DN4 is CD25-/CD44-. The mature SP cells are further analysed using CD62L/CD44: effector T cells are characterized by CD62L-/CD44+, central memory T cells carry CD62L+/CD44+, and naïve T cells are CD62L+/CD44-. Immature single positive (ISP) cells are marked by CD8 SP and then CD3-. (WT n=4 vs cKO n=4. * indicates a p-value of < 0.05).

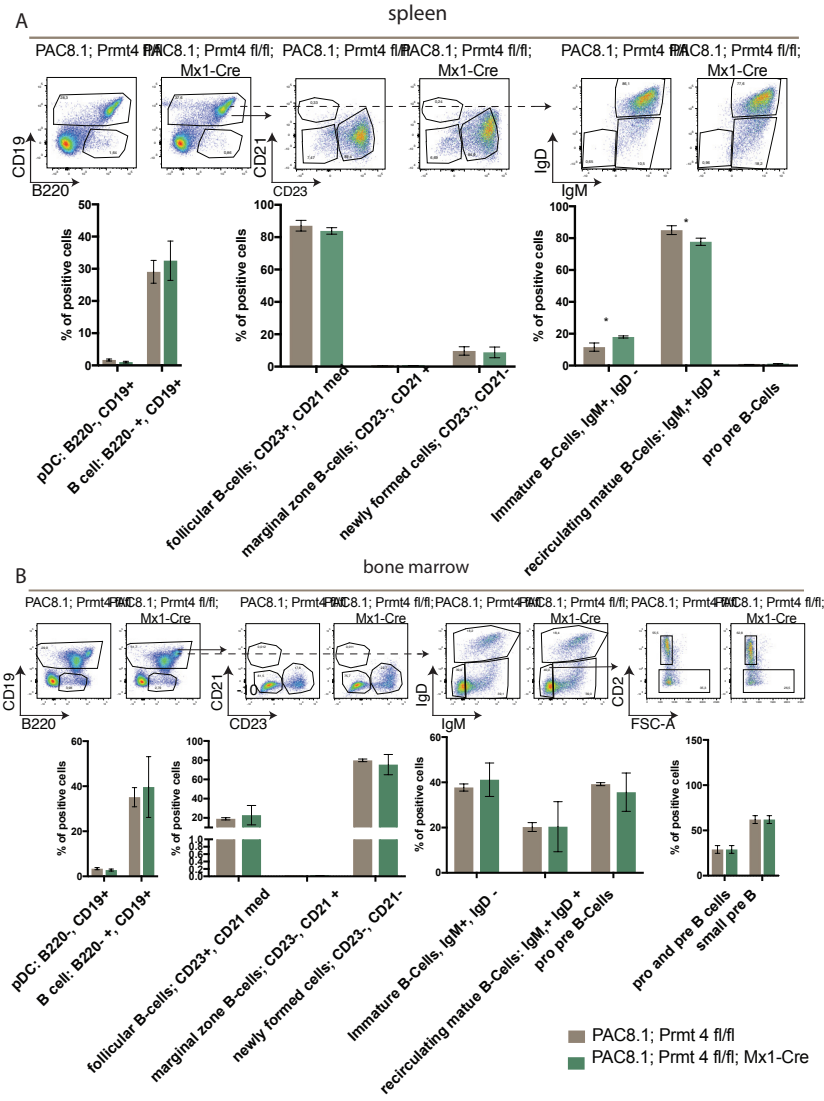

Figure 4. B cell flow cytometry analysis of control and Prmt4 cKO (A) spleen cells and (B) bone marrow. First, we gated for single cells, and lymphocytes using FSC-A/FSC-H and FSC-A/SSC-A. Subsequently we used the markers B220/CD19 markers to distinguish the plasmacytoid dendritic cells (pDC; CD19-/B220+) and B cells (CD19+/B220+ and -). The B cell population is thereafter subdivided in six groups. Three subpopulations are divined using CD23/CD21; follicular (CD23+/ CD21 medium); marginal zone (CD23-/CD21+) and newly formed (CD23-/CD21-) B cells. IgM/IgD markers are used to distinguish immature (IgM+/IgD-); recirculating (IgM+/IgD+) and pro/pre (IgM-/ IgD-) B cells. The last group is in BM cells further specified as pro/pre-B cells (CD2-) and small pre-B cells (CD2+) using CD2/FSC-A. (WT n=4 vs cKO n=4).

two differences that were significant, both in the peripheral blood. One was in the CD71-/KIT+ population, which is an increase of immature cells, that goes from 0.0027% to 0.0064%, which is so small that it is irrelevant. Those cells might be non-erythroid progenitors. The second difference was found in the CD71-/Ter119+ population, representing mature erythrocytes, which was decreased by ~3% in the

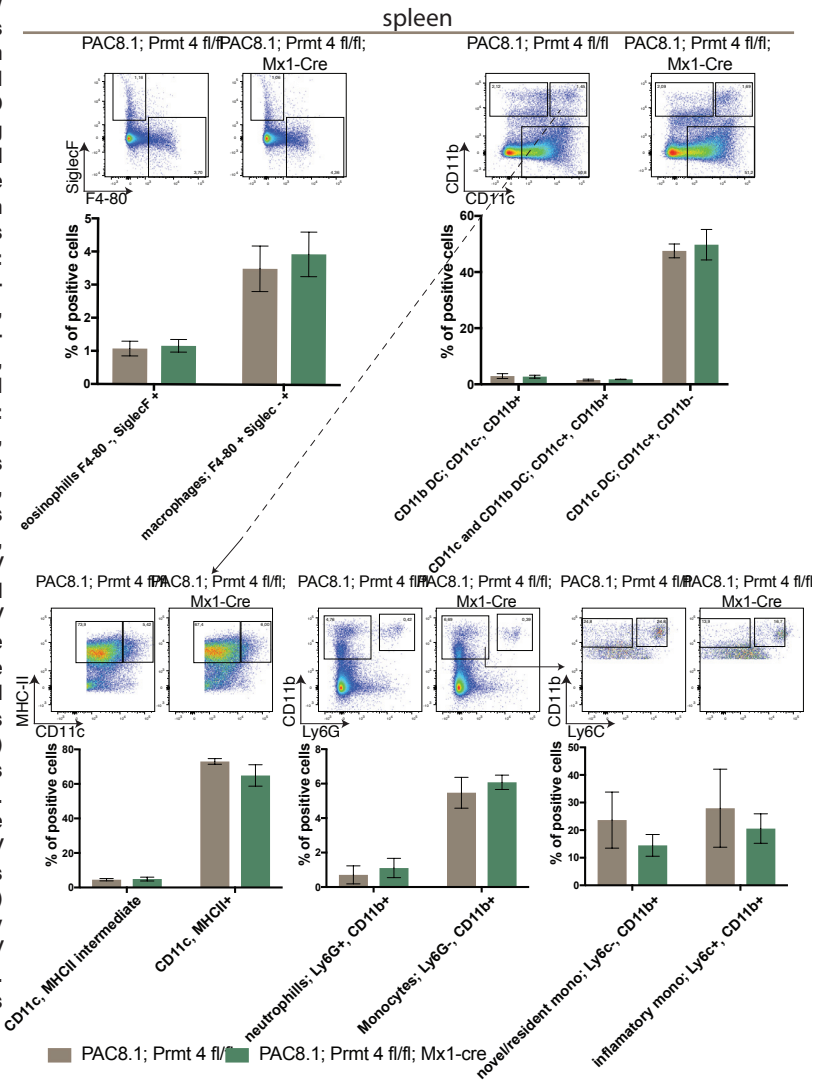

Figure 5. Flow cytometry analysis for myeloid cells in spleen from control and Prmt4 cKO mice. After gating for living cells and lymphocytes, we could distinguish 7 different types of myeloid cells: eosinophils (F4-80-/SiglegF+), macrophages (F4-80+/SiglegF+), conventional dendritic cells (DCs: CD11c+/CD11b+), immature DCs (CD11c+/CD11b-), other myeloid cells (CD11c-/CD11b+), neutrophils (Ly6G+/CD11b+) and monocytes (Ly6G-/CD11b+). The immature DCs are further categorised as small DCs (CD11c-/MHCII+) and large DCs (CD11b+/MHCII+). Monocytes are subdivided in novel/resident monocytes (CD11b+/Ly6C-) and inflammatory monocytes (CD11b+/Ly6C+). (WT n=4 vs. cKO n=4. * indicates p<0.05).

Prmt4 cKO animals. But this was not reflected in the blood parameters (Figure 1A). With specific interest, we looked at the different T cells populations, because we observed a reduced thymus in Prmt4-deleted mice (figure 1B), and because literature describes aberrant T cell development and maturation in embryos.[62] Figure 3 shows the different T cell populations in the spleen (panel A) and in the thymus (panel B). After gating for live/dead cells, we gated for CD3/FSC-A, as T cells are CD3- and NK cells CD3+. Immature T cells within the capsule of the thymus are CD8-/CD4-negative (DN). After moving to the cortex, the precursor T cells become CD8+/CD4+ positive (DP). Subsequently, the T cells become single positive (SP) for CD4 or CD8 and move to the spleen. Using CD62L and CD44 we can specify these cells further. CD4+ SP cells are subdivided in memory (CD62L-/CD44+) and naïve (CD62L+/CD44-and+) T cells. CD8 SP cells are divided in activated (CD62L+/CD44+), effector

(CD62L-/CD44+), and naïve (CD62+/CD44-) CD8+T cells.
In spleen, we observed a significant increase of almost 12% of CD4 SP cells, and a decrease of 11% of CD8 SP cells. Other populations were not affected by the conditional knockout of PRMT4.
In thymus, we observed a small decrease of 2% in the CD4 SP population. So, the differences in spleen are more pronounced than in the thymus. This could be caused by the maturation of the T cells, which first are DN, then become DP and then SP for CD4 or CD8. In thymus, the main population are the DP CD8+/CD4+ cells. When maturation is complete, the cells leave the thymus. Since the genotype of the *Prmt4* conditional knockout affects the SP CD4 and CD8 T cells, this would be observed more easily in the spleen where these cells accumulate, rather than in the thymus.
Next, we analysed the mice for different B cell populations present in spleen and BM using flow cytometry. After gating for living, single cells and lymphocytes, we used B220/CD19 to distinguish the plasmacytoid dendritic cells (pDCs: CD19-/B220+) from the total B cell population (CD19+/B220+and-). Subsequently we can specify 6 different B cell categories: follicular (CD23+/CD21-), marginal zone (CD23-/CD21+) and newly formed (CD23-/CD21-) B cells, and immature (IgM+/IgD-), recirculating (IgM-/IgD+), and pro/pre- (IgM-/IgD-) B cells. The last group can be further specified in BM using CD2/FSC-A, the small pre-B cells are CD2+ and conventional pro/pre-B cells are CD2 low. Figure 4 shows the percentages of those different cell populations in spleen (panel A) and BM (panel B). Two changes in the splenic B cell populations can be observed. The immature B cells (IgM+/IgD-) are increased by 7% in the *Prmt4* cKO animals compared to the controls. In contrast, the percentage of recirculating mature B cells was decreased by 8%. This suggests delayed B cell maturation in the absence of PRMT4. The other measurements of B cell populations did not reveal significant differences between the controls and the *Prmt4* cKO animals.
For different myeloid cell populations, we checked the spleen. First, we gated for living cells and leukocytes. Using F4-80/SiglegF we distinguished eosinophils (F4-80-/SiglegF+) and macrophages (F4-80+/SiglegF+). In addition, with the help of markers CD11c/CD11b, we distinguished different dendritic cell (DC) populations: conventional DCs are CD11c+/CD11b+, immature DCs are CD11c+/CD11b- and other myeloid cells within this staining are CD11c-/CD11b+. Finally, neutrophils are Ly6G+/CD11b+, and monocytes are Ly6G-/CD11b+. Monocytes are further specified in novel/resident (CD11b+/Ly6C-) and inflammatory (CD11b+/Ly6C+) monocytes. Figure 5 shows our findings concerning the myeloid cells in the *Prmt4* cKO mice; no significant changes were found in any of the myeloid populations analysed.

PRMT4: analysis of stress hematopoiesis

In mice, steady state erythropoiesis is located in BM. Stress erythropoiesis initiated by anemia, however, takes place in the spleen, and is controlled by distinct environmental factors. To investigate whether Prmt4 affects stress erythropoiesis in the spleen, anemia was induced in *Prmt4* cKO mice by administration of PHZ on 2 subsequent days. Three days after the second PHZ injection, blood was taken from the mandibular vein and analysed on the animal blood cell counter (Figure 6A and B). No significant differences were found between control and *Prmt4* cKO littermates. The number of cells in the BM, spleen and thymus were also not significantly different (Figure 6C).

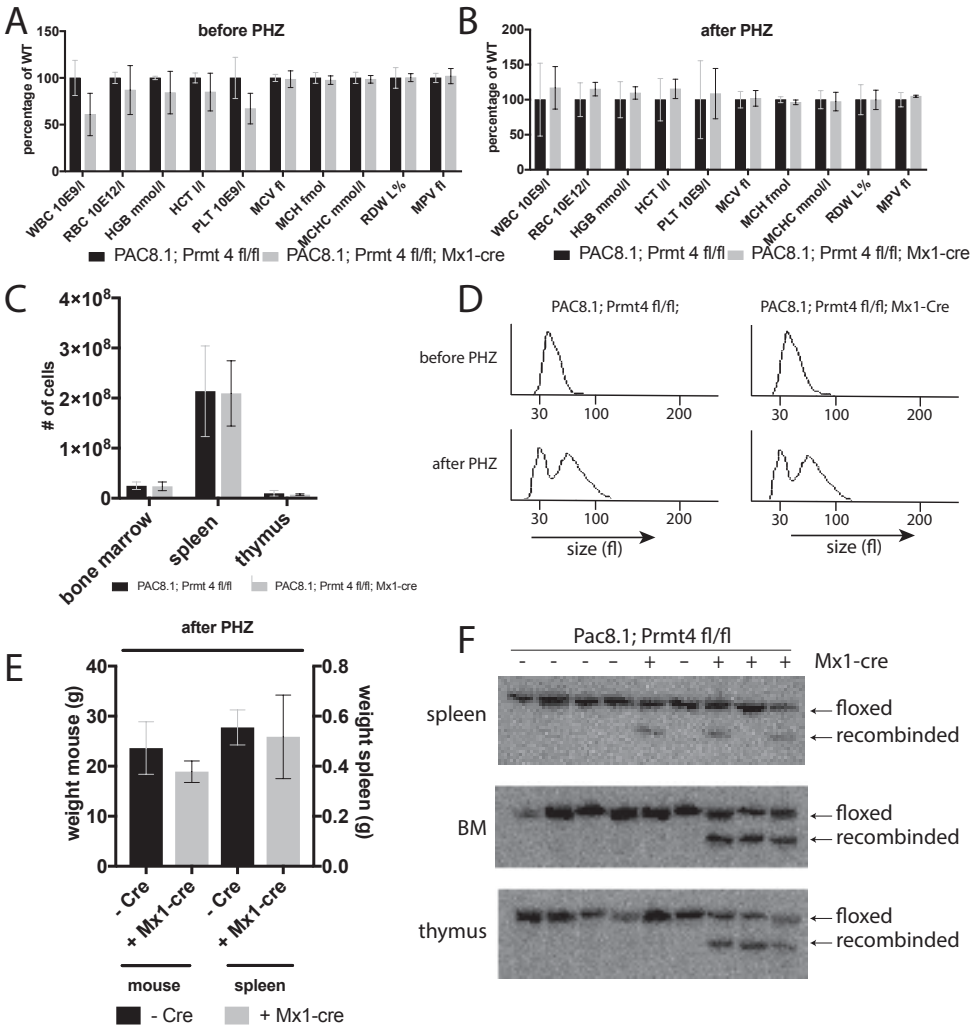

Figure 5. Flow cytometry analysis for myeloid cells in spleen from control and Prmt4 cKO mice. After gating for living cells and lymphocytes, we could distinguish 7 different types of myeloid cells: eosinophils (F4-80-/SiglegF+), macrophages (F4-80+/SiglegF+), conventional dendritic cells (DCs: CD11c+/CD11b+), immature DCs (CD11c+/CD11b-), other myeloid cells (CD11c-/CD11b+), neutrophils (Ly6G+/CD11b+) and monocytes (Ly6G-/CD11b+). The immature DCs are further categorised as small DCs (CD11c-/MHCII+) and large DCs (CD11b+/MHCII+). Monocytes are subdivided in novel/resident monocytes (CD11b+/Ly6C-) and inflammatory monocytes (CD11b+/Ly6C+). (WT n=4 vs. cKO n=4. * indicates p<0.05).

Histograms of RBCs size distribution revealed clear differences before and after PHZ treatment; in response to the anemia, a population of newly formed reticulocytes appears (Figure 6D). This response is similar between the control and *Prmt4* cKO littermates. This is in agreement with the MCV/MCH/MCHC values measured on the animal blood cell counter (Figure 6A). In addition, the body and spleen weights were not significantly different between the two groups of mice (Figure 6E). PHZ treatment did result in a ~5-fold increase in spleen weight (compare Figure 1), as a result of the stress erythropoiesis response.

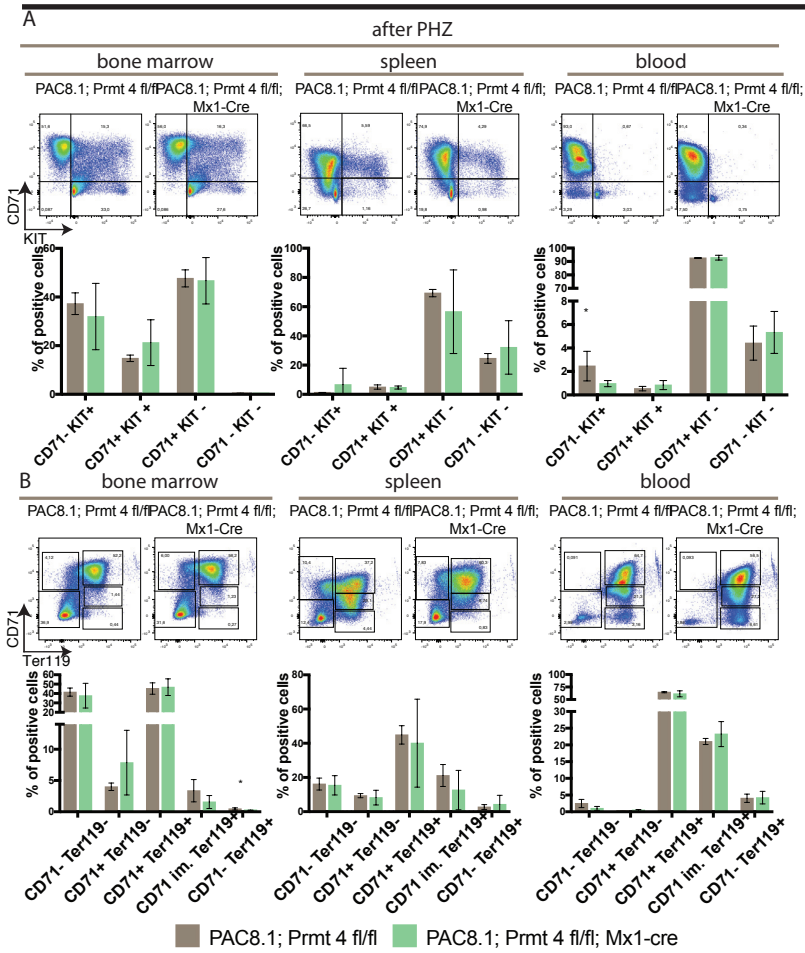

Figure 7. Flow cytometry analysis of erythroid cells in control and Prmt4 cKO mice after PHZ treatment. After live/dead gating we distinguished different erythroid progenitor cell populations using (A) CD71/KIT and (B) CD71/KIT. (WT=4 vs cKO n=4. * indicates a p-value of <0.05).

Figure 6F shows the accompanying Southern blot analysis. Unfortunately, the recombination rate was much lower, compared to the previous Southern blot (Figure 1G). In the best recombined samples, we observed a recombination of about 50%. Also, there are two animals with some recombination in the spleen, but not in BM, and vice versa. This is remarkable, since the recombination was 80-100% in all tissues in the experiment without PHZ. Apparently, the PHZ treatment results in the selection of cells that escaped *Mx1*-Cre mediated recombination. Therefore, we analysed erythropoiesis in more detail, using expression of KIT, CD71 and Ter119 to stage differentiation. The effect of PHZ treatment on the erythroid compartment was clearly observed in animals of both genotypes (compare Figure 7 with Figure 2). For example, blood is normally composed of 95% CD71-/Ter119+ erythrocytes;
after PHZ treatment this was reduced to about 5-10%, while many more CD71+/Ter119+ cells (reticulocytes) were found. This confirms the hemolytic effect of PHZ in the mice. It is striking that the variation in Prmt4 cKO samples is much larger than among control mice. As a result, we did not observe major differences. Yet, we observed two minor but significant differences between the control and *Prmt4* cKO animals after PHZ treatment. The CD71-/Ter119+ population halved from 0.4% to 0.2% (Figure 7) in bone marrow. These are mature cells within

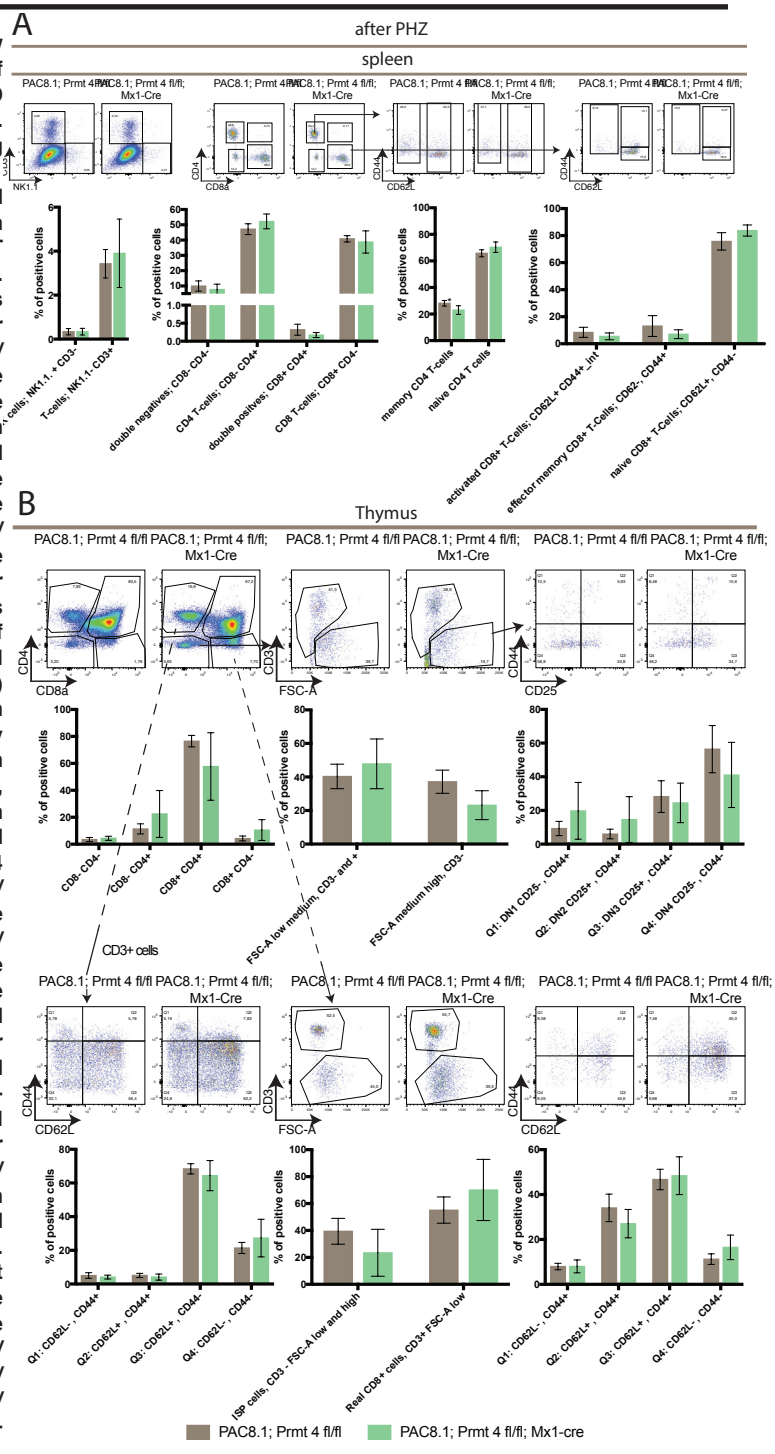

Figure 8. T cell flow cytometry analysis of control and Prmt4 cKO mice after PHZ treatment. After live/dead marking (not shown) CD3/NK1.1 or NK1.1/FSC-A was used to distinguish between NK-cells (NK1.1+) and T cells (NK1.1- /(CD3+)). Different populations of T cells were further specified using CD4/ CD8. CD4-/CD8- double negative (DN) cells are immature T cells, in thymus they are located in the capsule. In the thymus, they move to the cortex and become CD8+/ CD4+ double positive (DP) which are precursor cells. Mature T cells located in the medulla of the thymus are marked as single positive (SP) for CD4 or CD8. From here the gating strategy differs between spleen and thymus. In spleen, the CD4+ population is CD62L/CD44 used to distinguish CD4 memory (CD62L-/ CD44+) and naïve CD4 T cells (CD62L+/ CD44-and+). Within the CD8+ population we can specify activated (CD62L+/CD44+), effector (CD62L-/CD44+) and naïve (CD62L+/CD44-) T cells. In thymus DN and SPs are further categorized using CD3/ FSC-A, to distinguish immature negative and mature positive cells. Subsequently, different maturation stadia of the DN immature cells are marked using CD25/ CD44. DN1 is CD25-/ CD44+, DN2 CD25+/ CD44+, DN3 CD25+/CD44- and DN4 is CD25-/CD44-. The mature SP cells are further analysed using CD62L/CD44: effector T cells are characterized by CD62L-/CD44+, central memory T cells carry CD62L+/CD44+, and naïve T cells are CD62L+/CD44-. Immature single positive (ISP) cells are marked by CD8 SP and then CD3-. (WT n=4 vs cKO n=4. * indicates a p-value of < 0.05).

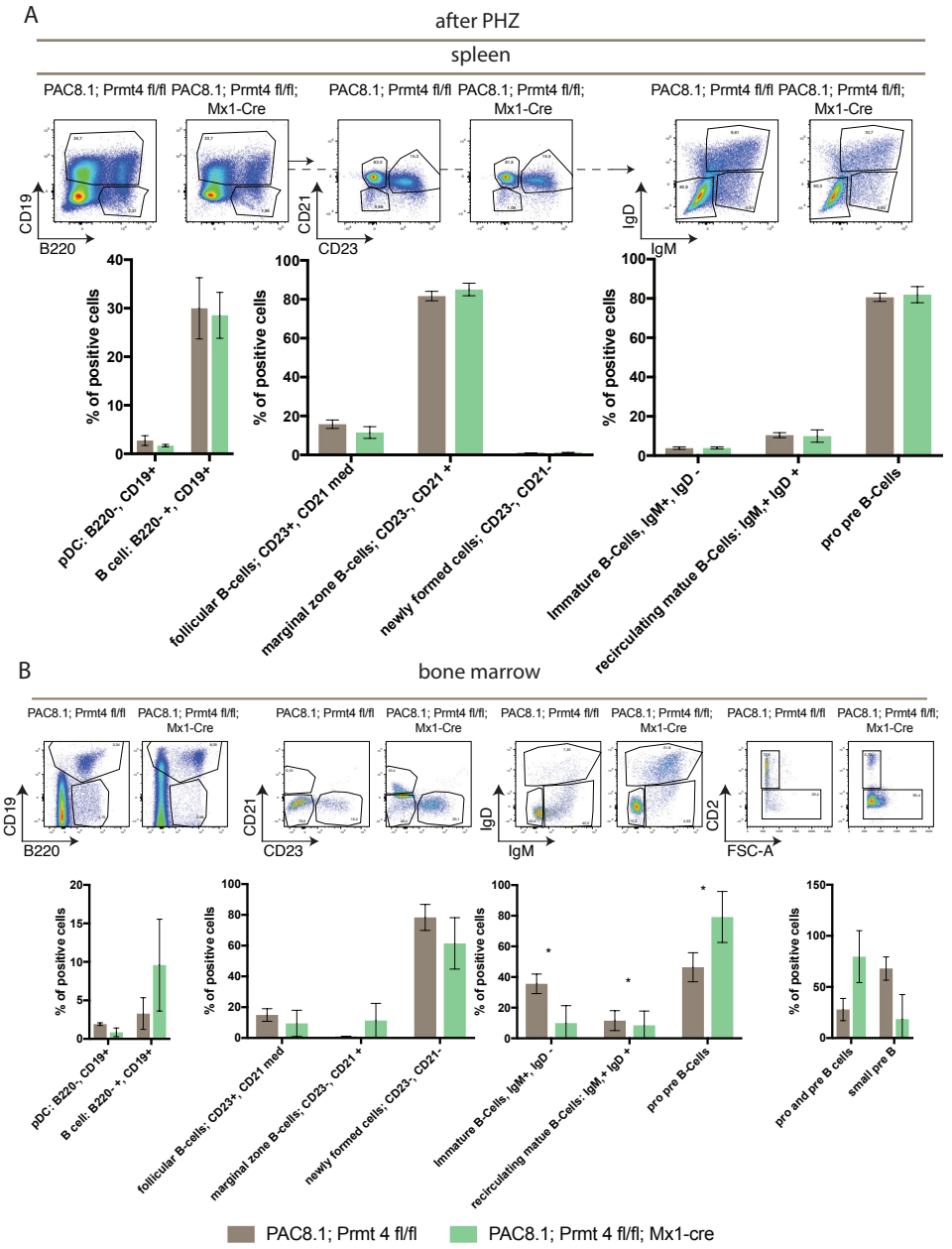

Figure 9. B cell flow cytometry analysis of control and Prmt4 cKO mice after PHZ treatment. First, we gated for single cells, and lymphocytes using FSC-A/FSC-H and FSC-A/SSC-A. Subsequently we used the markers B220/CD19 markers to distinguish the plasmacytoid dendritic cells (pDC; CD19-/B220+) and B cells (CD19+/B220+ and -). The B cell population is thereafter subdivided in six groups. Three subpopulations are divined using CD23/CD21; follicular (CD23+/CD21 medium); marginal zone (CD23-/CD21+) and newly formed (CD23-/CD21-) B cells. IgM/IgD markers are used to distinguish immature (IgM+/IgD-); recirculating (IgM+/IgD+) and pro/pre (IgM-/IgD-) B cells. The last group is in BM cells further specified as pro/pre-B cells (CD2-) and small pre-B cells (CD2+) using CD2/FSC-A. (WT n=4 vs cKO n=4. * indicates a p-value of <0.05).

the bone marrow, which are rare. In blood we also observed a decrease 2.3% in the controls to 0.9% of the early progenitor BFU-E cells (KIT+/CD71-) in the cKO animals. Although PHZ mainly affects erythropoiesis, the large scale decay of erythrocytes will also trigger an immunoreaction. The analysis of T cells is shown in Figure 8. In spleen (upper panel), we observed no significant differences between the control and *Prmt4* cKO mice. When comparing Figure 8 with Figure 3, we observed changes induced by the PHZ, but these were genotype independent. We can see the increase of CD8+ naïve cells and reduced activated and effector memory CD8+ T cells. So, the PHZ affects also the T cells maturation.

In the thymus, we didn't find any significant differences between the control and *Prmt4* cKO mice. CD3 positivity of SP cells, but mainly the activated CD8+ cell population is decreased from 50-60% to 10%, and the naïve CD8+ cell population is increased from 28% to 88 %.Figure 4 we can

For the B cells, we didn't observe significant differences between the PHZ-treated

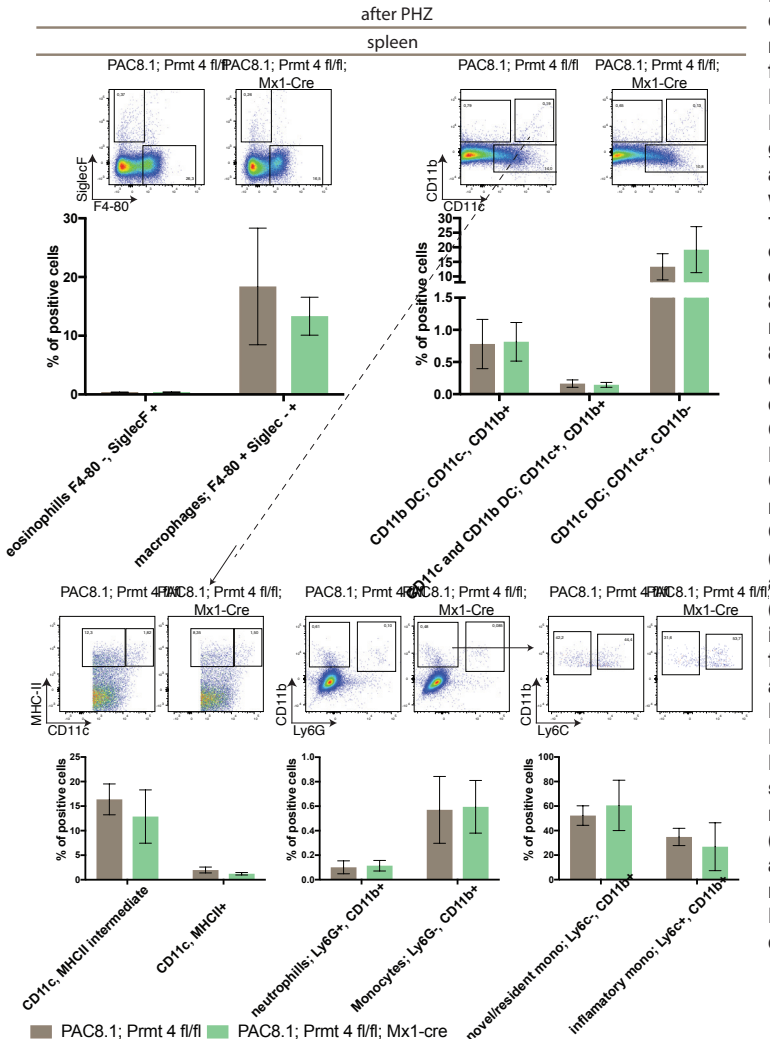

Figure 10. Flow cytometry analysis for myeloid cells in spleen from control and Prmt4 cKO mice after PHZ treatment. After gating for living cells and lymphocytes, we could distinguish 7 different types of myeloid cells: eosinophils (F4-80-/SiglecF+), macrophages (F4-80+/SiglecF+), conventional dendritic cells (DCs: CD11c+/CD11b+), immature DCs (CD11c+/CD11b-), other myeloid cells (CD11c-/CD11b+), neutrophils (Ly6G+/CD11b+) and monocytes (Ly6G-/CD11b+). The immature DCs are further categorised as small DCs (CD11c-/MHCII+) and large DCs (CD11b+/MHCII+). Monocytes are subdivided in novel/resident monocytes (CD11b+/Ly6C-) and inflammatory monocytes (CD11b+/Ly6C+). (WT n=4 vs. cKO n=4).

control and *Prmt4* cKO mice the spleen (Figure 9). Compared with see a decrease of follicular and increase of marginal zone B cells. Also, the recirculating B cells were decreased, and the pro/pre-B cell populations were highly increased after PHZ treatment.
PHZ treatment also caused changes in the BM B cell populations (Figure 9, lower panel). Whereas immature/recirculating B cells were decreased, the immature pro/pre-B cells were significantly increased compared to the control littermates. The pro/pre-B cells and small pre-B cells were highly variable, while these populations displayed stable values in the experiments without PHZ treatment (Figure 4).
Figure 10 shows our findings concerning the myeloid cells after pIpC induction and PHZ treatment. All myeloid cell populations were changed compared to the experiment without PHZ (Figure 5). PHZ treatment increased macrophages, and the dendritic cell population, especially the immature population. This was accompanied by a decrease in small and large conventional DCs, neutrophils and monocytes. However, we did not observe a significant difference between Mx1-Cre and control mice, the differen ces appear after the PHZ treatment.
In conclusion, lack of Prmt4 hardly affects erythropoiesis and only results in a small but significant reduction in peripheral blood erythrocytes. The thymus is hypocellular, and CD4+CD8- T cells are increased in peripheral blood at the expense of CD4-CD8+ T cells. In the B cell lineage immature cells are increased, whereas mature cells are decreased. Upon PHZ treatment, recovery of erythropoiesis was independent of Prmt4, and the block of B cell maturation persisted (increased immature B cells and a decrease of mature B cells). Following PHZ treatment, however, the percentage of cells in which the floxed *Prmt4* locus was recombined (and deleted) was clearly reduced. This suggests that Prmt4-deficient cells are less competitive compared to wt cells during stress erythropoiesis. Due to the PHZ treatment many erythrocytes were lysed in the blood stream, this massive lysis apparently affects other hematopoietic cell lineages. New erythroid cells are created quickly, which may affect the balance between the cells. Cells that have escaped recombination may contribute more efficiently to the fast generation of new cells. This might explain the observed low recombination frequency at the *Prmt4* locus after PHZ treatment.

We performed similar experiments for the genes *Prmt1 and Prmt5,* and for the combination of *Prmt1* with *Prmt4,* and *Prmt4* with *Prmt5*. We will discuss these experiments less extensively and will mainly focus on potential differences.

PRMT1: analysis of normal hematopoiesis

We crossed PAC8.1; *Prmt1* fl/fl mice with *Mx1*-Cre. Figure 11A shows blood parameters after pIpC injection. Most of the parameters showed no significant changes due to the loss of *Prmt1*, only the white blood cell (WBC) and platelets (PLT) counts were decreased. All red blood cell (RBC) values and the related hemoglobin (HGB), haematocrit (HCT), mean corpuscular hemoglobin (MCH), red blood cell distribution (RDW) were not changed. The RDW is a shows the variation in RBC size. Figure 11B shows the number of cells in BM, spleen and thymus measured on a CASY instrument. The *Prmt1* cKO appeared to have less BM cells and more spleen cells, but these differences were not significant. Figure 11C displays histograms of RBCs after pIpC induction of *Mx1*-Cre. Also, here no significant changes were observed.

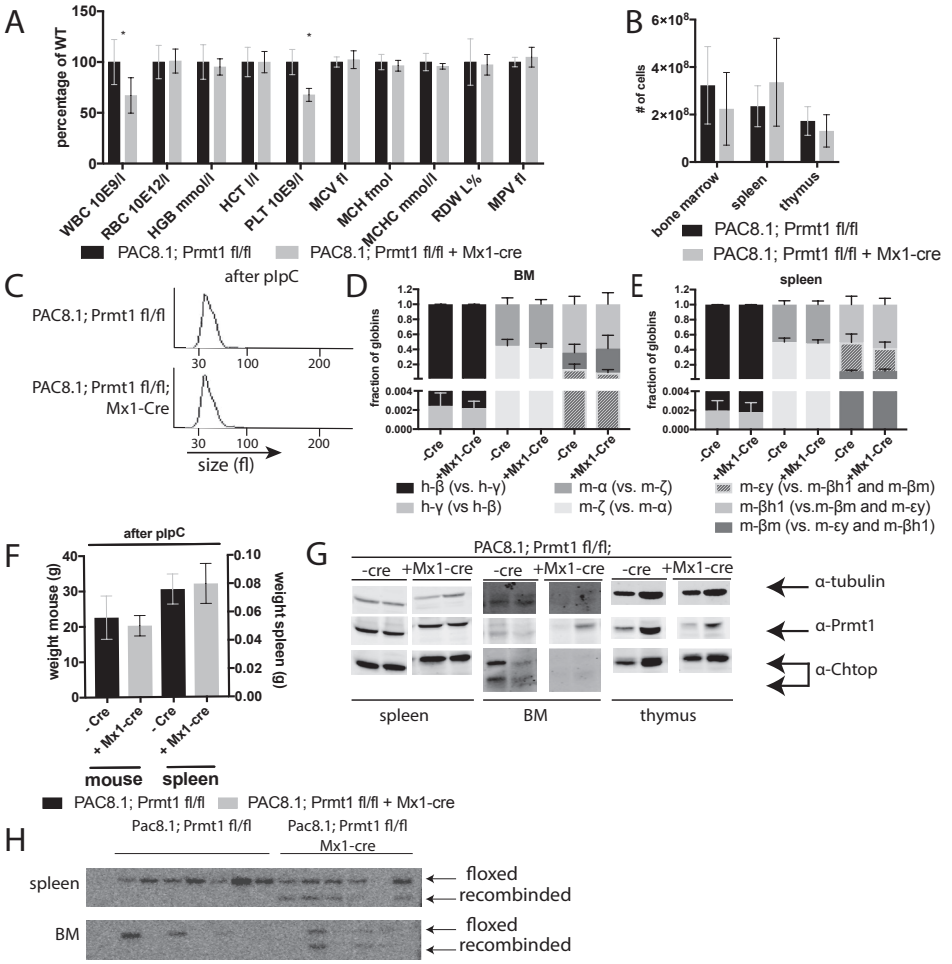

Figure 11. Control and Prmt1 cKO mice.(WT n=8 and cKO n=6. * indicates a p-value <0,05.) (A) Measured blood parameters: WBC (white blood cells); RBC (red blood cells); HGB (hemoglobin); HCT (haematocrit); PLT (platelets); MCV (Mean Corpuscular Volume); MCH (Mean Corpuscular Hemoglobin); MCHC (Mean Corpuscular Hemoglobin Concentration); RDW (RBC distribution width); MPV (mean platelet volume) measured one day before sacrifice. (B) Number of cells counted per tissue using a CASY TTC instrument. (C) Size distribution of RBCs after pIpC treatment, one day before sacrifice. (D) and (E) Expression of g-globin and mouse globins were determined using qRT-PCR. Fractions were calculated using g/g+b, z/(z+a) and bm/(bm+ey+bH1). Values were normalized to control littermates with no Mx1-Cre. (F) Mice were weighed (left panel), after sacrifice the spleen weight was determined (right panel). (G) Western blot analysis of RIPA lysates of spleen, BM and thymus. Shown are 2 representatives of each condition of each tissue. Tubulin was used as a loading control. We stained for PRMT1 and its interacting partner CHTOP. (H) Southern blot of spleen and bone marrow cells after pIpC induction. Left panel shows control littermates without Mx1-Cre, and right panel cKOs with Mx1-Cre.

To measure globin expression levels, we performed qRT-PCR on RNA isolated from BM and spleen (Figure 11D,E). We checked the human γ and mouse εy, βH1, βmajor, and ζ-globins. The expression of γ-globin was normalized against the PAC8.1-originated human β-globin. The mouse globins were normalized against α-globin. Here we did not observe any differences. In Figure 11F we show at the left panel the weights of the mice and at the right panel the spleen weights. There was

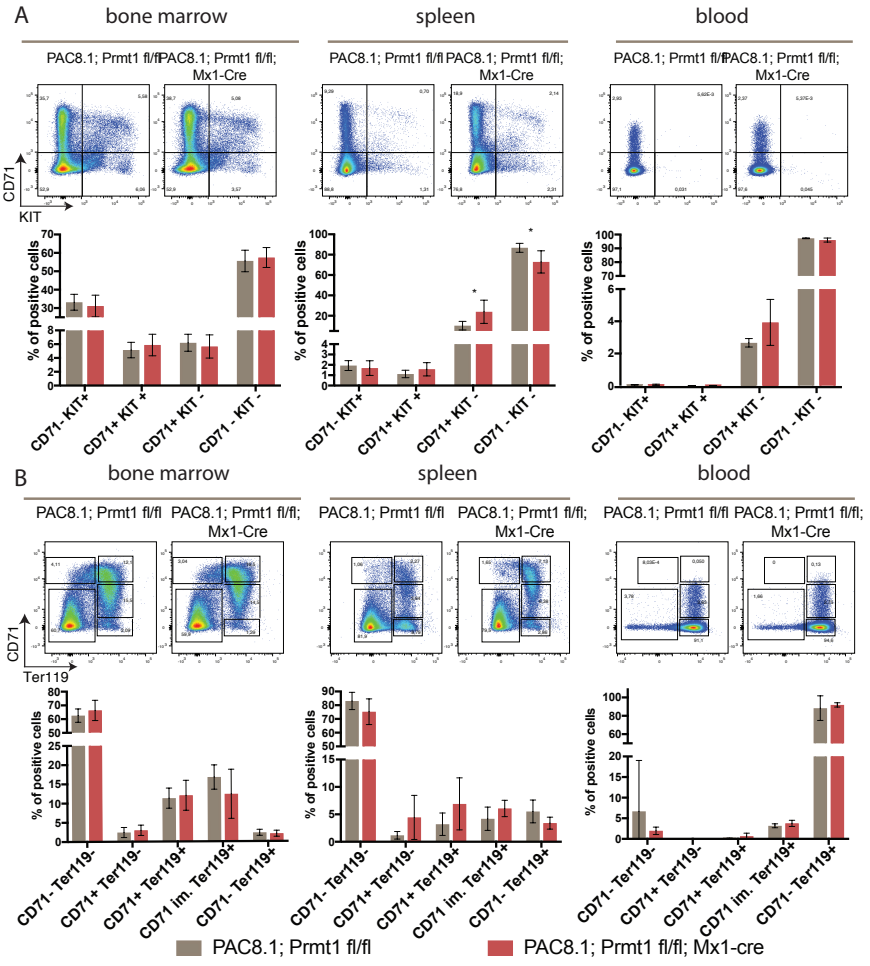

Figure 12. Flow cytometry analysis of erythroid cells in control and Prmt1 cKO mice. After live/dead gating we distinguish different erythroid progenitor cell populations using (A) CD71/KIT119 and (B) CD71/Ter119. (WT=6 vs cKO n=6. * indicates a p-value of <0.05).

no significant difference in spleen size and animal weight between the controls and the *Prmt1* cKO animals. We also performed Southern and western blotting to check recombination at genomic and expression at protein level, respectively (Figure 11G,H). The Southern blot revealed that recombination efficiency was much lower than expected, reaching ~50% at best. As a consequence, PRMT1 protein levels remain virtually unchanged (Figure 11G). In some *Prmt1* cKO animals, PRMT1 protein levels were slightly reduced, and this varied between the different tissues tested. For example, almost no differences were observed in spleen, while the effect was more pronounced in BM and thymus. This could be partly caused by our experimental setup, we did not select for erythroid cells in spleen. We also stained the western blot for the PRMT1 interaction partner CHTOP. In some samples, for example in BM where we observed less PRMT1, we also observed reduced levels of CHTOP. We therefore further analysed the effects of the reduction of PRMT1 in

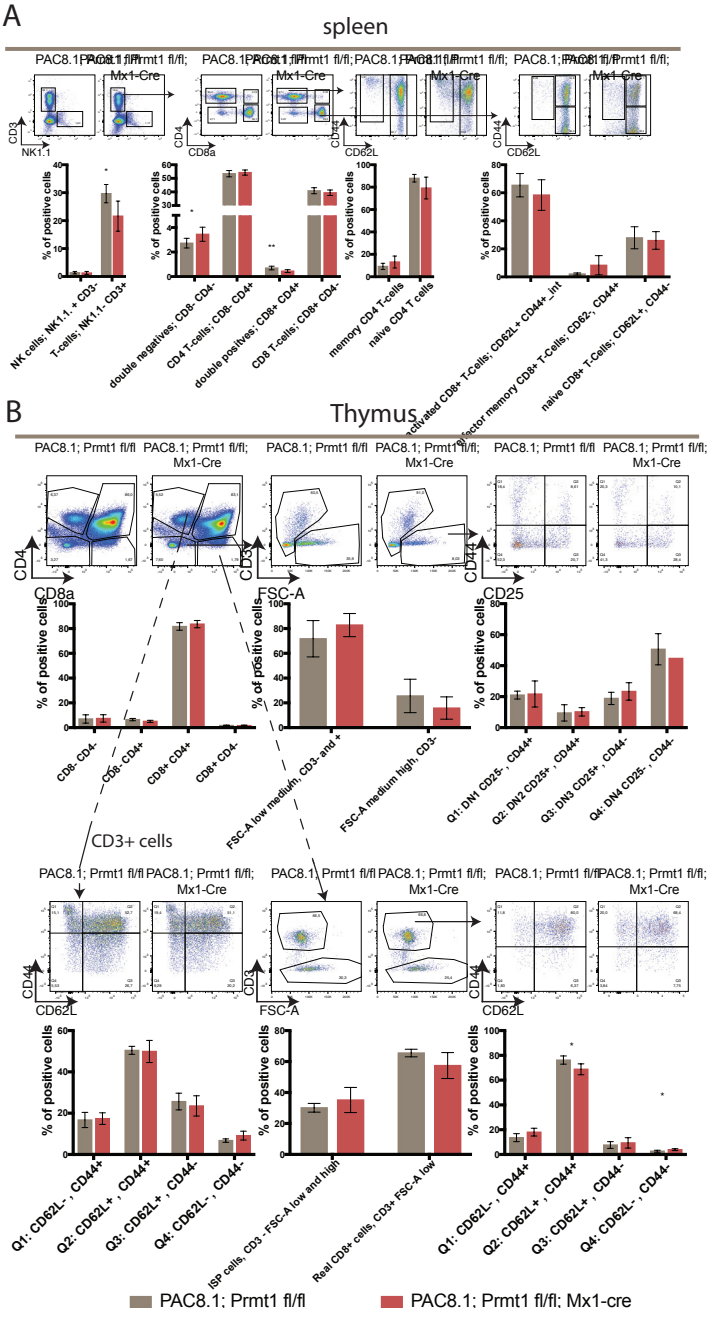

Figure 13. T cell flow cytometry analysis of control and Prmt1 cKO (A) spleen and (B) thymus cells after plpC treatment. After live/dead marking (not shown) CD3/NK1.1 (for spleen cells) or NK1.1/ FSC-A (for thymus cells) was used to distinguish between NK-cells (NK1.1+) and T cells (NK1.1- /(CD3+)). Different populations of T cells are further specified using CD4/ CD8. CD4-/CD8- double negative (DN) cells are immature T cells, in thymus they are located in the capsule. In the thymus, they move to the cortex and become CD8+/CD4+ double positive (DP) which are precursor cells. Mature T cells are characterized which are located in the medulla of the thymus are marked as single positive (SP) for CD4 or CD8. From here the gating strategy differs between spleen and thymus. In spleen, the CD4+ population is CD62L/CD44 used to distinguish CD4 memory (CD62L-/ CD44+) and naïve CD4 T cells (CD62L+/ CD44-and+). Within the CD8+ population we can specify activated (CD62L+/CD44+), effector (CD62L-/ CD44+) and naïve (CD62L+/CD44-) T cells. In thymus DN and SPs are further categorized using CD3/FSC-A, to distinguish immature negative and mature positive cells. Subsequently, different maturation stadia of the DN immature cells are marked using CD25/CD44. DN1 is CD25-/CD44+, DN2 CD25+/ CD44+, DN3 CD25+/CD44- and DN4 is CD25-/CD44-. The mature SP cells are further analysed using CD62L/CD44: effector T cells are characterized by CD62L-/CD44+, central memory T cells carry CD62L+/CD44+, and naïve T cells are CD62L+/CD44-. Immature single positive (ISP) cells are marked by CD8 SP and then CD3-. (WT n=6 vs cKO n=6 * indicates a p-value of < 0.05. ** indicates a p-value <0.01).

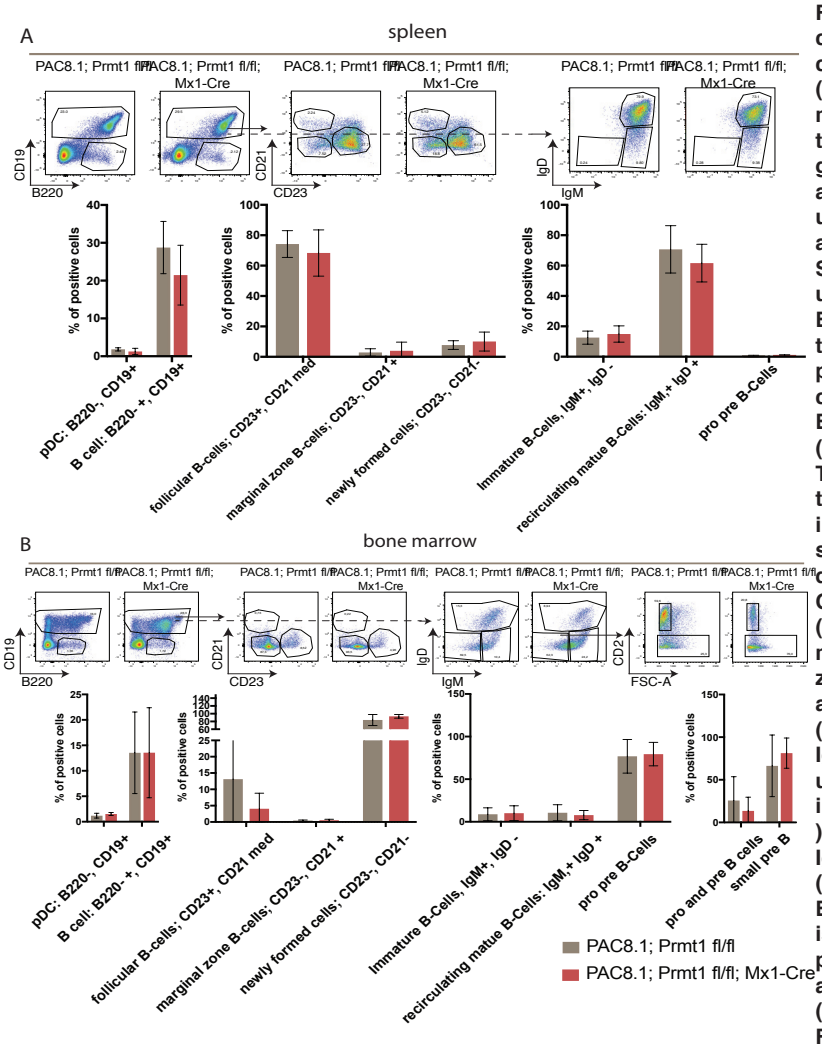

Figure 14. B cell flow cytometry analysis of control and Prmt1 cKO (A) spleen and (B) bone marrow cells after plpC treatment. First, we gated for single cells, and lymphocytes using FSC-A/FSC-H and FSC-A/SSC-A. Subsequently we used the markers B220/CD19 markers to distinguish the plasmacytoid dendritic cells (pDC; CD19-/B220+) and B cells (CD19+/B220+ and -). The B cell population is thereafter subdivided in six groups. Three subpopulations are divided using CD23/CD21; follicular (CD23+/CD21 medium); marginal zone (CD23-/CD21+) and newly formed (CD23-/CD21-) B cells. IgM/IgD markers are used to distinguish immature (IgM+/IgD-); recirculating (IgM+/IgD+) and pro/pre (IgM-/IgD-) B cells. In BM cells, the last group is further specified as pro/pre-B cells (CD2-) and small pre-B cells (CD2+) using CD2/FSC-A. (WT n=6 vs cKO n=6).

hematopoiesis by pan-hematopoietic flow cytometry analysis of spleen, BM, thymus and blood.

For the erythroid cells, we stained BM, spleen and blood with CD71, Ter119 and KIT, Figure 12. In *Prmt1* cKO mice no significant changes were observed in the Ter119+ compartments. In the spleen, we observed an increase of ~15% in the CD71+/KIT- population, and a ~15% decrease in the CD71-/KIT- population.

Additionally, we analysed T cells in the spleen and thymus (Figure 13). In the spleen (upper panel), using NK1.1. and CD3, the total population of T cells was reduced with ~ 9%. Within this T cell population the CD8/CD4 double negatives (DN) and double positives (DP) were slightly but significantly changed. CD8/CD4 DN are immature cells, and DP cells are precursor cells. DN cells within the spleen are thought to be activated SP cells that lost their marker and are DN cells that migrated already.[63,64] No differences between the cKO and control mice were observed within the single

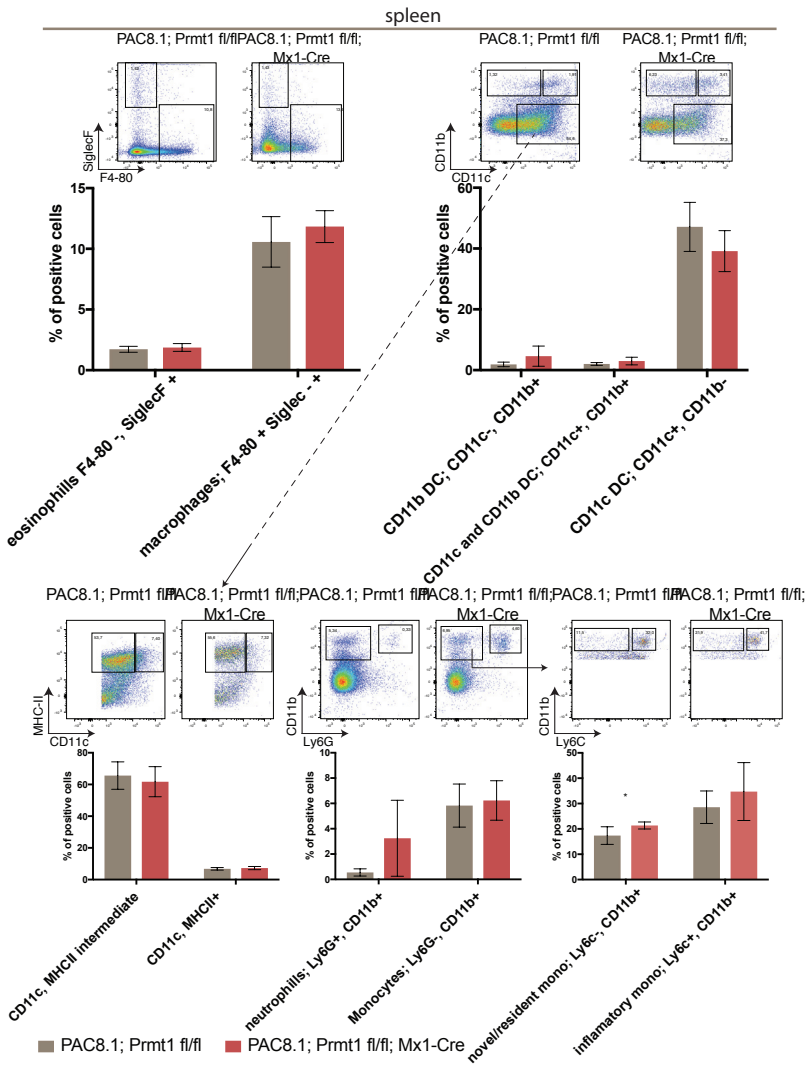

Figure 15. Flow cytometry analysis of myeloid cells in spleen from control and Prmt1 cKO mice after pIpC treatment. After gating for living cells and lymphocytes, we could distinguish 7 different types of myeloid cells: eosinophils (F4-80-/SiglegF+), macrophages (F4-80+/SiglegF+), conventional dendritic cells (DCs: CD11c+/CD11b+), immature DCs (CD11c+/CD11b-), other myeloid cells (CD11c-/CD11b+), neutrophils (Ly6G+/CD11b+) and monocytes (Ly6G-/CD11b+). The immature DCs are further categorised as small DCs (CD11c-/MHCII+) and large DCs (CD11b+/MHCII+). Monocytes are subdivided in novel/resident monocytes (CD11b+/Ly6C-) and inflammatory monocytes (CD11b+/Ly6C+). (WT n=6 vs. cKO n=6. * indicates p<0.05)

CD8 or CD4 positive T cell populations (Figure 13). Only further in the differentiation stage of CD8 SP cells, within the CD3+ group, the proportion of CD62L/CD44 double positives are decreased from 76% to 68%, and the CD62L/CD44 double negatives are increased from 2.7% to 3.7%.

Next, we analysed the B cell populations. Figure 14 shows the percentages of these populations in spleen (upper panel) and BM (lower panel). No significant changes were observed. This is in contrast with the literature; Infantion et al. found that PRMT1 is required for B cell activation and maturation *in vitro*.[65] The low recombination efficiency in the *Prmt1* cKO mice provides a likely explanation for this discrepancy.

For different myeloid cell populations, we checked the spleen. There was some variation in these populations between the control and *Prmt1* cKO mice (Figure 15). The immature CD11c+/CD11b- DCs were not significantly decreased in the *Prmt1*

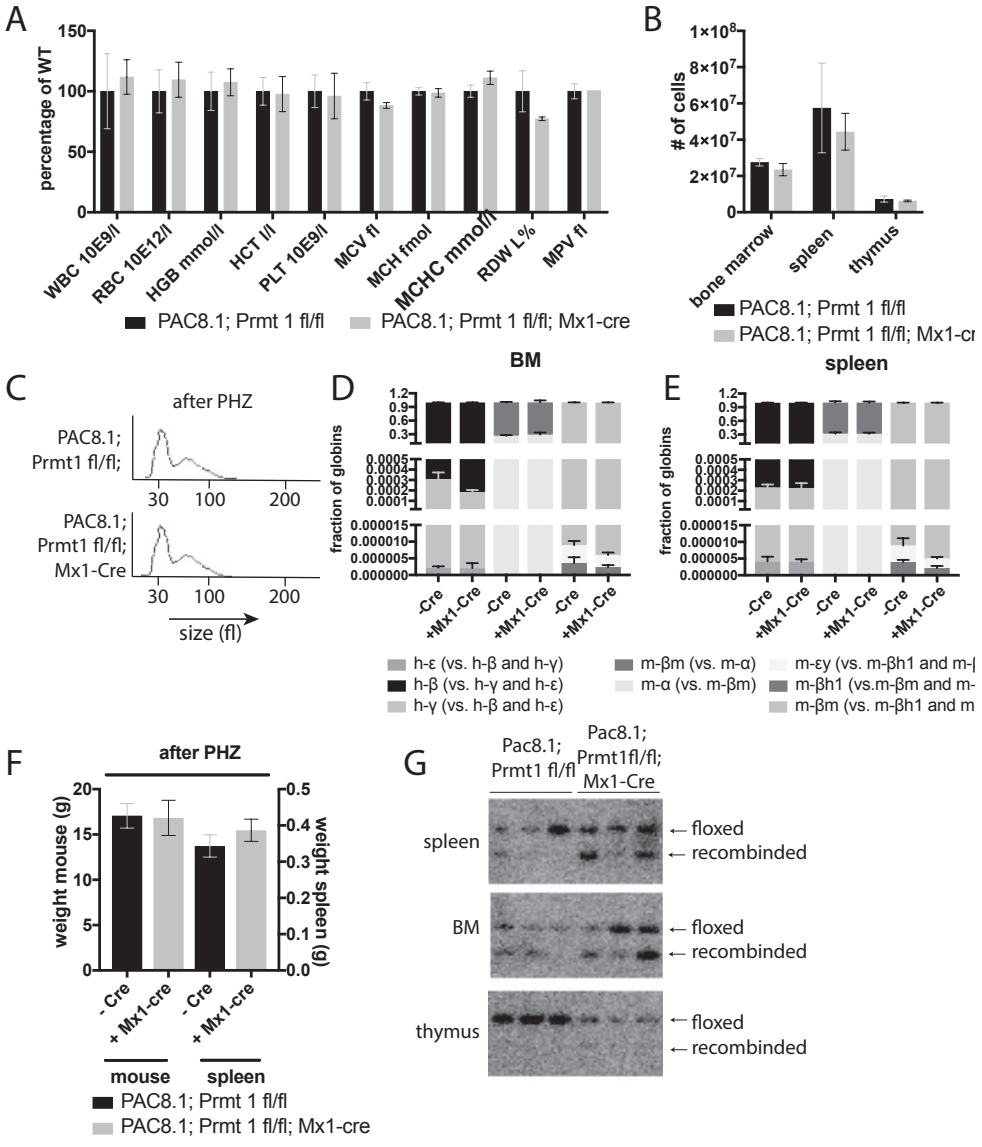

Figure 16. Control and Prmt1 cKO mice after treatment with pIpC and induction of stress erythropoiesis by PHZ treatment. (WT n=6 and cKO n=6). (A) Measured blood parameters: WBC (white blood cells); RBC (red blood cells); HGB (hemoglobin); HCT (haematocrit); PLT (platelets); MCV (Mean Corpuscular Volume); MCH (Mean Corpuscular Hemoglobin); MCHC (Mean Corpuscular Hemoglobin Concentration); RDW (RBC distribution width); MPV (mean platelet volume) measured one day before sacrificing. (B) Number of cells counted per tissue using CASY TTC instrument. (C) Size distribution of RBCs after PHZ treatment. (D) and (E) Expression ration of g-globin and mouse globins were determined using qRT-PCR. Fractions were calculated using g/g+b, bm/(bm+a) and bm/(bm+ey+bH1). Values were normalized to control littermates. (F) Mouse (left panel) and spleen weights (right panel) after PHZ treatment. (G) Southern blot of spleen, bone marrow and thymus cells after pIpC treatment. It looks like all except one contain Cre.

cKO mice. The only significant change concerned the population of novel/resident monocytes, which was increased with 4.3% in the *Prmt1* cKO animals.
In summary, in the pan-hematopoietic flow cytometry analysis we found no major differences between the control and *Prmt1* cKO animals. Whereas the total number of cells in the spleen was not altered, the KIT negative erythroid precursors were increased whereas (CD71-) CD3 positive T cells were decreased negative cells were decreased. In the B cell analysis we did not observe any significant changes. However, the low recombination efficiency in the *Prmt1* cKO animals indicate that PRMT1 activity has an important functional role in several hematopoietic lineages, resulting in selection of non-recombined cells. The low recombination also implies that the effect in various lineages is underestimated.
.

PRMT1: analysis of stress hematopoiesis

We also induced stress erythropoiesis by treating the mice with phenylhydrazine (PHZ). Blood parameters after PHZ treatment are shown in Figure 16A. We didn't observe significant differences between the controls and the *Prmt1* cKO animals. Total cell numbers of BM, spleen and thymus cells were counted on the CASY

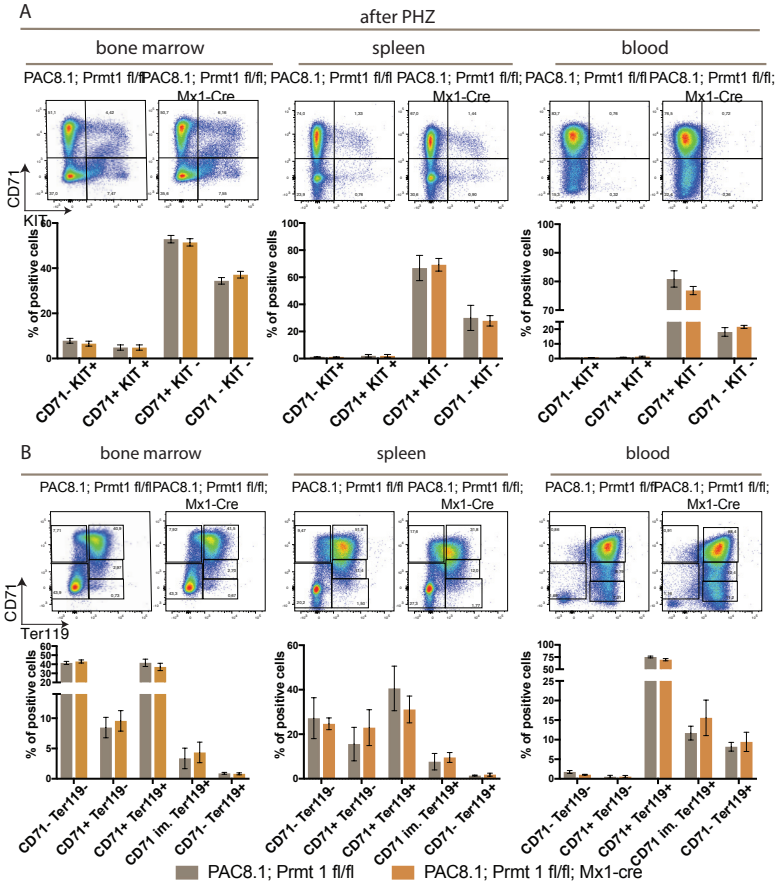

Figure 17. Flow cytometry analysis of erythroid cells in control and Prmt1 cKO mice after induction with plpC and PHZ treatment. After life/dead gating we distinguish different erythroid progenitor cell populations using (A) CD71/KIT and (B) CD71/Ter119 (WT=3 vs cKO n=3).

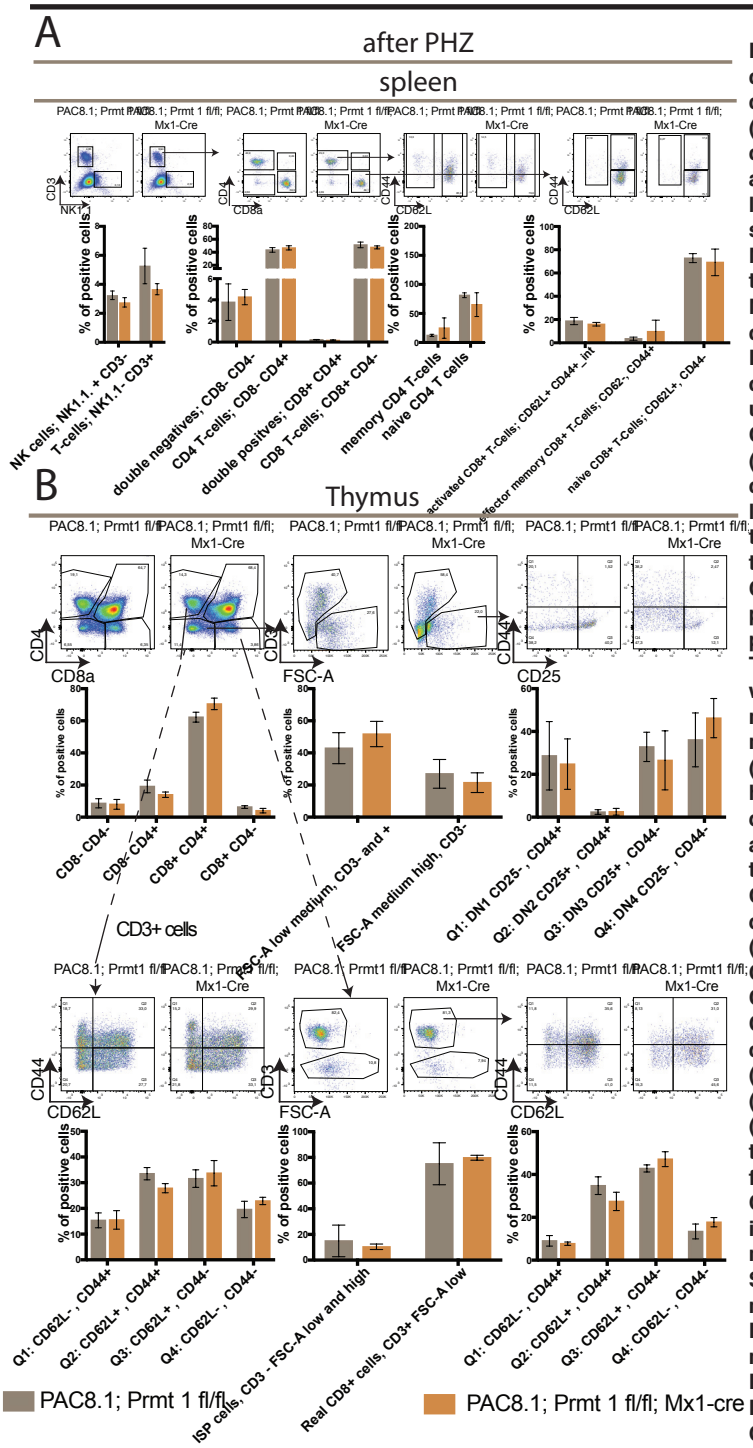

Figure 18. T cell flow cytometry analysis of control and Prmt1 cKO (A) spleen and (B) thymus cells after plpC induction and PHZ treatment. After life/dead marking (not shown) CD3/NK1.1 or NK1.1/FSC-A was used to distinguish between NK-cells (NK1.1+) and T cells (NK1.1- /(CD3+)). Different populations of T cells are further specified using CD4/CD8. CD4-/CD8- double negative (DN) cells are immature T cells, in thymus they are located in the capsule. In the thymus, they move to the cortex and become CD8+/CD4+ double positive (DP) which are precursor cells. Mature T cells are characterized which are located in the medulla of the thymus are marked as single positive (SP) for CD4 or CD8. From here the gating strategy differs between spleen and thymus. In spleen, the CD4+ population is CD62L/CD44 used to distinguish CD4 memory (CD62L-/CD44+) and naïve CD4 T cells (CD62L+/CD44-and+). Within the CD8+ population we can specify activated (CD62L+/CD44+), effector (CD62L-/CD44+) and naïve (CD62L+/CD44-) T cells. In thymus DN and SPs are further categorized using CD3/FSC-A, to distinguish immature negative and mature positive cells. Subsequently, different maturation stadia of the DN immature cells are marked using CD25/CD44. DN1 is CD25-/CD44+, DN2 CD25+/CD44+, DN3 CD25+/CD44- and DN4 is CD25-/CD44-. The mature SP cells are further analysed using CD62L/CD44: effector T cells are characterized by CD62L-/CD44+, central memory T cells carry CD62L+/CD44+, and naïve T cells are CD62L+/CD44-. Immature single positive (ISP) cells are marked by CD8 SP and then CD3-. (WT n=3 vs cKO n=3).

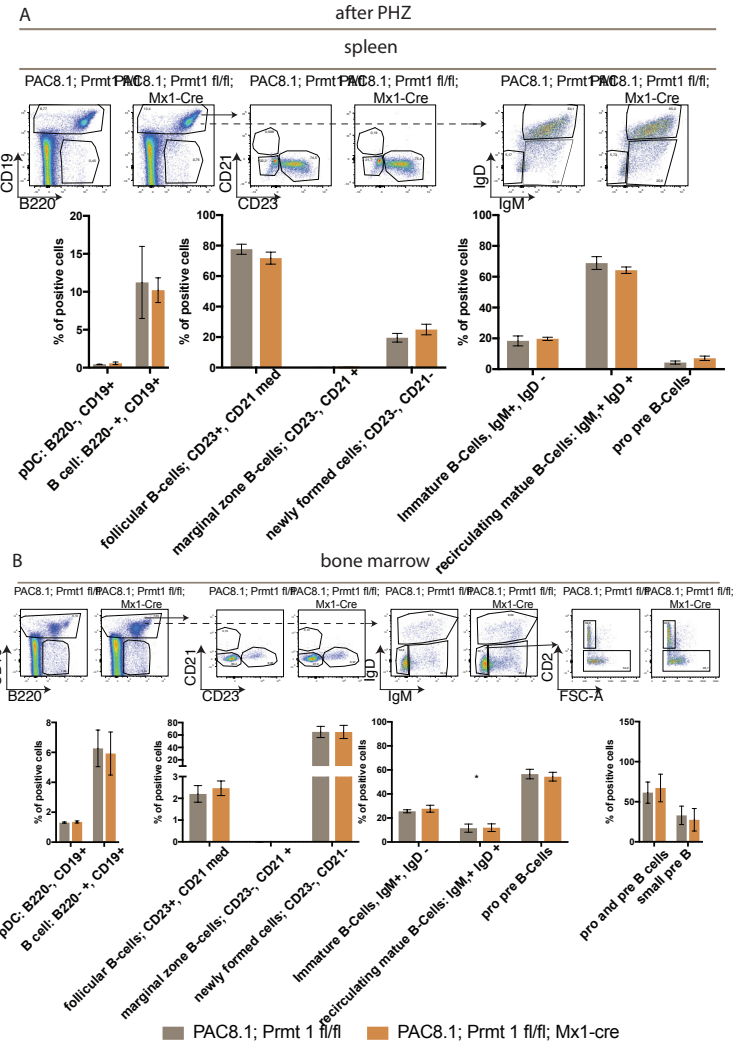

Figure 19. B cell flow cytometry analysis of control and Prmt1 cKO (A) spleen and (B) bone marrow cells after plpC induction and PHZ treatment. First, we gated for single cells, and lymphocytes using FSC-A/FSC-H and FSC-A/SSC-A. Subsequently we used the markers B220/CD19 markers to distinguish the plasmacytoid dendritic cells (pDC; CD19-/B220+) and B cells (CD19+/B220+ and -). The B cell population is thereafter subdivided in six groups. Three subpopulations are divined using CD23/CD21; follicular (CD23+/CD21 medium); marginal zone (CD23-/CD21+) and newly formed (CD23-/CD21-) B cells. IgM/IgD markers are used to distinguish immature (IgM+/IgD-); recirculating (IgM+/IgD+) and pro/pre (IgM-/IgD-) B cells. The last group is in BM cells further specified as pro/pre-B cells (CD2-) and small pre-B cells (CD2+) using CD2/FSC-A. (WT n=3 vs cKO n=3).

instrument (Figure 16B). Histograms of erythrocyte size distributions after PHZ treatment are shown in Figure 16C. After PHZ treatment a second peak appears (compare Figure 11A), representing newly formed reticulocytes in response to the PHZ-induced anaemia. No differences were found between the control and *Prmt1* cKO mice, indicating that mice of both genotypes are able to adequately mount the stress response. Expression of the globin genes was also similar between the two groups of mice (Figure 16D,E), as were animal and spleen weights (Figure 16F). Of note, spleen weights were increased ~5-fold upon PHZ treatment (compare Figure 11F) due to the fact that stress erythropoiesis had been activated in the spleen. Because in our previous experiment the Southern blots revealed poor recombination rates, we repeated that for these animals, Figure 16G. Recombination is better than observed in Figure 11H, but it appears that the genotyping by PCR on genomic DNA is not always correct. This shows the importance to double-check genotyping using independent methods: PCR and Southern blotting. For further analysis, we used the

Southern blotting results to group the data to cKO or control animals.
We also performed the same pan hematopoietic flow cytometry analysis on spleen, BM, blood and thymus cells of these mice. We started with the erythroid analysis on BM, spleen and blood. In BM, spleen and blood we observed changes due to PHZ treatment. There are more progenitor cells present in all the tissues analysed, in agreement with
Figure 16D, histogram of blood (Figure 17). The significant differences before PHZ treatment (Figure 11) are no longer observed after PHZ treatment. Figure 18 represents the T cells in spleen (upper panel) and thymus (lower pane). Although the significant differences observed before PHZ treatment (Figure 13) were not detected, we did observe the same trends. The lack of significance is likely explained by the fact that fewer animals were used for the PHZ treatment. In Figure 13 (lower panel), the differences between *PAC8.1*/wt; *Prmt1* fl/fl and *PAC8.1*/wt; *Prmt1* fl/fl; *Mx1-Cre*/wt mice after pIpC treatment are shown for T cells of the thymus. For B cells (Figure 14 and Figure 19), we observed that the percentage of B cells was reduced in spleen. This may be the result of the increase of spleen size due to activation of stress erythropoiesis in the PHZ treated mice (Figure 16B). In addition, in spleen the proportion of immature and pro/pre-B cells was increased. The decrease in marginal zone B cells in spleen could be caused by the enlargement of the spleen. Other B cell proportions in the spleen were not changed. In BM, we observed that the total proportion of B cells was reduced when comparing the mice without PHZ to the mice that received the PHZ. This affected a number of B cell subpopulations in the BM: follicular, newly formed and pro/pre-B cells, the immature B cells (IgM+/IgD-) were decreased with almost 20%.
This trend continued for the myeloid cells, where almost all the myeloid cell populations were decreased in spleen (compare Figure 20 to Figure 15). Interestingly, we also observed altered B cell populations after PHZ treatment of control and *Prmt4* cKO mice (Figure 9), but in the *Prmt4* fl/fl mice the effect of PHZ treatment is different. For example, in the *Prmt4* fl/fl mice the marginal zone cells and pro/pre-B cells were both increased within the spleen, where we observed decreases in the cKO *Prmt1* fl/fl. Those differences are less pronounced in BM.
In conclusion, the observed recombination efficiency of the floxed *Prmt1* allele after pIpC treatment is low (at best 50%). Since full knockouts of *Prmt1* die before birth because of developmental problems,[47] it is likely that *Prmt1* is also crucial for hematopoietic cells. If fully recombined cells die, the remaining heterozygote or unrecombined cells have a selective advantage and are apparently able to compensate for the lost cells. To tackle this problem, a Cre recombinase specific for B or T cells could be used. Examples are *Mb1*-Cre for B cells, and *Lck-Cre* for the T cells.[66,67] Since B and T cells are not essential for survival of the animal, this should show whether *Prmt1* has an essential role in these cells.

PRMT5: analysis of normal hematopoiesis

Next, we investigated conditional knockout mice for the Type II symmetric protein arginine methyl transferase *Prmt5*. In the blood parameters, we observed a decrease of WBC in general in the cKO animals compared to the control mice (Figure 21A). The other parameters were unaffected. The cellularity of BM and spleen was similar in cKO and the control mice. The cellularity of the thymus was almost 10-fold

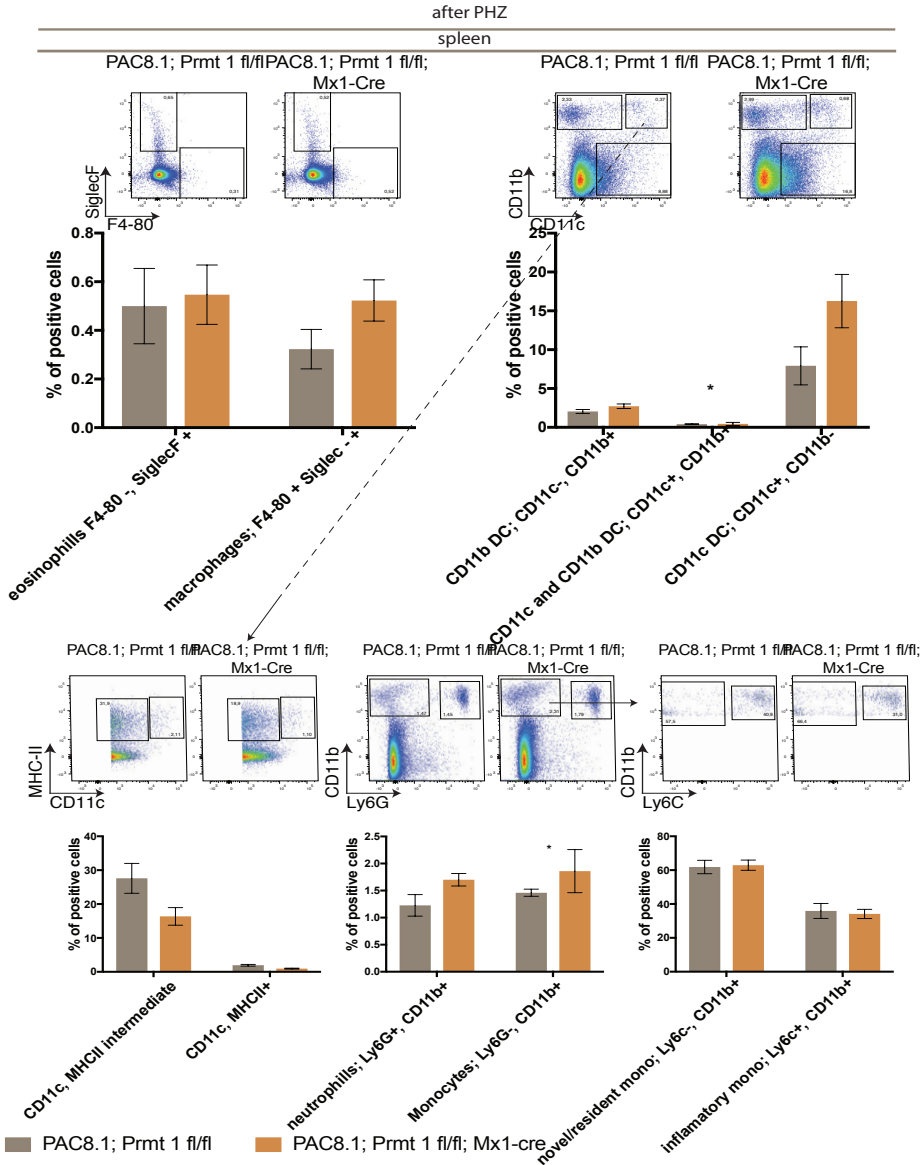

Figure 20. Flow cytometry analysis for myeloid cells in spleen from control and Prmt1 cKO mice after PHZ treatment. After gating for living cells and lymphocytes, we could distinguish 7 different types of myeloid cells: eosinophils (F4-80-/SiglegF+), macrophages (F4-80+/SiglegF+), conventional dendritic cells (DCs: CD11c+/CD11b+), immature DCs (CD11c+/CD11b-), other myeloid cells (CD11c-/CD11b+), neutrophils (Ly6G+/CD11b+) and monocytes (Ly6G-/CD11b+). The immature DCs are further categorised as small DCs (CD11c-/MHCII+) and large DCs (CD11b+/MHCII+). Monocytes are subdivided in novel/resident monocytes (CD11b+/Ly6C-) and inflammatory monocytes (CD11b+/Ly6C+). (WT n=3 vs. cKO n=3. * indicates p<0.05).

increased in the control mice compared to control mice in litters of *Prmt4* and *Prmt1* mice, which may be due to the fact that these mice were analysed at a younger age Figure 21B. Cellularity of *Prmt5* cKO does not show this increase and is much lower compared to wt littermates. The erythrocyte size distribution was not altered

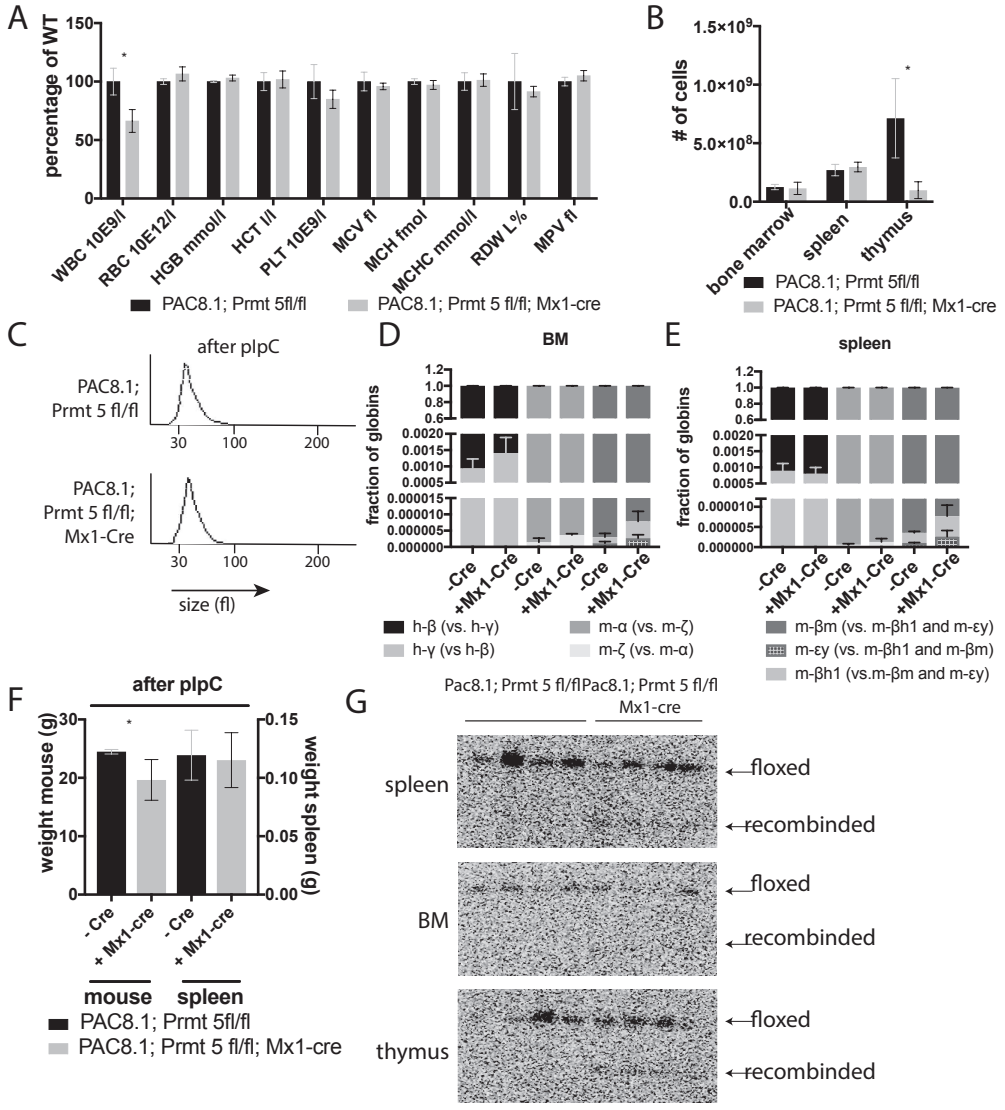

Figure 21. Control and Prmt5 cKO mice. (WT n=4 and cKO n=4. * indicates a p-value <0.05). (A) Measured blood parameters: WBC (white blood cells); RBC (red blood cells); HGB (hemoglobin); HCT (haematocrit); PLT (platelets); MCV (Mean Corpuscular Volume); MCH (Mean Corpuscular Hemoglobin); MCHC (Mean Corpuscular Hemoglobin Concentration); RDW (RBC distribution width); MPV (mean platelet volume) measured one day before sacrificing. (B) Number of cells counted per mice per tissue using CASY TTC instrument. (C) Blood parameter histograms of the red blood cells after pIpC treatment: one day before PHZ treatment and on the day of sacrificing after PHZ treatment. On the y-axis amount and x-axis, the size of the RBCs. (D) and (E) Expression ration of human g- and b-globin and mice globins were determined in BM and spleen using qRT-PCR Fractions were calculated using g/g+b, z/(z+a) and bm/(bm+ey+bH1). Values were normalized to WT littermates with no Mx1-Cre. (F) The mice were weighed (left panel), after sacrificing also the spleen weight was determined (right panel). (G) Southern blot analysis of spleen, bone marrow and thymus cells after pIpC induction. Left panel show 'WT' littermates without Mx1-Cre, and right panel cKO's with Mx1-Cre.

between *Prmt5* wt and cKO (Figure 21C).
The expression of the different globin genes was quantified using RT-qPCR in BM (Figure 21D) and spleen (Figure 21E). In BM we observed no significant changes. In spleen, we didn't observe any differences between the control and *Prmt5* cKO mice. Compared to the controls, the body weights of *Prmt5* cKO mice was significantly reduced from a mean of 24.5 grams to a mean of 19.9 grams (Figure 21F). This is partly caused by the male/female balance, as all mice were male in the control group, while this was 50% in the cKO group (2 out of 4). The average weight of the two male *Prmt5* cKO mice was 22.7 grams.
Southern blot of DNA isolated from spleen, BM and thymus demonstrated that recombination at the Prmt5 locus was very inefficient in the *Prmt5* cKO animals (Figure 21G), indicating that, similar to the *Prmt1* cKO animals, cells that had escaped recombination had outcompeted the cells with recombination at both floxed alleles. We isolated DNA from cells passed through a sieve. The significant effect of *Prmt5* cKO on thymus cellularity, may imply that selection for non-recombined cells was insufficient for the thymic cells, or may be due to changes in the stromal cells of the thymus that are not represented in the DNA tested by Southern blot.

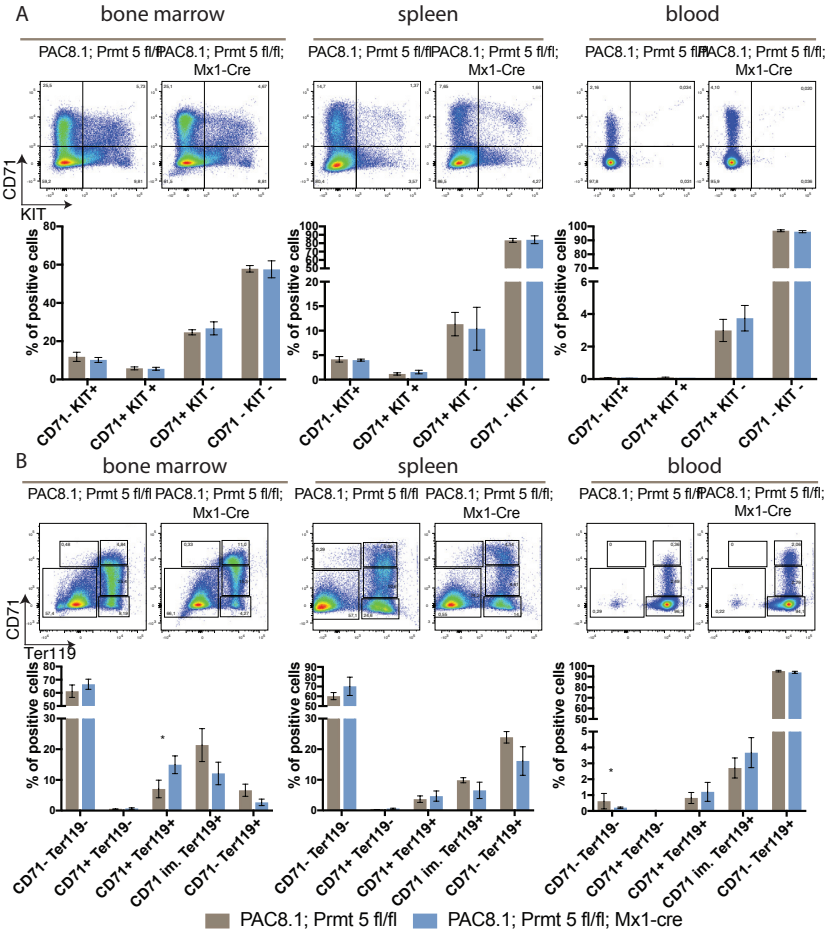

Figure 22. Flow cytometry analysis of erythroid cells in control and Prmt5 cKO mice. After live/dead gating we distinguish different erythroid progenitor cell populations using (A) CD71/KIT and (B) CD71/Ter119. (WT=4 vs cKO n=4. * indicates a p-value of <0.05)

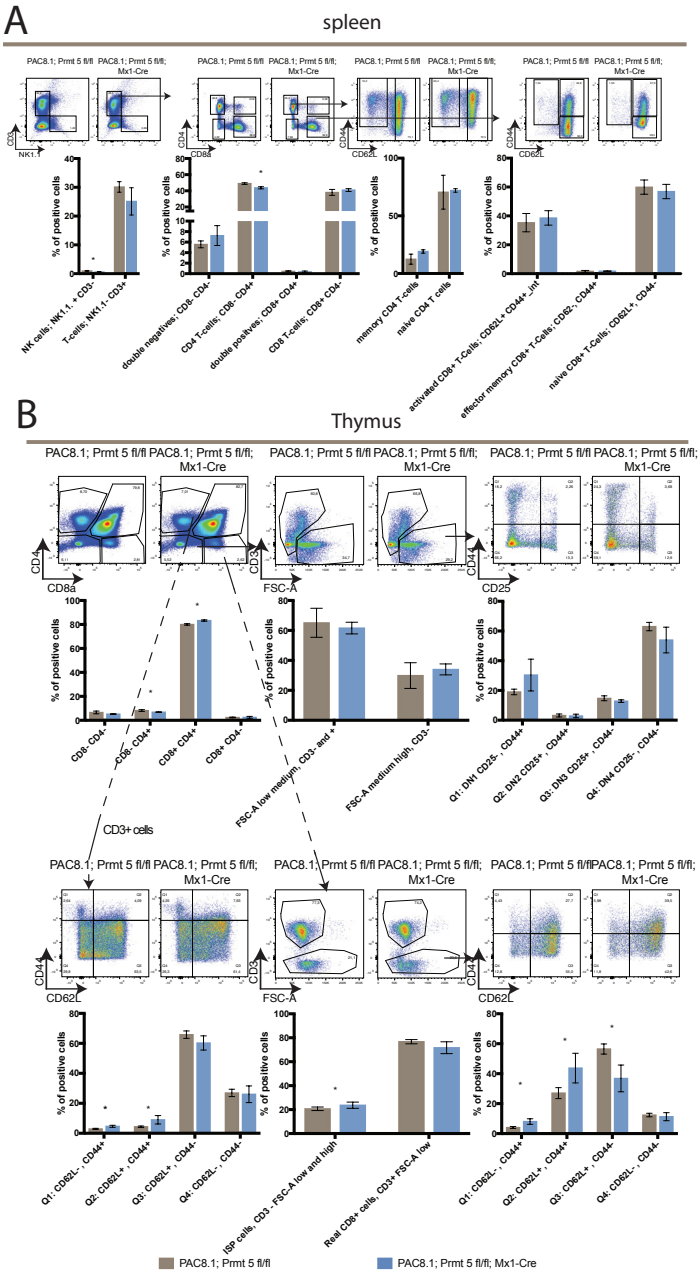

Figure 23. T cell flow cytometry analysis of Control and Prmt5 cKO (A) spleen and (B) thymus cells after PHZ treatment. After live/dead marking (not shown) CD3/NK1.1 or NK1.1/FSC-A was used to distinguish between NK-cells (NK1.1+) and T cells (NK1.1-/(CD3+)). Different populations of T cells are further specified using CD4/CD8. CD4-/CD8- double negative (DN) cells are immature T cells, in thymus they are located in the capsule. In the thymus, they move to the cortex and become CD8+/CD4+ double positive (DP) which are precursor cells. Mature T cells are characterized which are located in the medulla of the thymus are marked as single positive (SP) for CD4 or CD8. From here the gating strategy differs between spleen and thymus. In spleen, the CD4+ population is CD62L/CD44 used to distinguish CD4 memory (CD62L-/CD44+) and naïve CD4 T cells (CD62L+/CD44-and+). Within the CD8+ population we can specify activated (CD62L+/CD44+), effector (CD62L-/CD44+) and naïve (CD62L+/CD44-) T cells. In thymus DN and SPs are further categorized using CD3/FSC-A, to distinguish immature negative and mature positive cells. Subsequently, different maturation stadia of the DN immature cells are marked using CD25/CD44. DN1 is CD25-/CD44+, DN2 CD25+/CD44+, DN3 CD25+/CD44- and DN4 is CD25-/CD44-. The mature SP cells are further analysed using CD62L/CD44: effector T cells are characterized by CD62L-/CD44+, central memory T cells carry CD62L+/CD44+, and naïve T cells are CD62L+/CD44-. Immature single positive (ISP) cells are marked by CD8 SP and then CD3-. (WT n=4 vs cKO n=4. * indicates a p-value of < 0.05).

Nevertheless, in the pan-hematopoietic flow cytometry analysis we observed some significant differences between the control and *Prmt5* cKO mice.
In BM, the erythroid CD71+/Ter119+ population was increased from 6.5% in the controls to 15.5% in the *Prmt5* cKO mice, while the CD71 intermediate/Ter119+ population was decreased from 22% in the controls to 13% in the *Prmt5* cKO mice (Figure 22). This may be the result of delayed maturation of the erythroid cells, or reduced cell survival during maturation. In blood the CD71-/Ter119- population was reduced from 0.4% to 0.2% which are probably not erythroid cells but contamination of other cells, which is in accordance with the lower WBC count. All other populations were not significantly different, and especially with the CD71/KIT markers the values were very similar between the control and *Prmt5* cKO mice.
The analysis of the T cell compartment is shown in Figure 23. In the spleen, we observed a significant but small decrease of NK cells from 0.91% in the controls to 0.55% in the *Prmt5* cKO mice. In the T cells within the spleen, we observed a reduction in mature CD4 SP cells from 49% in the controls to 43% in the *Prmt5*

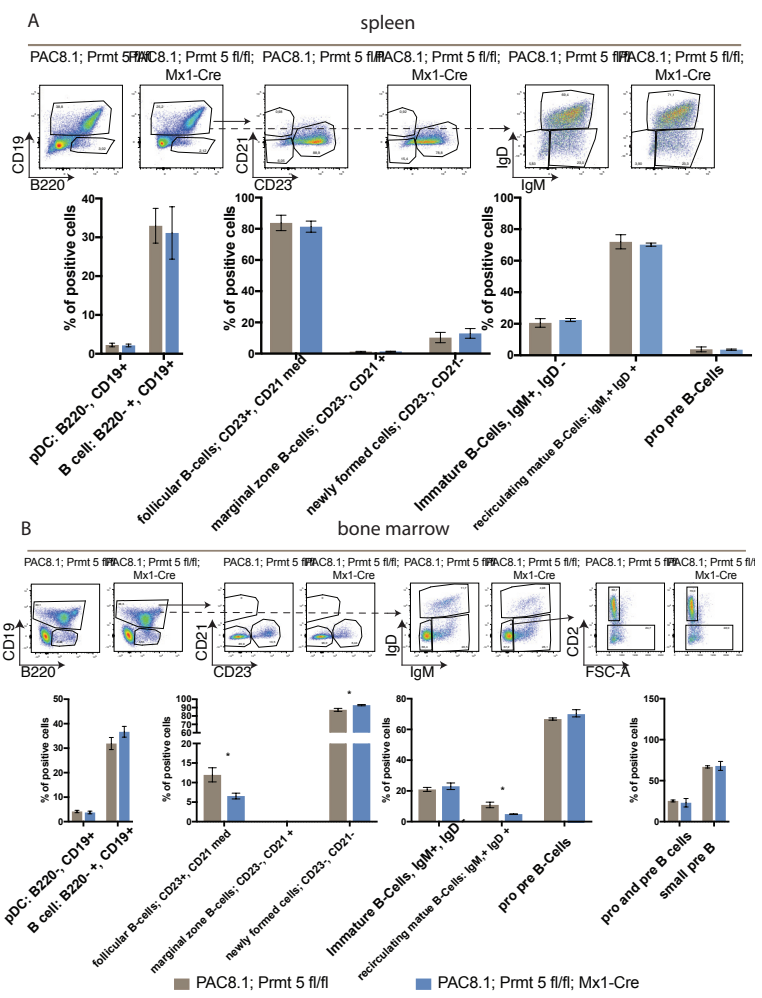

Figure 24. B cell flow cytometry analysis of Control and Prmt5 cKO (A) spleen cells and (B) spleen. First, we gated for single cells, and lymphocytes using FSC-A/FSC-H and FSC-A/SSC-A. Subsequently we used the markers B220/CD19 markers to distinguish the plasmacytoid dendritic cells (pDC; CD19-/B220+) and B cells (CD19+/B220+ and -). The B cell population is thereafter subdivided in six groups. Three subpopulations are divined using CD23/CD21; follicular (CD23+/CD21 medium); marginal zone (CD23-/CD21+) and newly formed (CD23-/CD21-) B cells. IgM/IgD markers are used to distinguish immature (IgM+/IgD-); recirculating (IgM+/IgD+) and pro/pre (IgM-/IgD-) B cells. The last group is in BM cells further specified as pro/pre-B cells (CD2-) and small pre-B cells (CD2+) using CD2/FSC-A. (WT n=4 vs cKO n=4. * indicates a p-value < 0.05).

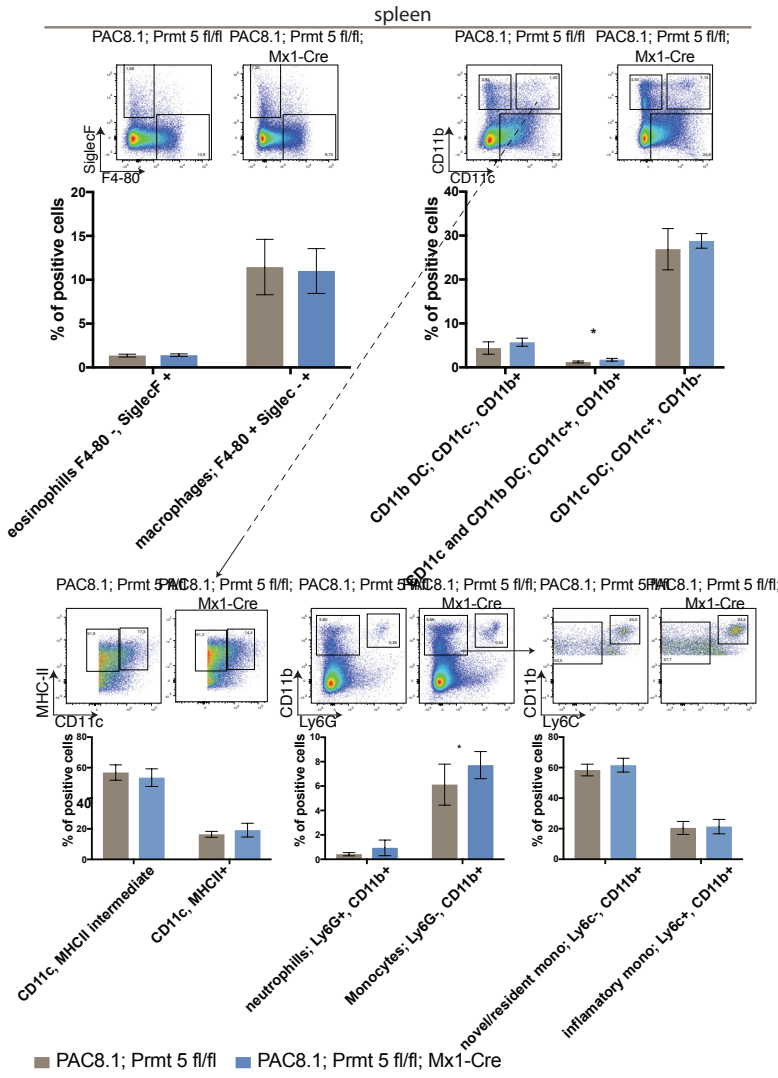

Figure 25. Flow cytometry analysis for myeloid cells in spleen from Control and Prmt5 cKO mice. After gating for living cells and lymphocytes, we could distinguish 7 different types of myeloid cells: eosinophils (F4-80-/SiglegF+), macrophages (F4-80+/SiglegF+), conventional dendritic cells (DCs: CD11c+/CD11b+), immature DCs (CD11c+/CD11b-), other myeloid cells (CD11c-/CD11b+), neutrophils (Ly6G+/CD11b+) and monocytes (Ly6G-/CD11b+). The immature DCs are further categorised as small DCs (CD11c-/MHCII+) and large DCs (CD11b+/MHCII+). Monocytes are subdivided in novel/resident monocytes (CD11b+/Ly6C-) and inflammatory monocytes (CD11b+/Ly6C+). (WT n=4 vs. cKO n=4. * indicates p<0.05).

cKO mice. This population was also reduced significantly in the thymus, from 8.4% to 6.9%. The double-positive progenitors CD8+/CD4+ were slightly but significantly increased from 80% in the controls to 83% in the *Prmt5* cKO mice. These small changes reach significance due to the fact that there was very little variation between the animals in each group. In the CD4 SP and CD8 SP T cell populations we observed that the effector memory (2,8% to 4.6%) and activated SP T cells (4,2% to 8.7%) populations were both significantly increased in thymus.

In the CD8 SP T cells also the naïve cells were decreased compared to the controls. Within the CD8 SP population, the ISP cells were slightly significantly increased in the *Prmt5* cKO mice from 21% to 22.9%.

It appears that in *Prmt5* cKO mice the balance in T cell populations is shifted slightly to the effector memory and activated side, and there are fewer naïve T cells present. Thus, the reduced cellularity of the thymus may be due to enhanced activation and

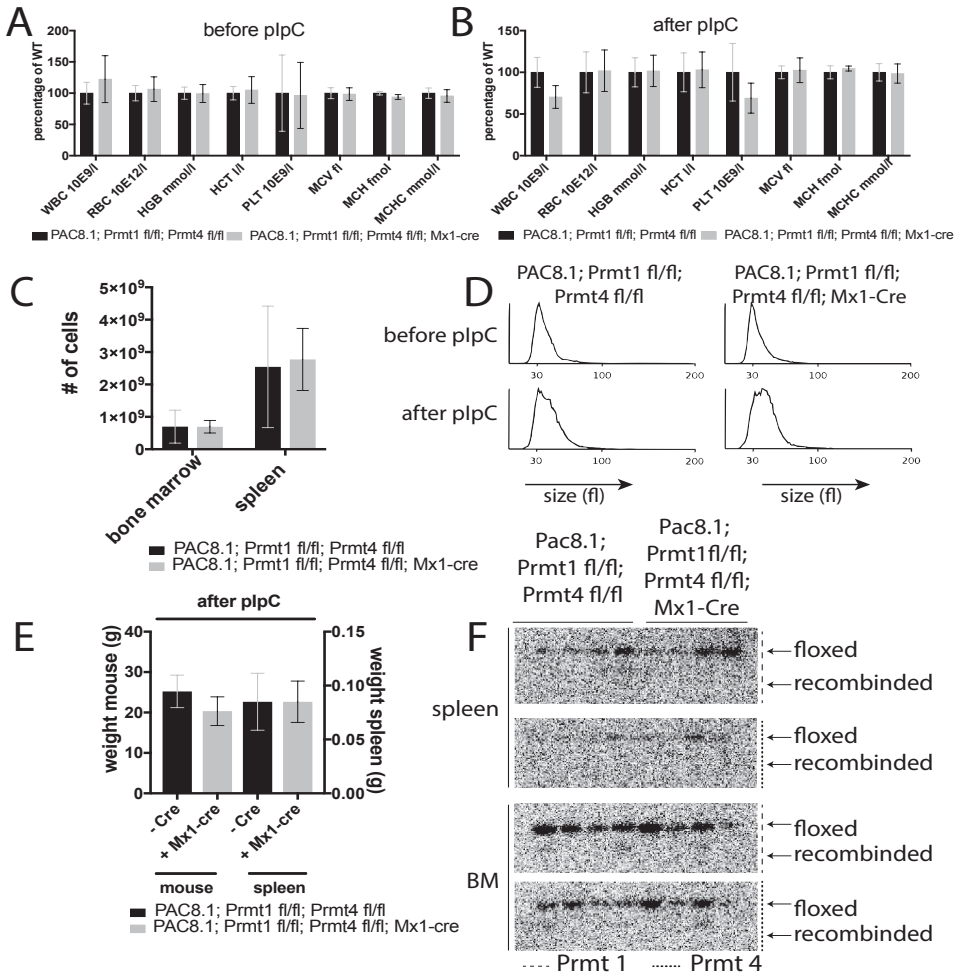

Figure 26. Control and Prmt1::Prmt4 cKO mice. (age of the mice at the moment of analysis 10-15 weeks) WT n=4 and cKO n=4). (A) Measured blood parameters before and (B) after pIpC treatment: WBC (white blood cells); RBC (red blood cells); HGB (hemoglobin); HCT (haematocrit); PLT (platelets); MCV (Mean Corpuscular Volume); MCH (Mean Corpuscular Hemoglobin); MCHC (Mean Corpuscular Hemoglobin Concentration); RDW (RBC distribution width); MPV (mean platelet volume) measured one day before sacrificing. (C) Number of cells counted per mice per tissue using CASY TTC instrument. (D) Blood parameter histograms of the red blood cells one day before pIpC induction and one day before sacrificing after pIpC induction. On the y-axis amount and x-axis, the size of the RBCs. (E) The mice were weighed (left panel), after sacrificing also the spleen weight was determined (right panel). (F) Southern blot analysis for both genes on spleen and bone marrow cells after pIpC induction. Left panel show 'WT' littermates without Mx1-Cre, and right panel cKOs with Mx1-Cre.

maturation of T cells, since the cells migrate from the thymus to the peripheric tissues in this stage.[68]

The analysis of the B cell compartment is presented in Figure 24. In the spleen (upper panel) we didn't observe any significant differences between the B cell populations of the control and *Prmt5* cKO mice. In BM (lower panel), we observed a reduction in follicular B cells from 12% in the controls to 6% in the *Prmt5* cKO

animals. An increase was observed for the newly formed B cells, from 87% to 92 % and a decrease from 10% to 5% of the recirculating mature B cells. Although not all changes were significant, compared to the controls the *Prmt5* cKO animals displayed a shift to more progenitor-like B cells.
Figure 25 represents the flow cytometry results of the myeloid cells in the control and *Prmt5* cKO mice. Most of the values were very similar between the two groups of mice. For example, the populations of eosinophils, macrophages and neutrophils appeared to be stable. The conventional DCs (CD11c+/CD11b+) were significantly increased from 1.2% to 1.7% and the monocytes from 6% to 7%. The subpopulations within these groups didn't show any changes.
In conclusion, interpretation of these data is limited by the low recombination efficiency observed in the *Prmt5* cKO animals. Nevertheless, the changes we observed in the hematopoietic cell populations point in general at an increase of progenitor cells populations, suggesting that PRMT5 is required for hematopoietic differentiation.

PRMT1 +PRMT4: analysis of normal hematopoiesis

In the next experiments, we bred mice compound homozygous for two *Prmt* conditional knockout alleles. We started with the combination of the PRMTs catalysing asymmetric arginine methylation: *Prmt1* and *Prmt4*.
Because the *Prmt1* floxed allele did not show efficient recombination after pIpC induction (Figure 11), we treated adult mice with pIpC, with the idea that the animals will have less time to mobilize unrecombined cells to take over from recombined cells. We injected mice between 8-13 weeks old every other day in a 3-treatment course, after 2 weeks we sacrificed the mice for analysis.
Measuring the blood parameters before and after pIpC induction, we didn't observe statistically significant differences between the controls and the *Prmt1::Prmt4* cKOs (Figure 26A and B). Similar to what was observed for Prmt1 cKO mice, however, WBC and PLT count is decreased in *Prmt1::Prmt4* cKO animals. Cellularity of BM and spleen, as well as red cell width distribution were similar between *Prmt1::Prmt4* cKO and wt mice (Figure 26C,D). After pIpC the RDW curves were changed, they were wider and less smooth.
Body and spleen weights were not affected by pIpC treatment (Figure 26E). To check recombination, we performed a Southern blot of spleen and BM cells (Figure 26F). Whereas the *Prmt4* floxed alleles showed very efficient recombination upon pIpC treatment (Figure 1) this was no longer the case in the compound *Prmt1::Prmt4* cKO animals. This strongly supports the notion that unrecombined cells have a strong selective advantage upon depletion of PRMT1 by recombination of the floxed *Prmt1* alleles (Figure 11).

PRMT4 and PRMT5: analysis of normal hematopoiesis

The final experiments were performed with PAC8.1/wt; Prmt4 fl/fl; Prmt 5 fl/fl and PAC8.1/wt; Prmt4 fl/fl; Prmt5 fl/fl; Mx1-Cre/wt mice. This combines conditional knockout alleles for two major PRMTs: PRMT4 belongs to the type 1 PRMTs and PRMT5 belongs to the type 2 PRMTs. The results are shown in Figure 27-35.
Analysis of blood parameters (Figure 27A), cell numbers (Figure 27B), RBC size distributions (Figure 27C), qRT-PCR results of the globins in BM and spleen (Figure 27 D,E), body- and spleen weights of the pIpC treated mice (Figure 27F) didn't reveal any significant differences between the control and Prmt4::Prmt5 cKO mice.

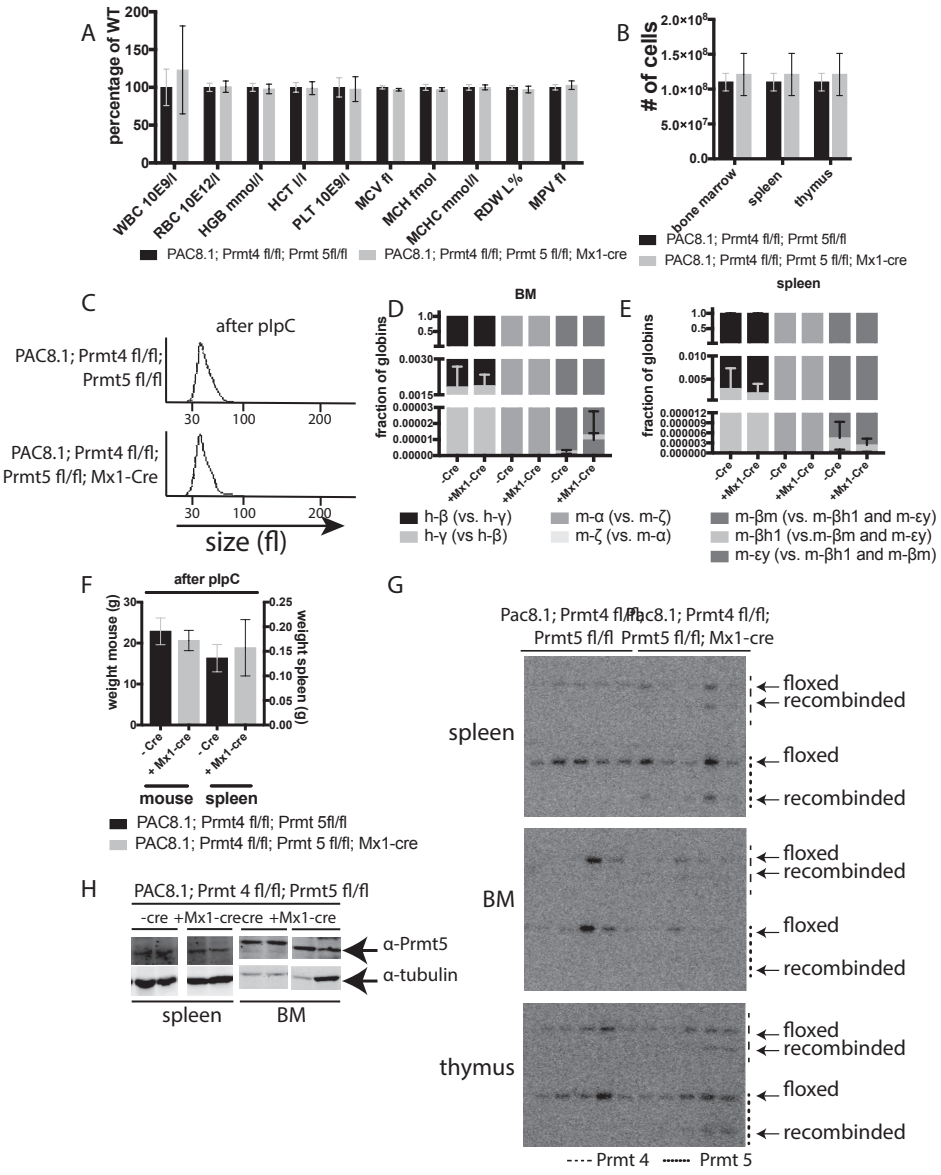

Figure 27. Control and Prmt4::Prmt5 cKO mice. (WT n=5 and cKO n=5). (A) Measured blood parameters: WBC (white blood cells); RBC (red blood cells); HGB (hemoglobin); HCT (haematocrit); PLT (platelets); MCV (Mean Corpuscular Volume); MCH (Mean Corpuscular Hemoglobin); MCHC (Mean Corpuscular Hemoglobin Concentration); RDW (RBC distribution width); MPV (mean platelet volume) measured one day before sacrificing. (B) Number of cells counted per mice per tissue using CASY TTC instrument. (C) Blood parameter histograms of the red blood cells one day before sacrificing after plpC induction. On the y-axis amount and x-axis, the size of the RBCs. (D) and (E) Expression ration of g-globin and mice globins were determined in BM and spleen using qRT-PCR. Fractions were calculated. (F) The mice were weighed (left panel), after sacrificing also the spleen weight was determined (right panel). (G) Southern blot analysis for both genes on spleen, bone marrow and thymus cells after plpC induction. Left panel show 'WT' littermates without Mx1-Cre, and right panel cKO's with Mx1-Cre. (H) Western blot analysis of RIPA lysates of complete tissues: spleen and BM. Shown are 2 representatives of each condition of each tissue. Tubulin was used as a loading control.

Southern blot analysis (Figure 27G) showed that there is some variation in recombination efficiency between the Prmt4::Prmt5 cKO mice, but on the whole the Prmt4 and Prmt5 floxed alleles displayed very inefficient recombination.
Western blot analysis of spleen and BM whole cell lysates (Figure 27H) could only be performed for PRMT5, since there is currently no antibody available for specific detection of PRMT4 in mouse tissues. For PRMT5 we observed that there appears to be some reduction in protein levels in some of the Prmt4::Prmt5 cKO tissues, but the great variability in expression between mice and tissues precludes a straightforward interpretation of these data.
Not surprisingly, the flow cytometry analyses did not reveal any exacting differences (Figure 28 to 35). The erythroid lineage displays a reduction of 0.5% of mature cells in the BM of Prmt4::Prmt5 cKO mice (Figure 28). For T cells we found a minor increase from 3% to 5% of the CD62-/CD44+ cell population within the CD3+ real CD4 SP cells of the thymus of Prmt4::Prmt5 cKO mice (Figure 29).
In the B cell lineage, no significant differences were found between the control and Prmt4::Prmt5 cKO mice (Figure 30).
For the myeloid cells we observed two increased cell populations, the CD11b DCs and the monocytes in the Prmt4::Prmt5 cKO mice (Figure 31).
We conclude that the minor differences between the controls and Prmt4::Prmt5 cKO

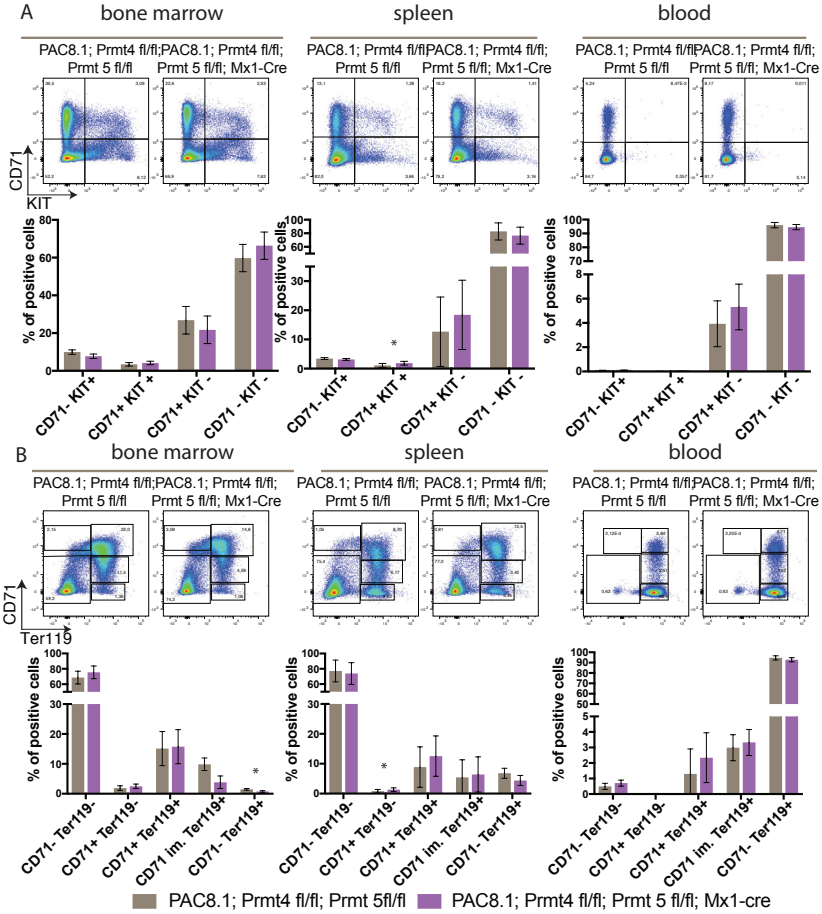

Figure 28. Flow cytometry analysis for erythroid cells in control and Prmt4::Prmt5 cKO mice. After live/dead gating we distinguish different erythroid progenitor cell populations using (A) CD71/KIT and (B) CD71/Ter119. (WT=5 vs cKO n=5).

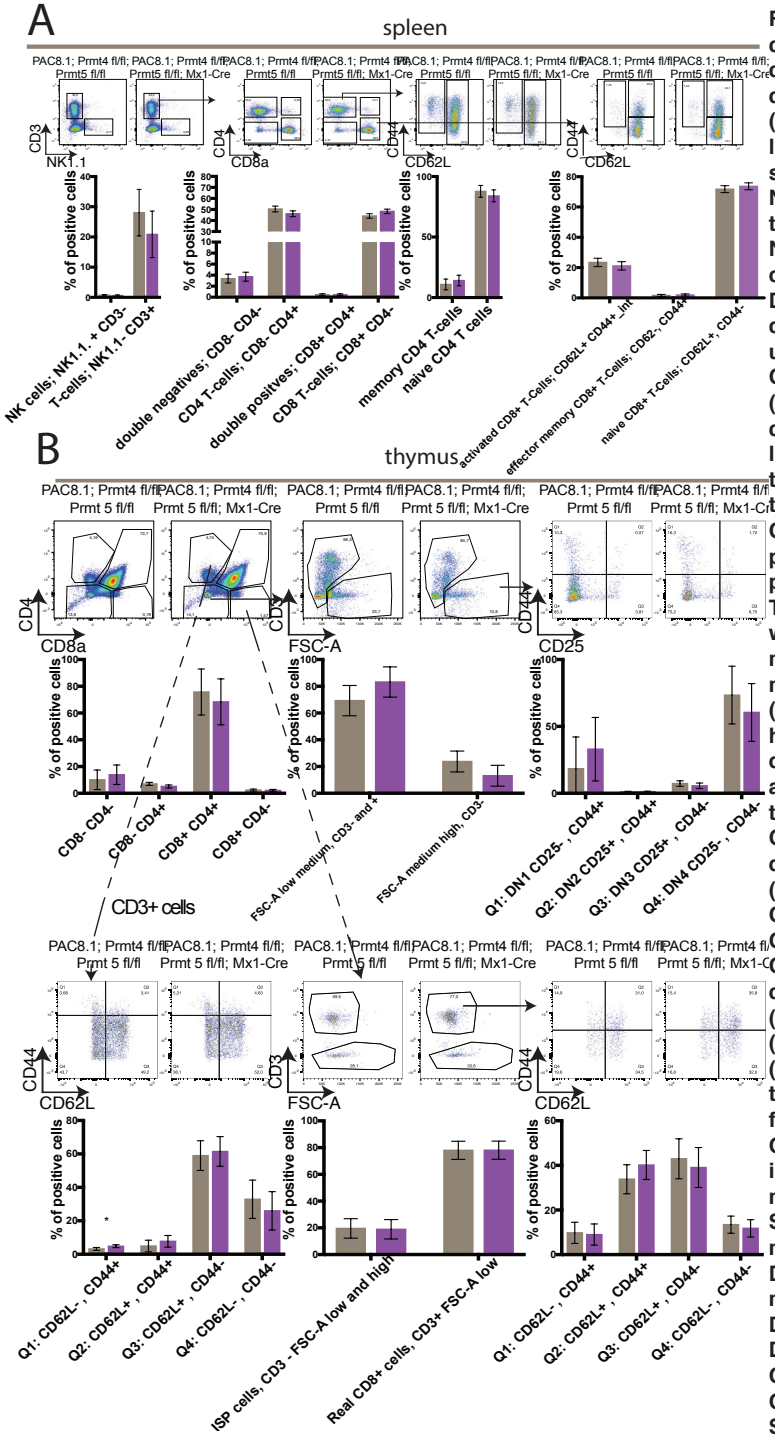

Figure 29. T cell flow cytometry analysis of control and Prmt4::Prmt5 cKO (A) spleen and (B) thymus cells. After live/dead marking (not shown) CD3/NK1.1 or NK1.1/FSC-A was used to distinguish between NK-cells (NK1.1+) and T cells (NK1.1- /(CD3+)). Different populations of T cells are further specified using CD4/CD8. CD4-/CD8- double negative (DN) cells are immature T cells, in thymus they are located in the capsule. In the thymus, they move to the cortex and become CD8+/CD4+ double positive (DP) which are precursor cells. Mature T cells are characterized which are located in the medulla of the thymus are marked as single positive (SP) for CD4 or CD8. From here the gating strategy differs between spleen and thymus. In spleen, the CD4+ population is CD62L/CD44 used to distinguish CD4 memory (CD62L-/CD44+) and naïve CD4 T cells (CD62L+/CD44-and+). Within the CD8+ population we can specify activated (CD62L+/CD44+), effector (CD62L-/CD44+) and naïve (CD62L+/CD44-) T cells. In thymus DN and SPs are further categorized using CD3/FSC-A, to distinguish immature negative and mature positive cells. Subsequently, different maturation stadia of the DN immature cells are marked using CD25/CD44. DN1 is CD25-/CD44+, DN2 CD25+/CD44+, DN3 CD25+/CD44- and DN4 is CD25-/CD44-. The mature SP cells are further analysed using CD62L/CD44: effector T cells are characterized by CD62L-/CD44+, central memory T cells carry CD62L+/CD44+, and naïve T cells are CD62L+/CD44-. Immature single positive (ISP) cells are marked by CD8 SP and then CD3-. (WT n=5 vs cKO n=5. * indicates a p-value of < 0.05).

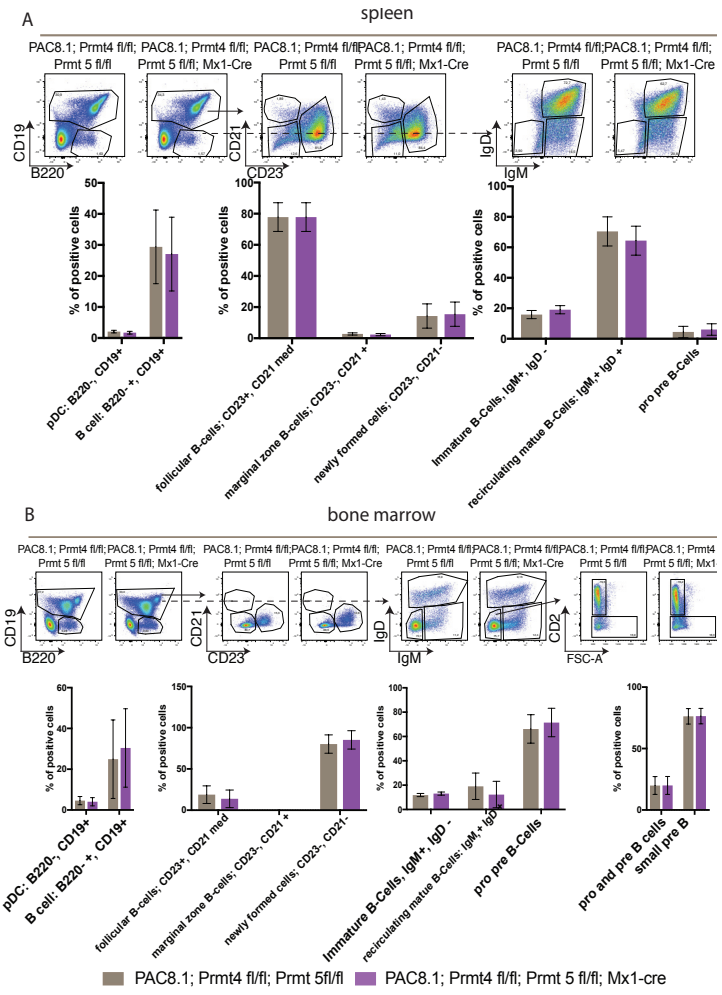

Figure 30. B cell flow cytometry analysis of control and Prmt4::Prmt5 cKO (A) spleen cells and (B) bone marrow. First, we gated for single cells, and lymphocytes using FSC-A/FSC-H and FSC-A/SSC-A. Subsequently we used the markers B220/CD19 markers to distinguish the plasmacytoid dendritic cells (pDC; CD19-/B220+) and B cells (CD19+/B220+ and -). The B cell population is thereafter subdivided in six groups. Three subpopulations are divined using CD23/CD21; follicular (CD23+/CD21 medium); marginal zone (CD23-/CD21+) and newly formed (CD23-/CD21-) B cells. IgM/IgD markers are used to distinguish immature (IgM+/IgD-); recirculating (IgM+/IgD+) and pro/pre (IgM-/IgD-) B cells. The last group is in BM cells further specified as pro/pre-B cells (CD2-) and small pre-B cells (CD2+) using CD2/FSC-A. (WT n=5 vs cKO n=5).

mice may reflect reduced expression of PRMT4/PRMT5 in a subset of the cells of the hematopoietic system. Since differences in the T cell compartment that were found with the Prmt4 single cKO mice were no longer detectable, the very low recombination efficiency obtained with the compound Prmt4::Prmt5 floxed mice indicates that cells escaping recombination have a selective advantage. This further supports the interpretation of the results obtained with the Prmt5 single cKO mice: the changes in the hematopoietic cell populations of Prmt5 single cKO mice point in general at an increase of progenitor cells populations, suggesting that PRMT5 is required for hematopoietic differentiation.

Experiments with *Vav1-Cre*

Because we could not exclude that pIpC-induced activation of CRE in the *Mxi-Cre* mice gave insufficient recombination of the Prmt1 and Prmt5 loci, we used tissue-specific, constitutively expressed, Cre recombinase lines. We chose *Vav1-Cre*, which drives Cre expression in the HSPC compartment [45], and *Vec-Cre*, which is already activated in endothelial cells before the first HSCs are formed [46]. Due to

expected embryonic lethality of loss of PRMT5, and to decrease selection of cells with non-recombined *Prmt*-loci, we chose a window for analysis during embryonic development. Timed matings were set up of mice harbouring PAC8.1; *Prmt5* floxed alleles, and Vav1-Cre recombinase, and embryos were collected on embryonic day (E) E13.5, E14.5, and E15.5. Western blot analysis was used to determine PRMT5 levels in RIPA lysates of fetal liver cells, and flow cytometry analysis was used to characterize cord blood and fetal liver cells.

All embryos collected at E13.5 contained *Vav1*-Cre, hence embryos with *Prmt5* fl/wt were used as controls. Western blot analysis revealed a reduction in *PRMT5* protein in *Prmt5* fl/fl embryos (Figure 32). Protein levels were halved in the embryos containing *Vav1*-Cre. Some of the embryos collected at E14.5 did not contain *Vav1*-Cre. Surprisingly, one of these appears have to lower levels of PRMT5 protein in the fetal liver than the embryos with *Vav1*-Cre. But in general the protein levels were reduced with 20%-50% in the embryos with *Vav1-Cre*.

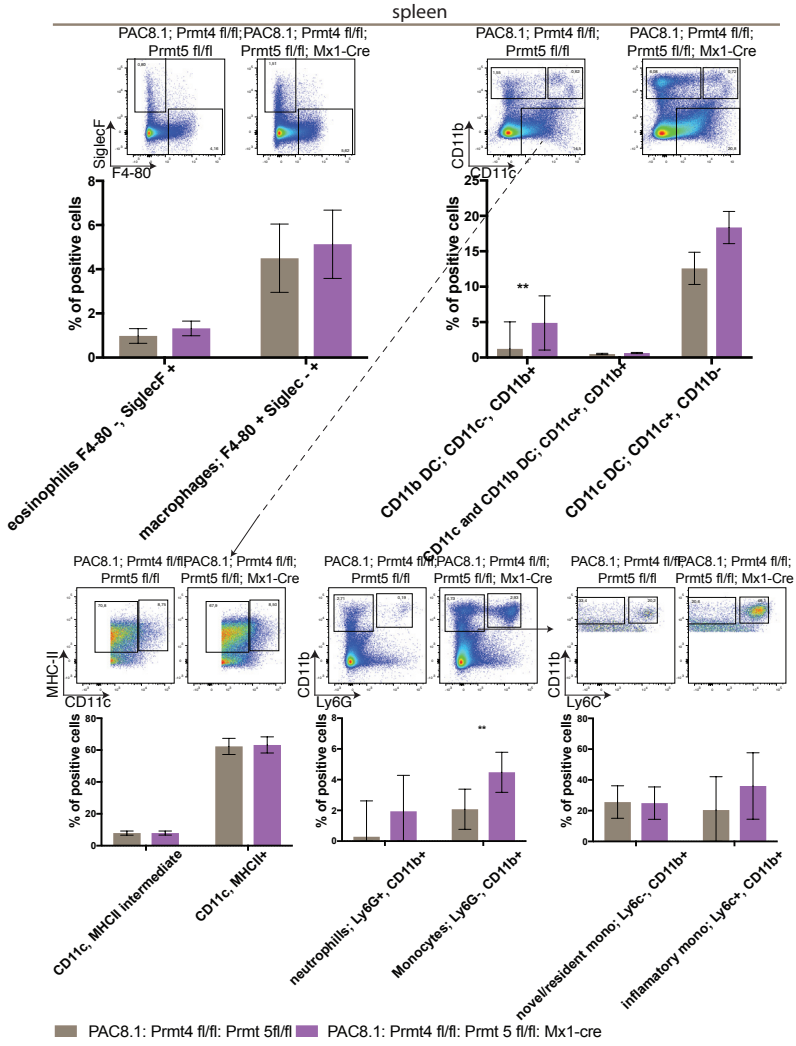

Figure 31. Flow cytometry analysis for myeloid cells in spleen from Control and Prmt4::Prmt5 cKO mice. After gating for living cells and lymphocytes, we could distinguish 7 different types of myeloid cells: eosinophils (F4-80-/SiglecF+), macrophages (F4-80+/SiglecF+), conventional dendritic cells (DCs: CD11c+/CD11b+), immature DCs (CD11c+/CD11b-), other myeloid cells (CD11c-/CD11b+), neutrophils (Ly6G+/CD11b+) and monocytes (Ly6G-/CD11b+). The immature DCs are further categorised as small DCs (CD11c-/MHCII+) and large DCs (CD11b+/MHCII+). Monocytes are subdivided in novel/resident monocytes (CD11b+/Ly6C-) and inflammatory monocytes (CD11b+/Ly6C+). (WT n=5 vs. cKO n=5. * indicates p<0.05).

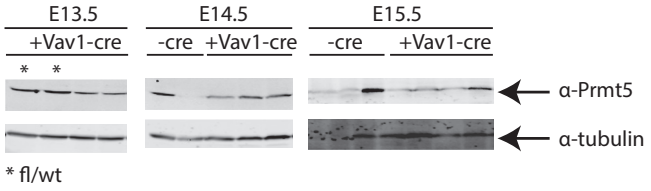

Figure 32. Western blot of fetal livers of E13.5, E14.5, and E15.5 embryos carrying PAC8.1/wt; Prmt5 fl/fl with(out) the Vav1-Cre recombinase. * heterozygote for Prmt5 floxed allele. Anti-tubulin was used as a loading control.

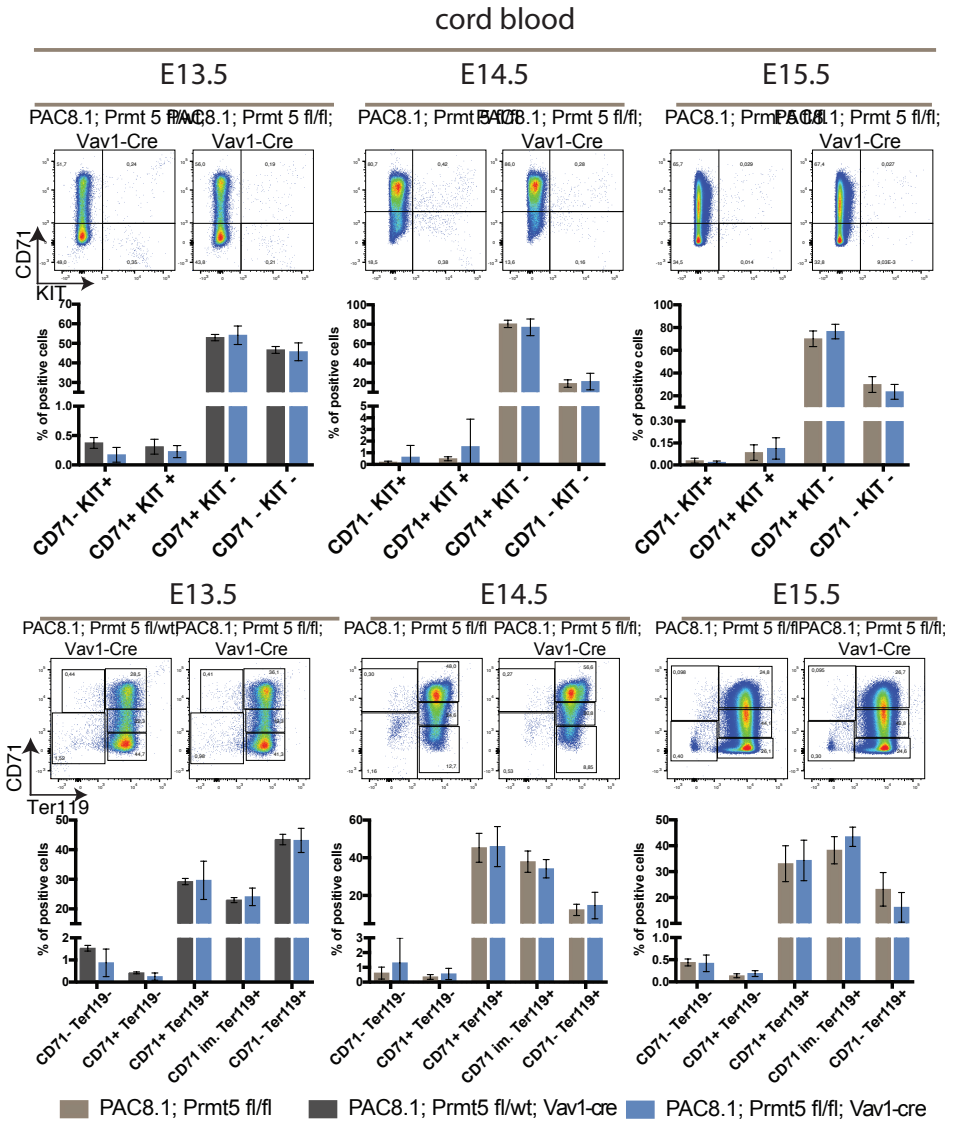

Figure 33. Flow cytometry analysis of erythroid cells in cord blood of PAC8.1/wt; Prmt5 fl/fl, PAC8.1/wt; Prmt5 fl/wt; Vav1-Cre/wt and PAC8.1/wt; Prmt5 fl/fl; Vav1-Cre/wt embryos at E13.5, E14.5, and E15.5. After live/dead gating we distinguished different erythroid progenitor cell populations using CD71/Ter119 and CD71/KIT. (E13.5 WT=2, cKO=7; E14.5 WT=5, cKO=4; E15.5 WT=4, cKO=6).

At E15.5 the fetal liver is no longer composed predominantly of erythroid cells, which could explain why there is so much PRMT5 protein left in E15.5 embryos containing *Vav1-Cre*. In conclusion, depletion of PRMT5 protein using *Vav1-Cre* was only partially successful; the best reduction was observed in E13.5 fetal livers.
Flow cytometry analysis did not reveal any major differences between the embryos of different genotypes in cord blood cells (Figure 33) and fetal liver cells (Figure 34). In E15.5 fetal liver, the CD71-/Ter119- population was reduced from 6% in the controls to 4.2% in the *Vav1*-Cre containing embryos. Because PRMT5 protein was

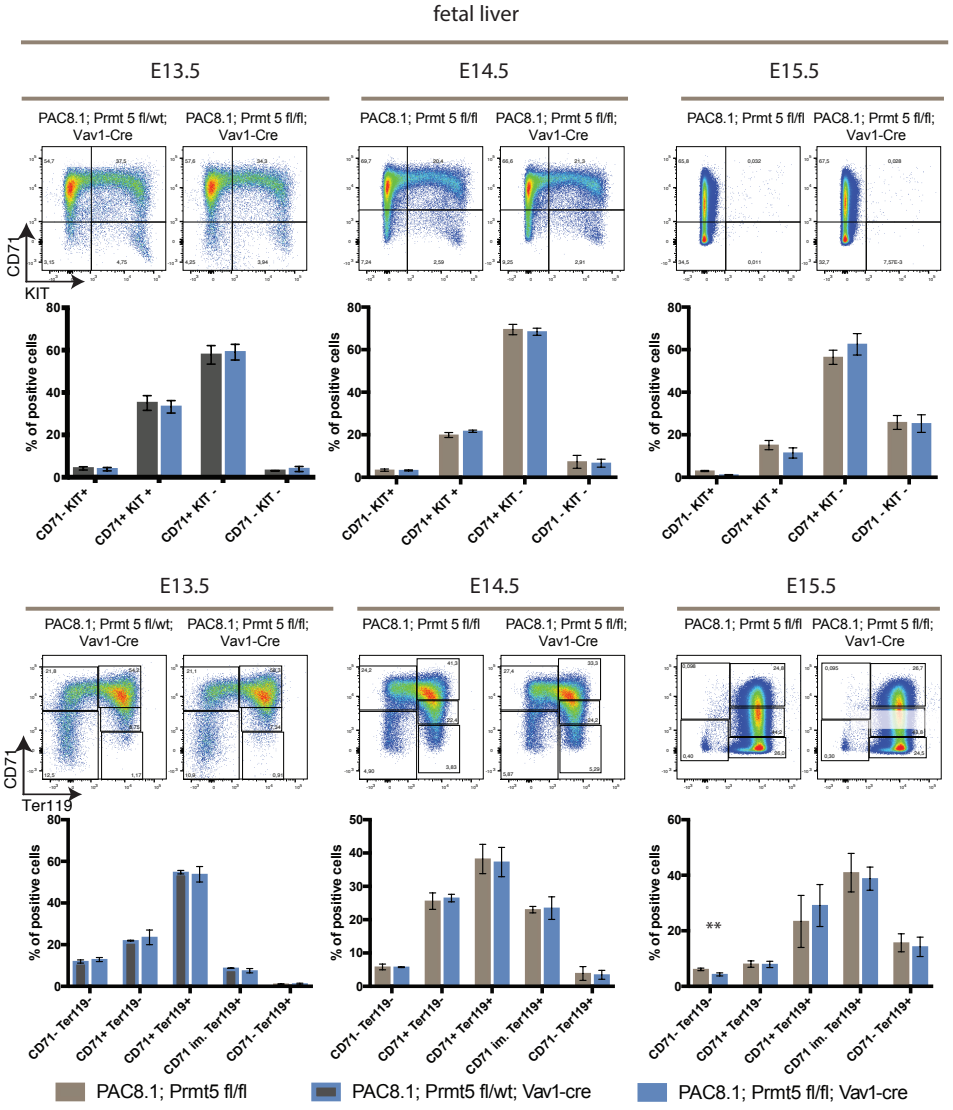

Figure 34. Flow cytometry analysis of erythroid cells of fetal livers of PAC8.1/wt; Prmt5 fl/fl, PAC8.1/wt; Prmt5 fl/wt; Vav1-Cre/wt and PAC8.1/wt; Prmt5 fl/fl; Vav1-Cre/wt embryos at E13.5, E14.5, and E15.5. After life/dead gating we distinguish different erythroid progenitor cell populations using CD71/Ter119 and CD71/KIT. (E13.5 WT=2, cKO=7; E14.5 WT=5, cKO=4; E15.5 WT=4, cKO=6).

still present, we did not perform a Southern blot.

Experiments with Vec-Cre

Since the results obtained with *Vav1-Cre* indicated incomplete recombination, we switched to the *Vec-Cre* line[46] which is active before the endothelial to hematopoietic transition during mouse development. Thus, recombination should have occurred before the appearance of the first HSCs.

Southern blot analysis was performed on fetal livers at E12.5, E13.5, E14.5, and E16.5 of PAC8.1/wt; *Prmt5* fl/fl and *fl/wt* embryos with and without *Vec-Cre* (Figure 35). Lanes containing DNA from *Prmt5 fl/wt* fetal livers are marked with an asterisk. Of note, the recombination efficiency observed in *Prmt5 fl/fl::Vec-Cre* fetal liver DNA is comparable to, or even less than the efficiency in *Prmt5 fl/wt::Vec-Cre* littermates. This difference becomes more marked at later developmental stages. This finally proofs that non-recombined cells have a selective advantage over PRMT5 depleted cells.

In Figure 36 we show the results of the erythroid flow cytometry analysis of fetal livers and cord blood. We did not observe significant changes in *Prmt5 Vec*-Cre cKO

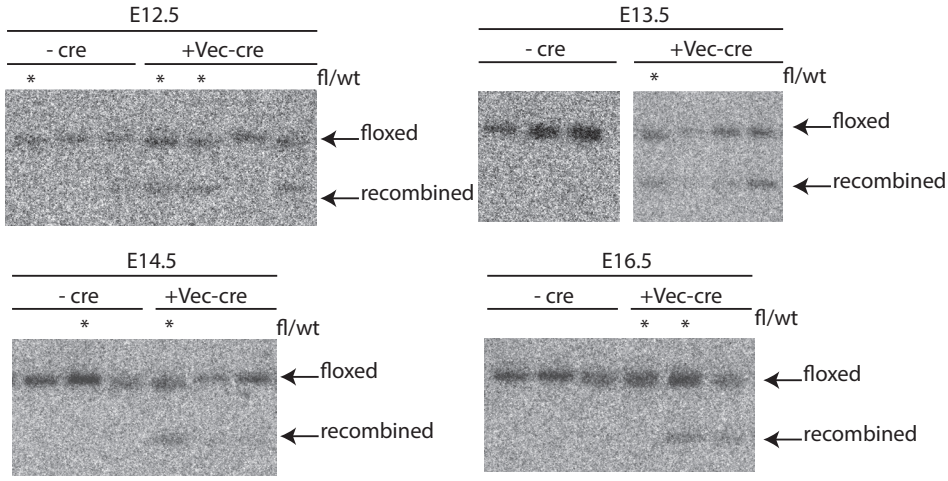

Figure 35. Southern blotting of PAC8.1/wt; Prmt5 fl/fl or fl/wt mice and PAC8.1/wt; Prmt5 fl/fl or fl/wt; Vec-Cre/wt fetal livers of embryos at E12.5, E13.5, E14.5, and E16.5. * Prmt5 fl/wt.

embryos.

CRISPR

Because of apparent selection for unrecombined cells in the conditional knockout mouse experiments, we wished to explore the role of the *PRMT* genes in the HUDEP-2 cell line[55] using CRISPR technology[69,70].

First, we lentivirally transduced HUDEP-2 cells using the lentiCas9-Blast vector, and we selected for the transduced cells with Blasticidine S. Cas9 expression in the pool of transduced cells was analysed by western blotting (Figure 37A, left panel). We noted that Cas9 expression was silenced upon removal of Blasticidine S from

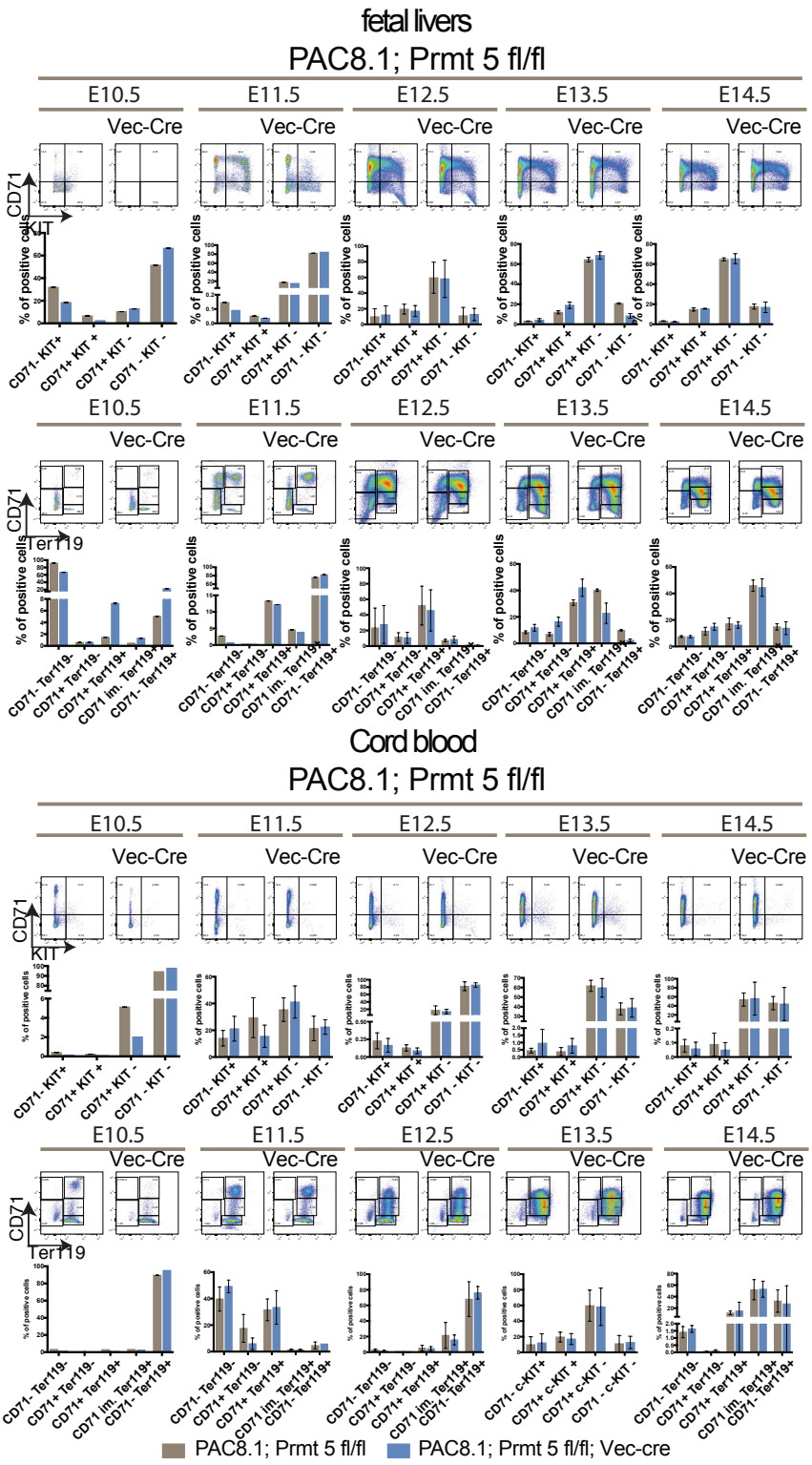
fetal livers
PAC8.1; Prmt 5 fl/fl
E10.5
E11.5
E12.5
E13.5
E14.5
Vec-Cre
CD71
KIT
Ter119
% of positive cells
CD71- KIT+
CD71+ KIT +
CD71+ KIT -
CD71 - KIT -
CD71- Ter119-
CD71+ Ter119-
CD71+ Ter119+
CD71 im. Ter119+
CD71- Ter119+
Cord blood
PAC8.1; Prmt 5 fl/fl
CD71- c-KIT+
CD71+ c-KIT +
CD71+ c-KIT -
CD71 - c-KIT -
PAC8.1; Prmt 5 fl/fl
PAC8.1; Prmt 5 fl/fl; Vec-cre

← Figure 36. Flow cytometry analysis of erythroid cells in cord blood and fetal livers of PAC8.1/wt; Prmt5 fl/fl, and PAC8.1/wt; Prmt5 fl/fl; Vec-Cre/wt embryos at E10.5 until E14.5. After live/dead gating we distinguished different erythroid progenitor cell populations using CD71/Ter119 and CD71/KIT. (E10.5 WT=3, cKO=3; E11.5 WT=6, cKO=2; E12.5 WT=4, cKO=5; E13.5 WT=2, cKO=7; E14.5 WT=6, cKO=2)

the medium (Figure 37A, midle and right panels); by selecting for Blasticidine S resistance again (not shown), high Cas9 expression levels can be restored.
After introducing the gRNAs into the HUDEP-2/Cas9 cells, we PCR-amplified the part of the target on the genomic DNA. For PRMT1, PRMT4, and PRMT5, this resulted in a product of ~523-553 bp. After gel purification of the PCR fragments, we used the surveyor assay to detect heteroduplexes (Figure 37B). Indels can be

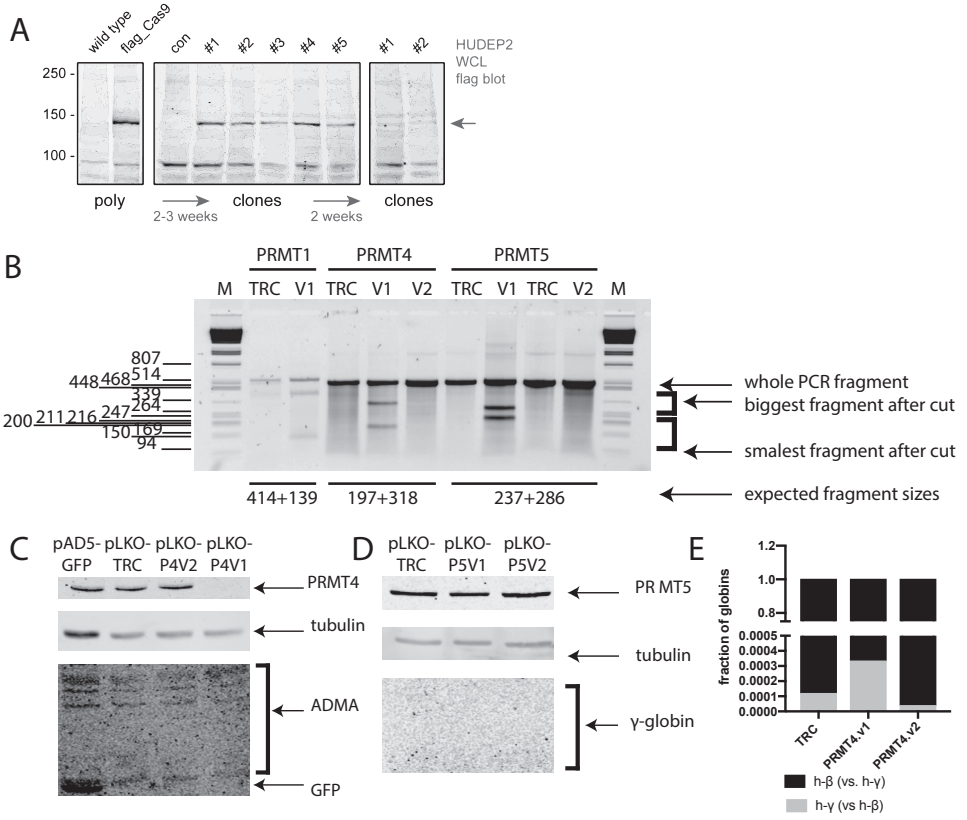

Figure 37. Results of CRISPR used in HUDEP-2 cells. (A) Western blot with anti-flag to check Cas9 expression in transduced HUDEP-2 cells after Blasticidine S selection. (B) Agarose /EtBr gel electrophoresis scan of the PCR fragments on genomic DNA of transduced HUDEP-2/Cas9 cells with the guide RNAs and controls after digestion with the surveyor endonuclease. (C) Western blot of the HUDEP-2/Cas9 cells after transduction with two different guide RNAs against PRMT4 and two controls. Single blot stained for PRMT4, tubulin as a loading control and asymmetric dimethyl arginine (ADMA). GFP of the first control gives non-specific signal. (D) Western blot of the HUDEP-2/Cas9 cells after transduction with two different guide RNAs against PRMT5 and one control. Single blot stained for PRMT5, tubulin as a loading control, and g-globin. (E) qRT-PCR results on mRNA of HUDEP-2/Cas9 cells after transduction with two different guide RNAs against PRMT4. g/g+b Normalized to TRC control.

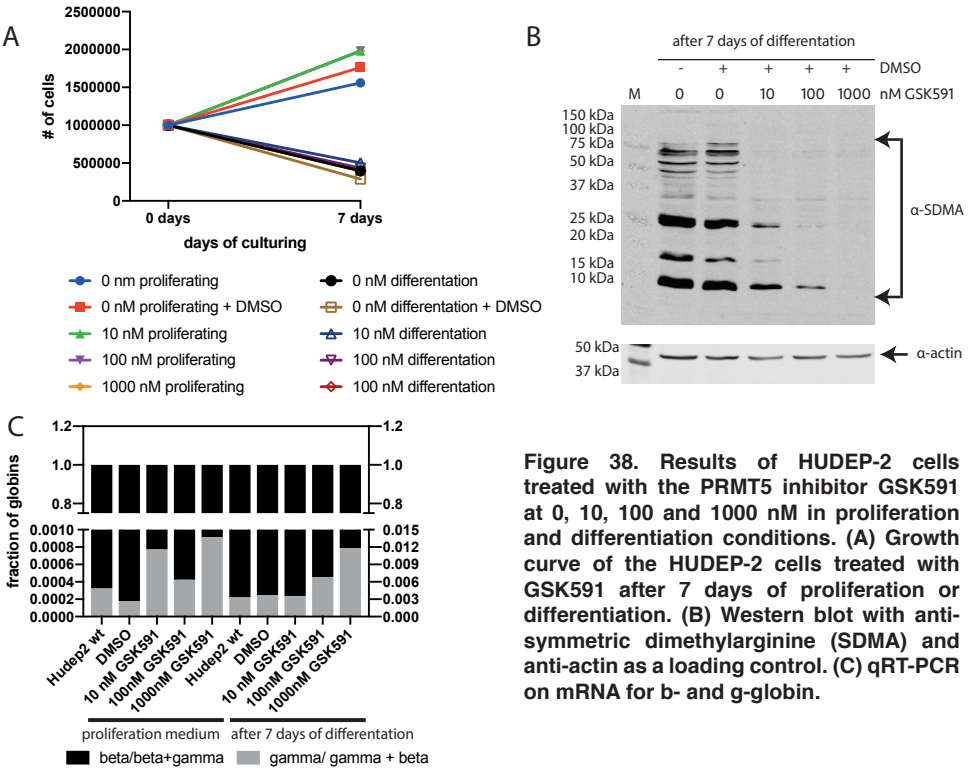

Figure 38. Results of HUDEP-2 cells treated with the PRMT5 inhibitor GSK591 at 0, 10, 100 and 1000 nM in proliferation and differentiation conditions. (A) Growth curve of the HUDEP-2 cells treated with GSK591 after 7 days of proliferation or differentiation. (B) Western blot with anti-symmetric dimethylarginine (SDMA) and anti-actin as a loading control. (C) qRT-PCR on mRNA for b- and g-globin.

detected specifically in the V1 samples of PRMT1, PRMT4, and PRMT5.

To confirm the effect of CRISPR-induced mutations on PRMT protein levels, we performed western blots for PRMT4 (Figure 37C) and PRMT5 (Figure 37D). In addition we also tested the PRMT4 blot for ADMA and the PRMT5 blot for γ-globin. HUDEP-2/Cas9 cells targeted by PRMT4-V1 displayed a strongly reduced PRMT4 protein level. In sharp contrast, HUDEP-2/Cas9 cells targeted by the two PRMT5 gRNAs did not display reduced PRMT5 reduced protein levels, despite the positive surveyor as say. This suggests that complete PRMT5 depletion is not compatible with survival of HUDEP-2 cells, a result that is in line with our observations on the *Prmt5* cKO mice. In Figure 37C at the lower panel, we checked whether the reduced protein levels of the PRMT4 protein were affecting asymmetric dimethyl arginine (ADMA) levels. We observed indeed a reduced ADMA level corresponding with the reduced PRMT4 protein. In Figure 37D we also tested for γ-globin levels, but as expected after the not reduced PRMT5 levels, there are no detectable γ-globin levels present.

To check the effect of the reduced PRMT4 level on globin expression, we performed qRT-PCR on mRNA of the CRISPRed HUDEP-2/Cas9 cells. Similar to the observations in the *Prmt4* cKO mice, we observed that depletion of PRMT4 had a minimal effect on expression of the γ-like and β-like globins, (Figure 37E). This indicates that PRMT4 is not involved in developmental regulation of globin expression.

For the PRMT1 CRISPRed HUDEP-2 cells we performed TIDE analysis on genomic DNA. Here we observed that only 9.4% was mutated due to the guide RNA (not shown). Because of this low efficiency we did not continue with this experiment.

In addition to the PRMT5 CRISPR experiments, we also tested the compound GSK591, an inhibitor of PRMT5 function. HUDEP-2 cells were seeded at 0,5x10^6 cells/ml and treated for 7 days with 10, 100 and 1000 nM GSK591 under proliferation and differentiation conditions. HUDEP-2 cells without any additives and with only DMSO were used as a control. The concentrations had no effect on the differentiation capacity of the cells (Figure 38A). In proliferation medium, cell expansion slightly is increased which already might an effect of the DMSO. In Figure 38B we show the Western blot stained with an antibody specific for symmetric dimethyl arginine (SDMA). The treated cells were showing depletion of SDMA, indicating that the inhibitor worked. Using RT-qPCR, we tested the mRNA levels of β- and γ-globin. We see an increase of γ-globin expression in the differentiated cells treated with the highest dose of GSK591(Figure 38C). Although the induction is ~10-fold, the absolute level of γ-globin is still very low. We conclude that inhibition of PRMT5 by GSK591 does not result in significantly increased γ-globin levels.

Discussion

Here we present our findings concerning conditional knockout mice of three different protein arginine methyl transferases: *Prmt1, Prmt4/Carm1, and Prmt5*. First, we will summarize the consequences of the cKOs in PAC8.1/wt mice with and without the hematopoietic specific *Mx1-Cre*/wt Cre-recombinase with a focus on erythroid cells and hemoglobin expression.

Earlier findings of our lab (not shown) revealed that use of the erythroid-specific *EpoR-Cre* line, which expresses Cre in erythroid progenitors, may leave residual mRNA and protein during terminal erythroid differentiation.

In literature, a defect of the earliest thymocyte progenitor subset is described at E18.5.[62] At the *PAC8.1*/wt; *Prmt4* fl/fl mice with and without *Mx1-Cre*/wt we can confirm changes within the T cell populations, but this is measured in adult spleen. Most of the changes that were found in literature we cannot find back in the thymus, where the T cells are originated from, although the cellularity of the thymus is reduced. Also, some B cell populations show a shift to the immature side due to the knockout. But this is only found in spleen and not in BM. After PHZ treatment we can't confirm the observed deregulations. But we found that the B cells are shifted to the pro/pre-B cells in BM instead of immature/recirculating B cells. Also, here we observed major changes in all cell populations, after PHZ addition compared to the experiment without PHZ.

For the *PAC8.1*/wt; *Prmt1* fl/fl and *PAC8.1*/wt; *Prmt5* fl/fl with and without *Mx1-Cre*/wt, we observed that the induction of recombination failed, probably due to selection for unrecombined cells. Nevertheless, we have described the observations made.

Within the *PAC8.1*/wt; *Prmt1* fl/fl mice with and without *Mx1-Cre*/wt, we see in spleen a small shift of early erythroid progenitor cells in the cKO animals, but this does not influence the other cell populations in BM and blood. In the other cells types we see some significant differences, but those are mostly shifts of few percentages from the progenitor-like stage(s) to the more mature-like cell stages.

Previously, a defect in B cell maturation when PRMT1 is absent has been reported.[65] sWe don't observe this. We only see some T cell and monocyte subpopulations that are shifting a few percentages to the more progenitor/immature like cells. After PHZ treatment all these significant deregulations have disappeared, but we can see major

shifts in all cells types to the progenitor/ immature cells presumably as a reaction to the red blood cell lysis, this is not due to the *Mx1-Cre* since the recombination was inefficient.
With PRMT5 we observe some shifts within the BM of the *Mx1-Cre* carrying animals. Also, the T cells in spleen and thymus show some altered cell population compositions, but more towards the mature cells.
Whereas the B cells are shifting in the BM more to the newly formed cells, this is not detected in spleen. Myeloid cells in spleen only show some minor changes due to activation of *Mx1-Cre*.
In the compound lines of Prmt1 fl/fl with Prmt4 fl/fl and Prmt4 fl/fl line with Prmt5 we didn't observe any significant changes in the pan-hematopoietic flow cytometry analysis.
To check recombination of the floxed allels, we analysed genomic DNA by Southern blotting. When we look at the *Prmt1* fl/fl mice and compare Southern blots of genomic DNA from spleen and BM of the mice with *Mx1-Cre*, we find considerable differences between animals. Also, there is fluctuation between the spleen and BM. This is also confirmed by western blot analysis; in some mice there is a clear protein reduction, and in other mice the protein is still abundant.
In the *Prmt4* fl/fl mice an even more interesting phenomenon is shown. In the normal *Mx1-Cre* pIpC induced mice we observe efficient recombination of close to 100%. If we treat these animals with PHZ, the recombination rate drops to 50% or even lower when comparing to the experiment without PHZ. Because the animals are sacrificed for analysis we cannot measure whether the recombination was better before the PHZ treatment. PHZ treatment causes massive lysis of the erythrocytes. As a result, new cells are quickly created, which might affect the balance between the hematopoietic lineages. Cells that escape recombination may contribute more efficiently to the newly formed cells. This would contribute to the observed low recombination frequency at the *Prmt4* locus after PHZ treatment.
When we look at the recombination efficiency of *Prmt5* fl/fl mice this is even more dramatic than the *Prmt1* fl/fl mice. If we combine *Prmt1* fl/fl with *Prmt4* fl/fl or *Prmt5* fl/fl with *Prmt4* fl/fl, recombination at the *Prmt4* locus is now also very inefficient. This indicates that the lack of efficient recombination of the floxed *Prmt1* and *Prmt5* alleles is not a locus-specific phenomenon, but more likely a consequence of strong selection bias for cells that have escaped recombination. This strongly suggests that PRMT1 and PRMT5 are essential proteins in the hematopoietic system.
According to literature, Vav1-Cre should have an effect from E11.5-E13.5 this is why we looked from E13.5. but we did not observe any effects of the cKO.[53,71]
In the embryo experiments with *Vec-Cre* and *Prmt5* floxed alleles we find that recombination of a heterozygous floxed *Prmt5* allele is efficient. In contrast, recombination rates of homozygous floxed *Prmt5* alleles is too inefficient to effectively deplete PRMT5 from the hematopoietic cells. These observations also support the notion that recombination of the *Prmt5* floxed locus is not intrinsically inefficient, and that PRMT5 is essential for hematopoietic cells. Collectively, our data shows that the conditional knockout approach can be applied successfully to non-essential *Prmt* genes such as *Prmt4*. For the study of essential *Prmt* genes such as *Prmt1* and *Prmt5*, it would be prudent to delete these genes in lineages not essential for survival of the animal such as megakaryocytes (*Pf4-Cre*), B (*Mb1-Cre*) and T cells (*Lck-Cre*).[67,68]

For the erythroid lineage, we used the human HUDEP-2 cell line as an alternative. We designed guide RNAs targeting the *PRMT1, PRMT4* and *PRMT5* genes. For *PRMT1* we performed TIDE analysis to check CRISPR-mediated genomic changes at the *PRMT1* locus. We found these to be too inefficient for analysis at population level. Improved gRNAs and/or selection of PRMT1-depleted cells will be required to study PRMT1 function in HUDEP-2 cells. For *PRMT5*, although one of the gRNAs appeared to be very efficient according to the Surveyor assay, PRMT5 protein was not successfully depleted from the cell population. As an alternative approach to PRMT5 inactivation, we tested GSK591 to inhibit PRMT5 catalytic activity. This resulted in clearly reduced levels of symmetric dimethyl arginines. We found a small increase in expression of γ-globin, although this remained well below therapeutically relevant levels.

Concerning the PRMT4 cells, the surveyor assay showed efficient modification of the genomic DNA. In HUDEP-2/Cas9 cells targeted by PRMT4-V1 gRNA a strongly reduced PRMT4 protein level was measured. But looking at the globin levels in these cells, we observed only minor γ-globin changes.

What changes did you observe?

These findings are in agreement with the data obtained with the *Prmt4* floxed mice that PRMT4 is not essential for the hematopoietic system and does not have a role in developmental regulation of globin expression.

In conclusion, PRMT4 yielded technically the best results in mice and HUDEP-2 cells, but the biological effects of PRMT4 depletion in hematopoietic cells appear to be very limited. Inactivation of *PRMT1* and *PRMT5* was technically challenging, most likely due to strong selection for cells with remaining activity of these proteins.

References

1 Franco, R. S. Measurement of red cell lifespan and aging. *Transfus Med Hemother* **39**, 302-307, doi:10.1159/000342232 (2012).

2 Schechter, A. N. Hemoglobin research and the origins of molecular medicine. *Blood* **112**, 3927-3938, doi:10.1182/blood-2008-04-078188 (2008).

3 Ingram, V. M. A specific chemical difference between the globins of normal human and sickle-cell anaemia haemoglobin. *Nature* **178**, 792-794 (1956).

4 Noguchi, C. T., Rodgers, G. P. & Schechter, A. N. Intracellular polymerization of sickle hemoglobin: disease severity and therapeutic goals. *Prog Clin Biol Res* **240**, 381-391 (1987).

5 Kumar, V., Abbas, A. K., Fausto, N. & Aster, J. C. *Robbins and Cotran pathologic basis of disease, professional edition e-book*. (elsevier health sciences, 2014).

6 Cunningham, M. J. & Nathan, D. G. New developments in iron chelators. *Current opinion in hematology* **12**, 129-134 (2005).

7 Borg, J. *et al.* Haploinsufficiency for the erythroid transcription factor KLF1 causes hereditary persistence of fetal hemoglobin. *Nat Genet* **42**, 801-805, doi:10.1038/ng.630 (2010).

8 Lanzkron, S. *et al.* Systematic review: Hydroxyurea for the treatment of adults with sickle cell disease. *Ann Intern Med* **148**, 939-955 (2008).

9 Platt, O. S. Hydroxyurea for the treatment of sickle cell anemia. *N Engl J Med* **358**, 1362-1369, doi:10.1056/NEJMct0708272 (2008).

10 Karkashon, S. *et al.* Intermediaries of branched chain amino acid metabolism induce fetal hemoglobin, and repress SOX6 and BCL11A, in definitive erythroid cells. *Blood Cells Mol Dis* **55**, 161-167, doi:10.1016/j.bcmd.2015.05.006 (2015).

11 Lettre, G. *et al.* DNA polymorphisms at the BCL11A, HBS1L-MYB, and beta-globin loci associate with fetal hemoglobin levels and pain crises in sickle cell disease. *Proc Natl Acad Sci U S A* **105**, 11869-11874, doi:10.1073/pnas.0804799105 (2008).

12 Thein, S. L., Menzel, S., Lathrop, M. & Garner, C. Control of fetal hemoglobin: new insights emerging from genomics and clinical implications. *Hum Mol Genet* **18**, R216-223, doi:10.1093/hmg/ddp401 (2009).

13 Uda, M. *et al.* Genome-wide association study shows BCL11A associated with persistent fetal hemoglobin and amelioration of the phenotype of beta-thalassemia. *Proc Natl Acad Sci U S A* **105**, 1620-1625, doi:10.1073/pnas.0711566105 (2008).

14 van Dijk, T. B. *et al.* Friend of Prmt1, a novel chromatin target of protein arginine methyltransferases. *Mol Cell Biol* **30**, 260-272, doi:10.1128/MCB.00645-09 (2010).

15 Wahlberg, K. *et al.* The HBS1L-MYB intergenic interval associated with elevated HbF levels shows characteristics of a distal regulatory region in erythroid cells. *Blood* **114**, 1254-1262, doi:10.1182/blood-2009-03-210146 (2009).

16 Wienert, B. *et al.* KLF1 drives the expression of fetal hemoglobin in British HPFH. *Blood* **130**, 803-807, doi:10.1182/blood-2017-02-767400 (2017).

17 Fanis, P. *et al.* Five friends of methylated chromatin target of protein-arginine-methyltransferase[prmt]-1 (chtop), a complex linking arginine methylation to desumoylation. *Mol Cell Proteomics* **11**, 1263-1273, doi:10.1074/mcp.M112.017194 (2012).

18 van Dijk, T. B. *et al.* Fetal globin expression is regulated by Friend of Prmt1. *Blood* **116**, 4349-4352, doi:10.1182/blood-2010-03-274399 (2010).

19 Li, X. *et al.* H4R3 methylation facilitates beta-globin transcription by regulating histone acetyltransferase binding and H3 acetylation. *Blood* **115**, 2028-2037, doi:10.1182/blood-2009-07-236059 (2010).

20 Li, J. *et al.* Coactivator-associated arginine methyltransferase 1 regulates fetal hematopoiesis and thymocyte development. *J Immunol* **190**, 597-604, doi:10.4049/jimmunol.1102513 (2013).

21 Mikropoulou, M. *An shRNA Screen for the Discovery of Suppressors of Fetal Hemoglobin*, Erasmus University Rotterdam, (2016).

22 Bedford, M. T. & Clarke, S. G. Protein Arginine Methylation in Mammals: Who, What, and Why. *Molecular Cell* **33**, 1-13, doi:10.1016/j.molcel.2008.12.013 (2009).

23 Gary, J. D. & Clarke, S. RNA and protein interactions modulated by protein arginine methylation. *Prog Nucleic Acid Res Mol Biol* **61**, 65-131 (1998).

24 Gray, K. A., Yates, B., Seal, R. L., Wright, M. W. & Bruford, E. A. Genenames.org: the HGNC resources in 2015. *Nucleic Acids Res* **43**, D1079-1085, doi:10.1093/nar/gku1071 (2015).

25 Huang, J., Vogel, G., Yu, Z., Almazan, G. & Richard, S. Type II arginine methyltransferase PRMT5 regulates gene expression of inhibitors of differentiation/DNA binding Id2 and Id4 during glial cell differentiation. *J Biol Chem* **286**, 44424-44432, doi:10.1074/jbc.M111.277046 (2011).

26 Yang, Y. *et al.* PRMT9 is a type II methyltransferase that methylates the splicing factor SAP145. *Nat Commun* **6**, 6428, doi:10.1038/ncomms7428 (2015).

27 Zurita-Lopez, C. I., Sandberg, T., Kelly, R. & Clarke, S. G. Human protein arginine methyltransferase 7 (PRMT7) is a type III enzyme forming omega-NG-monomethylated arginine residues. *J Biol Chem* **287**, 7859-7870, doi:10.1074/jbc.M111.336271 (2012).

28 Cheng, D., Côté, J., Shaaban, S. & Bedford, M. T. The Arginine Methyltransferase CARM1 Regulates the Coupling of Transcription and mRNA Processing. *Molecular Cell* **25**, 71-83, doi:10.1016/j.molcel.2006.11.019.

29 Fuhrmann, J., Clancy, K. W. & Thompson, P. R. Chemical biology of protein arginine modifications in epigenetic regulation. *Chem Rev* **115**, 5413-5461, doi:10.1021/acs.chemrev.5b00003 (2015).

30 Zhang, X. & Cheng, X. Structure of the predominant protein arginine methyltransferase PRMT1 and analysis

of its binding to substrate peptides. *Structure* **11**, 509-520 (2003).
31 Tang, J. *et al.* PRMT1 is the predominant type I protein arginine methyltransferase in mammalian cells. *Journal of Biological Chemistry* **275**, 7723-7730 (2000).
32 Lin, W.-J., Gary, J. D., Yang, M. C., Clarke, S. & Herschman, H. R. The mammalian immediate-early TIS21 protein and the leukemia-associated BTG1 protein interact with a protein-arginine N-methyltransferase. *Journal of Biological Chemistry* **271**, 15034-15044 (1996).
33 Fabbrizio, E. *et al.* Negative regulation of transcription by the type II arginine methyltransferase PRMT5. *EMBO reports* **3**, 641-645 (2002).
34 Kwak, Y. T. *et al.* Methylation of SPT5 Regulates Its Interaction with RNA Polymerase II and Transcriptional Elongation Properties. *Molecular Cell* **11**, 1055-1066, doi:10.1016/S1097-2765(03)00101-1.
35 Pal, S., Vishwanath, S. N., Erdjument-Bromage, H., Tempst, P. & Sif, S. Human SWI/SNF-Associated PRMT5 Methylates Histone H3 Arginine 8 and Negatively Regulates Expression of ST7 and NM23 Tumor Suppressor Genes. *Molecular and Cellular Biology* **24**, 9630-9645, doi:10.1128/mcb.24.21.9630-9645.2004 (2004).
36 Pollack, B. P. *et al.* The human homologue of the yeast proteins Skb1 and Hsl7p interacts with Jak kinases and contains protein methyltransferase activity. *J Biol Chem* **274**, 31531-31542 (1999).
37 Bezzi, M. *et al.* Regulation of constitutive and alternative splicing by PRMT5 reveals a role for Mdm4 pre-mRNA in sensing defects in the spliceosomal machinery. *Genes & Development* **27**, 1903-1916, doi:10.1101/gad.219899.113 (2013).
38 Yang, Y. & Bedford, M. T. Protein arginine methyltransferases and cancer. *Nature Reviews Cancer* **13**, 37, doi:10.1038/nrc3409 (2012).
39 Zhao, Q. *et al.* PRMT5-mediated methylation of histone H4R3 recruits DNMT3A, coupling histone and DNA methylation in gene silencing. *Nature Structural and Molecular Biology* **16**, 304 (2009).
40 Migliori, V. *et al.* Symmetric dimethylation of H3R2 is a newly identified histone mark that supports euchromatin maintenance. *Nature Structural and Molecular Biology* **19**, 136 (2012).
41 Blanc, R. S. & Richard, S. Arginine Methylation: The Coming of Age. *Mol Cell* **65**, 8-24, doi:10.1016/j.molcel.2016.11.003 (2017).
42 Hua, W. K. *et al.* Protein arginine methyltransferase 1 interacts with and activates p38alpha to facilitate erythroid differentiation. *PLoS One* **8**, e56715, doi:10.1371/journal.pone.0056715 (2013).
43 Greenblatt, S. M. *et al.* CARM1 Is Essential for Myeloid Leukemogenesis but Dispensable for Normal Hematopoiesis. *Cancer Cell* **33**, 1111-1127 e1115, doi:10.1016/j.ccell.2018.05.007 (2018).
44 Ju, J. *et al.* Human fetal globin gene expression is regulated by LYAR. *Nucleic Acids Res* **42**, 9740-9752, doi:10.1093/nar/gku718 (2014).
45 Rank, G. *et al.* Identification of a PRMT5-dependent repressor complex linked to silencing of human fetal globin gene expression. *Blood* **116**, 1585-1592, doi:10.1182/blood-2009-10-251116 (2010).
46 He, Y. *et al.* Induction of human fetal hemoglobin expression by adenosine-2',3'-dialdehyde. *J Transl Med* **11**, 14, doi:10.1186/1479-5876-11-14 (2013).
47 Pawlak, M. R., Scherer, C. A., Chen, J., Roshon, M. J. & Ruley, H. E. Arginine N-methyltransferase 1 is required for early postimplantation mouse development, but cells deficient in the enzyme are viable. *Molecular and cellular biology* **20**, 4859-4869 (2000).
48 Tee, W.-W. *et al.* Prmt5 is essential for early mouse development and acts in the cytoplasm to maintain ES cell pluripotency. *Genes & development* **24**, 2772-2777 (2010).
49 Yadav, N. *et al.* Specific protein methylation defects and gene expression perturbations in coactivator-associated arginine methyltransferase 1-deficient mice. *Proceedings of the National Academy of Sciences* **100**, 6464-6468 (2003).
50 de Krom, M., van de Corput, M., von Lindern, M., Grosveld, F. & Strouboulis, J. Stochastic patterns in globin gene expression are established prior to transcriptional activation and are clonally inherited. *Mol Cell* **9**, 1319-1326 (2002).
51 Koscielny, G. *et al.* The International Mouse Phenotyping Consortium Web Portal, a unified point of access for knockout mice and related phenotyping data. *Nucleic Acids Res* **42**, D802-809, doi:10.1093/nar/gkt977 (2014).
52 Stadtfeld, M. & Graf, T. Assessing the role of hematopoietic plasticity for endothelial and hepatocyte development by non-invasive lineage tracing. *Development* **132**, 203-213, doi:10.1242/dev.01558 (2005).
53 Chen, M. J., Yokomizo, T., Zeigler, B. M., Dzierzak, E. & Speck, N. A. Runx1 is required for the endothelial to haematopoietic cell transition but not thereafter. *Nature* **457**, 887-891, doi:10.1038/nature07619 (2009).
54 Kuhn, R., Schwenk, F., Aguet, M. & Rajewsky, K. Inducible gene targeting in mice. *Science* **269**, 1427-1429, doi:10.1126/science.7660125 (1995).
55 Kurita, R. *et al.* Establishment of immortalized human erythroid progenitor cell lines able to produce enucleated red blood cells. *PLoS One* **8**, e59890, doi:10.1371/journal.pone.0059890 (2013).
56 Sanjana, N. E., Shalem, O. & Zhang, F. Improved vectors and genome-wide libraries for CRISPR screening. *Nat Methods* **11**, 783-784, doi:10.1038/nmeth.3047 (2014).
57 Zufferey, R., Nagy, D., Mandel, R. J., Naldini, L. & Trono, D. Multiply attenuated lentiviral vector achieves efficient gene delivery in vivo. *Nature biotechnology* **15**, 871-875, doi:10.1038/nbt0997-871 (1997).
58 Zheng, S. *et al.* Arginine methylation-dependent reader-writer interplay governs growth control by E2F-1. *Mol Cell* **52**, 37-51, doi:10.1016/j.molcel.2013.08.039 (2013).
59 Stewart, S. A. *et al.* Lentivirus-delivered stable gene silencing by RNAi in primary cells. *RNA (New York, N.Y.)* **9**, 493-501 (2003).

60 Esteghamat, F. *et al.* The DNA binding factor Hmg20b is a repressor of erythroid differentiation. *Haematologica* **96**, 1252-1260, doi:10.3324/haematol.2011.045211 (2011).

61 Brinkman, E. K. *et al.* Easy quantification of template-directed CRISPR/Cas9 editing. *Nucleic Acids Research*, gky164-gky164, doi:10.1093/nar/gky164 (2018).

62 Kim, J. *et al.* Loss of CARM1 results in hypomethylation of thymocyte cyclic AMP-regulated phosphoprotein and deregulated early T cell development. *J Biol Chem* **279**, 25339-25344, doi:10.1074/jbc.M402544200 (2004).

63 Martina, M. N., Noel, S., Saxena, A., Rabb, H. & Hamad, A. R. Double negative (DN) alphabeta T cells: misperception and overdue recognition. *Immunol Cell Biol* **93**, 305-310, doi:10.1038/icb.2014.99 (2015).

64 Miyagawa, F., Okiyama, N., Villarroel, V. & Katz, S. I. Identification of CD3+CD4-CD8- T cells as potential regulatory cells in an experimental murine model of graft-versus-host skin disease (GVHD). *J Invest Dermatol* **133**, 2538-2545, doi:10.1038/jid.2013.212 (2013).

65 Infantino, S. *et al.* Arginine methylation catalyzed by PRMT1 is required for B cell activation and differentiation. *Nature Communications* **8**, 891, doi:10.1038/s41467-017-01009-1 (2017).

66 Carow, B., Gao, Y., Coquet, J., Reilly, M. & Rottenberg, M. E. lck-Driven Cre Expression Alters T Cell Development in the Thymus and the Frequencies and Functions of Peripheral T Cell Subsets. *J Immunol* **197**, 2261-2268, doi:10.4049/jimmunol.1600827 (2016).

67 Hobeika, E. *et al.* Testing gene function early in the B cell lineage in mb1-cre mice. *Proc Natl Acad Sci U S A* **103**, 13789-13794, doi:10.1073/pnas.0605944103 (2006).

68 Caramalho, Í., Nunes-Cabaço, H., Foxall, R. B. & Sousa, A. E. Regulatory T-Cell Development in the Human Thymus. *Frontiers in Immunology* **6**, doi:10.3389/fimmu.2015.00395 (2015).

69 Cong, L. *et al.* Multiplex genome engineering using CRISPR/Cas systems. *Science* **339**, 819-823, doi:10.1126/science.1231143 (2013).

70 Mali, P. *et al.* RNA-guided human genome engineering via Cas9. *Science* **339**, 823-826, doi:10.1126/science.1232033 (2013).

71 Tober, J., Yzaguirre, A. D., Piwarzyk, E. & Speck, N. A. Distinct temporal requirements for Runx1 in hematopoietic progenitors and stem cells. *Development* **140**, 3765-3776, doi:10.1242/dev.094961 (2013).

Supplementary material

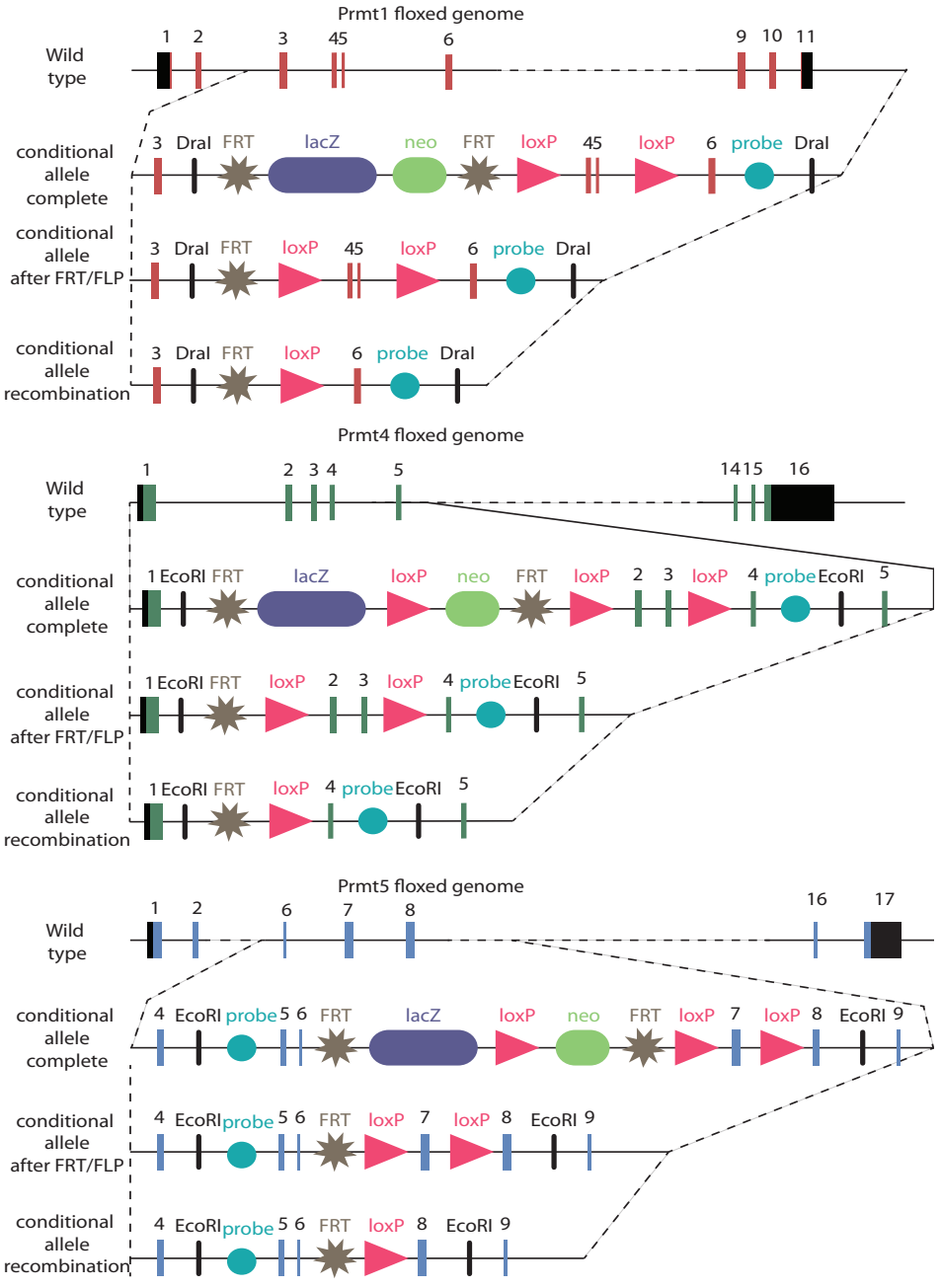

Supplementary Figure 1. Conditional knockout alleles of the Prmt1, Prmt4 and Prmt5 mice.

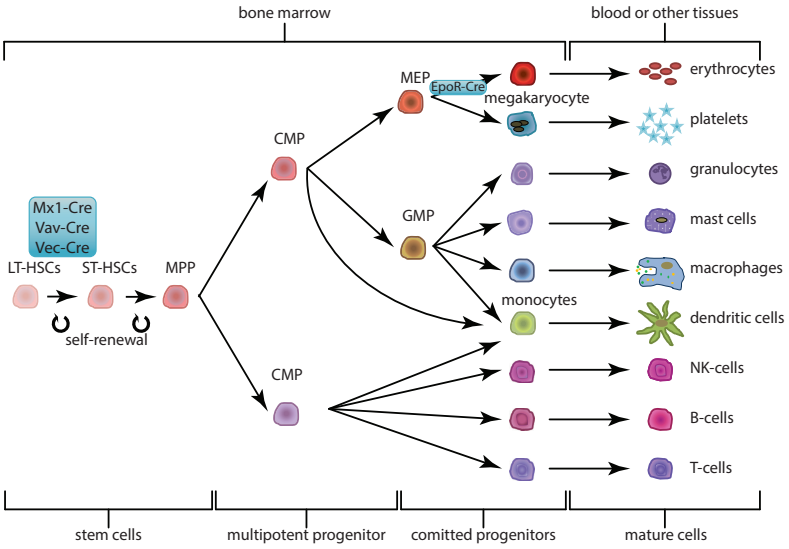

Supplementary Figure 2. Hematopoietic system and Cre recombinases used in this study.

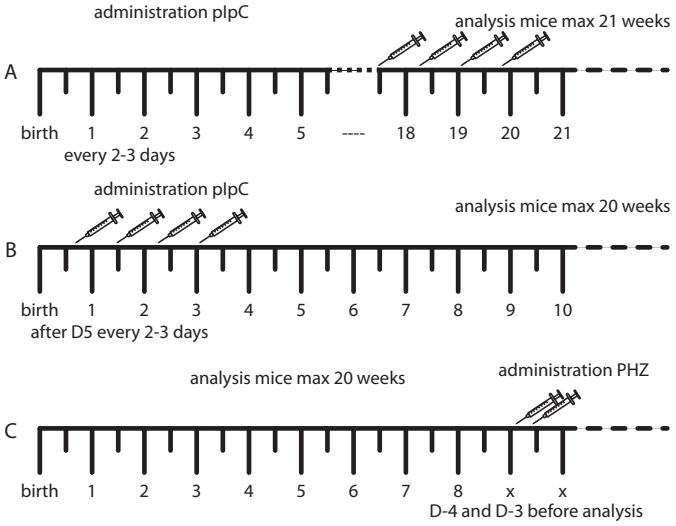

Supplementary Figure 3. Injection scheme for induction of Mx1-Cre and phenylhydrazine (PHZ) treatment. (A) Administration of pIpC in adult mice. (B) administration of pIpC in young mice. (C) Administration of PHZ. This can be combined with A and B.

Supplementary Table 1. List of primers used.

Gene[2]	Sequence	Purpose
PAC8.1_Fw	GCTGCTGTTATGACCACTAGAGGG	Genotyping
PAC8.1_Rv	AGACAGGGAAGGAGGTGTGG	Genotyping
EpoR-Cre_Fw	GTGTGGCTGCCCCTTCTGCCA	Genotyping
EpoR-Cre_Rv	CAGGAATTCAAGCTCAACCTCA	Genotyping
general-Cre_Fw	ACCCTGTTACGTATAGCCGA	Genotyping
general-Cre_Rv	CTCCGGTATTGAAACTCCAG	Genotyping
Vav-Cre_Fw	GGCGACAGTTACAGTCACAGAAGAGG	Genotyping
Vav-Cre_Rv	GCCTGGCGATCCCTGAACATG	Genotyping
CAG_Flp_Fw	CCCATTCCATGCGGGGTATCG	Genotyping
CAG_Flp_Rv	GCATCTGGGAGATCACTGAG	Genotyping
Prmt1_m_Fw	GAGTGCTTGCCATACAAGAGATCC	Genotyping
Prmt1_m_Rv	TACAAGGCCAGCCCTTAGATCACC	Genotyping
Prmt4_m_Fw	TACAAGGCCAGCCCTTAGATCACC	Genotyping
Prmt4_m_Rv	CTCTGATATGAGGGCATGACTGCG	Genotyping
Prmt5_m_Fw	CCAGAACTTCCTCTGGTTTCTGG	Genotyping
Prmt5_m_Rv	GAAAGCTGTGTGTCCTCACAC	Genotyping
Prmt1_m_Probe_Fw	GAGAAGGGACCAAAGGAATG	Southern blotting
Prmt1_m_Probe_Rv	TACAGACAGGGTCAGATGAG	Southern blotting
Prmt4_m_Probe_Fw	GCTCATCCAGGCTTTAG	Southern blotting
Prmt4_m_Probe_Rv	CAGACCCAATCCCATAG	Southern blotting
Prmt5_m_Probe_Fw	ACAAGCTAGGTATTTACACAAGGA	Southern blotting
Prmt5_m_Probe_Rv	GTCACACAGAGTCCGAAAGTTA	Southern blotting
Gapdh_m_qPCR_Fw	CTACTGGTGTCTTCACCACC	qPCR
Gapdh_m_qPCR_Rv	TCGTGGTTCACACCCATCAC	qPCR
α_m_qPCR_Fw	TTGGCTAGCCACCACCCT	qPCR
α_m_qPCR_Rv	CCAAGAGGTACAGGTGCA	qPCR
βmajor_m_qPCR_Fw	ATGGCCTGAATCACTTGGAC	qPCR
βmajor_m_qPCR_Rv	ACGATCATATTGCCCAGGAG	qPCR
βH1_m_qPCR_Fw	TGG ACA ACC TCA AGG AGA CC	qPCR
βH1_m_qPCR_Rv	ACC TCT GGG GTG AAT TCC TT	qPCR
εy_m_qPCR_Fw	TGGCCTGTGGAGTAAGGTCAA	qPCR
εy_m_qPCR_Rv	GAAGCAGAGCACAAGTTCCCA	qPCR
β_h_qPCR-Fw	TACAATTTGCTTCTGACACAAC	qPCR
β_h_qPCR-Rv	ACAGATCCCCAAAGGAC	qPCR
γ_h_qPCR-Fw	AGGTGCTGACTTCCTTGGG	qPCR
γ_h_qPCR-Rv	GGGTGAATTCTTTGCCGAA	qPCR
hPRMT1_5Fw1	CACCGCTGGACGTCGGCTCGGGCAC	CRISPR guide
hPRMT1_5Rv1	AAACGTGCCCGAGCCGACGTCCAGC	CRISPR guide
hPRMT1_deltest_Fw1	TGGTGGTGTGCACCTATAATC	CRISPR surveyor
hPRMT1_deltest_Rv1	CCCATCACCTCCATCCAATC	CRISPR surveyor
hPRMT4_exFw1	CACCGTGTGTTCAGCGAGCGGACGG	CRISPR guide
hPRMT4_exRv1	AAACCCGTCCGCTCGCTGAACACAC	CRISPR guide
hPRMT4_exFw2	CACCGGGAGCGGTCTGTGTTCAGCG	CRISPR guide
hPRMT4_exRv2	AAACCGCTGAACACAGACCGCTCCC	CRIPSR guide
hPRMT4_deltest_Fw1	CCCTGTATGTTCAAGGGAGAAA	CRISPR surveyor
hPRMT4_deltest_Rv1	AGGGCATTGTAACTGCTCTAC	CRISPR surveyor
hPRMT5_5Fw1	CACCGCTAATCATGTCATTGATCGC	CRISPR guide
hPRMT5_5Rv1	AAACGCGATCAATGACATGATTAGC	CRISPR guide
hPRMT5_5Fw2	CACCGGACCAATAAGAAGGGATTTC	CRISPR guide
hPRMT5_5Rv2	AAACGAAATCCCTTCTTATTGGTC	CRISPR guide
hPRMT5_deltest_Fw1	ATGGGTGTGGCTTCTCTTAC	CRISPR surveyor
hPRMT5_deltest_Rv1	CTAGGGCTACTACTGGCATTTAC	CRISPR surveyor

2 m_ = mouse; h_=human; Fw = sense; Rv = antisense

Supplementary Table 2 list of antibodies used

Flow cytometry			
Antibody	**Manufacturer**	**Order #**	**Dilution**
CD71-FITC	BD Pharmingen	553266	1:400
Ter119-PE	BD Pharmingen	553673	1:400
KIT-PE-Cy7	BD Pharmingen	558163	1:200
CD44-APC	BD Pharmingen	559250	1:400
Ly6C-Brilliant Violet 605	BD Horizon	563011	1:500
2,4G2 block	Homemade	-	1:300
Fixable Viability Dye eFluor® 506	eBioscience	65-0866-14	1:400
CD3-FITC	BD Pharmingen	553062	1:320
CD25-PERCP-Cy5.5	BD Pharmingen	551071	1:160 for spleen or 1:640 for thymus
CD4-APC-Cy7	BD Pharmingen	560181	1:200
NK1.1-Pacific Blue	BD Horizon	560524	1:50
CD8a-PE-Cy7	eBioscience	25-0081-82	1:1600
CD44-PE	BD Pharmingen	553134	1:1000
CD62L-APC	eBioscience	17-0621-82	1:5000
CD21-FITC	eBioscience	11-0212-85	1:500
CD19-PERCP-Cy5.5	eBioscience	45-0193-82	1:320
B220-Alexa Fluor 700	eBioscience	56-0452-82	1:160
IgM-Bio	BD Pharmingen	553436	1:80
Streptavidin-APC-eFluor 780	eBioscience	47-4317-82	1:400
CD2-PE	eBioscience	12-0021-83	1:2500
CD23-PE-Cy7	eBioscience	25-0232-81	1:500
IgD-APC	eBioscience	17-5993-82	1:2500
F4/80-FITC	eBioscience	11-4801-85	1:100
CD11b-PERCP-Cy5.5	BD Pharmingen	550993	1:100
MHCII-Alexa Fluor 700	eBioscience	56-5321-82	1:400
Ly6C-Brilliant Violet 605	BD Horizon	563011	1:500
SiglecF-PE	PD Pharmingen	552126	1:320
Ly6G-PE-Cy7	BD Pharmingen	560601	1:500
CD11c-PertexRed	Invitrogen	MDC11c17	1:100
7-aminoactinomycin D	Invitrogen	A1310	1:400
Western blotting			
Antibody	**Manufacturer**	**Order #**	**Dilution**
Prmt1	Upstate/Millipore	07-404	1:1000
Prmt4	Upstate/Millipore	09-818	1:1000
Prmt5	Upstate/Millipore	07-4051	1:1000
Gamma	Santa Cruz	sc-21756	1:1000
Actin	Santa Cruz	sc-1616	1:1000
tubulin	Thermo Fisher	A11126	1:100-
Asymmetric DMA	Cell Signalling	13522	1:1000
Symmetric DMA	Cell Signalling	13222	1:1000

Chapter 4

Chromatin Target of Prmt1 protein reduction does not affect fetal globin regulation

Chapter 4. Chromatin Target of Prmt1 protein reduction does not affect fetal globin regulation

Silvia Hoeboer[1], Nynke Gillemans[1], Ryo Kurita[2], Yukio Nakamura[2], Anne Korporaal[1], Marjolein de Bruijn[3], Rudi Hendriks[3], Thamar Bryn van Dijk[1] and Sjaak Philipsen[1]

[1] Department of Cell Biology, Erasmus MC, Rotterdam, The Netherlands
[2] Cell Engineering Division, RIKEN, BioResource Center, Tsukuba Ibaraki, Japan
[3] Department of Pulmonary Medicine, Erasmus MC, Rotterdam, The Netherlands.

Manuscript in preparation

Abstract

In an effort to find new therapeutic targets for the most common monogenetic diseases, β-thalassemia and sickle cell anaemia, Chromatin Target of Prmt1 (CHTOP) was previously found as a γ-globin regulator. In cell culture studies, where short hairpin-mediated knockdown of CHTOP was achieved in primary human erythroid progenitor cells, γ-globin levels of up to 25% of total β-like globin were found. Animal studies were hampered by the fact that constitutive *Chtop* knockout mice die around E16.5. Here we report results obtained with mice carrying a human *HBB* locus transgene, *Chtop* floxed alleles, and Cre recombinases specific for the erythroid and hematopoietic system. Using the *EpoR-Cre* line we observed a high recombination efficiency in erythroid cells. However, the protein levels of CHTOP were not affected, presumably due to the stage of differentiation at which Cre-mediated recombination occurs. We then switched to the pan-hematopoietic inducible *Mx1-Cre* line. Induction of *Mx1-Cre* in young mice resulted in efficient recombination, and importantly reduced CHTOP protein expression. These reduced levels of CHTOP protein did not increase γ-globin expression or lead to other strong hematopoietic phenotypes. To investigate the role of CHTOP in embryos, *in utero* induction of *Mx1-Cre* was not successful, and the constitutive pan-hematopoietic *Vav-Cre* line displayed poor recombination efficiency. With the constitutive hemo-endothelial *Vec-Cre* line we achieved efficient recombination and CHTOP protein reduction in fetal livers and cord blood of E12.5-E16.5 embryos. This had no discernible effect on γ-globin expression or the other erythroid parameters measured. Finally, we depleted CHTOP protein in Human Umbilical cord blood-Derived Erythroid Progenitor 2 (HUDEP-2) cells using CRIPSR technology. The *CHTOP* gene was targeted efficiently as shown by surveyor assays and TIDE analysis. However, we did not observe increased expression of γ-globin in CHTOP-depleted HUDEP-2 cells.

Introduction

In humans, the hemoglobin tetramer changes composition during the embryonic/fetal and fetal/adult transition. The first switch occurs halfway the first trimester when the major embryonic hemoglobin, a tetramer of ζ-globin and ε-globin peptides, changes to the fetal hemoglobin (HbF) tetramer composed of α-globin and γ-globin peptides. Around birth, a second switch occurs from HbF to adult hemoglobin (HbA), which is composed of a tetramer of α-globin peptides and β-globin peptides. In mice, there is only one switch, between embryonic day 11.5-13.5 the embryonic/fetal globins ζ, εy, and βh1 are replaced by the fetal/adult α, βmajor, and βminor globins. Every year around 300,000 people are born with the most common monogenetic disorders in the human population: β-thalassemia and sickle cell disease. In these diseases, the level and/or function of β-globin is disturbed due to mutations. Researchers discovered a benign condition called Hereditary Persistence of Fetal Hemoglobin (HPFH), whereby the affected people maintain increased γ-globin levels in adulthood.[1] When HPFH is combined with sickle cell disease or β-thalassemia, the disease burden of the patients is reduced.[2] Several therapeutic strategies to improve the condition of sickle cell disease and β-thalassemia patients aim to raise γ-globin levels in adults. An example is hydroxyurea treatment which elevates HbF to over 15% in some patients, but is ineffective in a sizeable fraction of patients.[3,4] Genome-wide association studies (GWAS) revealed several γ-globin regulators, including BCL11A and MYB.[5-7] About 50% of the variability in HbF levels can be assigned to the known γ-globin modifier loci.[7,8] An experimentally identified potential γ-globin modifier is Chromatin Target of Prmt1 (CHTOP), previously known as Friend of Prmt1 (FOP)[9] and small protein rich in arginine and glycine (SRAG). CHTOP is conserved in vertebrates. It is a 27 kDa nuclear protein, and also has isoforms of 25 kDa and 23 kDA.[9]

In studies of cultured human adult erythroid progenitor (HEP) cells, γ-globin levels of up to 30% of total hemoglobin were reached using short hairpin-mediated knockdown of CHTOP. [10] In mice, a full knockout of CHTOP is lethal around E16.5 due to multiple defects, including placental defects, precluding the use of this model to study developmental regulation of globin expression.[9,11]

Using mass spectroscopy, PRMT1 and PRMT5 were identified as CHTOP interacting partners.[9,10,12] Previous work linked those proteins to globin regulation.[13]

The protein arginine methyltransferase (PRMT) family consists of 9 members which are divided in 3 groups: Type I, II and III.[14,15] PRMTs catalyse the transfer of a methyl group from *S*-adenosyl-*L*-methionine (SAM) to the guanidino nitrogen atom of arginine. CHTOP interacting partner PRMT1 is a type I PRMT and is characterized by catalysing asymmetric ω-N^G,N^G-dimethylated arginines (aDMA). The type I enzymes include PRMT1, PRMT2, PRMT3, PRMT4/CARM1, PRMT6 and PRMT8. Type II enzymes are characterized by formation of symmetric ω-N^G,N^G-dimethylated arginines (sDMA), and include PRMT5 and PRMT9.[16,17] PRMT7 is thus far the only type III enzyme which is able to form ω-N^G-monomethyl arginine (MMA) on histones.[18] Most PRMTs methylate arginine- and glycine rich motifs, called RGG/RG motifs or GAR-domains, except for PRMT4/CARM1, which prefers proline, glycine and methionine (PGM)-rich motifs.[19] In general arginine methylation brings about changes in interacting partners, due to steric effects of hydrogen bond interactions without changing the charge of the molecule.[20] Full knockouts of PRMT1 and PRMT5

are, similar to the CHTOP full knock out, lethal in mice.[21,22]
The interaction between PRMT1 and CHTOP requires the GAR-domain of the CHTOP protein. CHTOP is ADMA-methylated by PRMT1. PRMT5 can also methylate CHTOP *in vitro* and *in vivo*.[9] Within the cell, CHTOP colocalizes with heterochromatin and is required for oestrogen-depended transcription of the *TTF1* gene.[9]
Another function of CHTOP works via a methylosome complex, which consists of the proteins PRMT1, PRTM5, methylosome protein 50 (MEP50) and enhancer of rudimentary homolog (ERH).[23,24] The CHTOP-methylosome complex is recruited by 5-hydroxymethylcytosine (5hmC), which are increased in glioblastoma cells.[23,24] Recruitment of the methylosome by 5hmC leads to methylation of histone H4 arginine 3 (H4R3), and the transcriptional activation of cancer-related genes such as ten-eleven translocation 1 (TET1).[23,24]
Furthermore, CHTOP is recruited by the UAP56 protein from the 'transcription/ export' complex TREX, together with the protein Alyref.[25] Together these factors show ATPase and RNA helicase activity. Within whole cell lysates, CHTOP is found to be hyper-methylated. In contrast, fractionation experiments show that CHTOP is hypo-methylated in the nuclear fraction.[25] In addition, hypo-methylated CHTOP crosslinks more efficiently to mRNA than the methylated form.[25]
Stable protein level of CHTOP is maintained via a negative feedback loop whereby CHTOP protein is binding to a stem-loop region in intron 2 within its own RNA, preventing splicing. As a stop codon is present in this sequence, this leads to degradation via nonsense-mediated mRNA decay (NMD).[26]
CHTOP has been shown to regulate γ-globin expression in cultured human erythroblasts.[10] Here, we present our findings concerning CHTOP function within the erythroid and hematopoietic system in the mouse. For this we used transgenic mice carrying the human β-globin (*HBB*) locus, floxed alleles of the *Chtop* gene, and Cre recombinase lines specific for the erythroid and hematopoietic system. We show here that although the erythroid-specific *EpoR-Cre* line efficiently activates recombination during erythroid differentiation, CHTOP protein remains abundantly present in the erythroid cells. For adult animals, we found that the inducible *Mx1-Cre* line effectively reduced CHTOP protein levels in the hematopoietic system, while for embryos the *Vec-Cre* line displayed efficient recombination in the fetal liver. Finally, we used CRISPR to deplete CHTOP protein from HUDEP-2 cells, a model for adult human erythropoiesis.[27]

Material and Methods

Mice

All animal studies were approved by the Erasmus MC Animal Ethics Committee. In this study, the following transgenic mouse strains were used: the human β-globin (*HBB*) locus PAC8.1 transgene [28], floxed *Chtop* alleles and Cre recombinase lines specific for the hematopoietic sytem. The JM8A3.N1 embryonic stem (ES) cell clone EPD0635_2_D03 with 'knockout first' L1L1_Bact_P cassette in the *Chtop* gene was obtained from the Wellcome Trust Sanger Institute (Hinxton, UK), as part of the International Mouse Knockout (now Phenotyping) Consortium. Supplementary Figure 1 displays the organization of the FRT/neo/LacZ and LoxP elements and the BclI restriction sites used for Southern blotting. Chimeras were derived by injecting ES cells into C57BL/6 blastocysts. Male chimeras were mated with C57BL/6 females

and the agouti offspring selected for presence of the targeted *Chtop* allele. To remove the LacZ-neo cassette, the mice were crossed with CAG-Flp mice. Offspring was selected for presence of floxed *Chtop* exon 4 (Supplementary Figure 1 lower panel). In addition, we used several Cre recombinase lines active in the hematopoietic system: the Epo Receptor locus (*EpoR*-Cre)[29], the endothelial, germ cell and pan hematopoietic *Vav1*-Cre[30]; vascular endothelial cadherin *Vec*-Cre[31], and interferon inducible *Mx1*-Cre line[32].
Genotyping was performed by PCR using genomic DNA isolated from toe biopsies. Primers are listed in Supplementary Table 1. Embryos were collected between embryonic day (E) 10.5 and E16.5; genotyping was performed by PCR on head DNA. Adults were analysed with a maximum age of 21 weeks. To detect Cre-mediated recombination of the *Chtop* locus, Southern blot analysis was done on erythroid tissues. The probes used listed in Supplementary Table 1. To induce *Mx1*-Cre mediated recombination, mice were injected subcutaneously (SC) 20mg/g body weight polyinosinic-polycytidylic ribonucleic acid (pIpC; P0913, Sigma Aldrich) for 3 times every other day starting at the end of the first week after birth, Supplementary Figure 2. After about 2 months, 1-2 weeks prior to collect, mice received one last pIpC injection. In some experiments, mice were subsequently treated with phenylhydrazine (PHZ P6926; Sigma Aldrich) to induce stress erythropoiesis. The mice were injected SC with 0.4% (w/v) PHZ in phosphate buffered saline (PBS) (12µl/g body weight) for 2 consecutive days (Day 1 and 2). Mice were collected at Day 5 for analysis.

Blood analysis

Peripheral blood was collected from the mandibular vein of adult mice (>10 weeks of age). Standard blood parameters were measured using an automated hematologic analyser Scil Vet Animal Blood Counter (Scil Vet ABC). Leftovers were stored in TRI-reagent (93289, Sigma Aldrich) at -20°C for RNA isolation.

Flow cytometry analysis

Single cell suspensions from blood, bone marrow, spleen, and thymus were made by flushing and crushing the material and passing through cell strainers (40 µm, 352340, BD Bioscience). The cells were diluted and washed in PBS containing 1mM EDTA. Before staining, the cells were washed in FACS buffer (PBS, 1% (w/v) bovine serum albumin (BSA) and 1 mM EDTA). ~10^6 cells were incubated for 30 minutes with the primary antibodies. Antibodies used are listed in Supplementary Table 2. Depending on the antibody combination, cells were washed in FACS buffer or PBS. Live cells were distinguished negatively by 7-aminoactinomycin D (7-AAD; A1310; Invitrogen) staining, and were directly analysed. Alternatively, the cells were stained for 30 minutes using the Fixable Viability Dye eFluor 506 (eBioscience), and washed in PBS. Cells were measured on the on a Fortessa flow cytometer (BD Bioscience).

MACS selection of CD71+ BM cells

To check recombination in erythroid cells, we selected for CD71 using the FITC labelled antibody annotated in Supplementary Table 2. We used MACS separation columns (Miltenyi Biotec) or FACS tubes and the EasySep kit (#18555; Stem Cell Technologies) and a magnet (18000; Stem Cell Technologies), according to the manufacturer's instructions.

Southern blot analysis

Genomic DNA (20 μg) of *Chtop* cKO mice was digested with 20 units of BclI enzyme overnight at 50°C. The fragments were separated on a 0.7% agarose gel, and subsequently transferred to a nylon membrane. Primers to generate the probe are listed in Supplementary Table 1. The probes were labelled with α^{32}P-dATP (PerkinElmer) using a nick translation kit (GE Healthcare). After hybridisation and washing, the blot was exposed to a phosphor screen which was scanned using a Typhoon FLA9500 instrument (GE Healthcare). The floxed *Chtop* allele will be visualised at 3.5 kb and the recombined allele at 2.7 kb.

Cell culture

Human Umbilical cord blood-Derived Erythroid Progenitor (HUDEP-2) cells were cultured in proprietary Cellquin medium (Sanquin Research, Amsterdam), supplemented with doxycycline (DOX, 1 mg/ml), stem cell factor (SCF, 100 ng/ml, R&D Systems), erythropoietin (EPO, 2 units/ml, Janssen-Cilag), and dexamethasone ($1x10^{-6}$M, Sigma) as described previously.[27] To induce differentiation, we used Cellquin medium supplemented with 500 μg/mL iron-saturated transferrin (Scipac) and EPO (10 units/ml). For cell counting we used a CASY TTC instrument (Roche).

Lentiviral production and transduction

For knockout experiments of *CHTOP* in HUDEP-2 cells, we transduced the cells first with lentiCas9-Blast (Addgene plasmid # 52962).[33] The lentiviral particles were produced in Human Embryonic Kidney (HEK) 293T cells as described previously.[34] Supernatant from the HEK-293T cells was collected and mixed on Day 1, 2, and 3 after transfection. On the third day, the supernatant was filtered using a 0.45μm filter. The virus particles were collected using centrifugation at 20,000 rpm for 2:15 hours at 4°C. The HUDEP-2 cells were exposed to the lentivirus for 78-92 hours. Blasticidin S (10 μg/mL; Santa Cruz #sc-495389) was added for the selection of transduced cells. After selection, we performed a second transduction with a vector containing the guide RNA (gRNA). This vector was made from the pSpCas9(BB)-2A-Puro (PX459) V2.0 plasmid, which was a gift from Feng Zhang (Addgene plasmid # 62988).[35] The gRNAs were designed with the online CRISPR design tool of the Zang lab at MIT (http://crispr.mit.edu/). As a threshold, we only used guides with a score higher than 85. Furthermore, we blasted the guide targets for predicted off target effects. The gRNA oligonucleotides (Integrated DNA Technologies) are listed in Supplementary Table 1. We transferred the gRNA part to a lentivirus producing vector, pLKO.1 puro, which was a gift from Bob Weinberg (Addgene plasmid # 8453). After transduction, we added puromycin (1 μg/mL; Sigma) for 24 hours to select for transduced cells.
To check the effect of the CRISPR, we designed a PCR around the gRNA target region. Using Platinum Taq polymerase (Invitrogen), we amplified a product of ~626 bp. Subsequently, we used the Surveyor Mutation Detection kit (Integrated DNA Technologies) according the manufacturer's instructions, to detect heteroduplexes indicative of CRISPR-induced mutations. When CRISPR succeeded, fragments of ~285 bp and ~341 bp are expected.

TIDE

On genomic DNA we performed TIDE analysis to check the efficiency of the CRISPR guides.[36]

Protein extraction and western blotting

Whole cell lysates of blood, BM, spleen, and HUDEP-2 cells were prepared using RIPA buffer (20mM Tris pH 7.4, 150 mM NaCl, 1% NP40, 0.1% SDS, 0.5% mM EDTA and 0.5% sodium deoxycholate) supplemented with complete protease inhibitor mix (Roche) and Pefablock (Roche).[37] The samples were lysed on ice for 15 minutes before centrifugation 15 minutes at 10,000 rpm at 4°C. Supernatant was collected and mixed with 4x Sample Buffer (50mM Tris pH6.8, 0.004% Bromophenol Blue, 8% SDS, 40% glycerol, 10% β-mercaptoethanol). To visualize γ-globin expression at the protein level, whole cell lysates were loaded on 10% or 12.5% SDS-PAGE, the gels were transferred to nitrocellulose membranes and probed with antibodies listed in Supplementary Table 2.

Results

In primary adult human erythroid progenitor (HEP) cells, CHTOP is associated with γ-globin regulation[10]. Upon shRNA-mediated knockdown, HbF levels of up to 30% of total Hb can be reached.[10] To test this *in vivo*, we performed knockout experiments in mice. Since the full knockout of *Chtop* is lethal in mice [9], we used a conditional knockout system.

We used mice carrying floxed *Chtop* alleles, the human *HBB* locus single copy transgene PAC8.1 [28], and a specific Cre recombinase. We started with the erythroid-specific *EpoR-Cre* line, containing a Cre recombinase knockin allele of the erythropoietin receptor gene [29]. This Cre recombinase will become active from the burst forming unit erythroid (BFU-E) progenitor stage and is specific for the erythroid linage.

The *PAC8.1/wt; Chtop fl/fl; EpoR-Cre/wt* mice were compared with littermates without *EpoR-Cre*. We also tested stress erythropoiesis induced by phenylhydrazine (PHZ) treatment. Before sacrificing the mice, we collected blood from the mandibular vein to measure blood parameters. We observed no differences comparing the *PAC8.1/wt; Chtop fl/fl* mice to the *PAC8.1/wt; Chtop fl/fl; EpoR-Cre/wt* mice (Figure 1A-B). As expected, there were significant effects on the erythroid compartment due to PHZ treatment; during stress erythropoiesis increased numbers of reticulocytes are released into the bloodstream. The histograms of the red blood illustrate these differences induced by PHZtreatment (Figure 1C), . However, when comparing the *EpoR-Cre/wt* mice with the controls no major differences were observed in the PHZ-treated mice. Figure 1D is showing the total body and spleen weights of animals without PHZ treatment. In addition, Figure 1E is showing the weights after PHZ treatment. No significant differences were found between the mice with *EpoR-Cre* and the controls. Comparing mice with and without PHZ treatment we observed, as expected, a significant increase in spleen size due to the activation of stress erythropoiesis.

Figure 1F-I shows the analysis of human and mouse β-like globin expression in bone marrow and spleen cells. An increase of almost 7% for γ-globin and 10% for ε-globin was found in PHZ-treated animals carrying *EpoR-Cre*, but due to the high variability between the animals, this did not reach statistical significance. To determine the recombination efficiency, we performed Southern blotting on spleen and bone marrow DNA (Figure 1J). For the mice without PHZ treatment we performed CD71+ cell selection to enrich for erythroid progenitor cells. This revealed very efficient

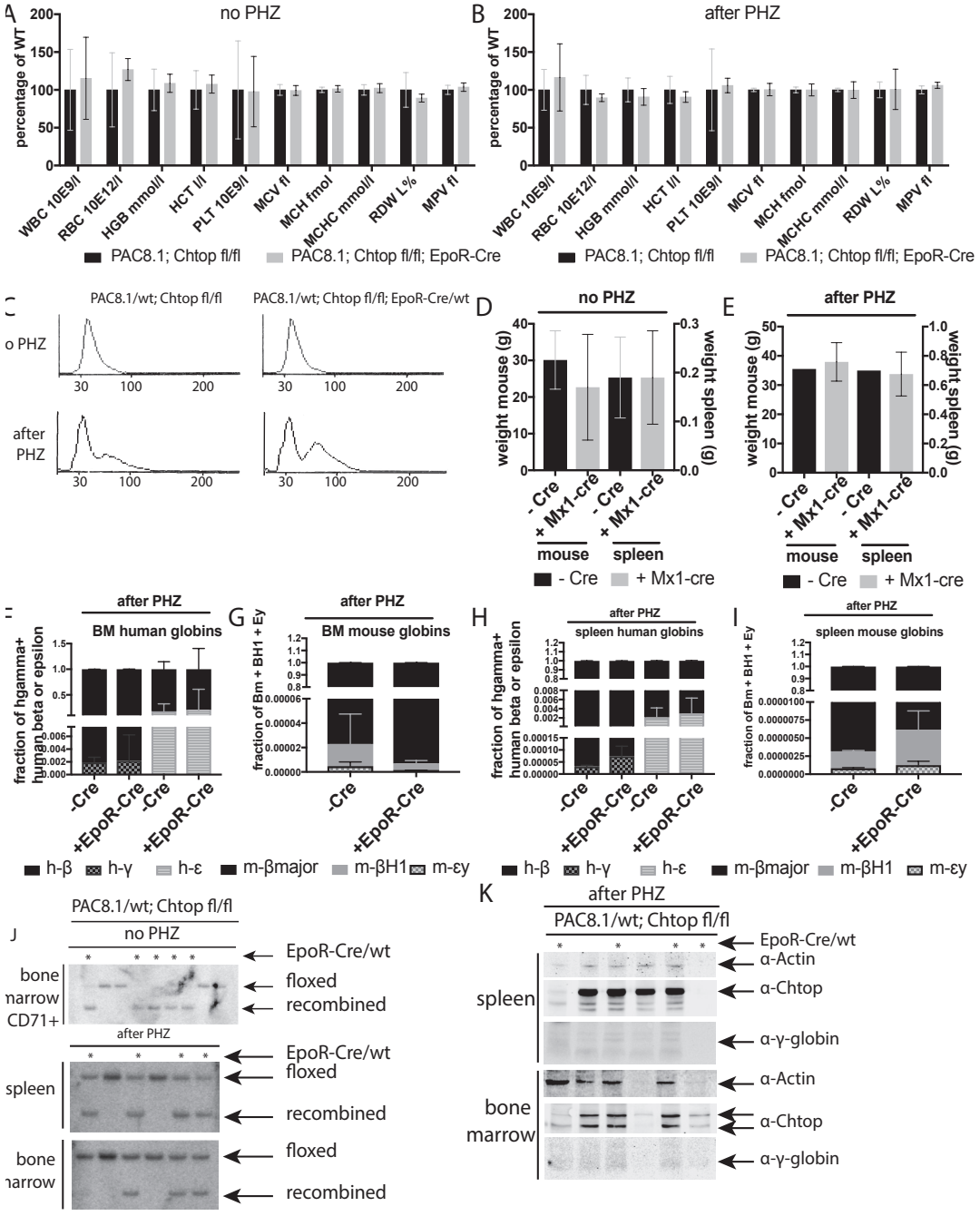
A
no PHZ
percentage of WT
WBC 10E9/l
RBC 10E12/l
HGB mmol/l
HCT l/l
PLT 10E9/l
MCV fl
MCH fmol
MCHC mmol/l
RDW L%
MPV fl
PAC8.1; Chtop fl/fl
PAC8.1; Chtop fl/fl; EpoR-Cre
B
after PHZ
C
PAC8.1/wt; Chtop fl/fl
PAC8.1/wt; Chtop fl/fl; EpoR-Cre/wt
o PHZ
after PHZ
D
no PHZ
weight mouse (g)
weight spleen (g)
- Cre
+ Mx1-cre
mouse
spleen
E
after PHZ
F
after PHZ
BM human globins
fraction of hgamma+ human beta or epsilon
G
after PHZ
BM mouse globins
fraction of Bm + BH1 + Ey
H
after PHZ
spleen human globins
I
after PHZ
spleen mouse globins
h-β
h-γ
h-ε
m-βmajor
m-βH1
m-εy
J
PAC8.1/wt; Chtop fl/fl
no PHZ
bone marrow CD71+
after PHZ
spleen
bone marrow
EpoR-Cre/wt
floxed
recombined
K
after PHZ
PAC8.1/wt; Chtop fl/fl
EpoR-Cre/wt
spleen
bone marrow
α-Actin
α-Chtop
α-γ-globin

←Figure 1. PAC8.1/wt; Chtop fl/fl mice with and without EpoR-Cre/wt before and after phenylhydrazine (PHZ) treatment (*indicates a p-<0.05 WT no PHZ n=8 / cKO no PHZ n=12 / WT after PHZ n=2 / cKO after PHZ n=4).(A-B) Blood parameters measured on the animal blood cell counter before (A) and after (B) PHZ treatment. White blood cells (WBC); red blood cells (RBC); hemoglobin (HGB); hematocrit (HCT); platelets (PLT); mean corpuscular volume (MCV); mean corpuscular hemoglobin (MCH); mean corpuscular hemoglobin concentration (MCHC); red blood cell distribution width (RDW); mean platelet volume (MPV). (C) RBC histograms, x-axis represents the size, y-axis the number of cells. After PHZ treatment, an additional peak is detected, representing larger non-nucleated RBCs: reticulocytes. (D-E) Average mouse body weights (left y-axis; two left bars), and spleen weights (right y-axis; two right bars) of mice before (D) and after (E) PHZ treatment. (F-I), Relative contribution of human (F, H) and mouse (G, I) b-like globins in bone marrow (F, G) and spleen (H, I) as measured by RT-qPCR. Relative fractions are calculated like g/(g +b) and bm/(bm + bH1 + ey). (J) Southern blot of genomic DNA after overnight digestion with the BclI enzyme at 50°C. Upper panel: CD71+ selected bone marrow cells; middle panel: spleen cells from PHZ treated mice; lower panel: total bone marrow (no selection) after PHZ treatment. (K) Western blot of spleen (upper panels) and BM (lower panels) cells after PHZ treatment. Blots were stained with anti- (a) actin, CHTOP and g-globin.

recombination of the *Chtop* locus, up to 100%, in the animals carrying *EpoR-Cre*. After PHZ treatment, the observed recombination rate was reduced to about 50%. Possibly, this can be explained by the fact that cells escaped recombination during the fast stress erythropoiesis response.

Figure 1K shows western blot results of spleen and bone marrow whole cell lysates. This confirmed that there was still CHTOP protein left owing to the incomplete recombination after PHZ treatment, although this varied between individual mice. In the first lane, containing protein of an *EpoR-Cre* mouse, less CHTOP protein was visible, but in the third lane, which also contains protein of an *EpoR-Cre* mouse, the level of CHTOP protein was similar to that observed in the second lane which contained protein isolated from a control mouse. We also stained the western blot for human γ-globin, but expression of γ-globin could not be detected.

Next, we performed CD71/Ter119 flow cytometry analysis on the bone marrow, spleen, and blood cells after PHZ treatment. We observed that there were no significant differences between the mice with and without *EpoR-Cre* (Figure 2). In conclusion, in the *EpoR*-Cre carring mice we detected a recombination efficiency of up to 100%, but no differences in erythroid parameters were observed. In addition, continued presence of CHTOP protein upon PHZ-induced stress erythropoiesis may have obscured any significant CHTOP-dependent changes in blood parameters, spleen and body weights, and alterations in globin expression. To circumvent this problem, we crossed the *PAC8.1/wt; Chtop fl/fl* mice with a line containing *Mx1-Cre*. This Cre is active from the early hematopoietic stem cell, so any remaining CHTOP protein should be diluted to undetectable levels due to the many cell divisions from that point when fully recombined. The *Mx1-Cre* line has the advantage that Cre expression is induced by activating the interferon response through injection of double stranded RNA (pIpC).

We measured the blood parameters before induction with pIpC, after pIpC induction, and after pIpC induction followed by PHZ treatment (Figure 3A-C). Most of the measured blood parameters were unaffected after *Mx1*-Cre induction by pIpC, (Figure 3B). We observed a reduction of 23% of the WBC in mice treated with pIpC and carrying *Mx1-Cre* (Figure 3B). We observed that in the control mice the RBCs were decreased with 19% after pIpC treatment, but that this did not occur in

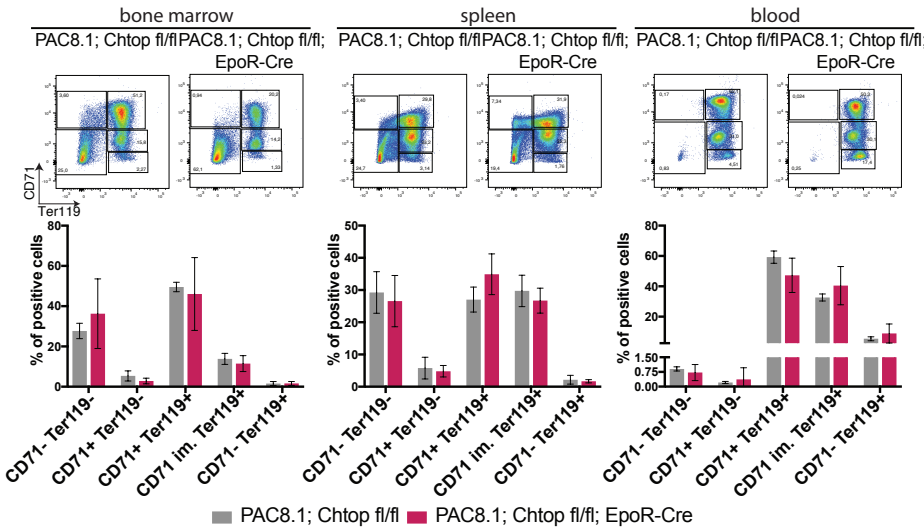

Figure 2. Flow cytometry analysis of bone marrow, spleen, and blood cells of PAC8.1/wt; Chtop fl/fl mice with and without EpoR-Cre/wt after PHZ treatment using the erythroid markers CD71 and Ter119. Maturation goes clockwise from CD71-/Ter119- → CD71+/Ter119- → CD71+ / Ter119+ → CD71 intermediate / Ter119+ → CD71- / Ter119+. (WT after PHZ n=2 / cKO after PHZ n=4).

mice with *Mx1-Cre,* where these values remained stable (not shown). Many blood parameters were affected by PHZ treatment in mice of both genotypes. The RBC size histograms (Figure 3D) illustrate the effect of PHZ treatment, with a peak of larger, newly-formed, reticulocytes appearing. We also measured the body and spleen weights (Figure 3E).

Although the body weights were slightly reduced within the group of *Mx1-Cre/wt* mice compared to the control mice, these differences were not significant. Interestingly the spleen weights of the PHZ treated mice showed a significant difference between the

Figure 3. (next page) PAC8.1/wt/ Chtop fl/fl mice with and without Mx1-Cre/wt, before and after pIpC induction, before and after PHZ treatment. (*indicates a p-<0,05 WT no pIpC no PHZ n=9 / cKO no pIpC no PHZ n=11 / WT after pIpC no PHZ n=8 / cKO after pIpC no PHZ n=10 / WT after pIpC and PHZ n=4 / cKO after pIpC and PHZ n= 4). (A) Before pIpC induction and before PHZ treatment, (B) After pIpC induction and before PHZ treatment and (C) after pIpC induction and after PHZ treatment: Blood parameters measured on the animal blood cell counter: White blood cells (WBC); red blood cells (RBC); hemoglobin (HGB); hematocrit (HCT); platelets (PLT); mean corpuscular volume (MCV); mean corpuscular hemoglobin (MCH); mean corpuscular hemoglobin concentration (MCHC); red blood cell distribution with (RDW); mean platelet volume (MPV). (D) Histograms of the red blood cells. X-axis represents the size, y-axis the number of cells. After PHZ treatment an extra peak is observed, representing larger non-nucleated RBCs: reticulocytes. (E) Body and spleen weights of the three conditions, on the left y-axis mouse weights are noted, and on the right y-axis the spleen weights. (F-G) Relative contribution of human and mouse b-like globins in bone marrow and spleen, after pIpC (F) and after pIpC and PHZ (G) as measured by RT-qPCR. Relative fractions are calculated like g / (g + b) and bm / (bm + bh1 +ey). (H) Southern blot of the BclI digested genomic DNA after pIpC induction of spleen cells and CD71+ and CD71- bone marrow cells. (I) Western blot of whole cell protein extracts after pIpC induction of spleen cells and CD71+ and CD71- bone marrow cells. Blots are stained with anti-tubulin and anti-CHTOP or anti-actin and anti g-globin. (J) Southern blot of BCLI digested genomic DNA of spleen and non-selected bone marrow cells after pIpC and PHZ treatment. (K) Western blot of whole cell protein extracts after pIpC and PHZ treatment of spleen and non-selected bone marrow cells. Blots were stained with anti-tubulin and anti-CHTOP.

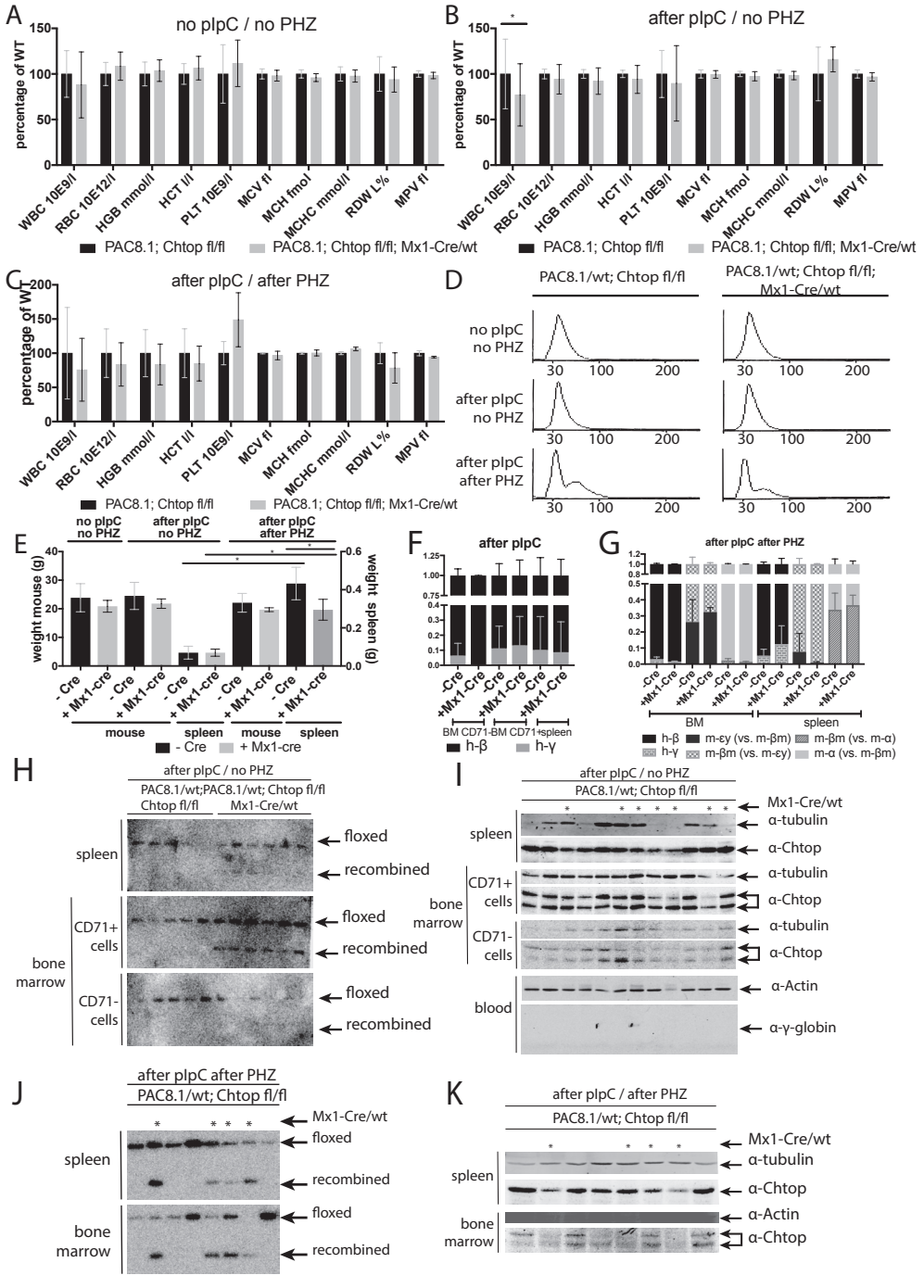
A
no pIpC / no PHZ
percentage of WT
WBC 10E9/l
RBC 10E12/l
HGB mmol/l
HCT l/l
PLT 10E9/l
MCV fl
MCH fmol
MCHC mmol/l
RDW L%
MPV fl
PAC8.1; Chtop fl/fl
PAC8.1; Chtop fl/fl; Mx1-Cre/wt
B
after pIpC / no PHZ
C
after pIpC / after PHZ
D
PAC8.1/wt; Chtop fl/fl
PAC8.1/wt; Chtop fl/fl; Mx1-Cre/wt
no pIpC no PHZ
after pIpC no PHZ
after pIpC after PHZ
E
weight mouse (g)
weight spleen (g)
mouse
spleen
- Cre
+ Mx1-cre
F
after pIpC
BM CD71-
BM CD71+
spleen
h-β
h-γ
G
after pIpC after PHZ
BM
spleen
h-β
m-εγ (vs. m-βm)
m-βm (vs. m-α)
h-γ
m-βm (vs. m-εγ)
m-α (vs. m-βm)
H
after pIpC / no PHZ
PAC8.1/wt;PAC8.1/wt; Chtop fl/fl
Chtop fl/fl
Mx1-Cre/wt
spleen
bone marrow
CD71+ cells
CD71- cells
floxed
recombined
I
after pIpC / no PHZ
PAC8.1/wt; Chtop fl/fl
Mx1-Cre/wt
α-tubulin
α-Chtop
α-Actin
α-γ-globin
blood
J
after pIpC after PHZ
PAC8.1/wt; Chtop fl/fl
K
after pIpC / after PHZ
PAC8.1/wt; Chtop fl/fl

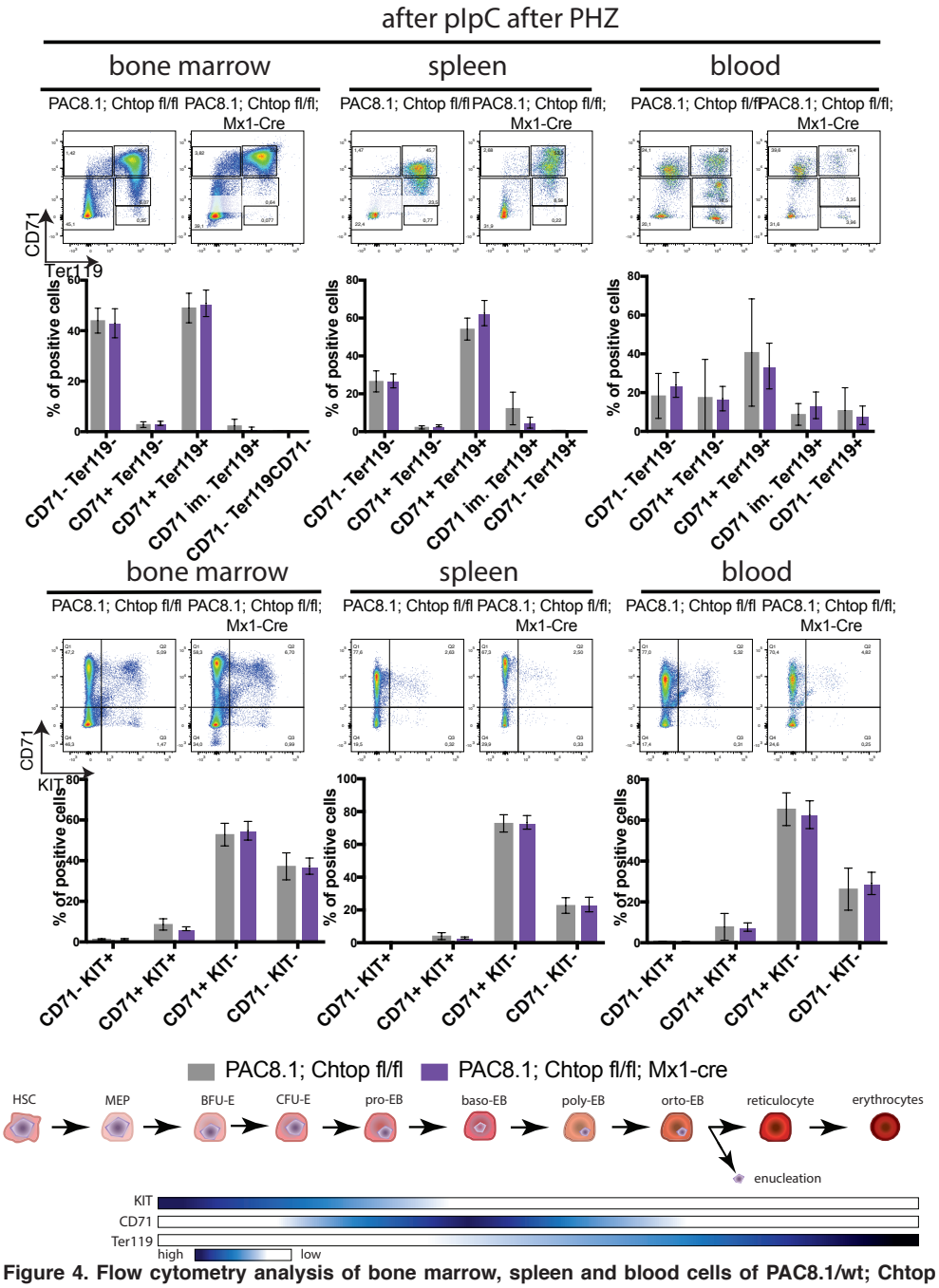

Figure 4. Flow cytometry analysis of bone marrow, spleen and blood cells of PAC8.1/wt; Chtop fl/fl mice with and without Mx1-Cre/wt after pIpC and PHZ treatment using the erythroid markers CD71, Ter119 and KIT. Maturation goes first from CD71-/KIT+, CD71+/KIT+, CD71+/KIT-, CD71-/KIT-. Using the CD71 and Ter119 combination, the maturation continues from CD71-/Ter119-, CD71+/Ter119-, CD71+/Ter119+, CD71+/Ter119 intermediate, CD71-/Ter119+, as described in the lower panel. HSC (hematopoietic stem cell), MEP (myeloid erythroid progenitor), BFU-E (burst forming unit erythroid), CFU-E (colony forming unit erythroid), pro-EB (pro-erythroblast), baso-EB (baso-erythroblast), poly-EB (poly-erythroblast), orto-EB (orto-erythroblast), reticulocytes, erythrocytes. (WT after pIpC and PHZ n=4 / cKO after pIpC and PHZ n=4).

mice with *Mx1-Cre* recombinase and without. We observed a reduction of 0.1 grams (median 0.415 grams without *Mx1-Cre*, 0.315 grams with *Mx1-Cre*) after pIpC and PHZ treatment. Due to PHZ-induced stress erythropoiesis, spleen sizes massively increased compared to the mice only treated with pIpC (0.07 grams in mice of both genotypes). Looking at γ-globin expression using qRT-PCR , we didn't observe changes in spleen, CD71-, and CD71+ bone marrow after *Mx1-Cre* induction (Figure 3F). We also quantified the expression of human and mouse β-like globins after PHZ treatment. Again, no changes due to the *Mx1-Cre* activity were found (Figure 3F).
To check the recombination efficiency and its effect on CHTOP protein levels, we performed Southern and western blotting on protein extracts of spleen and BM cells. In mice that were only treated with pIpC, we observed a lower recombination rate than observed with *EpoR-Cre* (compare Figure 3H with Figure 1J). Highest recombination efficiency was observed in CD71+ selected bone marrow cells, and reached levels of ~33%. On the western blot of these samples, we observed a slight reduction in CHTOP protein levels, but the effect was minimal (Figure 3I). In blood, no γ-globin protein could be detected by western blot analysis (Figure 3I lower panel). Figure 3J shows the Southern blot of the mice induced with pIpC and treated with PHZ. In both spleen and BM, the recombination efficiency was higher than observed in the animals without PHZ treatment. Furthermore, recombination in the BM appeared more efficient than in the spleen, with levels up to ~66%. Western blot analysis confirmed these results (Figure 3K).
In addition, we performed flow cytometry analysis after PHZ treatment. Figure 4 shows the flow cytometry results of the *PAC8.1/wt; Chtop fl/fl* with and without *Mx1-Cre* after pIpC induction and PHZ treatment. Here we included the cell surface markers CD71, Ter119, and KIT.
Comparing the PHZ treated (Figure 4) to the non-PHZ treated mice (not shown), it is clear that there were more CD71+/Ter119+ cells present after PHZ treatment. No significant differences were found between the conditional knockout mice with *Mx1-Cre* and their control littermates. The western and Southern blots (Figure 3 H-K) indicate that the poor recombination efficiency and the abundant presence of CHTOP protein could be the cause of the apparent lack of phenotype within the erythroid compartment. It is possible that we induced *Mx1-Cre* too late and/or analysed the mice too soon. The average lifespan of a mouse erythrocyte is 60 days; we analysed these mice already 1 month after induction. It is therefore possible that we were looking at a cell population that in part originated from before the pIpC treatment. To circumvent this problem, we repeated the experiment by inducing *Mx1-Cre* earlier, within the first week after birth. We waited until the mice reached an age of 16 weeks, so all newly formed cells should be derived from the hematopoietic system after Cre-mediated recombination of the *Chtop* locus. Because CHTOP depletion might also affect other blood cell populations originated form the hematopoietic stem cell, we set up a pan-hematopoietic flow cytometry analysis to observe whether there were changes due to *Mx1-Cre* activity.
After pIpC induction, just before sacrificing the mice, we measured the blood parameters (Figure 5A-C). We observed an effect of pIpC only within the conditional knockout mice carrying *Mx1-Cre* versus no pIpC at the RBC, HCT, MCH and MCHC levels, which all decreased. The RBC cell size histograms did not reveal any obvious changes (Figure 5C). The mouse and spleen weights were not affected

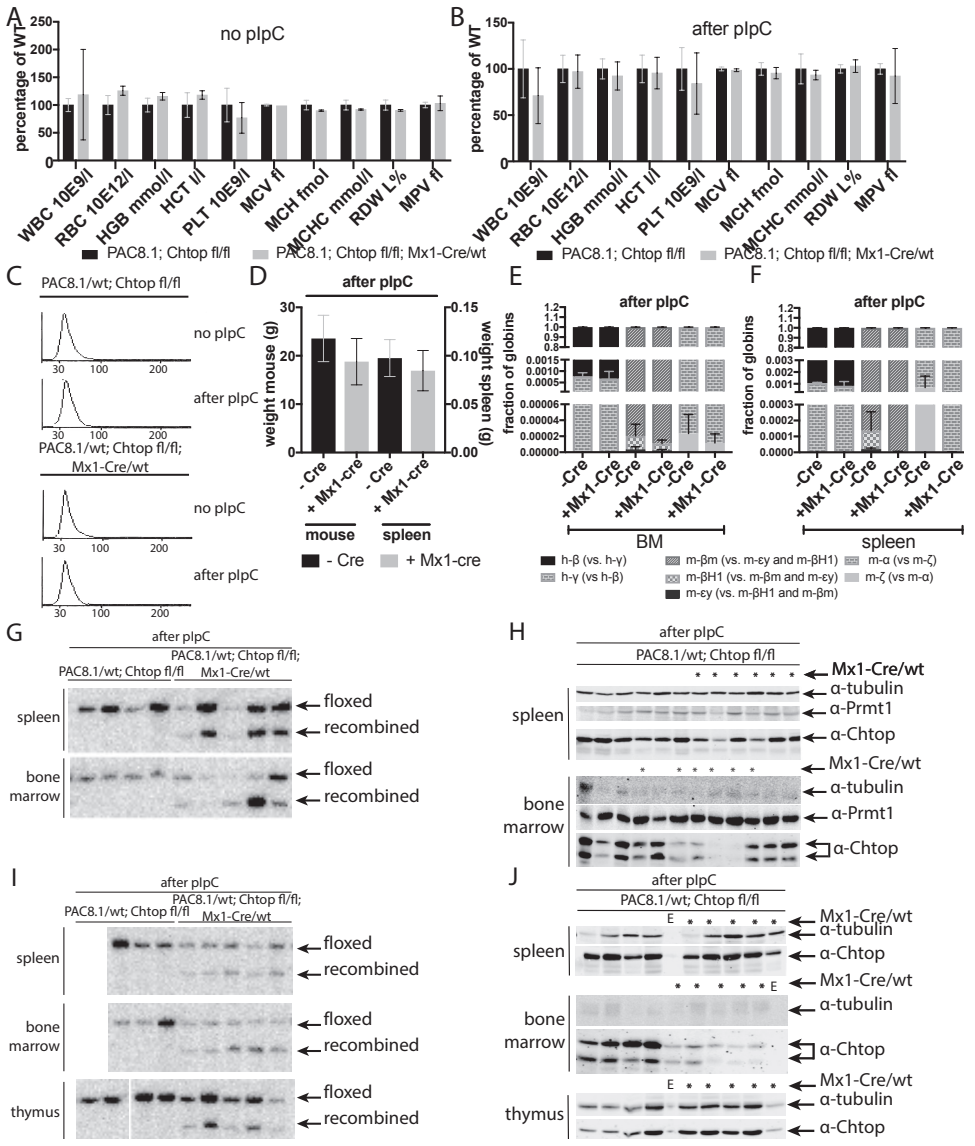

Figure 5. PAC8.1/wt/ Chtop fl/fl mice with and without Mx1-Cre/wt after starting the pIpC induction at a young age, including non-injected controls. (A) control littermates before and (B) after pIpC induction. Blood parameters were measured on the animal blood cell counter: White blood cells (WBC); red blood cells (RBC); hemoglobin (HGB); haematocrit (HCT); platelets (PLT); mean corpuscular volume (MCV); mean corpuscular hemoglobin (MCH); mean corpuscular hemoglobin concentration (MCHC); red blood cell distribution with (RDW); mean platelet volume (MPV). (C) Histograms of the RBCs. X-axis represents the size, y-axis the number of cells. (D) Mouse body and spleen weights after pIpC induction, on the left y-axis mouse weights are noted, and on the right y-axis spleen weights. (E) mRNA of bone marrow and (F) spleen cells was tested using RT-qPCR for human b and g globin and mouse ey, bH1, bmajor and z globins. (G) and (I) Southern blots of BCLI digested genomic DNA after pIpC of spleen and bone marrow cells. (H) and (J) Western blot of whole cell protein extracts after pIpC and PHZ treatment of spleen and non-selected bone marrow cells and thymus (J). Blots are stained with anti-tubulin, anti-CHTOP and its binding partner PRMT1. E=empty lane. (*indicates p-<0,05 or which samples carry Mx1-Cre recombinase, WT no pIpC no PHZ n=5 / cKO no pIpC no PHZ n=2 / WT after pIpC n=12 / cKO after pIpC n=12).

by the presence of *Mx1-Cre* (Figure 5D). Measuring the relative globins levels of human γ and mouse εy, βH1, βmajor, and ζ in bone marrow (Figure 5E) and spleen (Figure 5F) only small but not significant increases were observed. In Figure 5 G-J the Southern (G and I) and western blots (H and J) of the samples are shown. Interestingly, the recombination efficiency has considerably improved compared with the previous results obtained with *Mx1-Cre*, but it was still not as good as with *EpoR-Cre* (Figure 1J) although that was on CD71+ selected cells.
Western blots (Figure 5 H and J) demonstrated that there were samples with strongly reduced CHTOP protein signals. In conclusion, although there was considerable variation in the recombination efficiency, CHTOP protein signals were reduced in several samples after pIpC induction in young mice. Thus, *Mx1*-Cre pIpC in young animals yields better results than when induced in adult mice.
In Figure 6 – 9 we present our findings concerning the pan-hematopoietic flow cytometry analysis on blood, spleen, bone marrow, and thymus cells.
Figure 6 displays flow cytometry of the erythroid markers CD71/Ter119/KIT on bone marrow, spleen, and blood cells. We observed a large population of CD71-/Ter119- BFU-E/CFU-E cells and a smaller population of CD71+/Ter119+ basophilic/polychromatic erythroblast in spleen and BM. This is expected in an experiment without stress erythropoiesis. When comparing the samples with *Mx1-Cre* and with out *Mx1-Cre*, we observed some differences, but due to variation between animals of the same group these did not reach statistical significance. Altogether, the reduction in CHTOP protein did not appear to affect the erythroid cell populations.
We tested thymus and spleen cells using a variety of markers (Figure 7). T cells start as CD3-/CD4-/CD8- cells within the outer cortex of the thymus, which are called double negative (DN) T cells. Four different DN stages can be distinguished using CD44 and CD25. DN stage 1 (DN1) CD25-/CD44+, they become double positive in DN2 (CD25+/CD44+) after with they lose CD44 activity in DN3 (CD25+/CD44-) and finally in DN4 they are double negative (CD25-/CD44-). Subsequently, the cells move to the inner cortex of the thymus, where the T cells become double positive (DP) for CD4+/CD8+/CD3+. Then the T cells are moving to the medulla and peripheral tissues such as the spleen. In this process, they become single positive for CD4 or CD8 and will remain CD3+. Using CD62L/CD44 different types of mature T cells can be distinguished: naïve T cells (CD62L+/CD44-), central memory (CD62L+/CD44+) and effector memory (CD62L-/CD44+) T cells. Our observations did not reveal any aberrations in the T cell compartment upon CHTOP depletion. As expected, many immature and precursors were found within the thymus and the populations of mature cells were smaller. Also within the SP groups, the most abundant were the naïve SP T cells. In the spleen, the SP populations were larger than the immature / precursor populations. There were virtually no differences between the mice with *Mx1-Cre* and without *Mx1-Cre*, in fact the spread and variation within the groups was low. In conclusion, a reduction in the CHTOP protein does not appear to affect the T cell populations.
Subsequently, we looked at different B cell populations in spleen and bone marrow (Figure 8). In general, from progenitor to mature cell, B cells carry the markers B220/CD19, the progenitors start expressing CD2, and when they become a mature B cell they start expressing IgM and later IgD. Finally, the marginal zone and follicular B cells can be distinguished using the CD21/CD23 markers. Also, here we observed

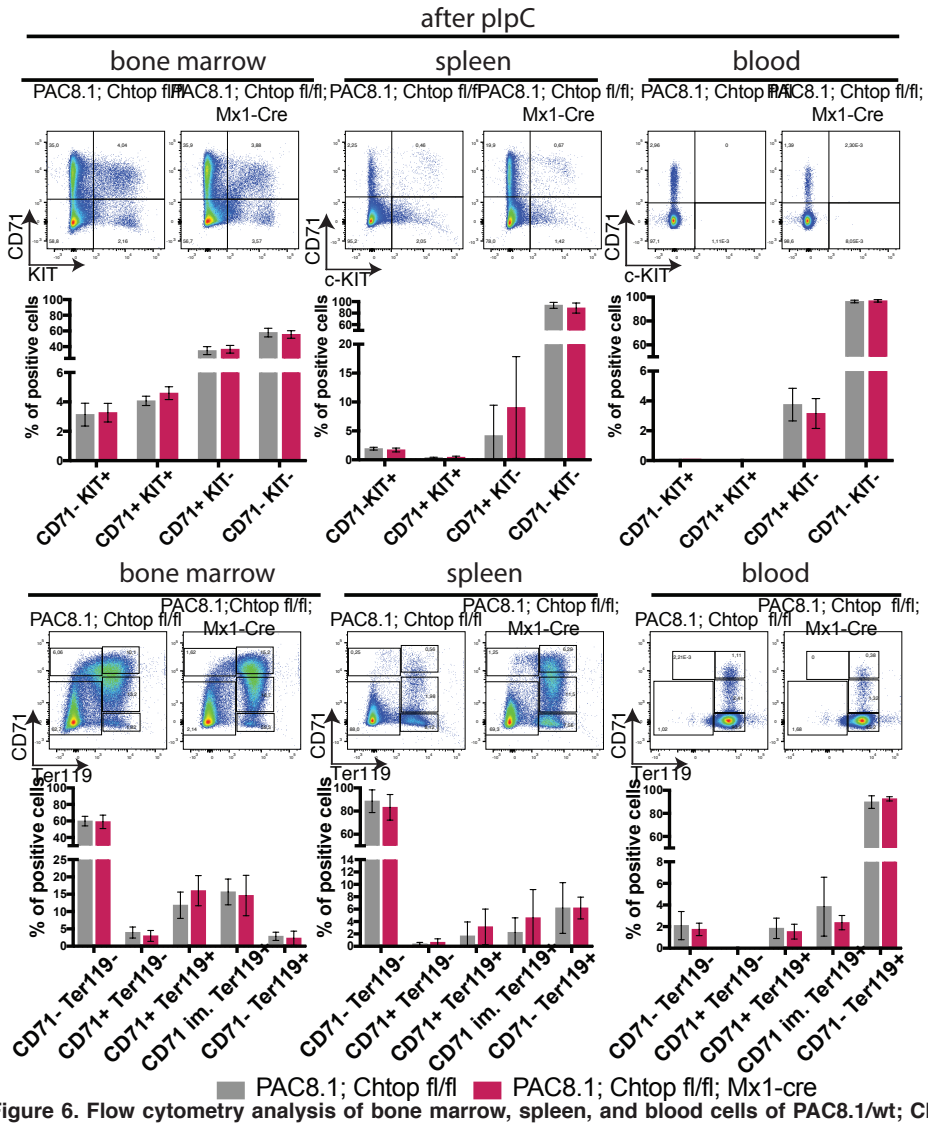

Figure 6. Flow cytometry analysis of bone marrow, spleen, and blood cells of PAC8.1/wt; Chtop fl/fl mice with and without Mx1-Cre/wt after pIpC induced at young age using the markers CD71, Ter119 and KIT. Maturation goes first from CD71-/KIT+, CD71+/KIT+, CD71+/KIT-, CD71-/KIT-. Using the CD71 and Ter119 combination, the maturation continues from CD71-/Ter119-, CD71+/Ter119, CD71+/Ter119+, CD71+/Ter119 intermediate, CD71-/Ter119+, as described in Figure 4 lower panel. (WT after pIpC n=4 / cKO after pIpC n=5).

changes in some cell populations. Due to the variation between the mice these differences did not reach statistical significance. In conclusion, reduction of CHTOP protein levels does not appear to affect the B cell populations within the spleen and bone marrow.

Finally, we checked different myeloid cells: granulocytes subdivided in eosinophils (F4-80-/SiglecF+) and neutrophils (Ly6G+/CD11b+); monocytes subdivided in novel/ resident (Ly6G-/CD11b+/Ly6C-) and inflammatory (Ly6G-/CD11b+/Ly6C+) cells,

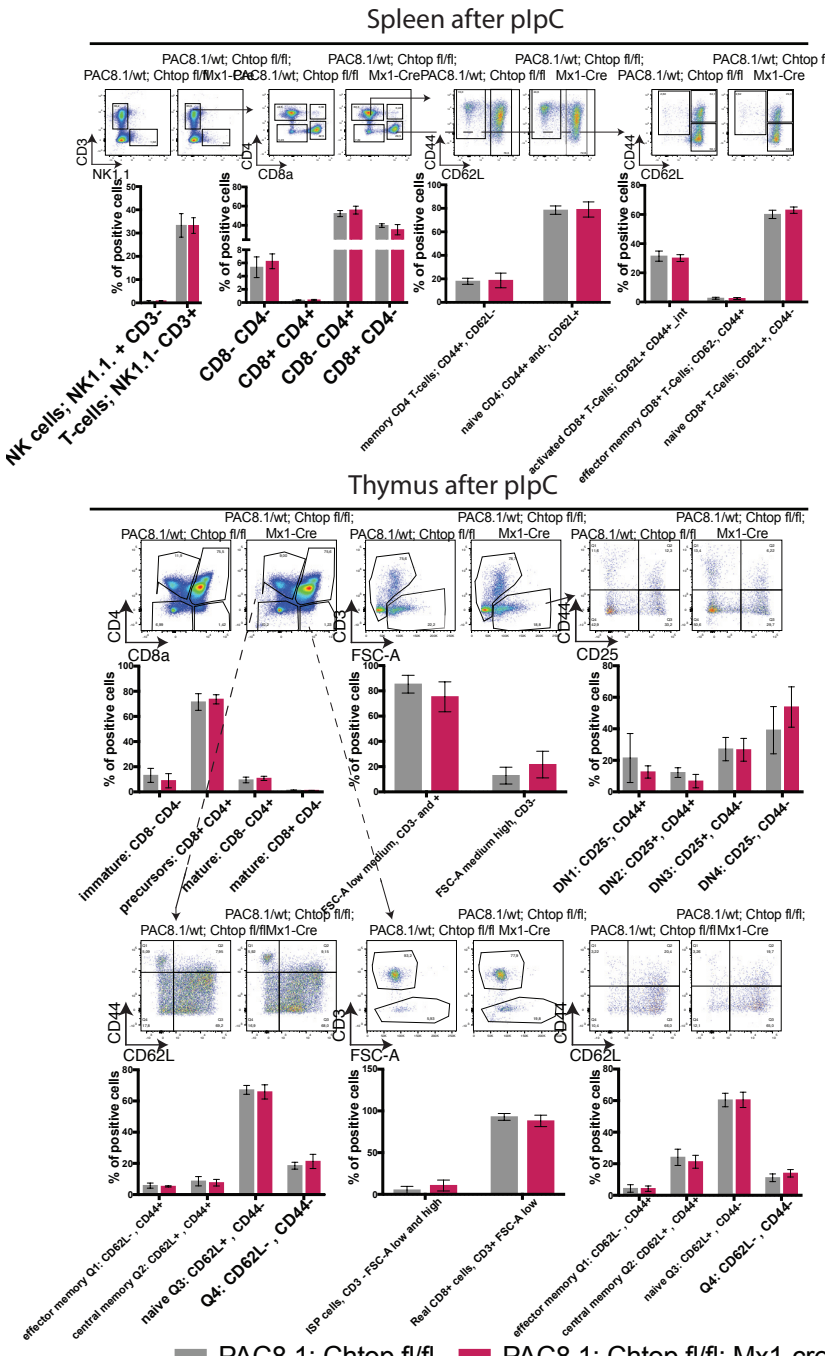

Figure 7. Flow cytometry T cell analysis of spleen (upper panel) and thymus (lower panel) cells after pIpC induction of PAC8.1/wt; Chtop fl/fl mice with and without Mx1-Cre/wt. After life/dead selection (not shown), natural killer cells (NK) were first distinguished from T cells using CD3/NK1.1 (spleen) or NK1.1/FSC-A (thymus). Subsequently the main categorisation of T cells within the spleen and thymus was done using CD4/CD8 markers: immature T cells are CD4-/CD8- double negative (DN), then the progenitor T cells become CD4+/CD8+ double positive (DP), then the mature T cells will lose one of the markers and become single positive (SP) CD4+/CD8- or CD4-/CD8+. Within the DN population in the thymus, CD3- cells were selected, using CD25/CD44 four different DN stages are distinguished in order of maturity: DN1 (CD25-/CD44+), DN2 (CD25+/CD44+), DN3 (CD25+/CD44-) and DN4 (CD25-/CD44-). Subsequently the single positive cells in thymus the CD3+ selection was done to distinguish the real SP cells and also the immature single positives (ISP) CD8+. In spleen as well the thymus, CD44/CD63 was used to distinguish within the single positive groups the: naïve (CD62L+/CD44-), central memory (CD62L+/CD44+) and central memory (CD62L-/CD44+) T cells. (WT after pIpC no PHZ n=4 / cKO after pIpC no PHZ n=5).

and dendritic cells (DCs) subdivided in pDCs (B220+/CD19-) (see Figure 8) immature LDCs/CD11b DCs (CD11c-/CD11b+, conventional DP DCs (CD11c+/CD11b+), small CD11c DCs (CD11c+/CD11b-/MHC-II intermediate/low) and large CD11c DCs (CD11c+/CD11b-/MHC-II high) (Figure 9).
Also here no significant differences were found following induction of *Mx1-Cre*.
Collectively, induction of *Mx1-Cre* with pIpC in the first week after birth resulted in more efficient recombination at the *Chtop* locus than when treatment was started at adult age. The CHTOP protein levels were also more reduced when the pIpC treatment was started in animals less than 7 days old. The protein reduction did affect the RBCs and some related parameters measured on the animal blood cell counter, but this could not be confirmed with the flow cytometry analysis. Hematopoietic deletion of CHTOP protein did not affect spleen and body weights, and also the globin mRNA levels measured using RT-qPCR did not change significantly. Since *Mx1-Cre* induction is active from the hematopoietic stem cell, we also looked at the T cell, B cell and myeloid cell populations, but we did not find any significant alterations due to the lowered CHTOP protein levels. Possibly, lowered protein levels are not enough to create a phenotype, and the protein should be removed completely.
Because our aim is to understand hemoglobin switching in order to increase γ-globin levels, we wished to extend the analysis of CHTOP function to embryonic development. For this purpose, we first setup a trial to induce *Mx1-Cre* in the embryos. We injected the pregnant mothers with the same doses as the adults (20 µg/g body weight) on E10.5 and E12.5. We analysed the embryos at E14.5 by Southern (Figure 10A and B) and western blotting (Figure 10 C and D). In DNA isolated from fetal livers of *Mx1-Cre* embryos isolated from mothers injected at E10.5 (Figure 10A and C) or E12.5 (Figure 10 B and D), we failed to observe recombination. In agreement with this observation, CHTOP protein levels remained similar to those observed in fetal livers from embryos without *Mx1-Cre*.
We therefore switched to the *Vav1-Cre* line, in which Cre recombinase is constitutively active in the hematopoietic stem cells. We tested recombination at the *Chtop* locus by Southern blotting of E14.5 fetal liver DNA (Figure 11). We also tested *Chtop* +/fl heterozygotes, since recombination might be more efficient if only one allele can be recombined. We observed recombination at the Chtop locus with a maximum efficiency of ~40%, in DNA isolated from *Chtop* fl/fl fetal livers. In DNA isolated from *Chtop* +/fl fetal livers no recombination was observed. However, we note that the genotyping does not match completely with the samples that show recombination. It is therefore possible that the *Chtop* +/fl fetal liver did not contain *Vav1-Cre*. Since 40% recombination efficiency in *Chtop* fl/fl fetal livers, is too low, we did not continue with *Vav1-Cre*.
We finally crossed the mice with the *Vec-Cre* line, which also expresses Cre recombinase constitutively in hematopoietic stem cells. We isolated fetal livers of E12.5/E14.5/E15.5/E16.5 embryos. On the Southern blot (Figure 12A) we observed efficient recombination rates varying between 60-90%. To confirm this, we also performed western blots (Figure 12B) which revealed a major reduction in CHTOP protein levels in the fetal livers from the samples with high recombination efficiency.
At E16.5 it was clear that liver cells, which are not affected by *Vec-Cre,* become more abundant. From the samples of E12.5, E14.5 and E16.5 that showed efficient recombination, we performed qRT-PCR to check the globin levels (Figure 12C-F).

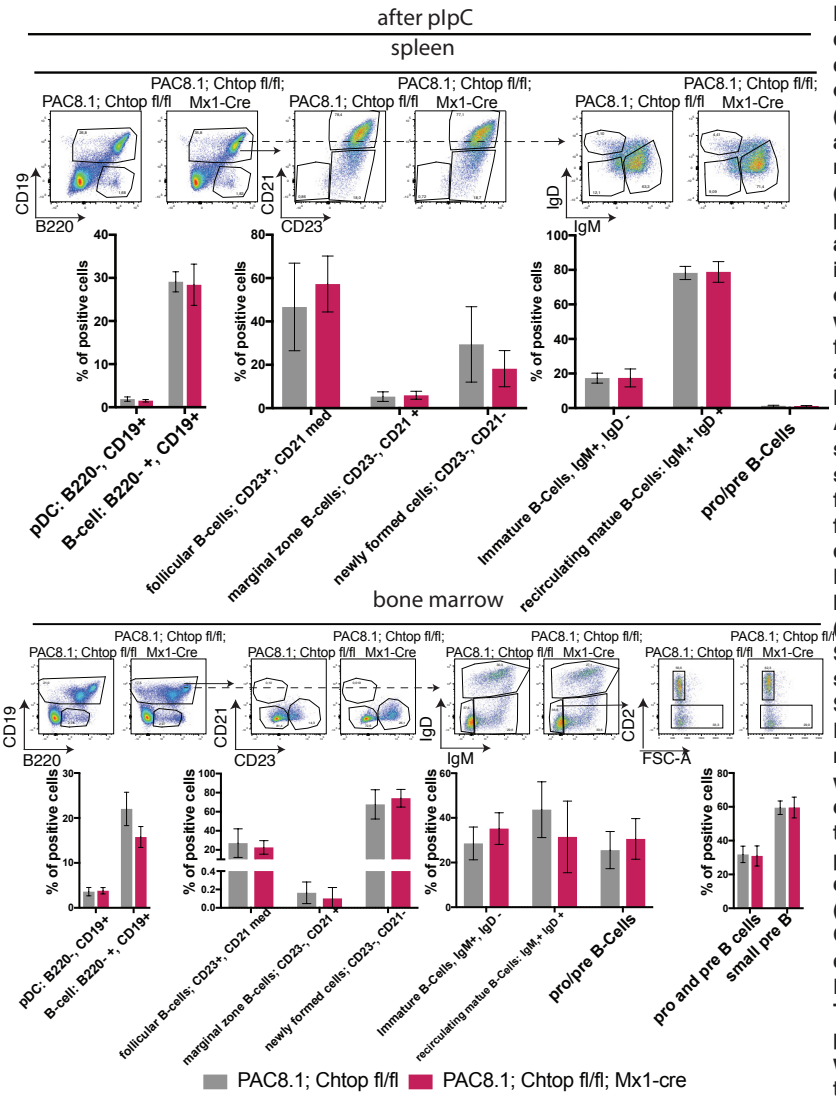

Figure 8. Flow cytometry B cell analysis of spleen (upper panel) and bone marrow (lower panel) cells after pIpC induction of PAC8.1/wt; Chtop fl/fl mice with and without Mx1-Cre/wt. After life/dead selection (not shown), we first gated for single cells (FSC-A/FSC-H) and lymphocytes (FSC-A/SSC-A) (not shown). Subsequent, B220/CD19 markers were used to distinguish the plasmacytoid dendritic cells (pDCs: B220-/CD19+) and B cells (CD19+/B220+and-). These B cell populations were there after subdivided into six specified groups: immature B cells (IgM+/IgD-), recirculating B cells (IgM+/IgD+), pro/pre-B cells (IgM-/IgD-/CD2-), small pre-B cells (IgM-/IgD-/CD2+), newly formed B cells (CD23-/CD21-), marginal zone B cells (CD23-/CD21+), follicular B cells (CD23+/CD21-). (WT after pIpC no PHZ n=4 / cKO after pIpC no PHZ n=5).

At E12.5 we used fetal liver and yolk sac RNA for the RT-qPCRs (Figure 12 C/D). Figure 12E shows the results of E14.5 fetal liver RNA and Figure 12F of E16.5 fetal liver RNA. We tested the relative levels of human globins γ and ε, and the mouse globins βmajor, βH1 and εy. In E12.5 yolk sac mRNA there appeared to be an increase of γ-globin and ε-globin expression, but these changes were not significant. In fetal liver RNA of E12.5 there was also an increase visible, but it is not significant. Fetal liver globin mRNA of E14.5 and E16.5 did not show any changes due to the reduction of CHTOP protein in the embryos with *Vec*-Cre.

We also performed flow cytometry analysis of cord blood (Figure 13) and fetal

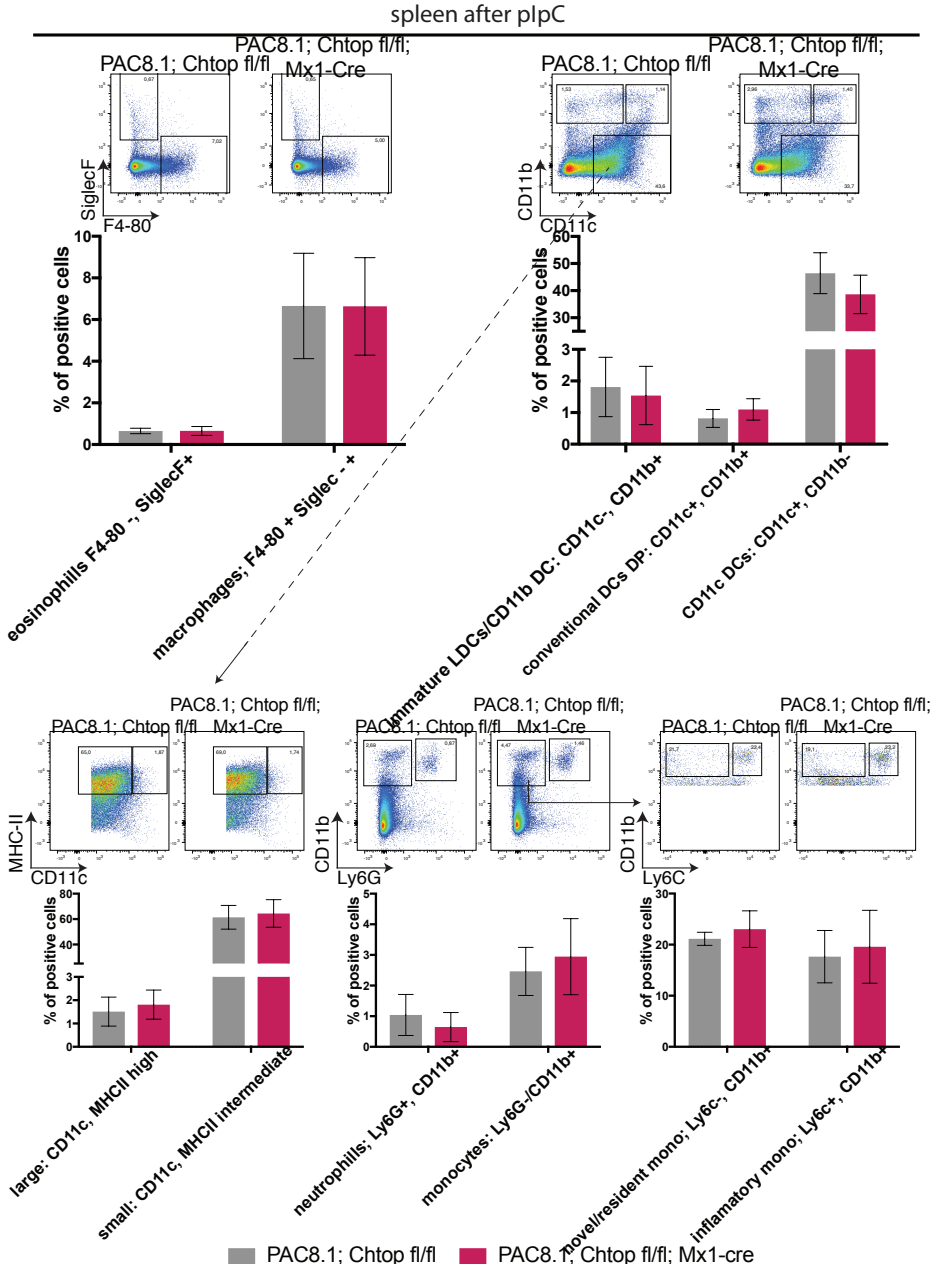

Figure 9. Flow cytometry analysis of myeloid spleen cells after pIpC induction of PAC8.1/wt; Chtop fl/fl mice with and without Mx1-Cre/wt. After life/dead marking and lymphocyte selection (FSC-A/SSC-A), we distinguished nine different myeloid cell types: eosinophils (F4-80-SiglegF+), macrophages (F4-80+/SiglegF + and -), neutrophils (Ly6G+/CD11b+), novel/resident monocytes (Ly6G-/CD11b+/Ly6C-), inflammatory monocytes (Ly6G-/CD11bb+/Ly6C+); immature LDCs /CD11b dendritic cells (DCs) (CD11c-/CD11b+), conventional DCs (CD11c+/CD11b+), large CD11c DCs (CD11c+/CD11b-/MHCII high) and small CD11c DCs (CD11c+/CD11b-/MHCII intermediate/low). (WT after pIpC no PHZ n=4 / cKO after pIpC no PHZ n=5).

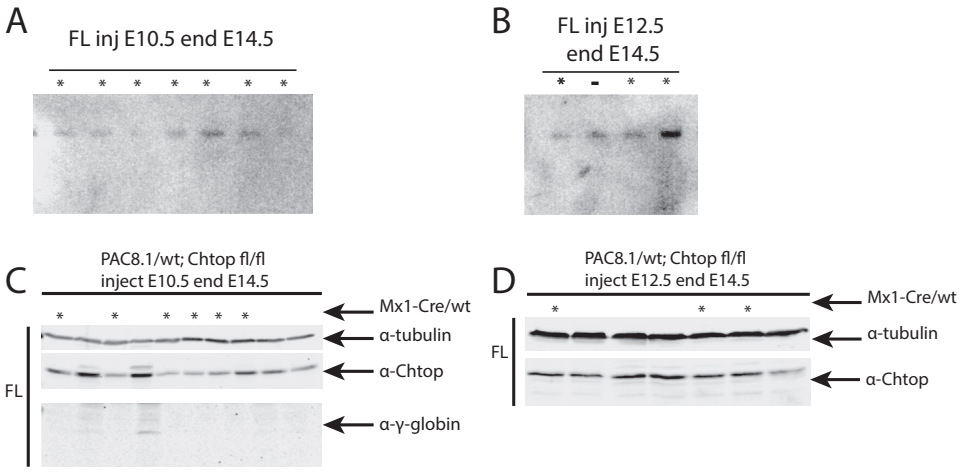

Figure 10. Induced PAC8.1/wt/ Chtop fl/fl embryos with and without Mx1-Cre/wt after induction with plpC by injecting pregnant dams on E10.5 or E12.5. (A) Southern blot of fetal liver (FL) genomic DNA BclI digests of mice dams at E10.5 and sacrificed at E14.5 embryos. (B) Southern blot of FL genomic DNA BclI digests of injected at E12.5 and sacrificed at E14.5 embryos. (C) Western blot of fetal liver whole cell RIPA lysates; embryos isolated from dams injected at E10.5 and sacrificed at E14.5. Western blot is stained with anti-tubulin, anti-CHTOP and anti g-globin. (D) Western blot of fetal liver whole cell RIPA lysates; embryos isolated from dams injected at E12.5 and sacrificed at E14.5. Western blot is stained with anti-tubulin an anti-CHTOP. Embryos with Mx1-Cre are marked with *.

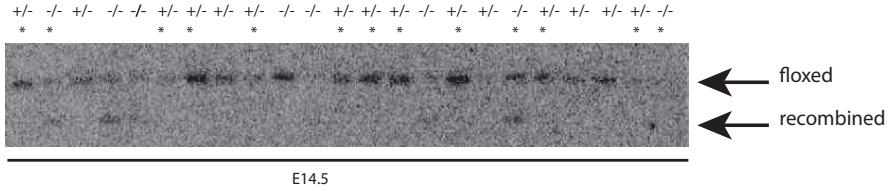

Figure 11. Southern blot of fetal liver genomic DNA BclI digests of E14.5 fetal livers of PAC8.1/wt; Chtop +/fl (+/-) or fl/fl (-/-) and with or without the Vav1-Cre recombinase allele. Embryos genotyped with Vav1-Cre are marked with *. Clearly genotyping is problematic.

liver cells (Figure 14) of E12.5-E16.5 embryos for the markers CD71/Ter119/KIT. Especially within the cord blood, almost no changes were detected. In the fetal liver samples we found more variation but no significant changes were detected.

We conclude that in fetal liver, cord blood, and yolk sac no significant changes are observed in the erythroid compartment due to the reduction of CHTOP protein. Of course, CHTOP is a crucial protein, since the full knockout is lethal.[9] The high γ-globin levels, up to 30%, in human erythroid progenitor cells (HEP) that were detected after depletion of CHTOP using short hairpins, suggested a major role for CHTOP in globin regulation.

While this work was in progress, the CRISPR technique was developed and we obtained access to a novel human erythroid cell line, HUDEP-2 (human umbilical cord-derived)[27], which is a model for adult human erythropoiesis. We therefore applied CISPR to deplete CHTOP from HUDEP-2 cells (Figure 15). As a first experiment, we used a lentiviral vector with blasticidin resistance to deliver Cas9 to the cells. Since we were unable to grow HUDEP-2 cells clonally, we selected an

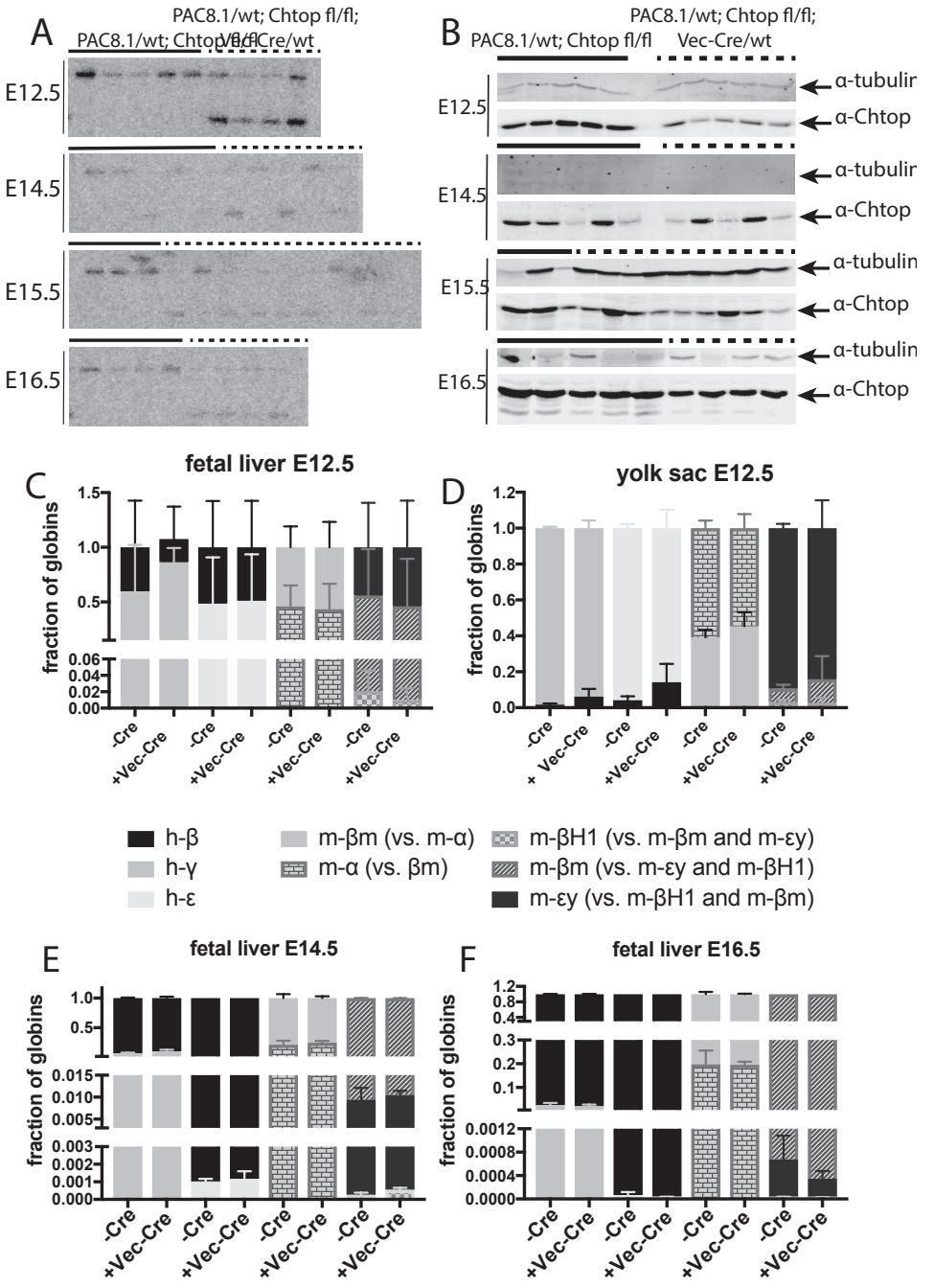

Figure 12. PAC8.1/wt; Chtop fl/fl embryos with or without Vec-Cre/wt at different days of gestation. (A) Southern blot of BclI digests of genomic DNA from fetal livers of E12.5 / E14.5 / E15.5 / E16.5 embryos. (B) Western blot of RIPA lysates of fetal livers of E12.5 / E14.5 / E15.5 / E16.5 fetal livers. The blot is stained with anti-tubulin and anti-CHTOP. (C-F) RT-qPCR relative fractions levels of human b-, g- and e-globin, and the mouse b-major, bH1 and ey globins of E12.5 fetal liver (C), E12.5 yolk sac (D), E14.5 fetal liver (E) and E16.5 fetal liver (F).

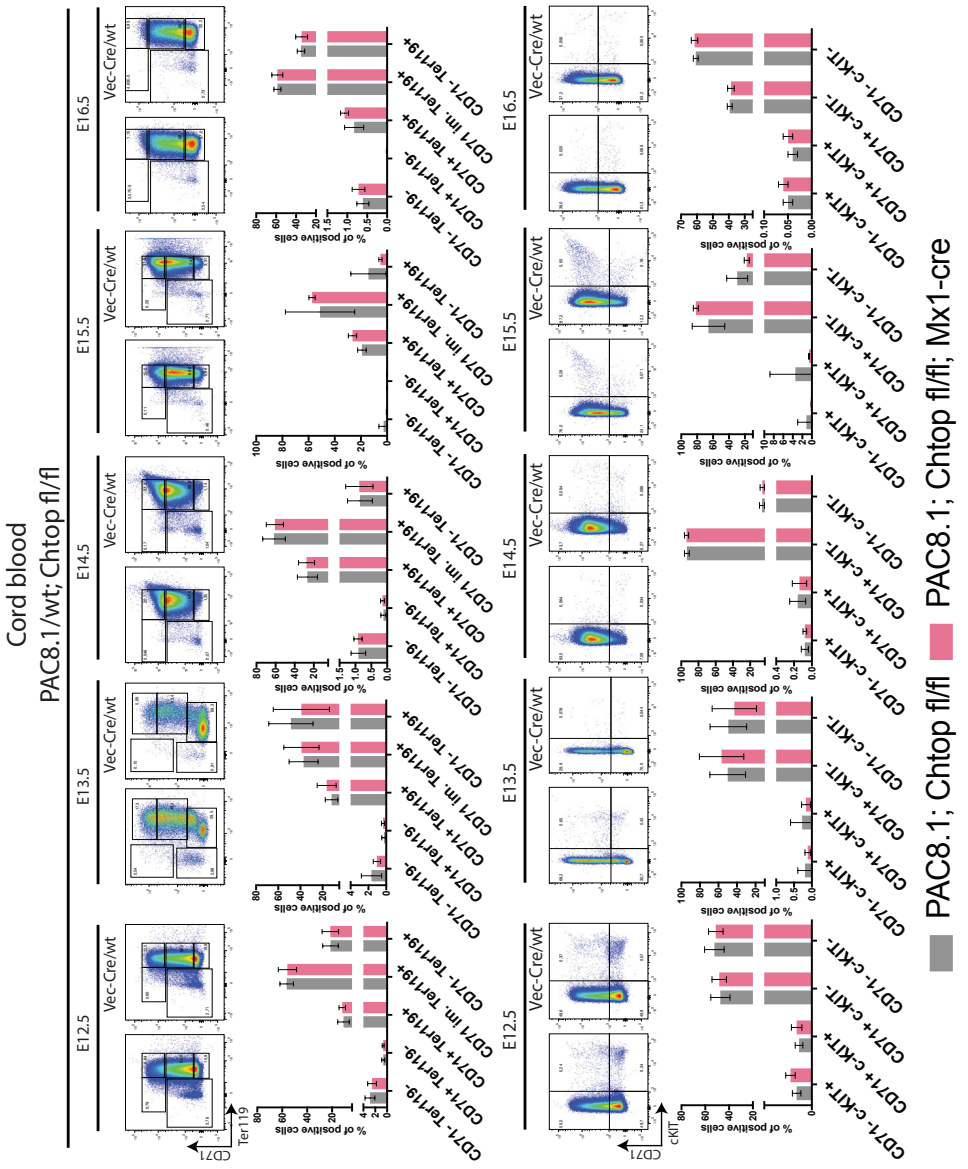

Figure 13. Flow cytometry analysis of PAC8.1/wt; Chtop fl/fl cord blood with and without Vec-Cre of E12.5 until E16.5 using the markers CD71/Ter119/KIT.

oligo-clonal culture of HUDEP-2 cells with average Cas9 expression. Subsequently we transferred the guide RNA expressing part of the pX459 vector including the guide RNA for CHTOP into the pLKO vector. We first tested functionality of the guide RNA targeting CHTOP by isolating genomic DNA from the cell pool, PCR the targeting region from 5' to 3' flanking part. These PCR fragments were purified and digested

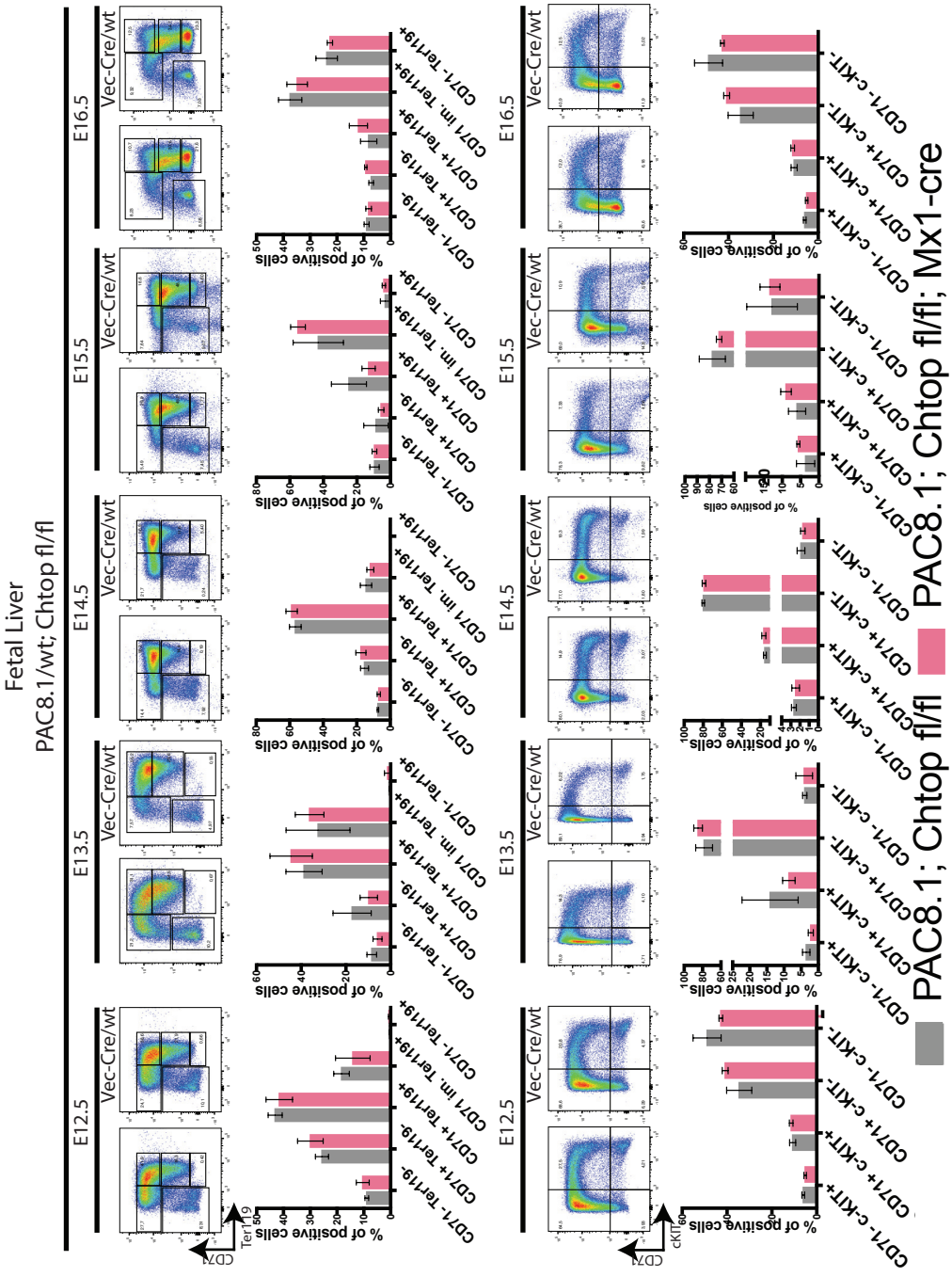

Figure 14. Flow cytometry analysis of PAC8.1/wt; Chtop fl/fl fetal liver cells with and without Vec-Cre of E12.3 until E16.5 using the markers CD71/Ter119/KIT.

using the Surveyor kit. After digestion, the samples were analysed on a 2% agarose (Figure 15A). We found that within the cell pool treated with the guide RNA targeting *CHTOP* two fragments were created from the PCR fragment. This indicated that there were hetero-duplexes within the pool of PCR fragments due to the action of Cas9. Subsequently we performed a western blot to see the effects on CHTOP protein levels, and whether the γ-globin levels were increased. In Figure 15B we observed a reduced amount of CHTOP protein in the cells treated with the guide RNA compared to the TRC and GFP controls. In addition to this we sequenced PCR fragments used TIDE analysis[38] to check the efficiency of our guide RNA (Figure 15C). Here we obtained a TIDE score of 61%, which is quite efficient. To check the effects on the levels of γ-globin and ε-globin we performed RT-qPCR on RNA isolated from the cell pool (Figure 15). We observed no alterations in the γ- and ε-globin levels in the CHTOP CRISPR cells. We conclude that although the CRISPR approach was successful, as shown by the surveyor assays and TIDE analysis, and led to a reduction of CHTOP protein, this did not appear to affect the γ-globin levels in HUDEP-2 cells.

Discussion

Previous work in cultured human primary erythroid progenitor cells showed an increase to 31% of γ-globin levels when CHTOP expression was depleted using shRNA constructs.[9,10] In addition, full *Chtop* knockout mice die from multiple defects.[9,10] Here, we investigated the function of CHTOP using conditional knockout mice carrying the human *HBB* locus, *Chtop* floxed alleles and Cre recombinases specific for the erythroid / hematopoietic system. We first started with *EpoR-Cre* which is specific for the erythroid compartment and does not need to be induced [29]. Here we observed deficient recombination but no apparent phenotype. When we treated the *EpoR-Cre* containing mice and their littermates with phenylhydrazine to induce stress erythropoiesis we observed an increase of erythroid progenitor cells and an increase in spleen size. But there was no difference between the *EpoR-Cre* carrying mice and the *EpoR-Cre* lacking mice. At protein level, we observed that the protein was still present at high levels. We also found that recombination at the *Chtop* locus was less efficient when the mice were treated with phenylhydrazine. We therefore switched to a Cre recombinase line that can be activated in the hematopoietic stem cell compartment by pIpC treatment: *Mx1-Cre*.[32] First, we injected animals that were already a few months old. We also induced stress erythropoiesis in these mice by injecting them with phenylhydrazine. Here we observed a small reduction in CHTOP protein levels, but the recombination efficiency varied considerably between the animals. We did not observe any differences in weight, erythroid-related blood parameters or flow cytometry of erythroid populations. Then we started the induction of *Mx1-Cre* at a young age (<7days). This led to improved genomic recombination, and more importantly a reduction in CHTOP protein levels in most of the samples. But even a reduced protein level within the hematopoietic tissues did not lead to significant differences between the *Mx1-Cre* and control littermates. The only changes observed were within the *Mx1-Cre* group before and after pIpC induction, within the erythroid related blood parameters: RBC, HCT, MCH and MCHC. Because *Mx1-Cre* mediated depletion of CHTOP might have an effect on other cell types, we set up a pan-hematopoietic flow cytometry analysis to check the B cell, T cell and

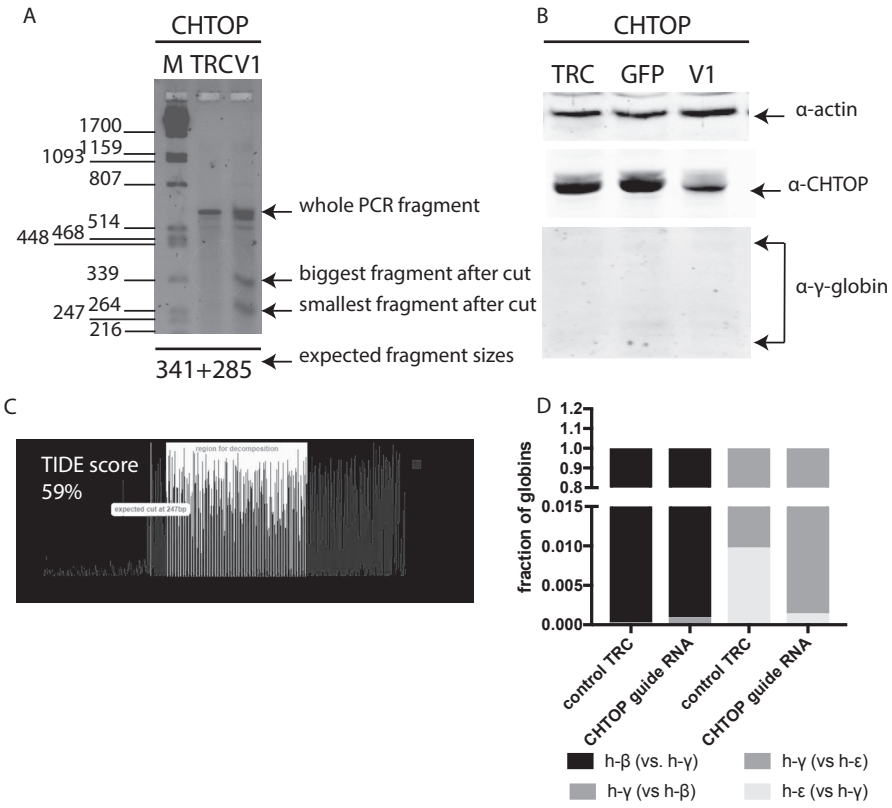

Figure 15. HUDEP-2 cells treated with CRISPR technology targeting the CHTOP gene within exon 2. (A) Surveyor assay; after PCR of the genomic DNA pool of the target region (626 bp). The PCR product was purified and digested with the surveyor enzyme that recognizes hetero-duplexes. This created two fragments of 341 bp and 285 bp. (B) Western blot of the HUDEP-2 RIPA lysates; the TRC and GFP controls were included. Blot was stained with anti-actin, anti-CHTOP and anti-g-globin. (C) Output of the TIDE analysis of sequences PCR fragments of the targeted region. The output score was 59%. (D) RT-qPCR analysis of b-, g- and e-globin expression.

In mice, γ-globin is an embryonic/fetal globin. We therefore investigated the effects of *Chtop* knockout on the erythroid system of embryos. We first attempted to induce *Mx1-Cre* in embryos by injecting the mothers with pIpC. Trial experiments revealed that this method does not work in our hands.

The *Vav1-Cre* line[30] was then used as an alternative approach, however when we checked recombination by Southern blot we found that recombination in the hematopoietic system was inefficient, precluding use of this Cre line to investigate the role of CHTOP in hematopoiesis. We then switched to the *Vec-Cre* line[31] which yielded efficient recombination and a reduction of the CHTOP protein levels in fetal livers at several developmental time points. Analysis of globin expression and flow cytometry for erythroid markers did not reveal significant changes due to reduced CHTOP levels.

Because the original observation on the potential role of CHTOP in globin regulation

was made by shRNA-mediated knockdown in primary human erythroid progenitor cells, we also investigated the effects of a CHTOP knockout in HUDEP-2 cells, a cell line modelling adult human erythropoiesis. Using the CRISPR-Cas9 lentiviral-based technique we targeted the *CHTOP* gene in HUDEP-2 cells. Although the CRISPR guide RNA was functional, as shown by surveyor assay, TIDE analysis, and protein reduction on western blot, no increase in γ-globin expression was observed.

In conclusion, our data do not support a role for CHTOP in γ-globin regulation. It is possible that CHTOP is a repressor of γ-globin but that it needs to be removed almost completely from the system. In all our experiments measureable levels of CHTOP protein were left. At least a reduction of CHTOP protein does not lead to an increase of γ-globin in mice and HUDEP-2 cells. Our findings are strengthened by a recent publication of Traxler, et al. These authors report that shRNA experiments are prone to off target effects, especially in erythroid cells.[39] This raises the possibility that the originally observed increased γ-globin levels upon CHTOP knockdown in HEP cells were due to off target effects.

For the HUDEP-2 cells, a full depletion could be achieved by deleting a larger part of the gene, for example an exon. Another approach would be introduction of a stop codon or frameshift mutation early within the gene, this will also lead to a non-functional protein.

For the mice this is more problematic, since full knockouts die before birth and cannot be studied to check the role of CHTOP in adults. A recent paper indicates that CHTOP lethality in full knockouts is caused by placental defects, which highlights the need to use a conditional approach to study the role of CHTOP in specific organs and tissues.[11] Alternatively, for the hematopoietic system, functional analysis of full *Chtop* knockout cells could be achieved by transplantation of *Chtop null* fetal liver cells into adult recipients.

References

1 Borg, J. *et al.* Haploinsufficiency for the erythroid transcription factor KLF1 causes hereditary persistence of fetal hemoglobin. *Nat Genet* **42**, 801-805, doi:10.1038/ng.630 (2010).

2 Sankaran, V. G. Targeted Therapeutic Strategies for Fetal Hemoglobin Induction. *ASH Education Program Book* **2011**, 459-465, doi:10.1182/asheducation-2011.1.459 (2011).

3 Platt, O. S. Hydroxyurea for the treatment of sickle cell anemia. *N Engl J Med* **358**, 1362-1369, doi:10.1056/NEJMct0708272 (2008).

4 Lanzkron, S. *et al.* Systematic review: Hydroxyurea for the treatment of adults with sickle cell disease. *Ann Intern Med* **148**, 939-955 (2008).

5 Uda, M. *et al.* Genome-wide association study shows BCL11A associated with persistent fetal hemoglobin and amelioration of the phenotype of beta-thalassemia. *Proc Natl Acad Sci U S A* **105**, 1620-1625, doi:10.1073/pnas.0711566105 (2008).

6 Thein, S. L. *et al.* Intergenic variants of HBS1L-MYB are responsible for a major quantitative trait locus on chromosome 6q23 influencing fetal hemoglobin levels in adults. *Proc Natl Acad Sci U S A* **104**, 11346-11351, doi:10.1073/pnas.0611393104 (2007).

7 Lettre, G. *et al.* DNA polymorphisms at the BCL11A, HBS1L-MYB, and beta-globin loci associate with fetal hemoglobin levels and pain crises in sickle cell disease. *Proc Natl Acad Sci U S A* **105**, 11869-11874, doi:10.1073/pnas.0804799105 (2008).

8 Thein, S. L., Menzel, S., Lathrop, M. & Garner, C. Control of fetal hemoglobin: new insights emerging from genomics and clinical implications. *Hum Mol Genet* **18**, R216-223, doi:10.1093/hmg/ddp401 (2009).

9 van Dijk, T. B. *et al.* Friend of Prmt1, a novel chromatin target of protein arginine methyltransferases. *Mol Cell Biol* **30**, 260-272, doi:10.1128/MCB.00645-09 (2010).

10 van Dijk, T. B. *et al.* Fetal globin expression is regulated by Friend of Prmt1. *Blood* **116**, 4349-4352, doi:10.1182/blood-2010-03-274399 (2010).

11 Perez-Garcia, V. *et al.* Placentation defects are highly prevalent in embryonic lethal mouse mutants. *Nature* **555**, 463-468, doi:10.1038/nature26002 (2018).

12 Fanis, P. *et al.* Five friends of methylated chromatin target of protein-arginine-methyltransferase[prmt]-1 (chtop), a complex linking arginine methylation to desumoylation. *Mol Cell Proteomics* **11**, 1263-1273, doi:10.1074/mcp.M112.017194 (2012).

13 Mikropoulou, M. *An shRNA Screen for the Discovery of Suppressors of Fetal Hemoglobin*, Erasmus University Rotterdam, (2016).

14 Gray, K. A., Yates, B., Seal, R. L., Wright, M. W. & Bruford, E. A. Genenames.org: the HGNC resources in 2015. *Nucleic Acids Res* **43**, D1079-1085, doi:10.1093/nar/gku1071 (2015).

15 Gary, J. D. & Clarke, S. RNA and protein interactions modulated by protein arginine methylation. *Prog Nucleic Acid Res Mol Biol* **61**, 65-131 (1998).

16 Yang, Y. *et al.* PRMT9 is a type II methyltransferase that methylates the splicing factor SAP145. *Nat Commun* **6**, 6428, doi:10.1038/ncomms7428 (2015).

17 Huang, J., Vogel, G., Yu, Z., Almazan, G. & Richard, S. Type II arginine methyltransferase PRMT5 regulates gene expression of inhibitors of differentiation/DNA binding Id2 and Id4 during glial cell differentiation. *J Biol Chem* **286**, 44424-44432, doi:10.1074/jbc.M111.277046 (2011).

18 Zurita-Lopez, C. I., Sandberg, T., Kelly, R. & Clarke, S. G. Human protein arginine methyltransferase 7 (PRMT7) is a type III enzyme forming omega-NG-monomethylated arginine residues. *J Biol Chem* **287**, 7859-7870, doi:10.1074/jbc.M111.336271 (2012).

19 Cheng, D., Côté, J., Shaaban, S. & Bedford, M. T. The Arginine Methyltransferase CARM1 Regulates the Coupling of Transcription and mRNA Processing. *Molecular Cell* **25**, 71-83, doi:10.1016/j.molcel.2006.11.019.

20 Fuhrmann, J., Clancy, K. W. & Thompson, P. R. Chemical biology of protein arginine modifications in epigenetic regulation. *Chem Rev* **115**, 5413-5461, doi:10.1021/acs.chemrev.5b00003 (2015).

21 Yadav, N. *et al.* Specific protein methylation defects and gene expression perturbations in coactivator-associated arginine methyltransferase 1-deficient mice. *Proceedings of the National Academy of Sciences* **100**, 6464-6468 (2003).

22 Pawlak, M. R., Scherer, C. A., Chen, J., Roshon, M. J. & Ruley, H. E. Arginine N-methyltransferase 1 is required for early postimplantation mouse development, but cells deficient in the enzyme are viable. *Molecular and cellular biology* **20**, 4859-4869 (2000).

23 Takai, H. *et al.* 5-Hydroxymethylcytosine Plays a Critical Role in Glioblastomagenesis by Recruiting the CHTOP-Methylosome Complex. *Cell Reports* **9**, 48-60, doi:10.1016/j.celrep.2014.08.071 (2014).

24 Lee, J. *et al.* Tumor stem cells derived from glioblastomas cultured in bFGF and EGF more closely mirror the phenotype and genotype of primary tumors than do serum-cultured cell lines. *Cancer Cell* **9**, 391-403, doi:10.1016/j.ccr.2006.03.030 (2006).

25 Chang, C. T. *et al.* Chtop is a component of the dynamic TREX mRNA export complex. *EMBO J* **32**, 473-486, doi:10.1038/emboj.2012.342 (2013).

26 Izumikawa, K. *et al.* Chtop (Chromatin target of Prmt1) auto-regulates its expression level via intron retention and nonsense-mediated decay of its own mRNA. *Nucleic Acids Res* **44**, 9847-9859, doi:10.1093/nar/gkw831 (2016).

27 Kurita, R. *et al.* Establishment of immortalized human erythroid progenitor cell lines able to produce enucleated red blood cells. *PLoS One* **8**, e59890, doi:10.1371/journal.pone.0059890 (2013).

28 de Krom, M., van de Corput, M., von Lindern, M., Grosveld, F. & Strouboulis, J. Stochastic patterns in globin gene expression are established prior to transcriptional activation and are clonally inherited. *Mol Cell* **9**, 1319-

1326 (2002).
29 Heinrich, A. C., Pelanda, R. & Klingmuller, U. A mouse model for visualization and conditional mutations in the erythroid lineage. *Blood* **104**, 659-666, doi:10.1182/blood-2003-05-1442 (2004).
30 Stadtfeld, M. & Graf, T. Assessing the role of hematopoietic plasticity for endothelial and hepatocyte development by non-invasive lineage tracing. *Development* **132**, 203-213, doi:10.1242/dev.01558 (2005).
31 Chen, M. J., Yokomizo, T., Zeigler, B. M., Dzierzak, E. & Speck, N. A. Runx1 is required for the endothelial to haematopoietic cell transition but not thereafter. *Nature* **457**, 887-891, doi:10.1038/nature07619 (2009).
32 Kuhn, R., Schwenk, F., Aguet, M. & Rajewsky, K. Inducible gene targeting in mice. *Science* **269**, 1427-1429, doi:10.1126/science.7660125 (1995).
33 Sanjana, N. E., Shalem, O. & Zhang, F. Improved vectors and genome-wide libraries for CRISPR screening. *Nat Methods* **11**, 783-784, doi:10.1038/nmeth.3047 (2014).
34 Zufferey, R., Nagy, D., Mandel, R. J., Naldini, L. & Trono, D. Multiply attenuated lentiviral vector achieves efficient gene delivery in vivo. *Nature biotechnology* **15**, 871-875, doi:10.1038/nbt0997-871 (1997).
35 Ran, F. A. *et al.* Genome engineering using the CRISPR-Cas9 system. *Nature protocols* **8**, 2281-2308, doi:10.1038/nprot.2013.143 (2013).
36 Brinkman, E. K. *et al.* Easy quantification of template-directed CRISPR/Cas9 editing. *Nucleic Acids Research*, gky164-gky164, doi:10.1093/nar/gky164 (2018).
37 Esteghamat, F. *et al.* The DNA binding factor Hmg20b is a repressor of erythroid differentiation. *Haematologica* **96**, 1252-1260, doi:10.3324/haematol.2011.045211 (2011).
38 Brinkman, E. K., Chen, T., Amendola, M. & van Steensel, B. Easy quantitative assessment of genome editing by sequence trace decomposition. *Nucleic Acids Res* **42**, e168, doi:gku936 [pii] 10.1093/nar/gku936 (2014).
39 Traxler, E. A., Thom, C. S., Yao, Y., Paralkar, V. & Weiss, M. J. Nonspecific inhibition of erythropoiesis by short hairpin RNAs. *Blood* **131**, 2733-2736, doi:10.1182/blood-2018-03-841304 (2018).

Supplementary Table 1. List of primers used.

Gene[3]	Sequence	Purpose
PAC8.1_Fw	GCTGCTGTTATGACCACTAGAGGG	Genotyping
PAC8.1_Rv	AGACAGGGAAGGAGGTGTGG	Genotyping
EpoR-Cre_Fw	GTGTGGCTGCCCCTTCTGCCA	Genotyping
EpoR-Cre_Rv	CAGGAATTCAAGCTCAACCTCA	Genotyping
general-Cre_Fw	ACCCTGTTACGTATAGCCGA	Genotyping
general-Cre_Rv	CTCCGGTATTGAAACTCCAG	Genotyping
Vav-Cre_Fw	GGCGACAGTTACAGTCACAGAAGAGG	Genotyping
Vav-Cre_Rv	GCCTGGCGATCCCTGAACATG	Genotyping
Vec-Cre_Fw1	CAGTTGGAAAACCTGCCTCCCTC	Genotyping
Vec-Cre_Fw2	CCCAGGCTGACCAAGCTGAG	Genotyping
Vec-Cre_Rv	GCCTGGCGATCCCTGAACATG	Genotyping
CAG_Flp_Fw	CCCATTCCATGCGGGGTATCG	Genotyping
CAG_Flp_Rv	GCATCTGGGAGATCACTGAG	Genotyping
Chtop_Fw	TGATTGTATTTGAGGCTGTATTGTC	Genotyping
Chtop_Rv	GGAAGTGCGTCACATTCTGG	Genotyping
Chtop_5'probe_Fw	CAGGCCTTTAGGCTTGGTTG	Southern blotting
Chtop_5'probe_Rv	CAAACTTGTTGATATCGTGG	Southern blotting
Gapdh_m_qPCR_Fw	CTACTGGTGTCTTCACCACC	qPCR
Gapdh_m_qPCR_Rv	TCGTGGTTCACACCCATCAC	qPCR
a_m_qPCR_Fw	TTGGCTAGCCACCACCCT	qPCR
a_m_qPCR_Rv	CCAAGAGGTACAGGTGCA	qPCR
bmajor_m_qPCR_Fw	ATGGCCTGAATCACTTGGAC	qPCR
bmajor_m_qPCR_Rv	ACGATCATATTGCCCAGGAG	qPCR
bH1_m_qPCR_Fw	TGG ACA ACC TCA AGG AGA CC	qPCR
bH1_m_qPCR_Rv	ACC TCT GGG GTG AAT TCC TT	qPCR
ey_m_qPCR_Fw	TGGCCTGTGGAGTAAGGTCAA	qPCR
ey_m_qPCR_Rv	GAAGCAGAGCACAAGTTCCCA	qPCR
b_h_qPCR-Fw	TACAATTTGCTTCTGACACAAC	qPCR
b_h_qPCR-Rv	ACAGATCCCCAAAGGAC	qPCR
g_h_qPCR-Fw	AGGTGCTGACTTCCTTGGG	qPCR
g_h_qPCR-Rv	GGGTGAATTCTTTGCCGAA	qPCR
hChtop_exFw1	CACCGACGGTTAGGCCGACCCATAG	CRISPR guide
hChtop_exRv1	AAACCTATGGGTCGGCCTAACCGTC	CRISPR guide
hChtop_deltest_Fw1	TGAGCTTCTTGGAGTTTCTG	CRISPR surveyor
hChtop_deltest_Rv1	GTTGTTACGCAGGTCATAGC	CRISPR surveyor

3 m_ = mouse; h_=human; Fw = sense; Rv = antisense

Supplementary Table 2 list of antibodies used

Flow cytometry			
Antibody	**Manufacturer**	**Order #**	**Dilution**
CD71-FITC	BD Pharmingen	553266	1:400
Ter119-PE	BD Pharmingen	553673	1:400
KIT-PE-Cy7	BD Pharmingen	558163	1:200
CD44-APC	BD Pharmingen	559250	1:400
Ly6C-Brilliant Violet 605	BD Horizon	563011	1:500
2,4G2 block	Homemade	-	1:300
Fixable Viability Dye eFluor® 506	eBioscience	65-0866-14	1:400
CD3-FITC	BD Pharmingen	553062	1:320
CD25-PERCP-Cy5.5	BD Pharmingen	551071	1:160 for spleen or 1:640 for thymus
CD4-APC-Cy7	BD Pharmingen	560181	1:200
NK1.1-Pacific Blue	BD Horizon	560524	1:50
CD8a-PE-Cy7	eBioscience	25-0081-82	1:1600
CD44-PE	BD Pharmingen	553134	1:1000
CD62L-APC	eBioscience	17-0621-82	1:5000
CD21-FITC	eBioscience	11-0212-85	1:500
CD19-PERCP-Cy5.5	eBioscience	45-0193-82	1:320
B220-Alexa Fluor 700	eBioscience	56-0452-82	1:160
IgM-Bio	BD Pharmingen	553436	1:80
Streptavidin-APC-eFluor 780	eBioscience	47-4317-82	1:400
CD2-PE	eBioscience	12-0021-83	1:2500
CD23-PE-Cy7	eBioscience	25-0232-81	1:500
IgD-APC	eBioscience	17-5993-82	1:2500
F4/80-FITC	eBioscience	11-4801-85	1:100
CD11b-PERCP-Cy5.5	BD Pharmingen	550993	1:100
MHCII-Alexa Fluor 700	eBioscience	56-5321-82	1:400
Ly6C-Brilliant Violet 605	BD Horizon	563011	1:500
SiglecF-PE	PD Pharmingen	552126	1:320
Ly6G-PE-Cy7	BD Pharmingen	560601	1:500
CD11c-PertexRed	Invitrogen	MDC11c17	1:100
7-aminoactinomycin D	Invitrogen	A1310	1:400
Western blotting			
Antibody	Manufacturer	Order #	Dilution
CHTOP	Absea Biotechnology	KT59	1:1000
CHTOP	Absea Biotechnology	KT64	1:1000
PRMT	Upstate/Millipore	07-404	1:1000
g-globin	Santa Cruz	sc-21756	1:1000
tubulin	ThermoFiser Scientific	A11126	1:1000
Actin	Santa Cruz	sc-1616	1:1000

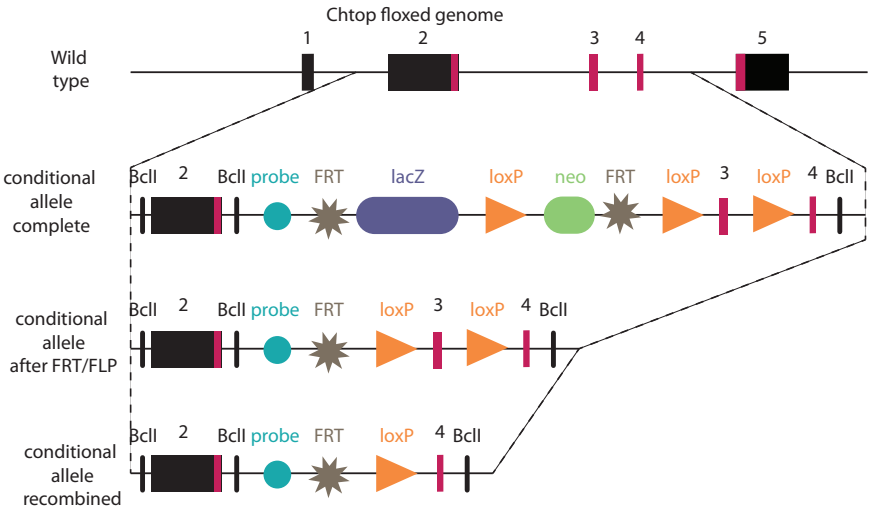

Supplementary Figure 1. Conditional knockout allele of Chtop gene. Before crossing with the hematopoietic Cre lines, we crossed the mice with the CAG-Flp line to remove the lacZ and neo cassette between the FRT sites. The resulting mice are referred to as Chtop fl/fl.

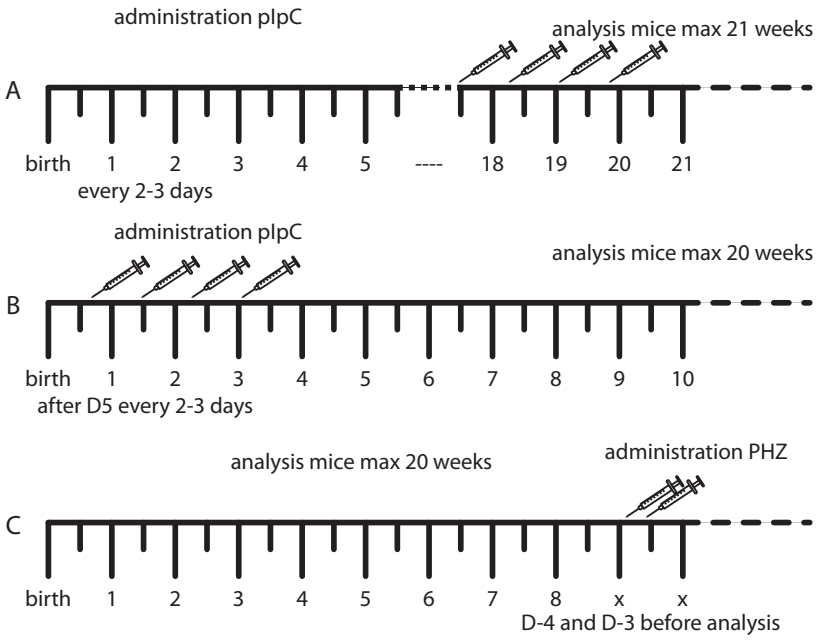

Supplementary Figure 2. Injection scheme for induction of Mx1-Cre and phenylhydrazine (PHZ) treatment. (A) induction of Mx1-Cre by pIpC in adults, (B) induction of Mx1-Cre by pIpC in young mice, (C) Administration of PHZ in EpoR-Cre mice or in combination with A or B. PHZ was administrated 4 days (D-4) and 3 days (D-3) before analysis.

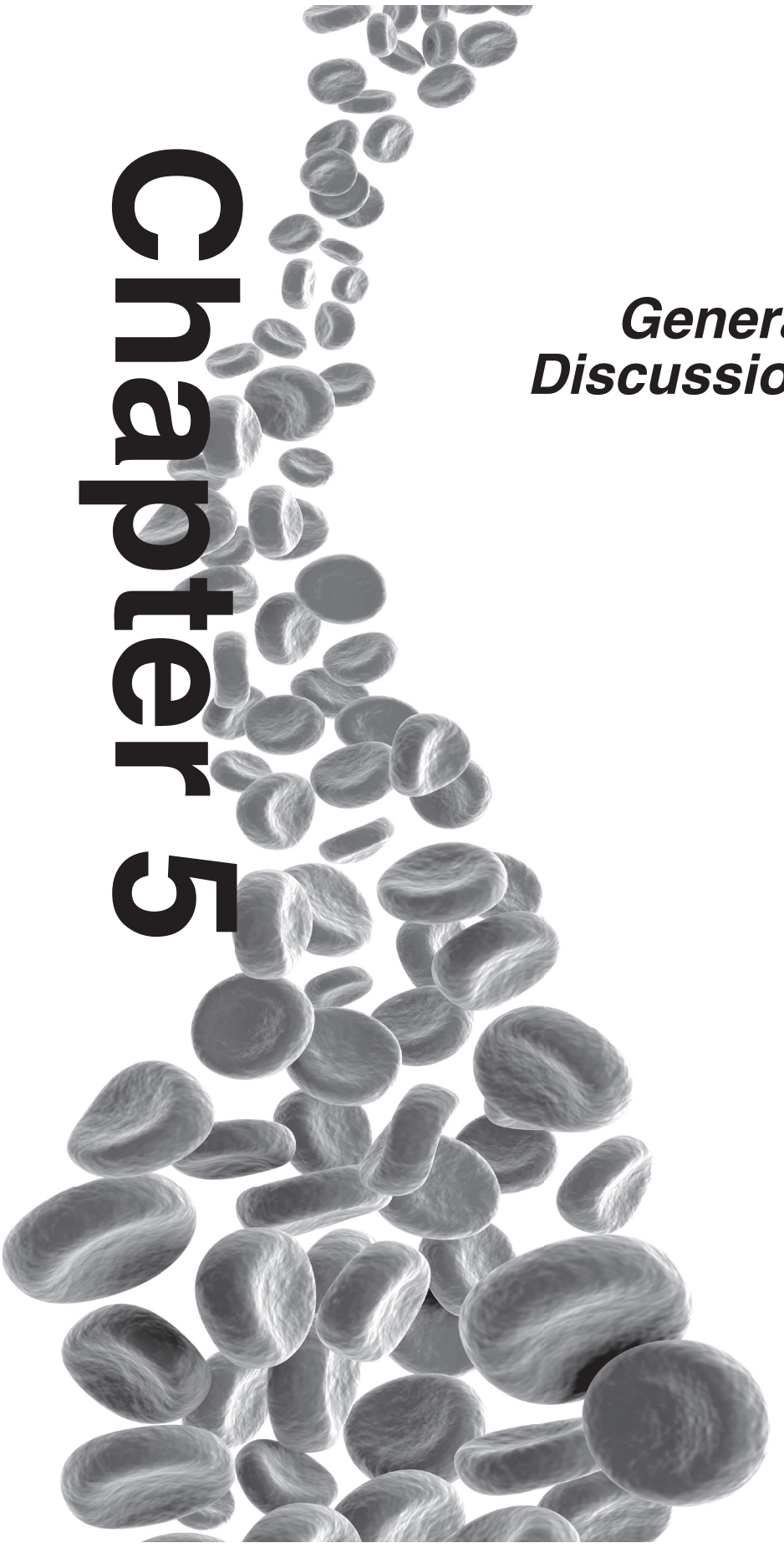

Chapter 5

General Discussion

Chapter 5 General Discussion

Hemoglobinopathies, including sickle cell disease (SCD) and thalassemia, are the most common monogenetic diseases within the human population.[1] Yearly, approximately 300,000 people are born with these diseases.[2] SCD and thalassemia manifest mainly in Mediterranean, African and Asian countries, and cause many problems within those societies.[2,3] Interestingly, a genetic condition called hereditary persistence of fetal hemoglobin (HPFH) is a natural symptom fighter.[4] In combination with SCD and β-thalassemia, HPFH ameliorates the worst symptoms of the diseases.[4,5] The degree of increase in fetal hemoglobin depends on the specific mutation that causes the HPFH. In SCD, levels of 20% HbF or higher result in a significant reduction of disease symptoms.[4]
Genome-wide association studies and linkage analysis have revealed transcription factors that were shown experimentally to be directly involved in hemoglobin regulation. Since transcription factors are poor targets for pharmacological intervention, the challenge is now to identify and functionally characterize the co-factors and epigenetic regulators interacting with these transcription factors.

Potential candidate KDM7A is not involved in globin regulation.

The first candidate fetal hemoglobin repressor tested in this thesis is KDM7A, also known as KDM7 or JHDM1D.[6] KDM7A is a histone demethylase, and is known to demethylate H3K9me2, H3K27me2 and H4K20Me1.[7] More specifically, demethylase activity of KDM7A towards H3K9me2 is only active in absence of H3K4me3, while demethylation of H3K27me2 is not affected by H3K4me3. H4K20me1 demethylation by KDM7A only occurs in the context of the complete nucleosome.[8] Dimethylation of H3K9 and H3K27 is associated with transcriptional repression.[9] It is known that is KDM7A is important during early neural differentiation via regulation of FGF4 expression.[10]
Chapter 2 shows the results of the use of a mouse model, which also carries the human *HBB* locus, together with erythroid specific Cre-recombinase *EpoR*-Cre and floxed alleles of the *Kdm7a* gene. Erythroid-specific recombination by *EpoR-Cre* was efficient but did not affect erythropoiesis. Since recombination by *EpoR-Cre* occurs late during erythroid differentiation, we extended the observations to pan-hematopoietic deletion by *Mx1-Cre*. Induction of Cre expression by pIpC injection resulted in highly efficient recombination at the *Kdm7a* locus. In the Mx1-Cre mice, we observed a delayed regenerative capicity of the erythroid cells. Although we observed minor changes in some hematopoietic cell populations, these changes did not influence the balance in the complete hematopoietic system. We conclude that KDM7A is dispensable for hematopoiesis and does not have role in repressing the *HBG1/2* genes in adult erythropoiesis.

PRMT1 and PRMT5 are essential for hematopoiesis

Next, we investigated the genes encoding protein arginine transferases *(PRMTs) PRMT1, PRMT4 and PRMT5*. In the literature, we can find a number of *in vitro* studies linking PRMT1 and PRMT5 to globin expression. *PRMT1* induction in K562 cells promotes erythroid differentiation, and a shRNA-mediated knockdown

of *PRMT1* leads to suppressed erythroid differentiation.[11] PRMT1 expression enhances the hemoglobin synthesis.[11] According to a recent publication loss of PRMT4 does not affect erythropoiesis and hematopoiesis, but is essential for myeloid leukomogenesis.[12]
Other K562 and human erythroid progenitor *in vitro* studies revealed that the PRMT5 protein binds to the γ-globin promoter via the nuclear zinc finger protein LYAR (Ly-1 antibody reactive clone) and DNA methyltransferase DNMT3A.[13,14] LYAR binds to the 5'untranslated region and silences γ-globin expression.[13] *In vitro* studies using the methyl transferase inhibitor Adox (adenosine-29,39-dialdehyde) led to inhibition of *PRMT5* and an increase of γ-globin expression in K562 cells.[15]
The PRMT-family consists of 9 members, and is divided in 3 groups: Type I, II and III.[16,17] PRMTs catalyse the transfer of a methyl group from *S*-adenosyl-*L*-methionine (SAM) to the guanidino nitrogen atom of arginine molecule. Type I is characterized by symmetric ω-N^G,N^G-arginine dimethylation (sDMA), and includes *PRMT5* and *PRMT9*.[18,19] Type II enzymes are characterized by asymmetric ω-N^G,N^G-arginine dimethylation (ADMA), and include PRMT1, PRMT2, PRMT3, PRMT4/CARM1, PRMT6 and PRMT8.[17] PRMT7 is thus far the only Type III enzyme which is able to from ω-N^G-monomethyl arginine (MMA) on histones.[20] Most PRMTs methylate arginine- and glycine rich motifs, called RGG/RG motifs or GAR-domains, except for PRMT4/CARM1, which prefers proline, glycine and methionine (PGM)-rich motifs.[21]
In general the effect of arginine methylation is changing interacting partners, due to steric effects of hydrogen bond interactions without changing the charge of the molecule.[22]
Many full knockouts of *Prmt*s in mice, for example, *Prmt1, Prmt4/Carm1* and *Prmt5* are lethal. [23-25] PRMTs are associated with many functions and roles *in vivo*: from the nerves, muscles and immune system to metabolic diseases, aging and cancer.[26,27]
Given the multiplicity of PRMT functions, we hoped to be able to link them to γ-globin regulation and erythroid cell development *in vivo*. In **Chapter 3** we describe our findings concerning PRMT1, PRMT4 and PRMT5.
The results for Prmt4 were in agreement with previous reports showing altered T cell development. Recombination of the floxed *Prmt4* allele was very efficient. Upon recombination of *Prmt1* and *Prmt5* alleles we observed modest changes in some hematopoietic cell populations. However, we found that recombination efficiency of the floxed *Prmt1* and *Prmt5* alleles was low, indicating selective survival of cells in which recombination had not occurred. Using tissue-specific constitutively active Cre lines, Vav1-Cre and Vec-Cre, we found more efficient recombination in *Prmt5* fl/wt mice compared to *Prmt5* fl/fl littermates. This supports the notion of selection for homozygous floxed cells that escaped recombination. The essential role of PRMT1 and PRMT5 was confirmed by CRISPR targeting in HUDEP-2 cells, a cell line modelling adult human erythropoiesis.

No confirmation of g-globin regulation by CHTOP *in vivo*

CHTOP (Chromatin Target of PRMT1) was previously found as a γ-globin regulator in an effort to find new therapeutic targets for β-thalassemia and sickle cell anaemia.[28] In cell culture studies, where a short hairpin-mediated knockdown of CHTOP was achieved in primary human erythroid progenitor cells, γ-globin levels of up to 25% of total β-like globin were found.[28,29] Animal studies are hampered by

the fact that constitutive *Chtop* knockout mice die around E16.5.[29] In **Chapter 4** we report results obtained with mice carrying a human *HBB* locus transgene, *Chtop* floxed alleles and Cre-recombinases specific for the erythroid and hematopoietic system. Using the EpoR-Cre line we observed a high recombination efficiency in erythroid cells but the protein levels of Chtop were not affected, presumably due to the stage of differentiation at which Cre-mediated recombination occurs. We then switched to the pan-hematopoietic inducible *Mx1*-Cre line. Induction of *Mx1*-Cre in young mice resulted in efficient recombination, and importantly reduced CHTOP protein expression. However, the low levels of CHTOP protein did not result in increased γ-globin expression or other hematopoietic phenotypes. When we investigated CHTOP in embryos, *Mx1*-Cre induction does not work. The constitutive pan-hematopoietic Vav-Cre line displayed poor recombination efficiency. With the constitutive hemo-endothelial Vec-Cre line we achieved efficient recombination and CHTOP protein reduction in fetal livers and cord blood of E12.5-E16.5 embryos. This had, however, no discernible effect on γ-globin expression or the other erythroid parameters measured. Finally, we depleted CHTOP protein in HUDEP-2 cells using CRIPSR technology. The *CHTOP* gene was targeted efficiently as shown by surveyor assays and TIDE analysis. However, we did not observe increased expression of γ-globin in CHTOP-depleted HUDEP-2 cells.

Future perspectives using CRISPR-Cas9

Recently developed technologies such as CRISPR-Cas9 and the establishment of the HUDEP-2 cell line, create new perspectives to look for other new candidate hemoglobin regulator genes.[30,31] First, CRISPR-Cas9 screens in combination of guide-RNA libraries in HUDEP-2 cells can reveal new γ-globin regulator genes. Recently, for example, the HRI gene was discovered to regulate γ-globin.[30,32-34]
Second, CRISPR-Cas9 can be applied to make use of homologous recombination to generate reporter lines.[30,31,35] Addition of GFP or another reporter to the γ-globin within HUDEP-2 cells can be used to detect γ-globin levels easily on the flow cytometer. When HUDEP-2 with γ-globin-GFP is created, these cells can be used in direct drug screen. Using flow cytometry the effects of compounds on γ-globin expression can be measured. In addition, a γ-globin-GFP fusion protein within embryonic stem cells can be used to create a genetically modified mouse model for further research on potential target genes of these drugs. Recently, pomalidomide was found to increase the HbF levels in CD34+ selected cord blood cells.[36] Pomalidomide is a drug used in the treatment of multiple myeloma with several side effects.
Third, CRISPR-Cas9 can be used in stem cells of human sickle cell and thalassemic patients CRISPR-Cas9 to correct mutations. This has, so far, been performed in cultured cells from the patients, such as induced pluripotent stem cells (iPS) cells or stem cells, and also in human embryos.[37-41] A risk of CRISPR-Cas9 technology are the off-target effects and larger deletions, which might damage other genes with unknown risks.[35] Because of the side effects, more research is required to create a safe CRISPR-Cas9 treatment.

Concluding remarks

Much time and effort was put in order to understand erythropoiesis and hemoglobin

switching, with the aim to increase the HbF levels in order to ameliorate most of the effects of SCD and β-thalassemia. Despite these efforts the mechanisms are not completely understood yet. In this thesis, we tried to couple the genes *KDM7A, PRMT1, PRMT4, PRMT5* and *CHTOP* to γ-globin regulation. Although we did not find increased HbF levels, we can only eliminate CHTOP, KDM7A and PRMT4 definitively as regulators of HbF inducers. The importance to check recombination efficiency in conditional knockout mice is clearly demonstrated by the *PRMT1* and *PRMT5* genes where cells escaping recombination appear to compensate for the loss of recombined cells. After a variety of experiments, we can conclude that PRMT1 and PRMT5 are likely important for hematopoiesis.

A similar selection mechanism occurred in CRISPR-Cas9 experiments aimed at inactivating PRMT1 and PRMT5 in HUDEP-2 cells, where we also did not observe increased expression of γ-globin. Thus, other experimental methods should be established to investigate the role of PRMT1 and PRMT5 in hematopoiesis, for example using one or more chemical compounds that inhibit the PRMT1 or PRMT5 function.

Finally, an unbiased CRISPR-Cas9 screen in HUDEP-2 γ-globin reporter cells could be performed to reveal novel genes involved in repression of the fetal globin genes, which will hopefully include druggable targets that can be used to develop affordable and safe oral drugs for β-hemoglobinopathy patients.

References

1 Angastiniotis, M. & Modell, B. Global epidemiology of hemoglobin disorders. Ann N Y Acad Sci 850, 251-269 (1998).

2 Weatherall, D. J. & Clegg, J. B. Inherited haemoglobin disorders: an increasing global health problem. Bull World Health Organ 79, 704-712 (2001).

3 Williams, T. N. & Weatherall, D. J. World distribution, population genetics, and health burden of the hemoglobinopathies. Cold Spring Harb Perspect Med 2, a011692, doi:10.1101/cshperspect.a011692 (2012).

4 Sankaran, V. G. Targeted Therapeutic Strategies for Fetal Hemoglobin Induction. ASH Education Program Book 2011, 459-465, doi:10.1182/asheducation-2011.1.459 (2011).

5 Borg, J. et al. Haploinsufficiency for the erythroid transcription factor KLF1 causes hereditary persistence of fetal hemoglobin. Nat Genet 42, 801-805, doi:10.1038/ng.630 (2010).

6 Nawrocki, M. J. et al. JHDM1D and HDAC1-3 mRNA expression levels in peripheral blood mononuclear cells of patients with systemic lupus erythematosus. Z Rheumatol 74, 902-910, doi:10.1007/s00393-015-1619-9 (2015).

7 Tsukada, Y.-i., Ishitani, T. & Nakayama, K. I. KDM7 is a dual demethylase for histone H3 Lys 9 and Lys 27 and functions in brain development. Genes & Development 24, 432-437, doi:10.1101/gad.1864410 (2010).

8 Qi, H. H. et al. Histone H4K20/H3K9 demethylase PHF8 regulates zebrafish brain and craniofacial development. Nature 466, 503-507, doi:http://www.nature.com/nature/journal/v466/n7305/abs/nature09261.html#supplementary-information (2010).

9 Horton, J. R. et al. Enzymatic and structural insights for substrate specificity of a family of jumonji histone lysine demethylases. Nat Struct Mol Biol 17, 38-43, doi:http://www.nature.com/nsmb/journal/v17/n1/suppinfo/nsmb.1753_S1.html (2010).

10 Huang, C. et al. Dual-specificity histone demethylase KIAA1718 (KDM7A) regulates neural differentiation through FGF4. Cell research 20, 154-165, doi:10.1038/cr.2010.5 (2010).

11 Hua, W. K. et al. Protein arginine methyltransferase 1 interacts with and activates p38alpha to facilitate erythroid differentiation. PLoS One 8, e56715, doi:10.1371/journal.pone.0056715 (2013).

12 Greenblatt, S. M. et al. CARM1 Is Essential for Myeloid Leukemogenesis but Dispensable for Normal Hematopoiesis. Cancer Cell 33, 1111-1127 e1115, doi:10.1016/j.ccell.2018.05.007 (2018).

13 Ju, J. et al. Human fetal globin gene expression is regulated by LYAR. Nucleic Acids Res 42, 9740-9752, doi:10.1093/nar/gku718 (2014).

14 Rank, G. et al. Identification of a PRMT5-dependent repressor complex linked to silencing of human fetal globin gene expression. Blood 116, 1585-1592, doi:10.1182/blood-2009-10-251116 (2010).

15 He, Y. et al. Induction of human fetal hemoglobin expression by adenosine-2',3'-dialdehyde. J Transl Med 11, 14, doi:10.1186/1479-5876-11-14 (2013).

16 Gray, K. A., Yates, B., Seal, R. L., Wright, M. W. & Bruford, E. A. Genenames.org: the HGNC resources in 2015. Nucleic Acids Res 43, D1079-1085, doi:10.1093/nar/gku1071 (2015).

17 Gary, J. D. & Clarke, S. RNA and protein interactions modulated by protein arginine methylation. Prog Nucleic Acid Res Mol Biol 61, 65-131 (1998).

18 Yang, Y. et al. PRMT9 is a type II methyltransferase that methylates the splicing factor SAP145. Nat Commun 6, 6428, doi:10.1038/ncomms7428 (2015).

19 Huang, J., Vogel, G., Yu, Z., Almazan, G. & Richard, S. Type II arginine methyltransferase PRMT5 regulates gene expression of inhibitors of differentiation/DNA binding Id2 and Id4 during glial cell differentiation. J Biol Chem 286, 44424-44432, doi:10.1074/jbc.M111.277046 (2011).

20 Zurita-Lopez, C. I., Sandberg, T., Kelly, R. & Clarke, S. G. Human protein arginine methyltransferase 7 (PRMT7) is a type III enzyme forming omega-NG-monomethylated arginine residues. J Biol Chem 287, 7859-7870, doi:10.1074/jbc.M111.336271 (2012).

21 Cheng, D., Côté, J., Shaaban, S. & Bedford, M. T. The Arginine Methyltransferase CARM1 Regulates the Coupling of Transcription and mRNA Processing. Molecular Cell 25, 71-83, doi:10.1016/j.molcel.2006.11.019.

22 Fuhrmann, J., Clancy, K. W. & Thompson, P. R. Chemical biology of protein arginine modifications in epigenetic regulation. Chem Rev 115, 5413-5461, doi:10.1021/acs.chemrev.5b00003 (2015).

23 Yadav, N. et al. Specific protein methylation defects and gene expression perturbations in coactivator-associated arginine methyltransferase 1-deficient mice. Proceedings of the National Academy of Sciences 100, 6464-6468 (2003).

24 Pawlak, M. R., Scherer, C. A., Chen, J., Roshon, M. J. & Ruley, H. E. Arginine N-methyltransferase 1 is required for early postimplantation mouse development, but cells deficient in the enzyme are viable. Molecular and cellular biology 20, 4859-4869 (2000).

25 Tee, W.-W. et al. Prmt5 is essential for early mouse development and acts in the cytoplasm to maintain ES cell pluripotency. Genes & development 24, 2772-2777 (2010).

26 Bedford, M. T. & Clarke, S. G. Protein Arginine Methylation in Mammals: Who, What, and Why. Molecular Cell 33, 1-13, doi:10.1016/j.molcel.2008.12.013 (2009).

27 Blanc, R. S. & Richard, S. Arginine Methylation: The Coming of Age. Mol Cell 65, 8-24, doi:10.1016/j.molcel.2016.11.003 (2017).

28 van Dijk, T. B. et al. Fetal globin expression is regulated by Friend of Prmt1. Blood 116, 4349-4352, doi:blood-2010-03-274399 [pii]
10.1182/blood-2010-03-274399 (2010).

29 van Dijk, T. B. et al. Friend of Prmt1, a novel chromatin target of protein arginine methyltransferases. Mol Cell Biol 30, 260-272, doi:10.1128/MCB.00645-09 (2010).

30 Ran, F. A. et al. Genome engineering using the CRISPR-Cas9 system. Nature protocols 8, 2281-2308, doi:10.1038/nprot.2013.143 (2013).
31 Sanjana, N. E., Shalem, O. & Zhang, F. Improved vectors and genome-wide libraries for CRISPR screening. Nat Methods 11, 783-784, doi:10.1038/nmeth.3047 (2014).
32 Grevet, J. D. et al. Domain-focused CRISPR screen identifies HRI as a fetal hemoglobin regulator in human erythroid cells. Science 361, 285-290, doi:10.1126/science.aao0932 (2018).
33 Manning, G., Whyte, D. B., Martinez, R., Hunter, T. & Sudarsanam, S. The Protein Kinase Complement of the Human Genome. Science 298, 1912-1934, doi:10.1126/science.1075762 (2002).
34 Shi, J. et al. Discovery of cancer drug targets by CRISPR-Cas9 screening of protein domains. Nature biotechnology 33, 661, doi:10.1038/nbt.3235
https://www.nature.com/articles/nbt.3235#supplementary-information (2015).
35 S., A. J. et al. CRISPR/Cas9 system: A promising technology for the treatment of inherited and neoplastic hematological diseases. ADVANCES IN CELL AND GENE THERAPY 1, e10, doi:doi:10.1002/acg2.10 (2018).
36 Dulmovits, B. M. et al. Pomalidomide reverses γ-globin silencing through the transcriptional reprogramming of adult hematopoietic progenitors. Blood 127, 1481-1492, doi:10.1182/blood-2015-09-667923 (2016).
37 Liang, P. et al. Correction of β-thalassemia mutant by base editor in human embryos. Protein & Cell 8, 811-822, doi:10.1007/s13238-017-0475-6 (2017).
38 Antoniani, C. et al. Induction of fetal hemoglobin synthesis by CRISPR/Cas9-mediated editing of the human β-globin locus. Blood 131, 1960-1973, doi:10.1182/blood-2017-10-811505 (2018).
39 Mettananda, S. et al. Editing an α-globin enhancer in primary human hematopoietic stem cells as a treatment for β-thalassemia. Nature Communications 8, 424, doi:10.1038/s41467-017-00479-7 (2017).
40 Hawksworth, J. et al. Enhancement of red blood cell transfusion compatibility using CRISPR-mediated erythroblast gene editing. EMBO Molecular Medicine 10, doi:10.15252/emmm.201708454 (2018).
41 Dever, D. P. et al. CRISPR/Cas9 β-globin gene targeting in human haematopoietic stem cells. Nature 539, 384, doi:10.1038/nature20134
https://www.nature.com/articles/nature20134#supplementary-information (2016).

Addendum

Summery
Samenvatting
Curriculum Vitae
PhD Portfolio
Acknowledgements

Summery

Around 300,000 people are born every year with sickle cell disease (SCD) and β-thalassemia worldwide. Asia, Africa and the Mediterranean area show the highest incidence of those monogenetic diseases. Because of the lower development in many of those countries, it causes many problems and treatments like blood transfusion or bone marrow transplantation are not possible. In those diseases, the function of adult hemoglobin (HbA) is affected. Research revealed another genetic condition that is characterized by high γ-globin fetal hemoglobin (HbF) levels in adults, called hereditary persistence of fetal hemoglobin (HPFH). Interestingly, HPFH ameliorates the symptoms of SCD and β-thalassemia. The best effects of HPFH are there when levels of 20% of higher are reached. Genome-wide association studies and linkage analysis have revealed transcription factors that were shown experimentally to be directly involved in hemoglobin regulation. Since transcription factors are poor targets for pharmacological intervention, the challenge is now to identify and functionally characterize the co-factors and epigenetic regulators interacting with these transcription factors.

The first candidate fetal hemoglobin repressor tested in this thesis is KDM7A, also known as KDM7 or JHDM1D. KDM7A is a histone demethylase, and is known to demethylate H3K9me2, H3K27me2 and H4K20Me1. **Chapter 2** shows the results of the use of a mouse model, which also carries the human *HBB* locus, together with erythroid specific Cre-recombinase *EpoR*-Cre and floxed alleles of the *Kdm7a* gene. Erythroid-specific recombination by *EpoR-Cre* was efficient but did not affect erythropoiesis. Since recombination by *EpoR-Cre* occurs late during erythroid differentiation, we extended the observations to pan-hematopoietic deletion by *Mx1-Cre*. Induction of Cre expression by pIpC injection resulted in highly efficient recombination at the *Kdm7a* locus. Although we observed minor changes in some hematopoietic cell populations, these changes did not influence the overall balance in the hematopoietic system. We conclude that KDM7A is dispensable for hematopoiesis and does not have role in repressing the *HBG1/2* genes in adult erythropoiesis.

Next, we investigated genes encoding protein arginine transferases (PRMTs) PRMT1, PRMT4 and PRMT5. The PRMT-family consists of 9 members, and is divided in 3 groups: Type I, II and III. PRMT1 and PRMT4 belong to the Type I group, that is characterized by asymmetric ω-N^G,N^G-arginine dimethylation (aDMA). PRMT5 belongs to the Type II groups, that is characterized by symmetric ω-N^G,N^G-arginine dimethylation (sDMA). Previous *in vitro* studies linked PRMT1 and PRMT5 to globin expression. PRMT4 loss does not affect the erythropoiesis and hematopoiesis, but is essential for myeloid leukemogenesis.

In **Chapter 3** we show our findings concerning PRMT1, PRMT4 and PRMT5. We used again the *HBB* caring mice, and the inducible pan hematopoietic Mx1-Cre. The results for *Prmt4* were in agreement with previous reports showing altered T cell development. Recombination of the floxed *Prmt4* allele was very efficient. For *Prmt1* and *Prmt5* we observed modest changes in some hematopoietic cell populations. We found that recombination efficiency of the floxed *Prmt1* and *Prmt5* alleles was low, indicating selective survival of cells in which recombination had not occurred. Using tissue-specific constitutively active Cre lines, *Vav1*-Cre and *Vec*-Cre, we found more efficient recombination in *Prmt5* fl/wt mice compared to *Prmt5* fl/fl littermates. This

supports the notion of selection for cells that escaped recombination. The essential role of PRMT1 and PRMT5 was confirmed by CRISPR targeting in HUDEP-2 cells, a cell line modelling adult human erythropoiesis.
Chromatin Target of Prmt1 (CHTOP) is the last gene that we tested in this thesis. It was previously found as a γ-globin regulator in an effort to find new therapeutic targets for β-thalassemia and SCD. In cell culture studies, where a short hairpin-mediated knockdown of CHTOP was achieved in primary human erythroid progenitor cells, γ-globin levels of up to 25% of total β-like globin were found. In **Chapter 4** we report results obtained with mice carrying the *HBB* locus transgene, *Chtop* floxed alleles and Cre-recombinases specific for the erythroid and hematopoietic system. Using the *EpoR*-Cre line we observed a high recombination efficiency in erythroid cells but the protein levels of CHTOP were not affected, presumably due to the stage of differentiation at which Cre-mediated recombination occurs. We then switched to the pan-hematopoietic inducible *Mx1*-Cre line. Induction of *Mx1*-Cre in young mice resulted in efficient recombination, and importantly reduced CHTOP protein expression. Even the low levels of CHTOP protein did not increase γ-globin expression or other strong hematopoietic phenotypes. We then investigated the role of CHTOP during development. We found that *Mx1*-Cre induction in embryos could not be achieved reproducibly. The constitutive pan-hematopoietic Vav-Cre line displayed poor recombination efficiency. With the constitutive hemo-endothelial Vec-Cre line we achieved efficient recombination and CHTOP protein reduction in fetal livers and cord blood of E12.5-E16.5 embryos. This had no discernible effect on γ-globin expression or the other erythroid parameters measured. Finally, we depleted CHTOP protein in HUDEP-2 cells using CRIPSR technology. The *CHTOP* gene was targeted efficiently as shown by surveyor assays and TIDE analysis. However, we did not observe increased expression of γ-globin in CHTOP-depleted HUDEP-2 cells. Finally, in **Chapter 5** I discuss the findings in this thesis in a broader context, indicating perspectives for future research aimed at revealing novel genes involved in repression of the fetal globin genes, which will hopefully include druggable targets that can be used to develop affordable and safe oral drugs for β-hemoglobinopathy patients.

Samenvatting

Elk jaar worden er wereldwijd rond de 300,000 mensen geboren met sikkel cel (SC) ziekte en β-thalassemie. Deze ziekten komen het meeste voor in Azië, Afrika en het Middellandse zeegebied. Vanwege de lagere ontwikkeling in de meeste van deze landen, veroorzaken de ziekten vele problemen en zijn behandelingen zoals bloedtransfusie en beenmergtransplantatie niet mogelijk. In deze ziekten is de functie van het volwassen hemoglobine (HbA) aangedaan. Onderzoek heeft nog een andere genetische aandoening gekarakteriseerd waarbij hoge niveaus van het foetale γ-globine (HbF) zijn gevonden, deze conditie heet erfelijke persistentie van foetaal hemoglobine (EPFH). Interessant hieraan is dat EPFH de meesten symptomen van de SC ziekte en β-thalassemia doet verminderen. De beste effecten van EPFH worden getoond als er een HbF niveau van 20% of hoger is. Genoom-wijde associatie studies en koppelingsanalyses hebben transcriptie factoren onthult die proefondervindelijk hun directe betrokkenheid bij hemoglobine regulatie hebben aangetoond. Doordat transcriptie factoren slechte mikpunten zijn voor farmacologische interventies, is de uitdaging nu om de cofactoren en epi-genetische regulatoren te identificeren die functioneel interacteren met deze transcriptie factoren.

De eerste kandidaat die het foetale hemoglobine onderdrukker getest in deze thesis is KDM7A, die ook bekend staat als KDM7 en JHDM1D. KDM7A is een histon demethylase, en is bekend H3K9me2, H3K27me2 en H4K20Me1 te demethyleren. **Hoofstuk 2** toont de resultaten van het gebruik van een muis model, die ook het humane *HBB* locus draagt, samen met een erytroïde specifieke Cre-recombinase *EpoR*-Cre en gefloxte allelen van het *Kdm7a* gen. Erytroïd-specifieke recombinatie door *EpoR*-Cre was efficiënt maar had geen effect op de erytropoëse. Doordat de recombinatie door *EpoR*-Cre laat in de erytroide differentiatie gebeurd, hebben we onze observaties uitgebreid naar een pan-hematopoëtische deletie door *Mx1*-Cre. Inductie van Cre expressie door pIpC injecties resulteren in een hoog efficiënte recombinatie op de *Kdm7a* locus. Ondanks dat we kleine veranderingen observeren in sommige hematopoëtische cel populaties, hebben deze veranderingen geen invloed op de algehele balans in het hematopoësche systeem. Wij concluderen dat KDM7a overbodig is voor de hematopoëse en geen rol speelt in de onderdrukking van de *HBG1/2* genen in de volwassen erytropoëse.

Vervolgens, onderzoeken we de genen die coderen voor de proteïne arginine transferases (PRMTs) PRMT1, PRMT4 en PRMT5. De PRMT-familie bestaat uit 9 leden en is onderverdeeld in 3 groepen: Type I, II en III. PRMT1 en PRMT4 behoren tot de Type I groep, die gekarakteriseerd wordt door asymmetrische ω-N^G,N^G-arginine dimethylatie (aDMA). PRMT5 behoort tot de Type II groep en wordt gekarakteriseerd door symmetrische ω-N^G,N^G-arginine dimethylatie (sDMA). Vorige *in vitro* studies hebben PRMT1 en PRMT5 gelinkt aan globine expressie. PRMT4 verlies heeft geen effect op de erytropoëse en hematopoëse, maar is essentieel voor myeloïde leukemogenese.

In **Hoofdstuk 3** tonen we onze bevindingen omtrent PRMT1, PRMT4 en PRMT5. We gebruikten weer de *HBB* dragende muizen en includeren pan hematopoëtische *Mx1*-Cre. De resultaten van *PRMT4* zijn in overeenstemming met de vorige verslagen, die een veranderde T cel ontwikkeling tonen. Recombinatie van gefloxte *PRMT4* allel was erg efficiënt. Voor *Prmt1* en *Prmt5* observeren we minimale veranderingen in sommige hematopoëtische cel populaties. We vonden dat de recombinatie efficiëntie

van gefloxte *Prmt1* en *Prmt5* was erg laag, wat wijst op selectieve overleving van cellen waarin de recombinatie niet gelukt is. Gebruik makend van constitutief actieve weefselspecifieke Cre-lijnen, *Vav1*-Cre en *Vec*-Cre, vonden we een efficiëntere recombinatie in *Prmt5* fl/wt muizen in vergelijking met *Prmt5* fl/fl nestgenoten. Dit ondersteund het idee van selectie van cellen die aan de recombinatie ontsnappen. De essentiële rol van PRMT1 en PRMT5 is bevestigd door CRISPR targeting in HUDEP-2 cellen, een cellijn die de humane volwassen erytropoëse modelleert.
Chromatine Target van PRMT1 (CHTOP) is het laatste gen die we hebben getest in deze thesis. Het is eerder gevonden als γ-globine regulator in een onderzoek om nieuwe therapeutische doelen voor β-thalassemie en SC ziekte te vinden. In eerdere celcultuur studies, waarbij een short hairpin-gemedieerde uitschakeling van het *CHTOP* gen was uitgevoerd in humane primaire erythroïde voorloper cellen, was er een verhoogd γ-globine niveau van zo'n 25% van het totaal β-achtige globine gevonden. In **Hoofstuk 4** rapporteren we de resultaten verkregen met muizen die het humane *HBB* locus dragen, gefloxte allelen van *Chtop* en Cre-recombinases specifiek voor het erytroïde en hematopoëtische systeem. Gebruikmakend van de *EpoR*-Cre lijn, observeren we een hoge recombinatie efficiëntie in erytroïde cellen, maar is het eiwit niveau van CHTOP niet aangedaan, dit komt waarschijnlijk door de differentiatie fase waarin de Cre-gemedieerde recombinatie plaatsvindt. Vervolgens zijn we overgestapt op de pan-hematopoëtische *Mx1*-Cre. Inductie van *Mx1*-Cre in jonge muizen resulteert in een efficiënte recombinatie en belangrijk een gereduceerd CHTOP eiwit niveau. Maar zelfs lage niveaus van het CHTOP eiwit leidt niet tot een toename van γ-globine of een ander sterk hematopoëtisch fenotype. Vervolgens hebben we gekeken naar de rol van CHTOP gedurende de ontwikkeling. Hier vonden we dat *Mx1*-Cre inductie in embryo's niet reproduceerbaar was. De constitutieve pan-hematopoëtische *Vav*-Cre lijn liet een slechte recombinatie efficiëntie zien. Bij de constitutieve hemo-endotheliale *Vec*-Cre verkregen we wel efficiënte recombinatie en CHTOP eiwit reductie in foetale levers en navelstrengbloed van E12.5-E16.5. Maar dit had geen waarneembaar effect op de expressie van γ-globine of andere gemeten erytroïde parameters. Tenslotte, verminderden we het CHTOP eiwit HUDEP-2 cellen door gebruik te maken van de CRISPR technologie. Het *CHTOP* gen was efficiënt getarget, wat is aangetoond met behulp van de surveyor assay en TIDE analyse. Desondanks, vonden we geen toename in de expressie van γ-globine in de CHTOP-verwijderde HUDEP-2 cellen.
Tenslotte in **Hoofstuk 5** bediscussieer ik de bevindingen in deze thesis in een breder context, bespreek mogelijkheden voor toekomstig onderzoek gericht op het vinden van nieuwe genen die betrokken zijn bij de repressie van de foetale globine genen, die hopelijk ook nieuwe medicinale doelen bevatten die kunnen worden gebruikt voor de ontwikkeling van betaalbare en veilig orale geneesmiddelen voor patiënten met β-hemoglobinopathiën.

Curriculum Vitae

PERSONAL INFORMATION

Name: Silvia Astrid Hoeboer
Date of Birth: 31 December 1987
Place of Birth: Rotterdam, the Netherlands
Nationality: Dutch

EDUCATION

2013 – 2019 **PhD Program Biomedical Science**
Department of Cell Biology, Erasmus Medical Centre, Rotterdam, the Netherlands
Promotor: Prof.dr. Sjaak Philipsen

2011 – 2012 **Master Life Science and Technology**
Leiden Institute of Chemistry, Leiden University, Leiden, the Netherlands
Mentor: Prof.dr. Mathieu Noteborn

2006 – 2010 **Bachelor Biology and Medical Laboratorial Research**
Hogeschool Rotterdam, Institute Engineering & Applied Science, Rotterdam, the Netherlands

TRAINING

2013 – 2018 **PhD research – Erasmus Medical Centre Rotterdam**
Department of Cell Biology, Erasmus Medical Centre, Rotterdam, the Netherlands
Promotor: Prof.dr. Sjaak Philipsen
Co-promotoren: Dr. Thamar van Dijk & Dr. Marieke von Lindern
Subject: Potential new gamma-globin regulators: *in vivo* analysis of their role in the hematopoietic system.

2011 – 2012 **Master Internship – Université Libre de Bruxelles**
Supervision: Prof. Dr. C. Blanpain & Dr. G. Driessens
Subject: Transcriptional analysis of human cutaneous squamous cell carcinomas.

2011 – 2011 **Master Internship – Leiden Universities Medical Center**
Supervision: Prof.dr. R. Willemse & Dr. C. Tensen & Dr. F.R. de Gruijl
Subject: Interspecies comparison of stem cell markers LGR5 and LGR6.

2009 – 2010 **HLO BML Bachelor of Applied Science Internship – Erasmus Medical Centre Rotterdam**
Supervision: Prof.dr. E.C. Zwarthoff – Dr. H. Vékony
Subject: Unravelling the mechanism of gene regulation by the leukemic oncogene MN1.

2008 – 2009 **HLO BML Bachelor of Applied Science Internship – Erasmus Medical Centre Rotterdam**
Supervision: Prof.dr. J.N.J. Philipsen - Dr. T.B. van Dijk
Subject: Fop and its 'friends': and the role of the GAR domain. And the production of GST-proteins.

AWARDS

2012 Best student award category "External Enrolled" Life Science and Technology, University of Leiden, Leiden, the Netherlands.

PUBLICATIONS

Not available

PhD Portfolio

Name PhD student:	Silvia Astrid Hoeboer
Erasmus MC Department:	Cell Biology
Research School:	Graduate School Medical Genetic Center
PhD teaching program:	Biomedical Science – Erasmus MC
PhD period:	April 2013 – September 2019
Promotor(s):	Prof.dr. J.N.J. Philipsen
Co-promotor(s):	Dr. T.B. van Dijk and Dr. M. von Lindern

General courses

Year	Title	Workload (ECTS)
2013	Laboratory animal science (Article 9)	3
2013	Genetics	3
2013	Biochemistry and Biophysics	3
2014	Cell and Developmental Biology	3
2014	Safely working in the laboratory	0,25
2014	Science Integrity for PhD Students	0,3
2015	Biostatistical Methods: basic Principles Part A	2
2017	Workshop on Photoshop and Illustrator	0,5
2017	Course and Master Classes on Molecular aspects of Hematological disorder	1

Meetings, Workshops and Symposia

Year	Title	Workload (ECTS)
2013-2017	Weekly Monday Morning Meetings, Cell Biology Department, Erasmus Medical Center	2
2013	20th MGC PhD Workshop, Luxembourg City, Luxembourg	2
2013	23th MGC Symposium, Rotterdam, Netherlands	0,5
2014	4th Winter School of the Collaborative Research Centre TRR81, Kleinwalsertal, Austria (oral presentation)	2
2014	21th MGC PhD Workshop, Munster, Germany	2
2014	24th MGC Symposium, Rotterdam, Netherlands	0,5
2015	5th Winter School of the Collaborative Research Centre TRR81, Kleinwalsertal, Austria (oral presentation)	2
2015	22th MGC PhD Workshop, Maastricht, Netherlands	2
2015	25th MGC Symposium, Leiden, Netherlands	0,5
2015	PhD Day Erasmus MC, Rotterdam, Netherlands	0,5
2016	6th Winter School of the Collaborative Research Centre TRR81, Kleinwalsertal, Austria (oral presentation)	2
2016	14th Dutch Chromatin Meeting Leiden, Netherlands	0,5
2017	Sanquin Spring Seminar, Amsterdam, Netherlands	1
2017	26th MGC Symposium, Rotterdam, Netherlands	0,5
2017	PhD Day Erasmus MC, Rotterdam, Netherlands	0,5

(Inter)National conferences

Year	Title	Workload (ECTS)
2015	9th Dutch Hematology Meeting, Papendal, Netherlands	1
2015	3th Symposium on Chromatin Changes in differentiation and malignancies, Marburg, Germany	2
2017	4th Symposium on Chromatin Changes in differentiation and malignancies, Egmond aan Zee, Netherlands	2

Additional Activities

Year	Title	Workload (ECTS)
2013-2017	Supervision of HLO/Master students	2
2014	Committee member Theme Biomedical Science EMC	2
2015	Organization PhD Workshop Maastricht, Netherlands	2

Acknowledgments

Poef… daar ligt hij dan… mijn proefschrift. Bloed, zweet en tranen heeft het zeker gekost. Dit had ik nooit kunnen bewerkstelligen zonder de steun van vele mensen.

Allereerst mijn (co)-promotoren, **Prof. Dr. Sjaak Philipsen, Dr. Thamar van Dijk** en **Dr. Marieke von Lindern.** In 2008 kwam ik als jonkie bij jullie op het lab mijn eerste HLO-stage doen, niet wetende dat ik in 2013 terug zou komen om van jullie de kans te krijg om een PhD te gaan doen. Nu weer een aantal jaren later, is het alweer 2019 en mag ik mijn proefschrift gaan verdedigen. Bedankt voor het vertrouwen dat jullie in mij getoond hebben en de discussies die we gehad hebben. **Sjaak** bedankt voor de positieve motivatie die je mij altijd gaf, en **Thamar** in het speciaal bedankt voor het leren van alle technieken die ik gebruikt heb tijdens de afgelopen jaren. **Marieke**, bedankt voor de feedback die je gegeven hebt tijdens het beoordelen van alle stukken en alle werkbesprekingen die we roulerend in Amsterdam en Rotterdam hadden.

Verder gaat mijn dank uit naar **Prof. Dr. Frank Grosveld, Prof. Dr. Joost Gribnau** en **Prof. Dr. Masja de Haas**. Bedankt voor het lezen van mijn proefschrift en het voorzien van commentaar erop. Beste **Frank**, bedankt voor alle feedback de afgelopen jaren op de geplande proeven tijdens de werkbesprekingen en de PhD-meetings. Ook ons gesprek over carrièremogelijkheden heeft mij wel goed geholpen. Beste **Joost,** wat leuk dat je nu in mijn commissie zit en nogmaals bedankt voor je praatje op het Wolfert Tweetalig afgelopen januari. **Prof. Dr. Danny Huylenbroeck** en **Dr. Marjon Cnossen**, bedankt voor het plaatsnemen in mijn promotie comité.

Mijn paranimfen, **Martijn** en **Anne.** Wat leuk en fijn om jullie bij mij te hebben op deze speciale dag. **Martijn** bedankt verder voor de leuke discussies en praatjes die we vaak in onze koffiepauzes hadden. Ik weet nu wat te doen als er zo'n Afrikaanse Indiër van Microsoft belt om mijn wachtwoorden te achterhalen. Het fluitje ligt er al klaar voor. **Anne,** wat heb jij in de laatste fase van mijn labwerk mij fijn geholpen tijdens je HLO-stage. Jij hebt het vak wel in je handen. Succes met je verdere carriere!

Deze thesis was zeker niet tot stand gekomen zonder de hulp en ervaringen van **Nynke**. Jouw enorme bak aan ervaring en inzichten hebben veel bijgedragen de resultaten van de inhoud van dit boekje. We werkten echt als een goed team en waren goed op elkaar in gespeeld op de dagen dat we grote experimenten deden. Super bedankt voor jouw inzet.

Maria and **Ileana** thank you for the warm welcoming within the Philipsen lab-team. You both already defended years ago, but I'm happy we still have contact every now and then. **Ileana and Dimitris,** thank you for the invitation to your beautiful wedding in Greece in 2017. Wish you and your little princess to be all the luck. **Maria** en **Thodoris,** veel geluk samen nu jullie ook getrouwd zijn maar nog wel steeds in Nederland zijn blijven wonen.
Other former Philpsen lab-members, **Sahar, Pavlos, Divine, Anna, Harmen, Mike, Bella, Juliette, Lieke, Dora,** thank you for the interest in my work and the interesting

lunch discussions.
Verder zijn er natuurlijk nog vele (oud-)celbiologie collega's die ik ook even wil bedanken voor de fijne tijd daar: **Johan, Maayke, Christina, Emma, Dubi, Rick, Andrea, Guillaume, Lucca, Sreya, Ralph**, **Judith, Ser, Johannes**, en iedereen die ik vergeet te noemen, bedankt voor jullie collegialiteit. **Martí**, we started the PhD together on the same day, and finally we graduated both (but not on the same day). Wish you and **Marta** and your son Bly all the luck. **Mieke, Evelien, Heleen, Jenniffer, Marjon** en anderen van het **Scholten-lab** bedankt voor jullie gezelschap tijdens de lunches en borrels. **Niels, Bob, Raymond, Kerstin** en **Derk** bedankt voor jullie adviezen en commentaren tijdens de MMM sessies.

Ook wil ik een aantal collega's van andere afdelingen bedanken. **Hegias**, thank you the nice traveling company in Greece. I enjoyed our road trip to the wedding. **Ruben, Joachim and Aristea** thank you for your company during the KWT trips. **Chiara**, thank you for the nice corridor talks. **Michael,** dank voor de intrigerende conversaties over 020 en dat voetbalclubje met dat lelijke UFO-stadion. **Mateusz, Atze** en **Fenne** ik vond het erg leuk om met jullie de MGC-workshop te organiseren. **Fenne** heel veel plezier en geluk aan de andere kant van de oceaan. **Marjolein** en **Rudi,** bedankt voor alle hulp bij het opzetten van de pan-hematopoeitsche screens. Dit was mij nooit gelukt zonder jullie kennis en ervaringen.

En achter de schermen, de mensen die de afdeling geordend houden, wil ik ook bedanken, **Marieke, Bep, Jasperina, Sonja, Leo, Melle, Koos** en de dames in de keuken.

De collega's van het Wolfert Tweetalig, **Wendy, Maayke, Anniek, Titus, Malyssa, Shiela, Menno, Ronald, Marcel, René, Michael, Michiel, Gerrie, Yvonne, Ada, Mehmet, Abdoel** en **Ronald** bedankt voor het mij zo welkom en thuis te laten voelen.

Alle **vrienden** en **vriendinnen,** het zijn er te veel om allemaal bij naam te noemen, maar ik wil jullie ook graag allemaal bedanken voor alle interesse en steun die ze mij hebben gegeven gedurende dit traject. **Jeske**, bedankt voor alle lunches en hardloop-sessies tijdens mijn mama-dagen, en ontspanning die het me gaf. **Barbara** en **Jony** bedankt voor de ontspannende sportuurtjes. **Patricia** en **Linda**, jullie waren er wanneer ik jullie nodig had, thanks! **Marloes** jij hebt altijd onvoorwaardelijk in mij geloofd. Super bedankt voor je onvermoeibare motivaties lieverd. **Lotte,** we kennen elkaar al zo lang. Ik hoop dat jij ook snel je weg weet te vinden.

Hier wil ik ook graag mijn familie leden, **Rob, Ingrid, Elise, Nienke, Joop, Saskia, Marlies, Roger, Opa, Adrie, Wilma, Henny, Maarten, Hanneke, Martijn, Gerine** bedanken voor alle interesse die jullie altijd hebben getoond in mijn werk en de voortgang ervan. Fijn om sommige van jullie erbij te hebben vandaag! Ook wil ik graag mijn schoonfamilie bedanken, **Hannie** en **Tom** voor het opvangen van Daan en ook Bram en jullie steun en intresse.. **Marije, Alexander, Renske, Hans, Marjan, Jan-Willem, Hilde, Gerard, Hugo, Nicolette, Timo, Marjolein, Steven, Lisette**, alle **neefjes** en **nichtjes**. Jullie ook allemaal bedankt voor de steun en interesse in de voortgang van mijn onderzoek.

In memoriam, **opaatje**, jammer dat je het einde van mijn onderzoek niet meer hebt mee kunnen maken. Bedankt dat je altijd interesse probeerde te tonen. *Ook in memoriam,* **Prof. Dr. Mathieu Noteborn**, tijdens mijn master heb je altijd in mij geloofd, ook al deed ik dat soms niet altijd meer. Sjaak en ik wilde je eigenlijk vragen in mijn commissie plaats te laten nemen. Helaas mocht dat niet zo zijn. Het ga je goed.

Adri en Marleen, Lieve Papa en Mama. De afgelopen jaren waren behoorlijk hektisch. Papa's opgeluk was wel een dieptepunt, maar de geboorte van Daan en Bram waren wel hoogte punten. Gelukkig nu weer een hoogtepunt! Bedankt voor jullie onvoorwaardelijke steun en hulp. Ik hoop dat we nog jaren van elkaar kunnen genieten.

Mijn kinderen **Daan** en **Bram**, jullie hebben dit allemaal niet zo meegekregen, het was soms zwaar om voor jullie te zorgen en tegelijkertijd aan mijn proefschrift te werken. Ik heb daardoor jullie soms minder aandacht kunnen geven die jullie verdienden. Nu is het gelukkig lekker klaar. Ik ben echt super trots en blij met jullie.

Lieve **Matthijs**, last but not least… we hebben een hoop doorstaan de afgelopen jaren, maar zonder jouw steun en motivatie was dit eindproduct er niet geweest. Via deze weg wil ik je hiervoor bedanken. Ik was niet altijd de gezelligste in sommige fasen van dit traject. Maar nu zie je wat ik allemaal uitgevoerd hebt. Super bedankt schat. Op naar de volgende fase. Ik hoop dat we elkaar nog jaren mogen ondersteunen.